MycoKeys 43: 1–21 (2018)
doi: 10.3897/mycokeys.43.25090
http://mycokeys.pensoft.net

RESEARCH ARTICLE

A peer-reviewed open-access journal
MycoKeys
Launched to accelerate biodiversity research

New host associations and a novel species for the gall-inducing acacia rust genus *Ravenelia* in South Africa

Malte Ebinghaus[1], Wolfgang Maier[2], Michael J. Wingfield[3], Dominik Begerow[1]

1 *AG Geobotanik, Ruhr-Universität Bochum, Germany* **2** *Institute for Epidemiology and Pathogen Diagnostics, Julius Kühn-Institut (JKI), Federal Research Centre for Cultivated Plants, Braunschweig, Germany* **3** *Forestry and Agricultural Biotechnology Institute (FABI), University of Pretoria, South Africa*

Corresponding author: *Malte Ebinghaus* (malte.ebinghaus@gmx.de)

Academic editor: *M. Thines* | Received 16 March 2018 | Accepted 9 November 2018 | Published 4 December 2018

Citation: Ebinghaus M, Maier W, Wingfield MJ, Begerow D (2018) New host associations and a novel species for the gall-inducing acacia rust genus *Ravenelia* in South Africa. MycoKeys 43: 1–21. https://doi.org/10.3897/mycokeys.43.25090

Abstract

Trees in the genus *Vachellia* (previously *Acacia*) are commonly infected by the gall-inducing rusts *Ravenelia macowaniana* and *R. evansii*. Rust galls bearing aecial infections and relating uredinial and telial infections on the leaves of nine *Vachellia* species not previously recorded to be infected by *Ravenelia* spp. have recently been collected in South Africa. The rust fungi causing these infections were characterised using molecular phylogenetic analyses of DNA sequence data of the LSU and ITS rDNA regions as well as morphological examinations. The host range of *R. macowaniana* and *R. evansii* was thus re-assessed and extended from four to nine species and from one to three species, respectively. Application of Principal Component Analyses (PCA) of telial morphological characters provided evidence of an effect of the host species on the teliospore morphology in *R. evansii*, but only minor effects in *R. macowaniana*. A novel gall-inducing *Ravenelia* sp. closely related to *R. macowaniana*, was found on *Vachellia xanthophloea* and it is described here as *R. xanthophloeae*.

Keywords

Ravenelia xanthophloeae sp. nov., *Vachellia xanthophloea*, novel host record, aecial galls, teliospore morphology, intraspecific variability, Principal Component Analysis

Introduction

Trees in the genus *Vachellia* (formerly *Acacia* subg. *Acacia*) and referred to here as acacias make up one of the most prominent floral elements of the Southern African

landscape. Acacias can be found in all South African biomes. Here they play important ecological roles by providing food for insects, birds and game, as well as improving soil fertility through nitrogen fixation by their associated rhizobia (Ross 1979, Coe and Coe 1987, Coates Palgrave 2005, Smit 2008, Grellier et al. 2012).

In South Africa, acacias are commonly infected by rust fungi (Pucciniales) of the genus *Ravenelia* (Doidge 1950). *Ravenelia* includes more than 200 described species and is amongst the most species-rich genera of rust fungi (Cummins and Hiratsuka 2003). These fungi are obligate parasites of various genera of the legumes (i.e. in subfamilies Mimosoideae, Faboideae, Caesalpinioideae) and they are globally distributed in the tropics and sub-tropics (Dietel 1906, Cummins and Hiratsuka 2003). While the aecial stage of several macrocyclic species is known to cause hypertrophied tissues such as galls and witches brooms within host organs (Dietel 1894, Hernandez and Hennen 2003), the multicellular teliospores of *Ravenelia* are amongst the most complex spore forms found in the rusts.

In South Africa, 20 species of *Ravenelia* have been described, the majority of which infect trees of the acacia genera *Senegalia* and *Vachellia* (Doidge 1939, 1950, van Reenen 1995). Four of these including *R. natalensis* Syd., P. Syd. & Pole-Evans, *R. deformans* (Maublanc) Dietel, *R. macowaniana* Pazschke and *R. evansii* Syd. & P. Syd. induce galls on their hosts. Based on the number of deposited specimens in the National Collection of Fungi, South Africa (PREM) and our own field observations, the macrocyclic and gall-inducing *R. macowaniana* and *R. evansii* are likely the most abundant *Ravenelia* species in South Africa. *Ravenelia macowaniana* has been reported from *V. karroo* only, which in turn is the most frequently occurring acacia in this region. *Ravenelia evansii* has been reported from four acacia species including *V. gerrardii* (Benth.) P.J.H. Hurter, *V. rehmanniana* (Schinz) Kyal. & Boatwr. *V. robusta* ssp. *robusta* (Burch.) Kyal. & Boatwr. and *V. sieberiana* var. *woodii* (Burtt Davy) Kyal. and Boatwr. (Doidge 1939, 1950). In contrast, *R. deformans* and *R. natalensis*, both reported from *V. karroo* (Hayne) Banfi and Galasso, have only rarely been collected (Doidge 1939, Farr and Rossman 2017).

During several field surveys focused on re-assessing the diversity of *Ravenelia* species in South Africa, we sampled rust infections associated with galls on eight *Vachellia* species. The aim of this study was to identify the collected rust specimens using morphological and phylogenetic analyses. In addition, new host associations and a new species were reported and the influence of the host on teliospore characters was analysed.

Material and methods

Specimens examined

Infected *V. borleae*, *V. davyi*, *V. exuvialis*, *V. hebeclada*, *V. natalitia*, *V. permixta*, *V. swazica* and *V. xanthophloea* trees were sampled during several field surveys in South Africa between 2004 and 2015. Leaves bearing uredinial and telial rust sori and short branch-

es having aecial galls were collected and subsequently dried between paper sheets in a plant press. In total, 49 specimens were studied based on morphology and 31 of these could be used for phylogenetic analyses based on DNA-sequence data. Ten of the 49 specimens were either type or voucher specimens collected in the late 19th and early 20th century and used by Doidge for her studies of the southern African *Ravenelia* spp. (Doidge 1927, 1939). These herbarium specimens were used only for morphological comparisons with the newly collected material (Table 1). Three specimens were deposited in KR, all others in PREM.

DNA extraction and PCR

Spores from individual sori were collected separately using sterile insect needles. Genomic DNA extractions were made using the INNUPrep Plant DNA Kit (Analytik Jena, Germany) following the manufacturer's protocols with the following modifications: Spores were crushed using a Retsch mixer mill MM2000 (Retsch, Haan, Germany) by shaking them together with 2 steel beads of 2.5 mm diameter in a 2.0 ml Eppendorf tube. This process was repeated in three consecutive cycles. In the first step, the closed tubes were cooled in liquid nitrogen and immediately shaken for 2 min at 100 Hz. Thereafter 10–40 µl of lysis buffer was added to the tube to loosen spore remnants from the inner side of the Eppendorf tube lid using a vortex mixer followed by a centrifugation step. Samples were again cooled in liquid nitrogen and shaken for an additional 2 min at 100 Hz followed by centrifugation for 1 min at 6000 rcf. The last two steps were repeated once.

For PCR of the ribosomal nrITS and LSU rDNA gene regions, the Taq-DNA-Polymerase Mix (PeqLab, Erlangen, Germany) was used with the primers ITS1F (Gardes and Bruns 1993) and RustITS1F (Toome and Aime 2014), respectively and ITS4BR (Vialle et al. 2009). PCR of the LSU rDNA region was performed using the primer pairs LR0R and LR6 (Vilgalys and Heester 1990). Two additional primers (5.8SrustF: 5'- CGA TGA AGA ACA CAG TGA AAT GTG; D1D2RustR: 5'- CTY TGC TAT CCT GAG GGA) were designed with improved specificity for *Ravenelia* and that reduced amplification of ascomycetous non-target organisms. The thermal cycling conditions for primers ITS1F/ITS4BR and RustITS1F/ITS4BR were as follows: 2 min at 96 °C followed by 40 cycles of 20 sec at 96 °C, 40 sec at 50 °C and 50 sec at 72 °C, final extension was for 5 min at 72 °C; for primers LR0R/LR6: 3 min at 96 °C followed by 40 cycles of 30 sec at 95 °C, 40 sec at 49 °C and 1 min at 72 °C, final extension was for 7 min at 72 °C; for primers 5.8SrustF/D1D2rustR: 3 min at 96 °C followed by 40 cycles of 30 sec at 96 °C, 45 sec at 54 °C and 1 min 20 sec at 72 °C, final extension was for 7 min at 72 °C.

PCR products were purified using Sephadex G-50 columns (Sigma-Aldrich, Steinheim, Germany). Where PCR products showed only weak bands on agarose gels, purification was undertaken using the Zymo Research DNA Clean & Concentrator™-5 Kit (Zymo Research GmbH, Freiburg, Germany) following the manufacturer's pro-

Table 1. List of specimens included in the present study, including host information, collection data and GenBank accession numbers of rDNA sequences.

Voucher	Species name	Host	Origin	Date	Collector	GenBank accession-Nos.	
						ITS	LSU
PREM61208	*Ravenelia evansii*	*Vachellia robusta* ssp. *robusta*	South Africa, North-West Province, Groot Marico, River Still Guest Farm	15 Apr 2009	W. Maier	MG945960	MG945992
PREM61209	" "	" "	South Africa, KwaZulu-Natal, Lake St. Lucia	18 Mar 2010	M. Ebinghaus	MG945959	MG945991
PREM2211	" "	" "	South Africa, Gauteng, Pretoria, The Willows	6 Apr 1912	I. B. Pole Evans	–	–
PREM6807	" "	" "	South Africa, KwaZulu-Natal, Verulam	3 Jul 1913	I. B. Pole Evans	–	–
PREM7105	" "	" "	South Africa, KwaZulu-Natal, Verulam	3 Jul 1913	I. B. Pole Evans	–	–
KR-M-43649	" "	" "	South Africa, KwaZulu-Natal, Mtunzini	20 Mar 2010	M. Ebinghaus	MG945958	MG945990
PREM61225†	" "	*Vachellia sieberiana* var. *woodii*	South Africa, Mpumalanga, R40 north of Nelspruit	22 June 2005	W. Maier	–	–
PREM61228	" "	" "	South Africa, KwaZulu-Natal; 30°52'S; 30°18'E	24 Nov 2005	A. R. Wood	MG945957	MG945989
PREM61223	" "	" "	South Africa, KwaZulu-Natal; 28°50'27"S; 29°26'5.8"E	23 Mar 2010	M. Ebinghaus	MG945956	MG945988
PREM2403	" "	" "	South Africa, KwaZulu-Natal, Cramond	3 June 1912	I. B. Pole Evans	–	–
PREM2539	" "	" "	South Africa, KwaZulu-Natal, Estcourt	31 Jul 1912	I. B. Pole Evans	–	–
PREM61881	" "	" "	South Africa, Mpumalanga; 25°23'41.8"S; 31°05'08.0"E	14. Feb 2015	M. Ebinghaus	MG945955	MG945987
PREM61224†	" "	*Vachellia davyi*	South Africa, Mpumalanga, R40 north of Nelspruit	27 June 2005	W. Maier	–	–
PREM61005	" "	" "	South Africa, Mpumalanga; 35 km east of MBombela; 25°34'21.6"S; 31°10'48.1"E	11 Apr 2013	M. Ebinghaus	MG945967	MG945999
PREM61845	" "	" "	South Africa, KwaZulu-Natal, near Pongola; 27°19'27.2"S; 31°26'39.6"E	13. Feb 2015	M. Ebinghaus	MG945968	MG946000
PREM61227	" "	*Vachellia hebeclada*	South Africa, North-West Province, Leeuwfontein Farm	30 Dec 2006	A. E. van Wyk	MG945969	MG946001
PREM61211†	" "	*Vachellia swazica*	South Africa, Mpumalanga; Marloth Park; 25°20'48.2"S; 31°46'45.7"E	9 Apr 2013	M. Ebinghaus	–	–
PREM61212†	" "	" "	South Africa, Mpumalanga; Marloth Park; 25°20'44.3"S; 31°46'26.2"E	9 Apr 2013	M. Ebinghaus	–	–
PREM61002	" "	" "	South Africa, Mpumalanga; Marloth Park; 25°20'43.0"S; 31°46'38.8"E	9 Apr 2013	M. Ebinghaus	MG945966	MG945998
PREM61008	" "	" "	South Africa, Mpumalanga; 25 km east of MBombela; 25°30'43.5"S; 31°10'3.3"E	12 Apr 2013	M. Ebinghaus	MG945965	MG945997
PREM61028	" "	" "	South Africa, Mpumalanga; Marloth Park; 25°20'44.4"S; 31°46'26.1"E	9 Apr 2013	M. Ebinghaus	MG945964	MG945996
PREM61846	" "	*Vachellia luederitzii* var. *retinens*	South Africa, KwaZulu-Natal; 15 km south of Jozini; 27°30'57.3"S; 32°00'39.1"E	12 Feb 2015	M. Ebinghaus	MG945961	MG945993
PREM61868	" "	*Vachellia exuvialis*	South Africa, Mpumalanga; Justicia; 24°52'52.6"S; 31°23'40.3"E	17 Feb 2015	M. Ebinghaus	MG945963	MG945995
PREM61876	" "	" "	South Africa, Mpumalanga, Belfast; 24°56'08.7"S; 31°21'52.5"E	17 Feb 2015	M. Ebinghaus	MG945962	MG945994

Voucher	Species name	Host	Origin	Date	Collector	GenBank accession-Nos.	
						ITS	LSU
ME384	" "	*Vachellia borleae*	South Africa, KwaZulu-Natal; 20 km north of Empangeni; 28°41'30.1"S; 31°43'16.9"E	9 Feb 2015	M. Ebinghaus	MG945971	MG946003
PREM61869	" "	" "	South Africa, Mpumalanga; Masibekela; 25°51'36.2"S; 31°49'51.8"E	16 Feb 2015	M. Ebinghaus	MG945970	MG946002
PREM61222	*Ravenelia macowaniana*	*Vachellia karroo*	South Africa, Limpopo, Sekhukhune Land, Winterveld Mine	23 June 2005	W. Maier	MG945975	MG946007
PREM61221	" "	" "	South Africa, North-West Province, Hartebeespoort Dam	June /Jul 2005	W. Maier	MG945973	MG946004
PREM61210	" "	" "	South Africa, Eastern Cape, Haga Haga	Dec 2005	W. Maier	MG945972	MG946004
PREM61220†	" "	" "	South Africa, unknown	15 May 2006	W. Maier	–	–
KR-M-43406	" "	" "	South Africa, Western Cape, Worcester	20 Dec 2004	M.J. Wingfield	MG945974	MG946006
KR-M-43657	" "	" "	South Africa, North-West Province; 25°30'08.2"S; 27°21'32.4"E	8 Mar 2015	M. Ebinghaus	MG945976	MG946008
PREM61875	" "	*Vachellia permixta*	South Africa, Limpopo, Mokopane; 24°08'52.4"S; 29°02'21.9"E	23 Feb 2015	M. Ebinghaus	MG945982	MG946014
PREM61862	" "	*Vachellia natalitia*	South Africa, Limpopo, Steelport; 24°41'32.3"S; 30°12'32.3"E	19 Feb 2015	M. Ebinghaus	MG945980	MG946012
PREM61218	" "	" "	South Africa, Mpumalanga, Nelspruit	10 Jan 2005	W. Maier	MG945979	MG946011
PREM61219	" "	" "	South Africa, Mpumalanga, Nelspruit	10 Jan 2005	W. Maier	MG945977	MG946009
PREM61888†	" "	" "	South Africa, Mpumalanga, Nelspruit	21 June 2005	W. Maier	–	–
PREM 61216	" "	" "	South Africa, Eastern Cape, Port St. John	28 Dec 2005	W. Maier	MG945978	MG946010
PREM61226†	" "	" "	South Africa, Mpumalanga, South of Nelspruit	16 Mar 2010	M. Ebinghaus	–	–
PREM61214	" "	" "	South Africa, Mpumalanga, East of Barberton	2 June 2012	M. Ebinghaus	MG945981	MG946013
PREM61215	*Ravenelia xanthophloeae*	*Vachellia xanthophloea*	South Africa, Mpumalanga, Barberton; 25°46'52.5"S; 31°03'10.7"E	3 Jul 2012	M. Ebinghaus	MG945985	MG946017
PREM61213	" "	" "	South Africa, KwaZulu-Natal, Mount Moreland; 29°38'21.6"S; 31°05'27.3"E	16 June 2012	M. Ebinghaus	MG945983	MG946015
PREM61213‡	" "	" "	South Africa, KwaZulu-Natal, Mount Moreland; 29°38'21.6"S; 31°05'27.3"E	16 June 2012	M. Ebinghaus	MG945986	–
PREM61000	" "	" "	South Africa, Mpumalanga, Komatipoort; 25°26'10.0"S; 31°57'48.6"E	9 Apr 2013	M. Ebinghaus	MG945984	MG946016
PREM1935†	*Ravenelia natalensis*	*Vachellia karroo*	South Africa, KwaZulu-Natal, Winkelspruit	29 Nov 1911	I. B. Pole Evans	–	–
PREM2514†	" "	" "	South Africa, KwaZulu-Natal, Winkelspruit	6 Jul 1912	E. M. Doidge	–	–
PREM2375†	*Ravenelia glabra*	*Calpurnia sylvatica*	South Africa, KwaZulu-Natal, Mulden	1 May 1912	P. MacOwan	–	–
PREM10698†	" "	" "	not known	not known	P. MacOwan	–	–
PREM20727†	" "	" "	South Africa, Western Cape, Somerset East	1875	P. MacOwan	–	–

†Specimens were only morphologically investigated.

‡Specimen representing the aecial infection state.

tocol. DNA sequencing was carried out in both directions using the same primers as those used for PCR on a 3130XL Genetic Analyzer (Applied Biosystems) at the sequencing service of the Faculty of Chemistry and Biochemistry of the Ruhr University Bochum, Germany.

Phylogenetic analyses

Sequences were screened against the NCBI GenBank using the BLASTn algorithm (Altschul et al. 1990) to exclude erroneously amplified contaminants from further processing. Forward and reverse strands of the rust sequences were assembled using Sequencher 5.0 software (Gene Codes Corp., Ann Arbor, MI, USA) and, where necessary, manually edited. In total, 32 sequences were used to construct an alignment of the nrITS and LSU rDNA sequence data, respectively, using MAFFT v6.832b (Katoh and Standley 2014) applying the L-INS-i strategy. Maximum likelihood analyses were conducted in RAxMLGUI v.1.3 (Silvestro and Michalak 2012) using RAxML 8.0.26 (Stamatakis 2014) using the general time reversible model of nucleotide substitution (Lanave et al. 1984) with gamma distributed substitution rates. The analyses were run with a rapid bootstrap analysis using 1000 bootstrap replicates. The analyses were first conducted for each dataset separately and topological congruence was checked visually. As no conflict of supported phylogenetic groupings was observed, the final phylogeny was inferred by combining both datasets of the nrITS and LSU rDNA sequences applying the same methodology as for individual datasets.

Parsimony network analyses were performed using TCS v1.21 (Clement et al. 2000) and the same sequence alignments that were used for the phylogenetic analyses. Gaps were deleted from calculations and the default connection limit of 95% was used.

Light- and electron microscopic investigations

The spores of the dried herbarium specimens (Table 1) were scraped from leaf surfaces and mounted in lactophenol on microscope slides. A minimum of ten teliospores and 30 urediniospores per specimen were examined. Minimum, maximum and mean values are provided in Table 2. The specimens PREM2211 (*R. evansii*), PREM2403 (*R. evansii*), PREM2539 (*R. evansii*), PREM6807 (*R. evansii*), PREM7105 (*R. evansii*), PREM1935 (*R. natalensis*), PREM2514 (*R. natalensis*), PREM2375 (*R. glabra*), PREM10698 (*R. glabra*) and PREM20727 (R. glabra) were examined at the facilities of the ARC-Plant Protection Institute (ARC-PPRI), Roodeplaat, South Africa using a Leica Dialux 22 EB microscope and a ColorView III CCD colour camera. Measurements were made using analySIS LS software (LS Research Software GmbH, Germany). The remaining specimens were studied at the Ruhr University Bochum, Germany, using a Zeiss Axioplan light microscope. Morphological characteristics were measured

Table 2. Measurements of morphological characters of *Ravenelia evansii*, *R. macowaniana* and *R. xanthophloeae* sp. nov., separately performed for each host species. All size measurements are given in µm. †Data taken from original descriptions by Doidge (1927).

Ravenelia on host species	Teliospore diameter	Probasidial cell length	Probasidial cell width	Epispore thickness	Ornamentation length	Cell numbers in diam.
R. evansii						
V. robusta†	50–80	25–30	17–23	4–6	4–6	4–6
V. borleae	(52)72–83(92)	(21)23–28(40)	(16)22–26(34)	(2.5)3–4.5(6.0)	(3)3.5–4.5(6)	3–6
V. davyi	(83)95–105(115)	1(9)25–30(34)	(12)19–24(32)	(2.5)4–5(6.5)	(2.0)3.5–5(7)	5–7
V. exuvialis	(47)70–85(101)	(19)23–28(33)	(15)21–26(30)	(2.5)3.5–4.5(6)	(3)4.5–6(7.5)	3–7
V. luederitzii	(79)94–100(115)	(18)23–30(36)	(15)19–25(32)	(2.5)3–5(7)	(1.5)3–5(6)	5–7
V. robusta	(81)90–110(118)	(20)22–29(35)	(14)19–25(33)	(3)3.5–5(6.5)	(1.5)3.5–6(8)	5–8
V. sieberiana	(63)85–97(112)	(19)23–29(35)	(15)21–24(33)	(2.5)3.5–4.5(6)	(2.5)4.5–6.5(8)	4–8
V. swazica	(71)85–105(124)	(16)22–29(39)	(12)18–27(32)	(2)3–5(7)	(2.5)3.5–6(7)	5–8
R. macowaniana						
V. karroo†	60–130	up to 45	18–28	not stated	–	4–7
V. karroo	(75)82–105(118)	(21)23–31(35)	(14)17–24(29)	(2)3–5.5(6.5)	–	4–7
V. natalitia	(50)80–105(114)	(19)24–34(45)	(14)19–26(34)	(2)3–4.5(5.5)	–	3–6
R. xanthophloeae						
V. xanthophloea	(40)65–75(84)	(19)22–28(40)	(12)18–25(29)	(2)3–4(6)	(0.5)1–2(3)	3–6

using Cell^D v. 3.1 imaging software (Olympus Soft Imaging Solutions GmbH, Germany) and Zen2 lite (Blue Edition) V. 2.0.0.0 (Carl Zeiss Microscopy, 2011, Jena, Germany). Photographs were obtained using a Color View microscope camera (Olympus Soft Imaging System, Germany). For detailed investigations of the spore-surface structures, scanning electron microscopy (SEM) was used. For this purpose, infected leaflets from the herbarium specimens were mounted on double-sided adhesive carbon tape on metal stubs and coated with gold in a sputter coater BAL-TEC SCD OSO (Capovani Brothers Inc, USA). Subsequently, the samples were examined using a ZEISS Sigma VP scanning electron microscope.

Principal Component Analyses (PCA)

For principal component analyses (PCA) the morphological data collected for all examined rust individuals were separated into sub-sets based on preliminary species assignments representing *R. evansii*, *R. macowaniana* and *Ravenelia* sp. (Groups A, B1 and B2). PCA for all subsets was conducted separately using the R-packages plyr and ggplot2 implemented in R (www.R-Project.org). Six characteristics of teliospores providing numeric data were defined and measured: teliospore diameter, probasidial cell length and probasidial cell width, number of cells in diameter, epispore thickness and ornamentation length. Mean values were calculated for the individual teliospore measurements, scaled and missing values were deleted from analyses.

Results

Phylogenetic Analyses

Sequence data from the nrITS and LSU rDNA gene regions were obtained for all 31 newly collected specimens. The alignment of the nrITS sequence dataset had a total length of 764 bp with 133 variable sites of which 131 positions were parsimony informative. The aligned sequences of the LSU rDNA dataset had a length of 922 bases and comprised 31 sequences with 45 variable sites and 40 parsimony informative positions. The combination of the nrITS and LSU rDNA datasets resulted in an alignment with a total length of 1686 nucleotides comprising 32 sequences. The sequence alignment and phylogenetic tree of the combined rDNA sequence data set was deposited at TreeBASE (http://purl.org/phylo; submission IDS22307).

Maximum likelihood analysis of the combined dataset resulted in a phylogenetic tree that consisted of three highly supported groups representing *R. evansii*, *R. macowaniana* and a novel *Ravenelia* species described below (Fig. 1A).

The phylogenetic group representing *R. evansii* consisted of 17 sequences. Three of these were obtained from *Vachellia sieberiana* var. *woodii* (PREM61223, PREM61228, PREM61881) and three from *V. robusta* ssp. *robusta* (KR-M-43649, PREM61208, PREM61209). These are tree species that had previously been reported as hosts of *R. evansii*. Rust specimens collected from the following five *Vachellia* species also clustered in this group: *V. borleae* (ME384 and PREM61869), *V. davyi* (PREM61005), *V. exuvialis* (PREM61868, PREM61876), *V. hebeclada* (PREM61227) and *V. swazica* (PREM61002, PREM61008, PREM61028). These are all newly reported hosts for *R. evansii*.

A second group included the sequences of eleven specimens, five of which originated from *V. karroo* and were identified as *R. macowaniana* (KR-M-43657, PREM61222, PREM61221, PREM61210, KR-M-43406). Five specimens were collected from *V. natalitia* (PREM61214, PREM61862, PREM61218, PREM61219, PREM61216) and one originating from *V. permixta* (PREM61875) also clustered in this group. The latter two hosts are newly reported for *R. macowaniana*.

A distinct clade, nested within the *R. macowaniana* group, was represented by three *Ravenelia* specimens that were isolated from *V. xanthophloea* (PREM61215, PREM61213, PREM61000) suggesting that it represents a novel taxon. For PREM61213, two identical sequences were obtained, one derived from aeciospores and one from teliospores.

The parsimony network analysis, based on the combined set of nrITS and LSU rDNA sequence data, separated three distinct groups each comprising the same specimens representing *R. evansii*, *R. macowaniana* and the novel *Ravenelia* species in our phylogenetic analysis, respectively (Fig. 1B). Network analysis relying on LSU alone could not separate *R. macowaniana* from the novel taxon, while separation of these two groups was observed based on nrITS alone (not shown). The *R.*

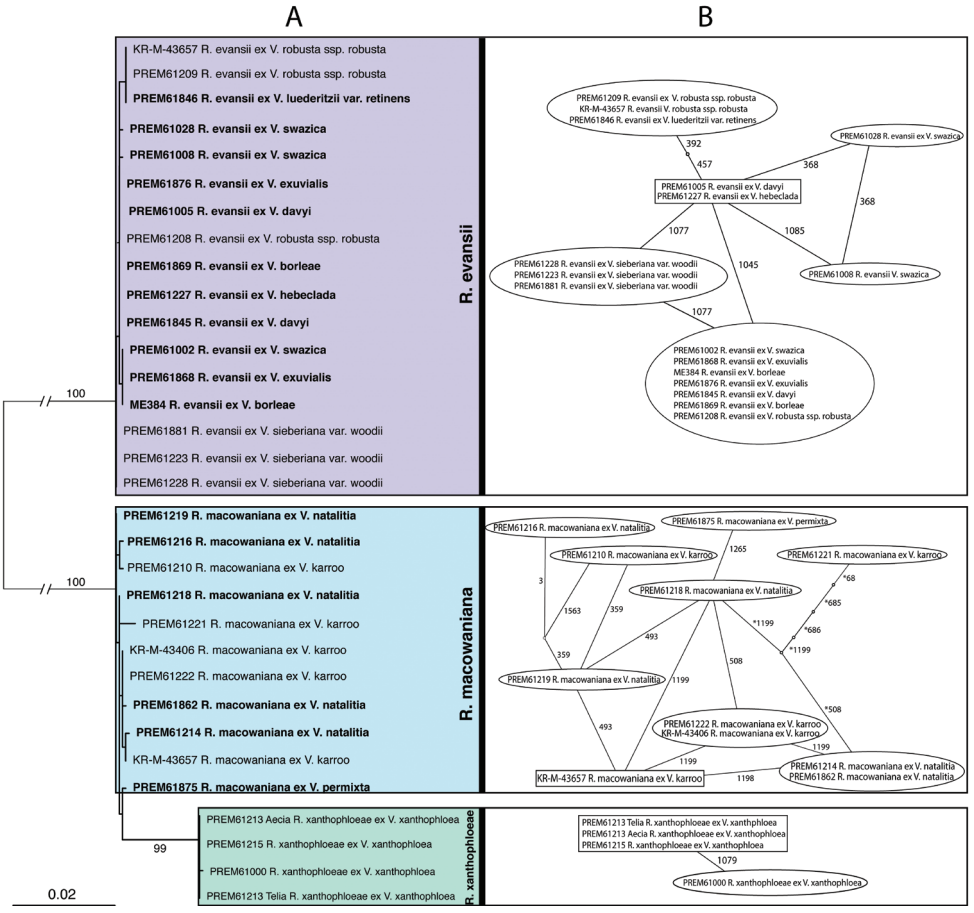

Figure 1. Phylogenetic reconstruction of *Ravenelia* species on different *Vachellia* hosts **A** Maximum likelihood tree with 1000 bootstrap repeats based on combined nrITS and LSU rDNA sequence data. Bootstrap values below 75 are not shown. Three highly supported groups represent *R. evansii*, *R. macowaniana* and *R. xanthophloeae* sp. nov., respectively. Specimens that originated from formerly unreported host species are highlighted in bold **B** Parsimony network analysis based on the same dataset as in the ML-analysis. Each line represents one base substitution while small circles represent intermediate but missing sequences. Numbers next to lines indicate the positions of the substitutions in the alignment. Sequences in rectangular boxes were inferred as ancestral by this analysis.

evansii group consisted of six haplotypes of 17 sequences that differed by a maximum of two substitutions from the inferred ancestral sequences (PREM61005 and PREM61227). In *R. macowaniana*, sequence divergence was more pronounced and consisted of nine haplotypes in a total of eleven sequences. The highest rate of six substitutions was observed for specimen PREM61221 relative to the inferred ancestral sequence (KR-M-43657). Specimens collected on *V. xanthophloea* had only one substitution.

Morphological analyses

Ravenelia evansii

The teliospore morphology of *R. evansii* specimens showed a considerable overall variability in all six investigated teliospore characteristics (Suppl. material 1: Fig. S1, Table 2). The voucher specimens PREM61869 (on *V. borleae*), PREM61876 and PREM61868 (both on *V. exuvialis*) had significantly smaller teliospores compared to the remaining specimens, but variation in this trait could also be observed within single host associations, e.g. within those from *V. davyi* and *V. robusta* (Suppl. material 1: Fig. S1).

The principal component analysis (PCA) of teliospore characteristics clustered several individuals derived from specific hosts into distinct groups (Fig. 2C, D). Individuals that originated from *V. borleae* and *V. exuvialis* clustered more closely and could be separated from those individuals that were collected from *V. davyi* (Fig. 2D). The separation of these individuals was supported by PC1 which could explain 37.6% of the overall variability. The traits 'cells in diameter' and 'teliospore diameter' were characteristics that corresponded best with this axis (Fig. 2C). These results indicated, that the latter two characters were the most variable traits to separate these individuals with different host associations. However, individuals from *V. luederitzii* var. *retinens, V. robusta* var. *robusta*, *V. sieberiana* var. *woodii* and *V. swazica* showed only weak separation, i.e. less clear patterns of morphological separation.

Ravenelia macowaniana

Specimens representing *R. macowaniana* were morphologically more homogeneous compared to *R. evansii*. Here, only spore characteristics such as 'probasidial cell width' and 'epispore thickness' were often significantly different between investigated specimens (Suppl. material 2: Fig. S2). There was little variation for the characters 'teliospore diameter', 'probasidial cell length' and the number of 'cells in diameter'. These characters varied distinctly only between single specimens, e.g. PREM61226 originating from *V. natalitia* had significantly larger teliospores in comparison to specimen PREM61888 that was also collected from this host (Suppl. material 2: Fig. S2).

For the specimens of *R. macowaniana*, PC1 and PC2 could explain 36.2% and 22.4% of the similarity, respectively. However, unlike in *R. evansii*, single teliospore characteristics did not differ significantly in terms of host association (Fig. 2A).

Ravenelia sp. nov.

Due to similar teliospore characteristics, *R. macowaniana* was compared using PCA to individuals of the undescribed *Ravenelia* species collected on *V. xanthophloea* in order to characterise and, if possible, to contrast both morphologies. The PCA separated two groups that corresponded well with *R. macowaniana* and the novel *Ravenelia* species and

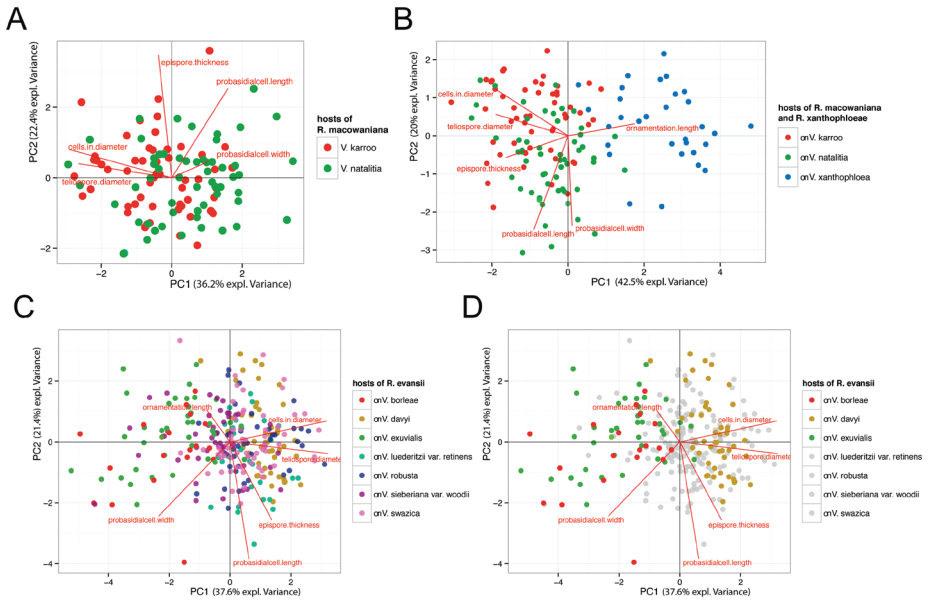

Figure 2. Biplots of a principal component analysis (PCA) of six teliospore characteristics of specimens of **A** *Ravenelia macowaniana* originating from *Vachellia karroo* (red) and *V. natalitia* (green) and **B** in comparison with *R. xanthophloeae* sp. nov. collected from *V. xanthophloea* (blue) **C, D** represent *R. evansii* originating from seven distinct *Vachellia* species. Each dot represents an individual teliospore for which mean values of multiple measurements of all six defined morphological characteristics were calculated. Each colour represents the host species of the individual rust specimen. In **D** only spore representatives collected from *V. borleae*, *V. exuvialis* and *V. davyi* were highlighted to gain better visibility.

showed very little overlap in morphological characteristics (Fig. 2B). Separation between both species groups was mostly seen in PC1 that could explain 42.5% of the overall variability with the 'ornamentation length' corresponding best to this axis (Fig. 2B). Although less distinct in the PCA, mean values of teliospore characters also revealed that the characters 'epispore thickness', 'probasidial cell length' and especially the 'teliospore diameter' and 'cells in diameter' are valuable characters for the discrimination of both species (Fig. 3). All spore measurements, derived from the six defined spore characteristics that were used for PCA, are available as an excel-file in the Suppl. materials 3, 4: tables S1, S2: 'PCA-table *R. evansii*' and 'PCA-table *R. macowaniana*', respectively.

Taxonomy

***Ravenelia xanthophloeae* Ebinghaus, W. Maier & Begerow, sp. nov.**
Mycobank: MB824073
Figure 4A–H

Type. South Africa, KwaZulu-Natal, 29°38'21.6"S; 31°05'27.3"E, on leaves and gall-transformed inflorescences of *Vachellia xanthophloea* (Benth.) P.J.H. Hurter (Fabaceae:

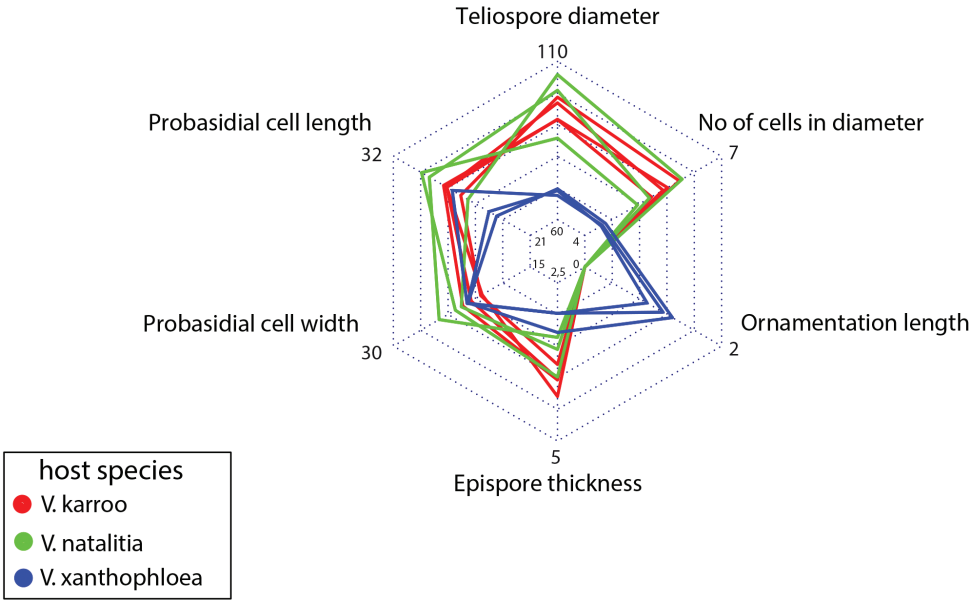

Figure 3. Radarchart of mean values of the morphological investigations of teliospore characteristics of *Ravenelia macowaniana* originated from *Vachellia karroo* (red), *V. natalitia* (green) and *R. xanthophloeae* on *V. xanthophloea* (blue). Numbers on y-axis represent the respective minimum and maximum values. This radarchart reveals the morphological differences between *R. macowaniana* and *R. xanthophloeae*.

Mimosoideae), 16 June 2012, M. Ebinghaus ME188, (holotype: PREM61213); South Africa, Mpumalanga, 25°46'52.5"S; 31°03'10.7"E, on leaves of *Vachellia xanthophloea* (Benth.) P.J.H. Hurter (Fabaceae: Mimosoideae), 3 July 2012, M. Ebinghaus ME174, (paratype: PREM61215); South Africa, Mpumalanga, 25°26'10.0"S; 31°57'48.6"E, on leaves of *Vachellia xanthophloea* (Benth.) P.J.H. Hurter (Fabaceae: Mimosoideae), 9 April 2013, M. Ebinghaus ME248, (paratype: PREM61000)

Etymology. The name refers to the host tree, *Vachellia xanthophloea.*

Description. Spermogonia not found. Aecia on rust-induced galls, which are formed instead of inflorescences. Aeciospores globose to sub-globose, often angular, yellowish-transparent in light microscopy, light brown when dry (19.0)21.0–24.0(28.5) × (14.5)18.0–20(21.5) µm, cell wall (1.0–)2.0(–3.0) µm thick, densely verrucose, germ pores numerous, scattered (Figure 4C). Peridia and peridial cells could not be described because only disintegrated aecia were present in the dried herbarium material.

Uredinia amphigenous on leaves, but mostly on the abaxial side of the leaflets, scattered or in small groups, minute, 0.1–0.2 mm, erumpent and surrounded by the torn epidermis; ellipsoidal to roundish, light-brown to blackish; paraphyses numerous, scattered within sorus; capitate, thickened end ovoidal, about 19–20 × 11–13 µm, cell wall 2–3 µm, light-brown, smooth; urediniospores ovoidal to broadly ellipsoidal or sometimes subglobose, (18)23–26(38) × (13)16–20(25) µm, spore wall evenly 1.5–2.0 µm thick with densely echinulate aculei (Figure 4D), germ pores 5–6, subequatorial to equatorial (Figure 4E).

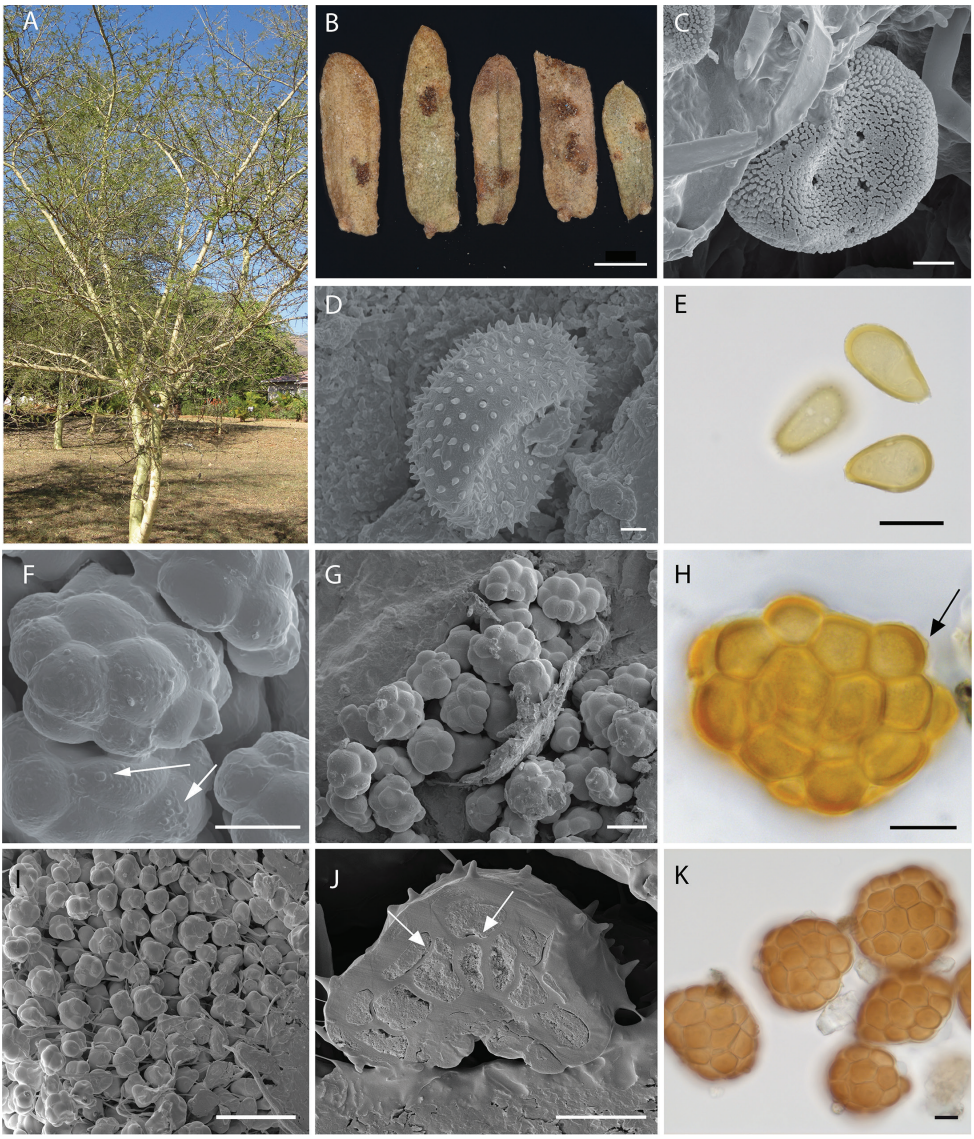

Figure 4. Infected host organs and spore images of *R. xanthophloeae* (**A–H**), *R. natalensis* (**I**), *R. evansii* (**J**) and *R. macowaniana* (**K**) **A** Infected individual of *V. xanthophloea*. Leaves were prematurely shed in comparison with uninfected trees **B** Telia on leaflets of *V. xanthophloea* **C** SEM of an aeciospore showing scattered germpores **D** SEM of an urediniospore **E** Urediniospores seen in LM **F** SEM view of a teliospore of *R. xanthophloeae*. The arrows indicate irregularly arranged verrucose ornamentations **G** Telium of *R. xanthophloeae* seen in SEM **H** LM view of a teliospore. The arrow indicates irregularly arranged verrucose ornamentations **I** Teliospores of *R. natalensis* with long pedicels **J** SEM picture of median section of a teliospore of *R. evansii*. Arrows indicate 2-celled probasidial cells **K** LM picture of teliospores of *R. macowaniana*. Scale bars: 1 mm (**B**), 4 µm (**C**), 2 µm (**D**), 20 µm (**E**), 20 µm (**F–H, J–K**), 40 µm (**I**).

Telia replacing the uredinia; teliospores often irregularly shaped from top view; single probasidial cells distinctly arched upwards (Figure 4F–H), orange-brown to pale brown, teliospore surface in general smooth but with single and irregularly arranged small verrucae, (Figure 4F–I); teliospores varying in size from (40)65–75(84) µm in diameter with mostly 4–5 probasidial cells in a cross-section, rarely 3 or 6 cells; central cells in two layers, 32–40 µm in lateral view; marginal cells in a single layer, (19)22–28(33) µm in lateral view and (12)18–25(29) µm from above; upper cellwall (2)3–4(6) µm thick; verrucose ornamentations (0.5)1–2(3) µm in height (Figure 4F, H), rarely with protuberances of up to 7 µm in height; cysts smooth and hyaline, of variable number but often appear in same number as marginal probasidial cells, swelling in water but only slightly in lactophenol, pedicels compound, not persisting.

Notes. In South Africa, *R. macowaniana*, *R. glabra* Kalchbr. & Cooke and *R. deformans* (Maublanc) Dietel are the only known species that exhibit two-layered probasidial cells and smooth teliospores. While the first character is shared by *R. xanthophloeae,* the teliospore surface bears small and irregularly arranged small warts clearly visible in SEM (Fig. 4F). However, these can easily be overlooked in light microscopy (Fig. 4H) and could potentially lead to misidentification. Specifically, *R. macowaniana* differs from *R. xanthophloeae* in the overall size of its teliospores (Table 2; Figure 4K) and the urediniospores have four equatorial germ pores whereas those of *R. xanthophloeae* have five to six equatorial germ pores. The teliospores of the microcyclic *R. glabra* Kalchbr. & Cooke are about twice the size (120–160 µm) of those of *R. xanthophloeae* and its oblong urediniospores are significantly larger (32–48 × 14–21 µm). This rust has also been reported only from *Calpurnia sylvatica* (Burch.) E. Mey (Fabaceae) (Doidge 1927). The demicyclic *R. deformans* (Maublanc) Dietel was synonymised with the neotropical *R. hieronymi* Speg. based on nearly identical morphology and congruent life cycle characteristics (Hernandez and Hennen 2003; Hennen et al. 2005) but conspecificity of these two rust fungi is doubtful as they infect distinct host species and occur each on different continents. However, both species produce aecia that induce malformations in young branches, which is a characteristic similar to the newly described *R. xanthophloeae*. With a size of 60–120 µm and 75–120 µm, respectively, the teliospores of *R. deformans* and *R. hieronymi* are, however, on average significantly larger and develop intermingled with the aecia (Doidge 1927), while *R. xanthophloeae* is macrocyclic and aecia, uredinia and telia are produced in spatially separated sori.

The teliospores of *R. xanthophloeae* may also be confused with those of *R. natalensis* Syd., P. Syd & Pole-Evans, but they are significantly smaller in size (30–50 µm diam.) and possess extraordinarily long and persistent pedicels (up to 110 µm; Sydow 1912, Fig. 4I). In *R. natalensis,* the aparaphysate uredinia and telia are confluent and cover large areas on the branches of the host (Sydow and Sydow 1912; own observations), while the specimens of *R. xanthophloeae* examined in this study have minute uredinia with numerous paraphyses and telia not exceeding 200 µm in diameter.

New host records. Morphological and molecular phylogenetic analyses based on nrITS and nrLSU data confirmed new host records for *R. macowaniana* and *R. evansii* that will be reported in the following section. An emended species decription for *R. evansii* is also provided.

***Ravenelia macowaniana* Pazschke & Hedwigia, 23: 30 and 59 (1894)**
Figure 4K

Ravenelia macowaniana Pazschke & Hedwigia, 23: 30 and 59 (1894). On leaves and in gall-transformed inflorescences of *Vachellia natalitia* (E.Mey) Kyal. & Boatwr. and on leaves of *V. permixta* (Burtt Davy) Kyal. & Boatwr. (Fabaceae: Mimosoideae).

Specimens examined. South Africa, Limpopo, Steelport, 24°41'32.3"S; 30°12'32.3"E, on leaves of *Vachellia permixta*, 23 February 2015, M. Ebinghaus ME424 (PREM61875); South Africa, Limpopo, Steelport, 24°41'32.3"S; 30°12'32.3"E, on leaves of *V. natalitia*, 19 February 2015, M. Ebinghaus ME416 (PREM61862); South Africa, Mpumalanga, East of Barberton, on leaves of *V. natalitia*, 2 June 2012, M. Ebinghaus ME158 (PREM61214); South Africa, Mpumalanga, Nelspruit, on leaves of *V. natalitia*, 10 January 2005, W. Maier WM3292 (PREM61218) and WM3294 (PREM61219); South Africa, Mpumalanga, South of Nelspruit, on leaves of *V. natalitia*, 10 March 2010, W. Maier WM3590 (PREM61226); South Africa, Mpumalanga, Nelspruit, on leaves of *V. natalitia*, 21 June 2005, W. Maier WM3423 (PREM61888); South Africa, Eastern Cape, Port St. Johns, on leaves of *V. natalitia*, 28 December 2005, W. Maier WM3453 (PREM61216); South Africa , Limpopo, Sekhukhune Land, Winterveld Mine, on leaves of *V. karroo* 23 June 2005, W. Maier WM3433 (PREM61222); South Africa, North-West Province, Hartebeesspoort Dam, on leaves of *V. karroo* June/July 2005, W. Maier WM3448 (PREM61221); South Africa, Eastern Cape, Haga Haga, on leaves of *V. karroo*, December 2004, W. Maier WM3485 (PREM61210); South Africa, on leaves of *V. karroo*, 15 May 2006, W. Maier WM3512 (PREM61220); South Africa, Western Cape, Worcester, on inflorescences of *V. karroo*, 20 December 2004, W. Maier WM3577 (KR-M-43406); South Africa, North-West Province 25°30'08.2"S; 27°21'32.4"E, on leaves of *V. karroo*, M. Ebinghaus ME433 (KR-M-43657).

Notes. Morphological as well as phylogenetic analyses, based on nrITS and nrLSU sequence data of the specimens PREM61214, PREM61216, PREM61218, PREM61219, PREM61862 and PREM61875 collected from *V. natalitia* and *V. permixta*, respectively, supported conspecificity and their placement in *R. macowaniana*. Therefore, we report *V. natalitia* and *V. permixta* as new hosts for *R. macowaniana*.

***Ravenelia evansii* Sydow, Ann. Mycol. 10, p. 440, Monograph. Ured. 3, p. 234**
Figure 4J

Ravenelia evansii Sydow, Ann. Mycol. 10, p. 440, Monograph. Ured. 3, p. 234 On *Vachellia borleae* (Burtt Davy) Kyal. & Boatwr., *V. davyi* (N.E.Br.) Kyal. & Boatwr., *V. exuvialis* (I. Verd.) Kyal. & Boatwr., *V. hebeclada* (DC.) Kyal. & Boatwr., *V. luederitzii* var. *retinens* (Sim.) (JH Ross & Brenan) Kyal. & Boatwr. and *V. swazica* (Burtt Davy) Kyal. & Boatwr. (Fabaceae: Mimosoideae).

Emended description. Telia subepidermally erumpent, dark brown to blackish, scattered or in loose groups on the abaxial side of leaflets, sori on the comparatively large leaflets of *V. robusta* ssp. *robusta* often forming concentric rings of 2.2–3.3 mm in diameter, single sori (120)230–500(710) µm in diameter with the largest telia appearing to develop in concentric arranged groups, subcircular to elongated; paraphyses lacking; teliospores circular to subcircular from topview, topside convex to almost hemispherical from lateral view, chestnut brown, (47)74–103(124) µm in diameter with (3)5–7(8) probasidial cells in a cross-section; single probasidial cells mostly single-layered, sometimes central cells and in rare events single cells two-layered, (16)23–30(39) µm from lateral view and (11)18–25(34) µm from top view; each probasidial cell with 3–5(8) spines; cysts hyaline and smooth, uniseriate and each cyst appears to be divided by a faint constriction, of the same number as peripheral probasidial cells, swelling in water but only slightly in lactophenol, pedicels compound, not persisting.

Specimens examined. All specimens examined for the emended species description of *R. evansii* representing new host associations are given in Table 1.

Notes. Rust infections on specimens of *Vachellia borleae* (ME384, PREM61869), *V. davyi* (PREM61845, PREM61005), *V. exuvialis* (PREM61876, PREM61868), *V. hebeclada* (PREM61227), *V. luederitzii* var. *retinens* (PREM61846) and *Vachellia swazica*.(PREM61002, PREM61028, PREM61008) were identified using morphological characters of the teliospores. These generally matched those of *R. evansii* Syd. & P. Syd. given in Doidge (1927) and Shivas et al. (2013) and were supported by molecular phylogenetic analyses of nrITS and nrLSU sequence data. These *Vachellia* species are reported as new hosts for *Ravenelia evansii*. Despite major congruence of teliospore characters, the range of the teliospore diameter observed by our examinations exceeded the size range of 50–80 µm and 63–90 µm given in Doidge (1927) and Shivas et al. (2013), respectively. Furthermore, the occurrence of two-layered probasidial cells is reported here for the first time Figure 4J). Therefore, we present an emended description of the telial stage of *R. evansii* Syd. & P. Syd. emend. Ebinghaus, W. Maier and Begerow.

Table 3. Summary of morphological characters and spore sizes of *Ravenelia evansii*, *R. macowaniana* and *R. xanthophloeae*. All size measurements are given in µm, minimum and maximum values in parentheses. †Measurements and observations according to Doidge (1939).

	Teliospores			
	Diameter	**Probasidial cell size**	**Ornamentation**	**No. of Cells in diameter**
R. evansii	(47)70–95(124)	(16)24–29(40) × (12)18–25(34)	(1.5)4–6(8)	(3)5–7(8)
R. macowaniana	(50)82–105(118)	(19)23–32(40) × (13.5)18–24(34)	–	(3)5–6(7)
R. xanthophloeae	(40.5)65–75(82)	(19)22–25(39.5) × (12.5)19–23(32)	(0.5)1–2(3)	(3)4–5(6)
	Aeciospores	**Urediniospores**		
	Size	**Size**	**Germ pores**	
			Number	**Arrangement**
R. evansii	23–40 × 16–26†	25–35 × 18–24†	4†	equatorial†
R. macowaniana	24–35 × 17–28†	20–30 × 12.5–15†	4†	equatorial†
R. xanthophloeae	(19)21–24(29)×(14)17–19(23)	(18)23–26(38) × (13)16–20(25)	5–6	equatorial

Discussion

The new rust species, *R. xanthophloeae*, was found only on the fever tree *Vachellia xanthophloea*. In South Africa, this tree species is naturally confined to habitats with shallow watertables in low-altitude areas of the northeastern KwaZulu-Natal, Mpumalanga and Limpopo Provinces (Coates Palgrave 2005, Smit 2008). However, it is frequently planted as ornamental at higher altitudes throughout Southern Africa, where infections by *R. macowaniana* on *V. karroo* are common. Yet, despite extensive sampling efforts, no rust has been reported from *V. xanthophloea* in these regions, suggesting that *R. xanthophloeae* might currently be restricted to the native range of its host tree. Furthermore, *V. xanthophloea* is apparently resistant to infection by the frequently co-occurring and closely related *R. macowaniana*. This observation lends additional support to the separation of *R. macowaniana* and *R. xanthophloeae* as distinct species.

Sequence divergence was smaller amongst the specimens of *R. evansii* than within *R. macowaniana* (Fig. 1). This is in contrast to teliospore morphology, where the six examined teliospore traits showed considerable variability in *R. evansii*, but very little variation in *R. macowaniana*. Specifically, an effect of the host association on teliospore morphology could be demonstrated and this was most pronounced in specimens of *R. evansii* collected from *V. borleae*, *V. davyi* and *V. exuvialis*. It has been demonstrated in other fungal and oomycetous plant pathogens that infraspecific variation of spore traits might correlate with host species (Savile 1976, Lutz et al 2005, Runge and Thines 2011). However, mechanisms leading to such host-associated differences in rust fungi remain obscure. Savile (1976) hypothesised that differences in host compatibility of rust fungi potentially lead to differences in nutrient supply and could consequently influence morphological features. It was also speculated that host anatomy such as the thickness of the cuticle and epidermis might influence spore morphology (Scholler et al. 2011). Clearly, experimental studies that focus on the differential effects of the host and environment on morphological character expression in the rust fungi are needed to resolve this question.

In the present study, the host ranges of *R. macowaniana* and *R. evansii* were expanded from one to three and from four to nine hosts, respectively. Thus, these two rust species have a broader host range then previously reported and parasitise several co-occurring acacia species in the South African savannah biome. This is in contrast to recent findings in the genus *Endoraecium* that infect Australian wattles (*Acacia* s. str., formerly *Acacia* subg. *Phyllodineae*). Based on morphological and molecular phylogenetic studies, species previously thought to have a broad host range were split into several species infecting mostly a single tree species (Berndt 2011, McTaggart et al. 2015). In this case, a general pattern of co-speciation of the parasites with their hosts was suggested (McTaggart et al. 2015). In the South African acacia rusts however, the shared distribution ranges of their hosts may prevent the rusts from speciation by recurrent gene flow between metapopulations. In contrast, *Ravenelia xanthophloeae* appears to infect only *V. xanthophloea.* In the phylogenetic analyses, this rust was closely related to *R. macowaniana*, which suggests a more recent speciation of both species. The host of *R. xanthophloeae* is eco-geographically clearly separated from the hosts of *R. macowaniana* and the different niches of the host most likely contributed considerably to the divergence of the parasite species.

Acknowledgements

We thank Dr. Isabel Rong and Dr. Adriaana Jacobs for organising field trips and for obtaining access to the National Collections of Fungi of South Africa as well as for general support and Dr. Martin Kemler for helpful suggestions on the manuscript. We gratefully acknowledge the DAAD (German Academic Exchange Service) and the Studienstiftung für mykologische Systematik und Ökologie for financial support. We further acknowledge support by the DFG Open Access Publication Funds of the Ruhr University Bochum.

References

Altschul SF, Gish W, Miller M, Myers EW, Lipman DJ (1990) Basic Local Alignment Search Tool. J Mol Biol 215: 403–410. https://doi.org/10.1016/S0022-2836(05)80360-2

Berndt R (2011) Taxonomic revision of *Endoraecium digitatum* (rust fungi, Uredinales) with description of four new species from Australia and Hawaii. Mycol Prog 10: 497–517. https://doi.org/10.1007/s11557-010-0719-9

Palgrave CM (2005) Keith Coates Palgrave Trees of Southern Africa. 3rd Edition, imp. 3. Struik Publishers, Cape Town.

Coe M, Coe C (1987) Large herbivores, *Acacia* trees and bruchid beetles. S Afr J Sci. 83: 624–635.

Dietel P (1894) Die Gattung *Ravenelia*. Hedwigia. Vol. 33. Verlag C. Heinrich, Dresden, 49–69.

Dietel P (1906) Monographie der Gattung *Ravenelia* Berk. Beihefte Bot. Centralbl. 20: 343–413.

Doidge E (1927) A preliminary study of the South African rust fungi. Bothalia 2: 1–228.

Doidge E (1939) South African rust fungi III. Bothalia 3: 487–512. https://doi.org/10.4102/abc.v3i4.1757

Doidge E (1950) The South African Fungi and Lichens to the End of 1945. Bothalia 5: 432.

Farr DF, Rossman AY (2017) Fungal Databases, Systematic Mycology and Microbiology Laboratory, ARS, USDA. http://nt.ars-grin.gov/fungaldatabases/ [Accessed 20 April 2017]

Gardes M, Bruns TD (1993) ITS primers with enhanced specificity for Basidiomycetes-application to the identification of mycorrhizae and rusts. Mol Ecol 2: 113–118. https://doi.org/10.1111/j.1365-294X.1993.tb00005.x

Grellier S, Barot S, Janeau J-L, Ward D (2012) Grass competition is more important than seed ingestion by livestock for *Acacia* recruitment in South Africa. Plant Ecol 213: 899–908. https://doi.org/10.1007/s11258-012-0051-3

Hernandez JR, Hennen JF (2003) Rust fungi causing galls, witches' brooms, and other abnormal growths in northwestern Argentina. Mycologia 95: 728–755. https://doi.org/10.1080/15572536.2004.11833076

Katoh K, Standley DM (2014) MAFFT Multiple Sequence Alignment Software Version 7: Improvements in Performance and Usability. Mol Biol Evol 30: 772–780. https://doi.org/10.1093/molbev/mst010

Lanave C, Preparata G, Saccone C, Serio G (1984) A new Method for calculating evolutionary Substitution rates. J Mol Evol 20: 86–93. https://doi.org/10.1007/BF02101990

Lutz M, Göker M, Piatek M, Kemler M, Begerow D, Oberwinkler F (2005) Anther smuts of Caryophyllaceae: molecular characters indicate host-dependent species delimitation. Mycol Prog 4: 225–238. https://doi.org/10.1007/s11557-006-0126-4

McTaggart AR, Doungsa-ard C, Wingfield MJ, Roux J (2015) *Uromycladium acaciae*, the cause of a sudden, severe disease epidemic on *Acacia mearnsii* in South Africa. Australasian Plant Pathol. 44: 637–645. https://doi.org/10.1007/s13313-015-0381-4

Pazschke EO (1894) In: Dietel P (Ed.) Die Gattung *Ravenelia*. Hedwigia 33. Verlag C. Heinrich, Dresden.

Ritschel A, Berndt R, Oberwinkler F (2007) New observations of rust fungi (Uredinales) from northern Namibia. Mycol Prog 6: 137–150. https://doi.org/10.1007/s11557-007-0533-1

Ross JH (1979) *Acacia karroo* in Southern Africa. Bothalia 10: 385–401.

Runge F, Thines M (2011) Host matrix has major impact on the morphology of *Pseudoperonospora cubensis*. Eur J Plant Pathol 129: 147–156. doi: 10.1007/s10658-010-9650-9

Scholler M, Lutz M, Wood AR, Hagedorn G, Menniken M (2011) Taxonomy and phylogeny of *Puccinia lagenophorae*: a study using rDNA sequence data, morphological and host range features. Mycol Prog 10: 175–187. https://doi.org/10.1007/s11557-010-0687-0

Shivas RG, Balu A, Singh S, Ahmed SI, Dhileepan K (2013) *Ravenelia acacia-arabicae* and *Ravenelia evansii* are distinct species on *Acacia nilotica* subsp. *indica* in India. Australasian Mycologist 31: 31–37.

Silvestro D, Michalak I (2012) raxmlGUI: a graphical front-end for RAxML. Org Divers Evol 12: 335–337. https://doi.org/10.1007/s13127-011-0056-0

Smit N (2008) Field Guide to the Acacias of South Africa. Briza Publications, Pretoria.

Stamatakis A (2014) RAxML version 8: a tool for phylogenetic analysis and post-analysis of large phylogenies. Bioinformatics 30: 1312–1313. https://doi.org/10.1093/bioinformatics/btu033

Sydow H, Sydow P (1912) Beschreibungen neuer südafrikanischer Pilze. Ann Mycol 10: 440.

Toome M, Aime MC (2014) Reassessment of rust fungi on weeping willows in the Americas and description of *Melampsora ferrinii* sp. nov. Plant Pathol 64: 1.

van Reenen M (1995) An annotated list of Urediniomycetes (rust fungi) from South Africa 1: Melampsoraceae and Pucciniaceae, excluding *Puccinia* and *Uromyces*. Bothalia 25.2: 173–181. https://doi.org/10.4102/abc.v25i2.726

Vialle A, Feau N, Allaire M, Didukh M, Martin F, Moncalvos J-M, Hamelin RC (2009) Evaluation of mitochondrial genes as DNA barcode for Basidiomycota. Mol Ecol Resour 9: 99–113. https://doi.org/10.1111/j.1755-0998.2009.02637.x

Vilgalys R, Hester M (1990) Rapid genetic identification and mapping of enzymatically amplified ribosomal DNA from several *Cryptococcus* species. J Bacteriol 172: 4239–4246. https://doi.org/10.1128/jb.172.8.4238-4246.1990

Supplementary material 1

Figure S1

Authors: Malte Ebinghaus, Wolfgang Maier, Michael J. Wingfield, Dominik Begerow

Data type: statistical data

Explanation note: Boxplot of measurements of the six defined teliospore characters of *R. evansii*. Values were obtained from teliospores derived from seven different host species of in total 18 individual trees. The boxplots are based on mean values calculated for all investigated teliospores for each specimen, respectively.

Link: https://doi.org/10.3897/mycokeys.43.25090.suppl

Supplementary material 2

Figure S2

Authors: Malte Ebinghaus, Wolfgang Maier, Michael J. Wingfield, Dominik Begerow

Data type: statistical data

Explanation note: Boxplot of measurements of the six defined teliospore characteristics of *R. macowaniana* and *R. xanthophloeae*. Values were obtained from teliospores derived from three different host species of in total 10 individual trees. The boxplots are based on mean values calculated for all investigated teliospores for each specimen, respectively.

Link: https://doi.org/10.3897/mycokeys.43.25090.suppl2

Supplementary material 3

Table S1

Authors: Malte Ebinghaus, Wolfgang Maier, Michael J. Wingfield, Dominik Begerow

Data type: species data

Explanation note: List of measurements of teliospore characters of *R. evansii*. Obtained values were sorted by voucher and by individual teliospores. All measurements are given in µm.

Link: https://doi.org/10.3897/mycokeys.43.25090.suppl3

Supplementary material 4

Table S2

Authors: Malte Ebinghaus, Wolfgang Maier, Michael J. Wingfield, Dominik Begerow

Data type: species data

Explanation note: List of measurements of teliospore characters of *R. macowaniana* and *R. xanthophloeae*. Obtained values were sorted by voucher and by individual teliospores. All measurements are given in µm.

Link: https://doi.org/10.3897/mycokeys.43.25090.suppl4

MycoKeys 43: 23–57 (2018)
doi: 10.3897/mycokeys.43.25081
http://mycokeys.pensoft.net

RESEARCH ARTICLE

A peer-reviewed open-access journal
MycoKeys
Launched to accelerate biodiversity research

Endophytic *Colletotrichum* species from *Dendrobium* spp. in China and Northern Thailand

Xiaoya Ma[1,2,3], Sureeporn Nontachaiyapoom[2,3], Ruvishika S. Jayawardena[2,3], Kevin D. Hyde[2,3], Eleni Gentekaki[3], Sixuan Zhou[1,4], Yixin Qian[1], Tingchi Wen[1], Jichuan Kang[1]

1 *Engineering and Research Center for Southwest Biopharmaceutical Resource of National Education Ministry of China, Guizhou University, Guiyang 550025, Guizhou Province, People's Republic of China* **2** *Center of Excellence in Fungal Research, Mae Fah Luang University, Chiang Rai 57100, Thailand* **3** *School of Science, Mae Fah Luang University, Chiang Rai 57100, Thailand* **4** *Guizhou Institute of Animal Husbandry and Veterinary, Guiyang, Guizhou province, 550005, People's Republic of China*

Corresponding author: *Jichuan Kang* (jckang@gzu.edu.cn)

Academic editor: *Andrew Miller* | Received 16 March 2018 | Accepted 3 November 2018 | Published 4 December 2018

Citation: Ma X, Nontachaiyapoom S, Jayawardena RS, Hyde KD, Gentekaki E, Zhou S, Qian Y, Wen T, Kang J (2018) Endophytic *Colletotrichum* species from *Dendrobium* spp. in China and Northern Thailandle. MycoKeys 43: 23–57. https://doi.org/10.3897/mycokeys.43.25081

Abstract

Species of *Colletotrichum* are commonly found in many plant hosts as pathogens, endophytes and occasionally saprobes. Twenty-two *Colletotrichum* strains were isolated from three *Dendrobium* species – *D. cariniferum*, *D. catenatum* and *D. harveyanum,* as well as three unidentified species. The taxa were identified using morphological characterisation and phylogenetic analyses of ITS, GAPDH, ACT and ß–tubulin sequence data. This is the first time to identify endophytic fungi from *Dendrobium* orchids using the above method. The known species, *Colletotrichum boninense*, *C. camelliae-japonicae*, *C. fructicola, C. jiangxiense* and *C. orchidophilum* were identified as fungal endophytes of *Dendrobium* spp., along with the new species, *C. cariniferi*, *C. chiangraiense*, *C. doitungense*, *C. parallelophorum* and *C. watphraense*, which are introduced in this paper. One strain is recorded as an unidentified species. Corn meal agar is recommended as a good sporulation medium for *Colletotrichum* species. This is the first report of fungal endophytes associated with *Dendrobium cariniferum* and *D. harveyanum*. *Colletotrichum camelliae-japonicae*, *C. jiangxiense*, and *C. orchidophilum* are new host records for Thailand.

Keywords

Colletotrichum, *Dendrobium*, Endophytic fungi, multi-loci, new species

Introduction

Colletotrichum is the sole genus in family *Glomerellaceae* (Glomerellales) (Maharachchikumbura et al. 2015, 2016; Jayawardena et al. 2016b; Hongsanan et al. 2017). Presently, there are 193 accepted *Colletotrichum* species in eleven species complexes and 23 accepted singleton species (Hyde et al. 2014; Jayawardena et al. 2016a). *Colletotrichum* species has been listed as one of the top ten fungal pathogenic genera in molecular plant pathology based on scientific/economic importance (Dean et al. 2012). Anthracnose caused by *Colletotrichum* species can be a devastating disease in many economically important crops, including fruit crops, vegetables, cassava, sorghum, as well as ornamental plant such as orchids (Prusky and Plumbley 1992; Hyde et al. 2009a, b; Cannon et al. 2012; Dean et al. 2012; Jadrane et al. 2012; Jayawardena et al. 2016a; Diao et al. 2017). Many pathogenic *Colletotrichum* species that adopt biotrophic life strategies are present as symptomless endophytes in living plant tissues (Photita et al. 2004), although a large number of non-pathogenic species also occur as endophytes (e.g. Mendgen and Matthias 2002; Lu et al. 2004; Rojas et al. 2010; Cannon et al. 2012; Kleemann et al. 2012). Interestingly, experiments of Redman et al. (2001) showed that pathogenic *Colletotrichum* species could express mutualistic lifestyles in plants not known to be hosts and conferred disease resistance, drought tolerance, and/or growth enhancement to the host plants. Even though the diversity of *Colletotrichum* species associated with cultivated plant hosts have extensively been studied (Yang et al. 2009), a very limited number of studies has been conducted on *Colletotrichum* species from non-cultivated plants in natural and semi-natural habitats (Cannon et al. 2012).

Dendrobium SW. is the second largest genus in *Orchidaceae* (The Plant List 2013). Most *Dendrobium* species/hybrids are important ornamental/floricultural crops, but some species within this genus also possess medicinal values (Xu et al. 1995; Ng et al. 2012). Many *Dendrobium* orchids have been listed as Chinese medicinal herbs and are used for the treatments of atrophic gastritis, diabetes, faucitis, fever, red tongue, and/or thirsty (Ping et al. 2003; Bulpitt et al. 2007; Xing et al. 2011; Xia et al. 2012; Xu et al. 2014). Moreover, some *Dendrobium* orchids including *D. catenatum* Lindl. (widely known as *D. officinale* Kimura & Migo) have been listed as critically endangered species by the International Union for Conservation of Nature (IUCN) (www.iucnredlist.org). Due to their significance, *Dendrobium* orchids have been the subject of many studies including the diversity of endophytic fungi (Ma et al. 2015). However, only a limited number of studies on endophytic *Colletotrichum* in *Dendrobium* species have been reported and the number of *Dendrobium* species included in these studies are very few (Yuan et al. 2009; Yang et al. 2011; Mangunwardoyo et al. 2011; Chen et al. 2012; Noireung et al. 2012; Tao et al. 2013). In the present study, we investigated the diversity of endophytic *Colletotrichum* in five *Dendrobium* orchid species collected from a mountain (at an elevation of 1,300–1,400 m) close to the Thailand-Myanmar border and *D. catenatum* collected from Guizhou Province in China. A total of 22 endophytic *Colletotrichum* strains were isolated and identified based on both mor-

phological and molecular characteristics. Five *Colletotrichum* strains, *C. cariniferi*, *C. chiangraiense*, *C. doitungense*, *C. parallelophorum* and *C. watphraense* are introduced as new species. The results of this study will contribute to the knowledge on diversity and phylogeny of *Colletotrichum*.

Material and methods

Sample collection

Healthy roots, stems and leaves of *D. cariniferum*, *D. harveyanum* and three unidentified *Dendrobium* taxa (referred to as *Dendrobium* sp. 1, 2 and 3) were collected from Wat Phra That Doi Tung (Temple of Doi Tung Pagoda), Mae Fah Luang District, Chiang Rai, Thailand. Healthy roots, stems and leaves of *D. catenatum* were collected from Guizhou Province in China. Materials were packed in zip-lock bags or tubes containing silica gel on ice. Fungal isolation was carried out within 48 hours following collection.

Fungal isolation and cultivation

Surface sterilization and endophyte isolation were carried out as described by Nontachaiyapoom et al. (2010) with some modifications. First, materials were washed with running water. Roots, stems and leaves were immersed in a solution containing 3% (v/v) H_2O_2 and 70% (v/v) ethanol for 5 minutes, and then rinsed with sterile distilled water for three times. Sterilized materials were cut into 2 mm^2 and placed on potato dextrose agar (PDA) containing 50 µg/ml oxytetracycline, 50 µg/ml penicillin and 50 µg/ml streptomycin (Otero et al. 2002). Samples were incubated at 28 °C under natural light. Single spores were transferred to fresh PDA to obtain pure cultures. The pure cultures were deposited at China General Microbiological Culture Collection Center (CGMCC), International Collection of Microorganisms from Plants (ICMP) and Mae Fah Luang University Culture Collection (MFLUCC). The dry cultures of new species were deposited in Mae Fah Luang University herbarium (MFLC).

DNA extraction and amplification

DNA samples were prepared from mycelium of pure fungal culture using EZgene Fungal gDNA Kit (GD2416, Biomiga, USA) as described by the manufacturer. Amplification reactions were performed using reagents purchased from BIOMIGA (San Diego, USA). Each 20-µl amplification reaction contained 10 µl of 2*Bench Top Taq Master Mix (0.05 units/µl Taq DNA polymerase, 0.4 mM dNTPs and 4mM $MgCl_2$); 2 µl forward and reverse primers; 1µl of DNA template and 7 µl of water. The primers

Table 1. PCR thermal cycling process.

Region/gene	Initial denaturation	Cycle number	PCR amplification			
			Denaturation	Annealing	Elongation	Final elongation
ITS	95 °C 3 min	30	95 °C 1 min	53 °C 1 min	72 °C 1 min	72 °C 10 min
GAPDH	95 °C 3 min	35	95 °C 1 min	60 °C 30 s	72 °C 45 s	
ACT	95 °C 3 min	40	94 °C 45 s	52 °C 30 s	72 °C 90 s	
ß-tubulin	95 °C 3 min	35	94 °C 1 min	55 °C 55 s	72 °C 1 min	

used in this study were ITS1/ITS4 (White et al. 1990), GDF/GDR (Templeton et al. 1992), 512F/783R (Carbone and Kohn 1999) and BT2A/BT2B (Glass and Donaldson 1995; Maharachchikumbura et al. 2012). The thermal cycling programs are presented in Table 1. PCR products were sent to Invitrogen (USA), Sangon Biotech and Sino GenoMax (China) for purification and sequencing.

Sequence analysis

Either single-directional sequencing results (for ITS and GAPDH) or bi -directional sequencing results (for ACT and TUB2) were manually trimmed and/or assembled into contigs using CodonCode aligner software (CodonCode Corporation, Dedham, Massachusetts). Through the latest publications and the observation for ML tree topology, a selected set of ITS, GAPDH, ACT and TUB2 sequences especially those of ex-type/ex-epitype materials used in the phylogenetic analysis were downloaded from GenBank (Table 2). Five datasets of *Colletotrichum* spp. ITS (134nt), GAPDH (113nt), ACT (119nt), ß–tubulin (125nt) and a concatenated dataset were constructed. Sequences were aligned using MAFFT version 6 (Katoh and Toh 2008; mafft. cbrc. jp/ alignment/ server/). Aligned datasets were visually inspected and misaligned regions were manually edited where necessary using Bio-Edit version 7.2.5 (Hall 1999). Ambiguous regions were trimmed using trimAL version 1.3 (Capella–Gutierrez, Silla–Martinez and Gabaldon 2009) available online through Phylemon 2.0 (http://phylemon.bioinfo.cipf.es/). After trimming, the final alignments contained 578 sites for ITS, 298 sites for GAPDH, 290 sites for ACT and 480 sites for ß–tubulin. The concatenated dataset contained a total of 134 taxa and 1646 sites that were used for all subsequent analyses and submitted to TreeBase (http://purl.org/phylo/treebase/phylows/study/TB2:S22431). Gaps were treated as missing data in maximum likelihood (ML), Bayesian inference (BI) and parsimony trees. Parsimony trees were constructed with PAUP (Phylogenetic Analysis Using Parsimony) version 4.0 beta 10 (Swofford 2002). Heuristic searches were conducted as follows: 1000 starting trees were generated using stepwise addition and random addition sequence replicates, followed by branch swapping using the tree–bisection–reconnection (TBR) algorithm. The inferences for MP tree were length = 6732 steps, CI = 0.294, RI = 0.760, RC = 0.223, HI = 0.706. Maximum likelihood analyse

Table 2. *Colletotrichum* strains and species isolated from *Dendrobium* orchids.

Orchid sample	Sample site	Tissue	Number of fungal strains	*Colletotrichum* species	Code
D. cariniferum	Chiang Rai, Thailand	Root	0	0	–
		Stem	1	***C. cariniferi***	**MFLUCC 14-0100**
		Leaf	0	0	–
D. harveyanum	Chiang Rai, Thailand	Root	0	0	–
		Stem	0	0	–
		Leaf	2	*C. orchidophilum*	MFLUCC 14-0161 MFLUCC 14-0162
Dendrobium sp. 1	Chiang Rai, Thailand	Root	2	***C. parallelophorum***	**MFLUCC 14-0077** **MFLUCC 14-0079**
		Stem	3	***C.parallelophorum***	**MFLUCC 14-0082** **MFLUCC 14-0083** **MFLUCC 14-0085**
		Leaf	4	*C. boninense*, *C. jiangxiense*, *C. fructicola*	MFLUCC 14-0086 MFLUCC 14-0087 MFLUCC 14-0091 MFLUCC 14-0092
Dendrobium sp. 2	Chiang Rai, Thailand	Root	2	***C. chiangraiense***; *C. fructicola*	**MFLUCC 14-0119** MFLUCC 15-0262
		Stem	3	*C. boninense*, ***C. watphraense***, *C.* sp.indet.	MFLUCC 15-0120 **MFLUCC 15-0123** MFLUCC 15-0124
		Leaf	3	*C. citricola*, ***C. doitungense***	**MFLUCC 15-0128** MFLUCC 15-0129 MFLUCC 15-0131
Dendrobium sp. 3	Chiang Rai, Thailand	Root	0	0	–
		Stem	0	0	–
		Leaf	1	*C. boninense*	MFLUCC 15-0148
D. catenatum	Xing Yi, China	Root	0	0	–
		Stem	0	0	–
		Leaf	1	*C. boninense*	MFLUCC 15-0261

"–" means that no strain was isolated. The strains of new species are in **bold** font.

was conducted with RAxMLGui 1.31 (Silvestro and Michalak 2012). The general time reversible (GTR) model of nucleotide substitution was used and the inverse gamma distribution option was implemented. The topology of the resulting tree was similar to that of the maximum parsimony tree. Bootstrap support was calculated from 1000 replicates, which were subsequently mapped onto the best-scoring ML tree. Bayesian inference trees were computed using MrBayes version 3.1.2 (Ronquist and Huelsenbeck 2003). The concatenated dataset was partitioned and the ultrafast bootstrap (Minh et al. 2013) implemented in the IQ-TREE software (Nguyen et al. 2015) as well as Mrmodeltest 2.3 (Nylander 2004) were used to estimate the best fitting models according to the Bayesian information criterion (BIC). The GTR model with inverse gamma dis-

tribution and HKY model with gamma distribution were used as the most appropriate for the ITS and GAPDH respectively. The Hasegawa, Kishino & Yano (HKY) model with inverse gamma distribution and GTR model with gamma distribution were selected for the ACT and ß-tubulin datasets. Two sets of four simultaneous independent chains of Markov chains Monte Carlo (MCMC) simulations were run for 6,000,000 generations, 25% of trees were discarded as burn-in and the remaining trees were used to calculate the posterior probabilities. Convergence was assumed when the standard deviation of split sequences was less than 0.01. The fungal isolates and sequences of region/genes used in *Colletotrichum* phylogenetic analysis are listed in Appendix A.

Morphological analysis

Sporulation of studied fungi was induced on thin pieces of Corn malt agar medium (CMA). The strains that did not sporulate on CMA were cultured on PDA or Sabouraud dextrose agar (SDA) with sterilized orchid tissues in order to induce sporulation. An autoclaved toothpick was placed on CMA for one strain *C. cariniferi* to induce sporulation. Cultures were grown in a dark cabinet at room temperature (28 °C) and observed for every seven days or less. The growth rate was evaluated when mycelia nearly covered the whole medium surface. Once an acervuli or ascomata were observed, photos were taken with a stereomicroscope (SteREO Discovery. V8, Carl Zeiss Microscopy GmBH, Germany). Cross-sections and conidiomata crushed in water were observed under a compound microscope (EOS 600D, Nikon, Japan). Ascomata and conidiomata were observed under a Motic SMZ–140 microscope (China). Conidiophore, conidia, appressoria, ascomata, asci, ascospores and other visible structures such as chlamydospore were used for evaluating morphological characteristics in this study (Damm et al. 2014). The recommendations of Jeewon and Hyde (2016) were followed in establishing new species.

Results

Fungal isolation and Identification

Twenty-two endophytic *Colletotrichum* strains were isolated from six *Dendrobium* species (Table 2). The highest number of *Colletotrichum* strains and species were isolated from *Dendrobium* sp.1 followed by *Dendrobium* sp.2. All three tissue types of the two orchids hosted at least one strains of *Colletotrichum*. Among the three tissue types, the highest number of *Colletotrichum* strains and species were isolated from leaves. *Colletotrichum boninense* and *C. fructicola* were respectively the most frequently isolated *Colletotrichum* species. Interestingly, *C. boninense* was isolated from *Dendrobium* species collected from both geographical areas studied (i.e., Chiang Rai, Thailand and Guizhou, China).

Table 3. Synopsis of size (μm) of structures of Colletotrichum species identified in this study.

			Sexual morph				Asexual morph		
***Colletotrichum* species**	**N**	**Vegetative hyphae diam (μm)**	**Setae (μm)**	**Ascomata (μm)**	**Size of asci (μm)**	**Size of ascospores (μm)**	**Size of conidiomata (μm)**	**Size of conidiophore (μm)**	**Size of conidia (μm)**
C. cariniferi sp. nov.	1	3.5–8.2	–	–	–	–	50 ×50	(37.5–) 42.3–65 (–71.6) × (3.1–) 3.8–5.9 (–6)	(24.1–) 26.8–33.0 (–36.1) × (7.9–) 8.3–9.6 (–10.2), L/W=3.4
C. chiangraiense sp. nov.	1	4.6.± 1.8	–	(14.4–) 15.3–19.6 (–20.5) × (7.4–) 7.3–7.9 (–8)	(30.7–) 33.4–52.7 (–72.2) × (5.7–) 6.5–8.2 (–9.4)	(11–) 11.9–15.4 (–16.7) × (2.2–) 2.8–3.8 (–4.4), L/W=4.2	–	–	–
C. citricola	3	3.1 ± 1.1	(51.8–) 54.1–67.8 (–68.5) × (2.3–) 2.4–5.8 (–7.2)	(34.5–) 46.4–84.9 (–87.1) × (31.7–) 33.8–46.5 (–50.9)	(41.3–) 49.4–65.0 (–71.6) × (8.3–) 9.5–12.9 (–14.3)	(14.4–) 14.8–17.5 (–19.3) × (5.4–) 5.7–7.1 (–7.6), L/W = 2.5	–	(10.8–) 16.7–25.6 (–30.6) × (3.1–) 4–5.3 (–5.6)	(12.5–) 13.4–15 (16.5–) × (5–) 5.9–6.9 (–7.2), L/W = 2.2
C. doitungense sp.nov.	2	1.1–3.5	–	(125.5–) 126.9–133.7 (–135.1) × (101.3–) 101.8–104.3 (–104.8)	(51.1–) 53.7–70.6 (–71.6) × (8.5–) 8.8–10.1 (–10.4)	(16.1–) 17.5–21.5 (–23.4) × (4.5–) 5.1–7(–7.5), L/W=3.2	–	(9.1–) 14.3–26.8 (–29.4) × (3–) 3.1–4.5 (–5)	(6.6–) 8.6–13.8 (–15) × (2.6–) 3.8–8.9 (–13.8), L/W=1.75
C. fructicola	3	2.6–5	(53–) 57.2–73.1 (–83.3) × (3.4–) 3.5–4 (–4.1)	(131.9–) 138.4–163.6 (–171.5) × (120.9–) 123.6–142.1 (–143.2)	(57.6–) 61.2–82.6 (–94.3) × (8.7–) 9.3–13.3 (–15.8)	(10–) 12.0–20.0 (–20.9) × (3.6–) 4.1–5.2 (–5.3), L/W=3.4	500×400	–	(12.8–) 13.8–16.6 (–18.6) × (2.7–) 3.5–7.8 (–16), L/W=2.9
C. jiangxiense	2	1.3–2.1	–	–	–	–	–	(12.7–) 13.5–21.4 (–23.4) × (1.9–) 2–3 (–3.2)	(8.6–) 9–12.4 (–13.2) × (3.5–) 3.6–4.4 (–4.5), L/W=2.6
C. orchidophilum	2	1.9–5.4	–	–	–	–	200×300	–	(9.6–) 11.7–14.1 (–14.7) × (2.9–) 3.5–4.4 (–4.8), L/W=3.3
C. parallelophorum sp.nov.	2	2–4.3	(56.7–) 60.2–79.2 (–81.2) × (2.8–) 2.9–3.7 (–3.9)	(267–) 261.4–342.3 (–346.2) × (190.4–) 173–272.5 (–280)	(43.3–) 44.1–63.3 (–66.5) × (7.6–) 8–9.8 (–10)	(13.9–) 14.1–18 (–20.9) × (3.1–) 3.9–5.4 (–5.8), L/W=3.5	200×200	(18.3–) 20.82–34 (–41.2) × (2.6–) 2.8–4.3 (–5.4)	(12.1–) 13.8–16.8 (–18.9) × (3.3–) 4.4–7.5 (–7.9), L/W=2.6
C. watphraense sp. nov.	1	1.6–4.3	–	–	–	–	200×300	(15.8–) 18.5–26.8 (–29.1) × (3.4–) 3.8–5.1 (–5.7)	(12.4–) 12.5–14.6 (–15.2) × (4.4–) 4.5–5.8 (–6.1), L/W=2.3

*"N"means the number of cultures that were used in measuring the characteristics.

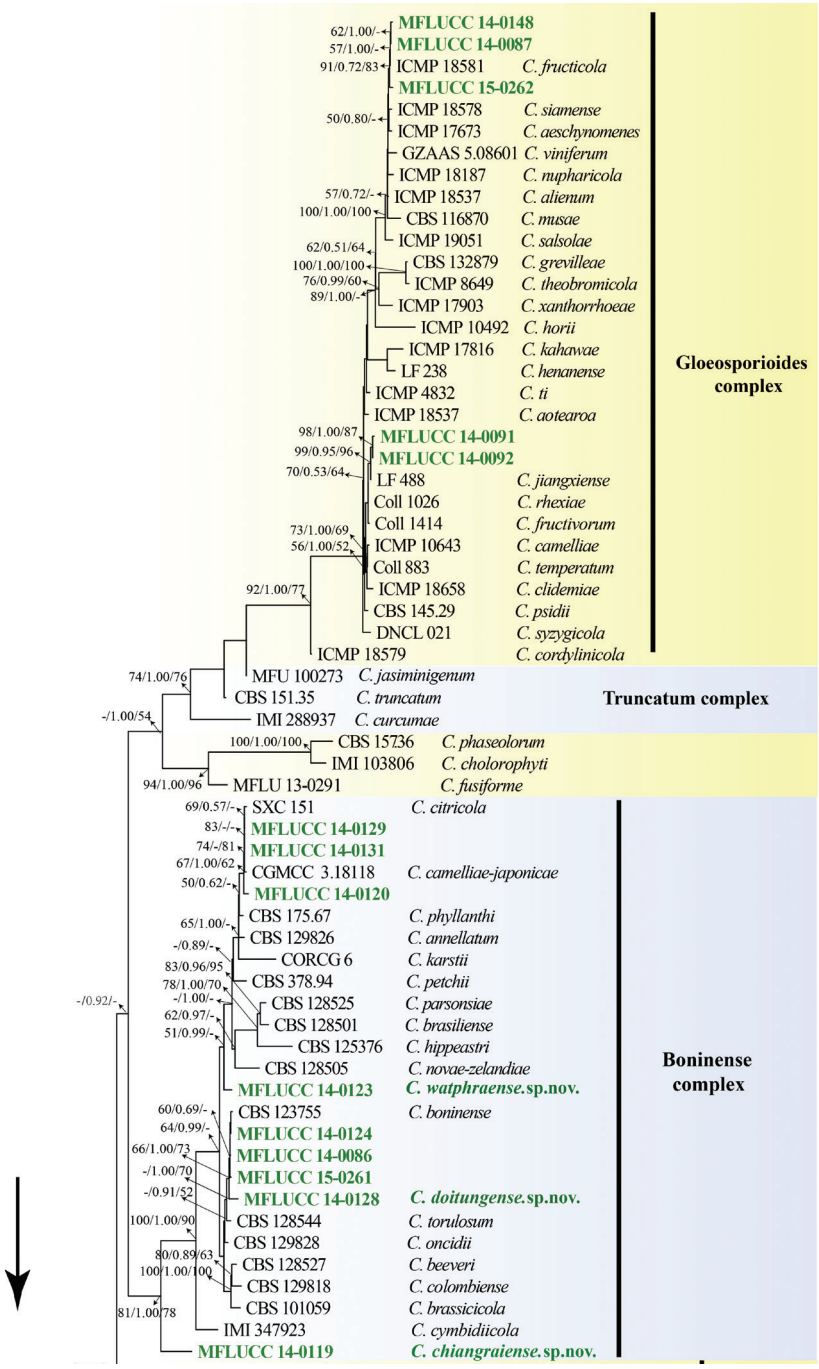

Figure 1. Maximum likelihood (ML) tree of *Colletotrichum* inferred from 134 taxa and 1646 sites from a concatenated dataset containing ITS, GAPDH, ACT and ß-tubulin sequence data. Values at nodes indicate bootstrap percentages (BP) for ML, Bayesian posterior probabilities (PP) and BP for maximum parsimony (MP) in this order. Only BP over 50%, PP over 0.50 and MP over 50 are shown. Dashes correspond to lower than the above-mentioned values. The isolated fungal endophytes in this study are shown in green **bold** text. Scale bar corresponds to 0.08 substitutions per site. "*" indicates the new species.

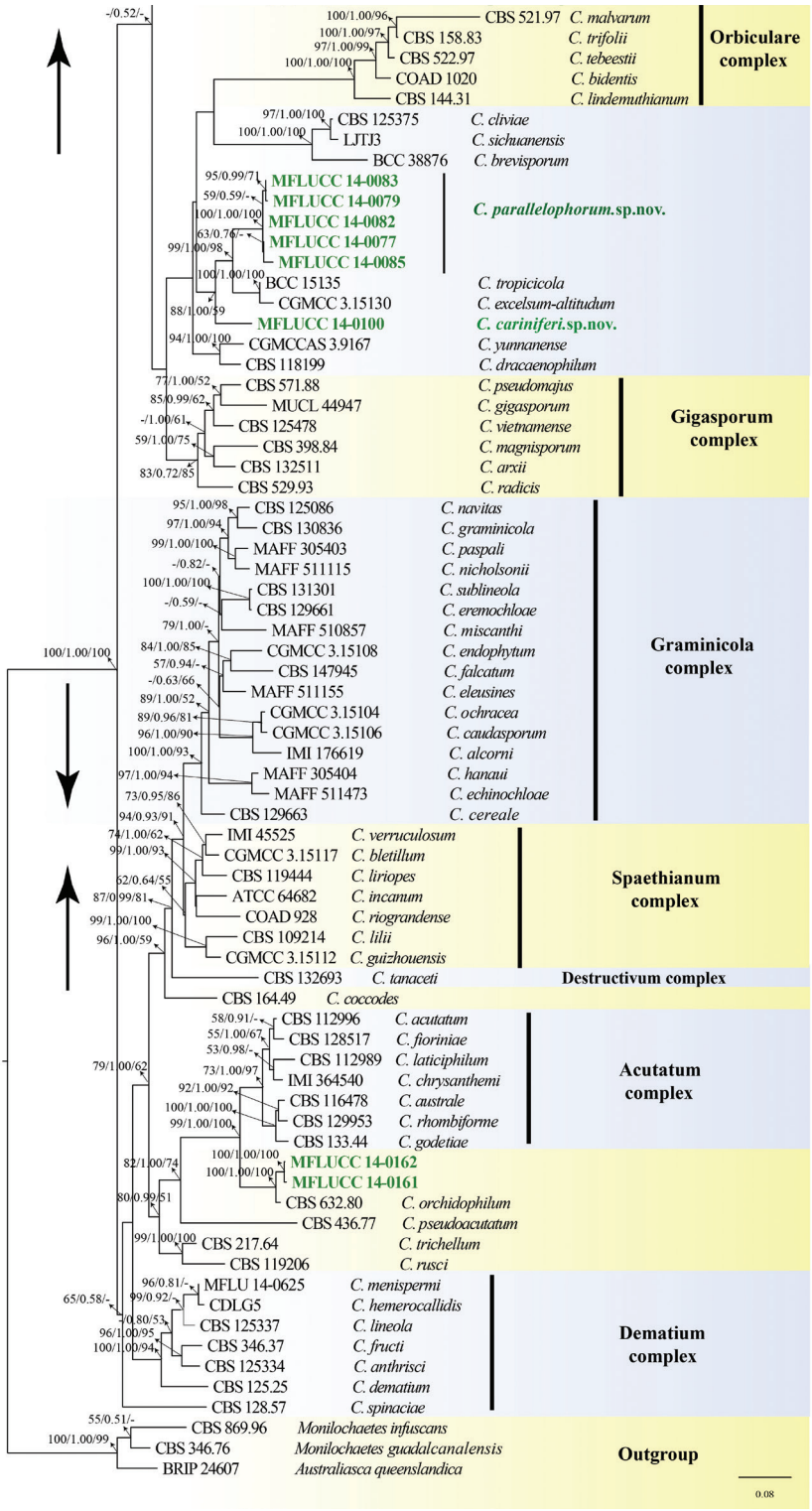

Figure 1. Continued.

Sporulation results

All *Colletotrichum* strains could grow on three kinds of media. *Colletotrichum citricola, C. doitungense*, *C. fructicola* and *C. parallelophorum* produced both sexual and asexual morphs in culture. *Colletotrichum boninense*, *C. cariniferi*, *C. orchidophilum* and *C. watphraense* produced only the asexual morph and *C. chiangraiense* produced only sexual morph in culture. Measurements of important vegetative and reproductive characteristics of isolated strains are given in Table 3.

Phylogenetic results

Phylogenetic analyses

All the sequences of ITS, GAPDH, ACT and β-tubulin of 22 strains of *Colletotrichum* obtained in this study were deposited in GenBank (List in Appendix B). The three selected outgroup species (i.e. *Australiasca queenslandica* BRIP 24607; *Monilochaetes infuscans* CBS 869.96 and *Monilochaetes guadalcanalensis* CBS 346.76) formed a strongly supported cluster (100ML/1.00BI/99MP). The ingroup consisted of all *Colletotrichum* sequences and was fully supported by all three methods of analysis (100ML/1.00BI/100MP). Five strains grouped within the gloeosporioides complex: MFLUCC 14-0087, MFLCCC 14-0091, MFLUCC 14-0092,

MFLUCC 14-0148 and MFLUCC 14-0262. The sequences of MFLCCC 14-0091 and MFLUCC 14-0092 were nearly identical and close to *C. jiangxiense* with strong support (99ML/0.95BI/96MP). MFLUCC 14-0087, MFLUCC 14-0148 and MFLUCC 15-0262 clustered with *C. fructicola* (ICMP 181873) (91ML/0.72BI/83MP).

Nine of the newly sequenced strains clustered within the boninense species complex: MFLUC 14-0086, MFLUCC 14-0119, MFLUCC 14-0120, MFLUCC 14-0123, MFLUCC 14-0124, MFLUCC 14-0128, MFLUCC 14-0129, MFLUCC 14-0131, MFLUCC 15-0261. MFLUCC 14-0086, MFLUCC 14-0124 and MFLUCC 14-0261 shared very similar sequences. MFLUCC 14-0128 grouped as sister to the three abovementioned strains (66ML/1.00BI/73MP). MFLUCC 14-0123 formed a separated clade from other species by only Bayesian analysis (1.00BI). MFLUCC 14-0120, MFLUCC 14-0129 and MFLUCC 14-0131 formed a cluster with *C. camelliae-japonicae* and *C. fructicola* (76ML/1.00BI/62MP). MFLUCC 14-0120 and MFLUCC 14-0129 differed by only three base pairs in trimmed concatenated alignment. MFULCC 14-0119 was placed basally to the boninense species complex with strong support (100ML/0.96BI/90MP).

MFLUCC 14-0161 and MFLUCC 14-0162 grouped outside the currently accepted species complexes. The two had a close relationship and formed a clade with *C. orchidophilum*, which is a singleton and a sister taxon to the acutatum species complex. They hold the maximum support with all three methods of analysis. *Colletotrichum orchidophilum* differed 1.5% and 1.3% with MFLUCC 14-0161 and MFLUCC 14-0162 respectively. MFLUCC 14-0077, MFLUCC 14-0079, MFLUCC 14-0082, MFLUCC

14–0083 and MFLUCC 14-0085 formed a novel clade (100ML/1.00BI/100MP), which grouped as sister clade to the *C. excelsum-altitudum*/*C. tropicicola* clade and MFLUCC 14-0100 (88ML/1.00BI/59MP). MFLUCC 14-0100 took a solo branch in the basal position among them (99ML/1.0BI/98MP).

Taxonomy

The 22 strains isolated as endophytes were assigned to eleven species, five known species, five new species and one undetermined species. We obtained the sexual and asexual morphs for four strains. The sexual morph only was obtained in the case of *C. chiangraiense.* The descriptions of the fungal endophytes identified in this study are as follows.

***Colletotrichum cariniferi* X.Y. Ma, K.D. Hyde & Jayawardena, sp.nov.**
Fungal Name Number: FN570511

Etymology. In reference to the host epithet cariniferum.

Holotype. MFLC 17-1199 (ex-holotype culture: MFLUCC 14-0100).

Description. *Sexual morph* not observed.

Asexual morph on CMA. Vegetative hyphae 3.5–8.2 µm diam (N=20), hyaline to brown, smooth-walled, septate, branched. Appressoria (9.7–) 10.4–17 (–20.5) × (6.5–) 7.1–11.3 (–13.6) µm (N=6), globose to sub-globose, light brown. Conidiomata 50 × 50 µm (N=10), developing with mycelia, globose to irregular, milk orange to orange, in mass brown. Conidiophores (37.5–) 42.3–65 (–71.6) × (3.1–) 3.8–5.9 (–6) µm (N=6), smooth-walled, unbranched, hyaline. The part connected with conidia of conidiogenous cell inflated and some with large guttules. Conidia (24.1–) 26.8–33.0 (–36.1) × (7.9–) 8.3–9.6 (–10.2) µm (N=30), L/W = 3.4, ellipsoidal to cylindrical, with one end inflated when immature state, both ends rounded when mature, with 2 to 3 guttules, hyaline.

Cultures on CMA flat with entire margin. Growth rate: 0.23cm/day, with 50-days for sporulation. Cottony, pale cinnamon to light brown, scattered pale mycelia in spots around the middle inoculum clump, sometimes covered short, floccose-felty, white, aerial mycelium, reverse buff brown.

Material examined. Thailand, Chiang Rai, Wat Phra That Doi Tung (Temple of Doi Tung Pagodas), the host *Dendrobium cariniferum* was sampled on 19 December 2013, Collector: Sureeporn Nontachaiyapoom, Natdanai Aewsakul, Xiaoya Ma.

Notes. *Colletotrichum cariniferi* (MFLUCC 14-0100) clusters in a separate branch with a good support (88ML/1.00BI/59MP). The species is most phylogenetically close to *Colletotrichum excelsum-altitudum* and *C. tropicicola,* but they are morphologically different. *C. cariniferi* holds 77 and 91 different base pairs compared with *C. tropicicola* and *C. excelsum-altitudum* respectively. *Colletotrichum cariniferi* has much larger conidia than that of closely related strains in the tree (conidia (24.1–) 26.8–33 (–36.1) × (7.9–) 8.3–9.6 (–10.2) µm (N=30), L/W = 3.4 vs. conidia of *C. tropicicola* 13–16.5×5–7 µm and *C.*

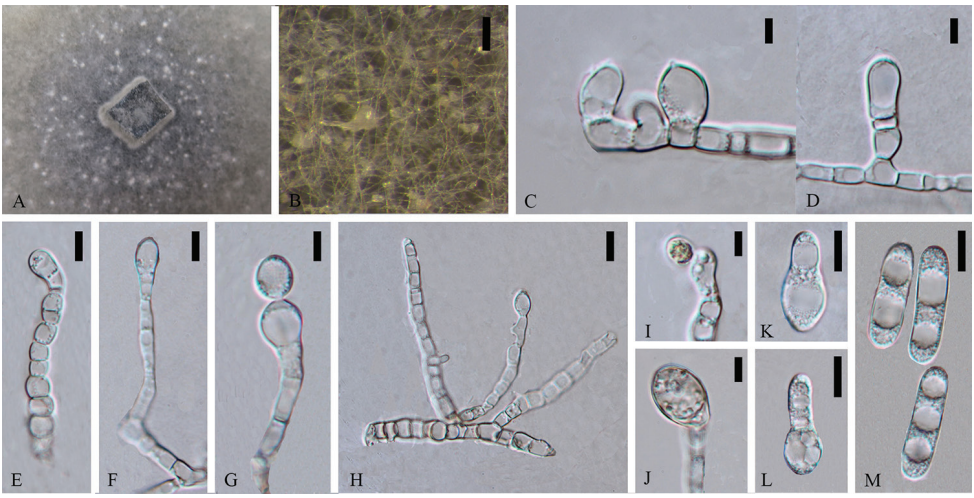

Figure 2. *Colletotrichum cariniferi* (holotype). **A** Colony **B** Conidiomata **C, I–J** Appressoria **D–H** Conidiophores **K–M** Conidia. Scale bars: 100 μm (**B**), 5 μm (**C–D**), 10 μm (**E–H**), 5 μm (**I–M**).

excelsum-altitudum 14.8 ± 0.8 × 5.8 ± 0.4 μm) (Noireung 2012; Tao et al. 2013). Blastn searches with sequence of MFLUCC 14-0100 resulted in 100% matches with ITS sequence of endophytic *Colletotrichum* sp. strain S4 isolated from *Dendrobuim nobile* in China (GenBank FJ042517, Yuan et al. 2009) and 96% identity with TUB2 sequences of *C. arxii* strain CBS 169.59 isolated from *Oncidium excavatum* (GenBank KF687868, Liu et al. 2014) in Netherlands and another *C. arxii* strain CBS 132511 isolated from *Paphlopedilum* sp. in Germany (GenBank KF687881, Liu et al. 2014) respectively. *Colletotrichum cariniferi* from stems of *D. cariniferum* is introduced as a new species.

Colletotrichum chiangraiense **X.Y. Ma, K.D. Hyde & Jayawardena, sp.nov.**
Fungal Name Number: FN570512
Figure 3

Etymology. In reference to the host sample site Chiang Rai, Thailand.

Holotype. MFLU 17-1201 (ex-holotype culture: MFLUCC 14-0119).

Description. *Asexual morph* not observed.

Sexual morph on CMA. Vegetative hyphae 4.6.± 1.8 μm diam (N=20), hyaline to pale brown, smooth-walled, septate, branched. Chlamydospore globose, brown. Hyphae fusion and crozier observed. Ascomata rare, covered by mycelia, black. Appressoria (14.4–) 15.3–19.6 (–20.5) × (7.4–) 7.3–7.9 (–8) μm (N=2), single, outline ampulliform or ovate, pale brown. Asci (30.7–) 33.4–52.7 (–72.18) × (5.7–) 6.5–8.2 (–9.4) μm (N=15), cylindrical, straight to curved, unitunicate, 8–spored. Ascospores (11–) 11.9–15.4 (–16.7) × (2.2–) 2.8–3.8 (–4.4) μm (N=20), L/W = 4.2, bi-seriately, smooth-walled, cylindrical or fusiform, one guttule in the middle, hyaline.

Cultures on CMA flat with entire margin. Growth rate: 0.6cm/day, with 20-days for sporulation. Fluffy, dark green in the middle and white margin, reverse black in the middle.

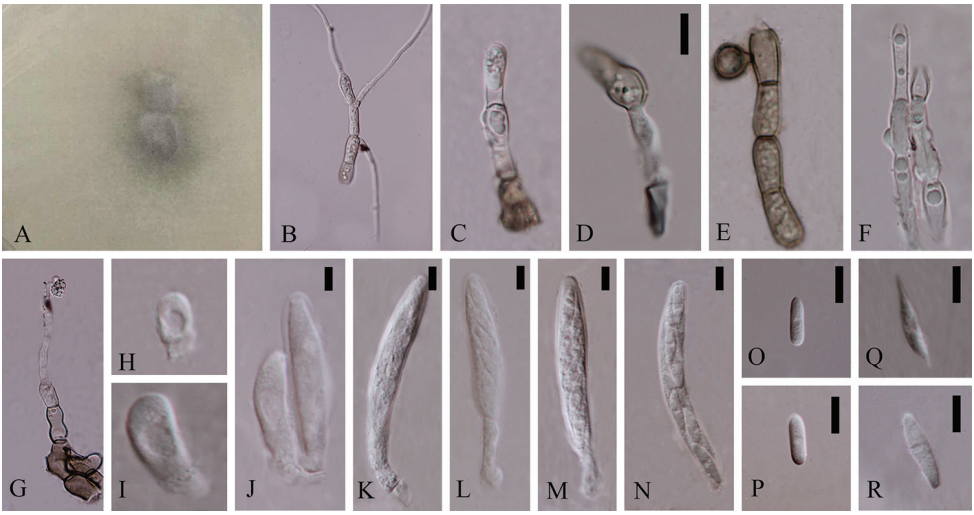

Figure 3. *Colletotrichum chiangraiense* (holotype). **A** Colony **B** Spore germination **C** Conidiophore **D** Appressoria **E** Chlamydospore **F** Mycelia fusion **G** Crozier **H–N** Asci **O–R** Ascospores. Scale bars: 20 μm (**D**), 20 μm (**G**), 5 μm (**J–N**), 10 μm (**O–R**).

Material examined. Thailand, Chiang Rai, Wat Phra That Doi Tung (Temple of Doi Tung Pagodas), the host *Dendrobium* sp.2 was collected on 19 December 2013, Collector: Sureeporn Nontachaiyapoom, Natdanai Aewsakul, Xiaoya Ma.

Notes. *Colletotrichum chiangraiense* (MFLUCC 14-0119) formed a single branch with the support of 81ML/1.00BI/78MP in boninense species complex. It has 125 different base pairs (mainly in ITS and ACT) from the closest strain *C. cymbidiicola.* Blastn searches with sequences of MFLUCC 14-0119 resulted in 99% identity with ITS of the endophytic *C. crassipes* strain DO93 (GenBank KP050648) isolated from *Dendrobium officinale* in China (Unpublished), 99% identity with ACT of the endophytic *Colletotrichum* sp. strain COAD 2105 (GenBank KY407893) isolated from *Cattleya jongheana* in Brazil (Unpublished), 98% identity with TUB2 of the endophytic *C. boninense* strain CBS 125502 (GenBank KJ955336) isolated from *Camellia sinensis* in China (Liu et al. 2015) and 98% identity with TUB2 of the endophytic *C. boninense* strain CGMCC 3.15165 (GenBank KC244156) isolated from *Bletilla ochracea* in China (Tao et al. 2013). This species was observed antheridium, mycelia fusion and crozier, which indicates that this species may be homothallic. Here we introduce the strain isolated from root of *Dendrobium* sp.2 as a new species.

Colletotrichum watphraense **X.Y. Ma, K.D. Hyde & Jayawardena, sp. nov.**
Fungal Name Number: FN570513
Figure 4

Etymology. In reference to the host sample site – Wat Phra temple in Chiang Rai, Thailand.

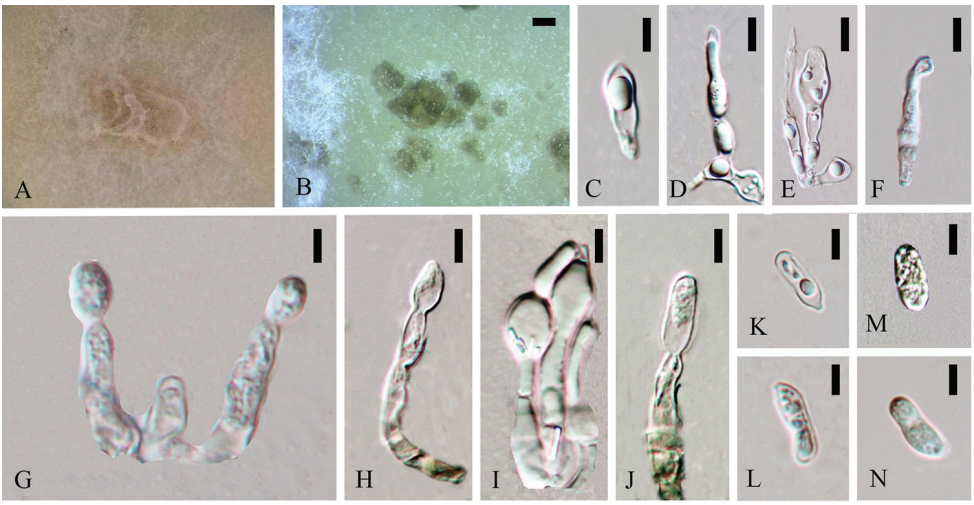

Figure 4. *Colletotrichum watphraense* (holotype). **A** Colony **B** Fruiting body **C–J** Conidiophores **K–N** Conidia. Scale bars: 200 μm (**B**), 5 μm (**C–N**).

Holotype. MFLU 17-1202 (ex-holotype culture: MFLUCC 14-0123).

Description. *Sexual morph* not observed.

Asexual morph on CMA. Vegetative hyphae 1.6–4.3 μm diam (N=20), smooth-walled, septate, branched, hyaline. Chlamydospores and appressoria not observed. Conidiomata 200 × 300 μm, brown, Conidiophores (15.8–) 18.5–26.8 (–29.1) × (3.4–) 3.8–5.1 (–5.7) μm (N=16), smooth-walled, septate, branched or single, periclinal thickening, hyaline. Conidia (12.4–) 12.5–14.6 (–15.2) × (4.4–) 4.5–5.8 (–6.1) μm (N=5), L/W = 2.3, aseptate, ellipsoidal, single guttules in the middle, the one part inflated, hyaline.

Cultures on CMA flat with entire margin. Growth rate: 0.45cm/day, with 30-days for sporulation. Fluffy, white to light buff orange. Perithecia isolated. Acervuli under white cotton-like mycelia, irregular, asymmetrical surface, light brown to brown.

Material examined. Thailand, Chiang Rai, Wat Phra That Doi Tung (Temple of Doi Tung Pagodas), the host *Dendrobium* sp.2 was collected on 19 December 2013, Collector: Sureeporn Nontachaiyapoom, Natdanai Aewsakul, Xiaoya Ma.

Note. MFLUCC 14-0123 formed a singular branch with other species and only supported by 1.00BI in boninense species complex. There were 42bp (2.6%) and 85bp (5.2%) differences in GAPDH between *Colletotrichum watphraense* and its close strains *Colletotrichum boninense*/*C. novae-zelandiae* respectively. The closest matches in a blastn search with ITS sequences of the strain MFLUCC 14-0123 are *C. cymbidiicola* strain FS21 (GenBank KP689224) iaolated from a rare medical plant *Huperzia serrata* with 99% identity in China (Wang et al. 2016), *C. gloeosporioides* strain Trtsf02 (GenBank GU479899) isolated from *Trillum tschonoskii* with 99% identity in China (Unpublished) and pathogenic *C. boninense* strain CO5016 (GenBank GU935883) isolated from ginseng with 99% identity in Korea (Unpublished). GAPDH and ACT sequences blastn results showed its closest matches are pathogenic *C. citricola* strain

SXC 151 (GenBank KC293736) isolated from Proteaceae with 99% identity in Netherlands (Liu et al. 2012) and *C. boninense* strain CBS 125502 (GenBank KJ954462) isolated from *Camellia* sp. with 99% identity in unknown locality (Liu et al. 2015). Blastn search with TUB2 sequence results in 99% identity with two *C. boninense* strains CBS 125502 (GenBank KJ955336) and the strain CGMCC 3.15165 (GenBank KC244156) as mentioned above. The conidiophores were much longer (40 µm long) in *C. boninense*. Conidia of the strain CBS 123755 have straight, cylindrical to clavate, conidia with a rounded apex; and base with a prominent hilum, sometimes with two large polar guttules, which is different from *Colletotrichum watphraense*. Here we assigned the strain isolated from stem of *Dendrobium* sp.2 as a new species.

Colletotrichum doitungense **X.Y. Ma, K.D. Hyde & Jayawardena, sp.nov.**
Fungal Name Number: FN570514
Figure 5

Etymology. In reference to the host sample site Doi tung, Chiang Rai, Thailand.

Holotype. MFLU 17-1200 (ex-holotype culture: MFLUCC 14-0128).

Description. Asexual morph on CMA. Vegetative hyphae 1.1–3.5 µm diam, hyaline, smooth-walled, septate, branched. Setae and chlamydospores not observed. Conidiomata and ascomata cluster together. Conidiophores (9.1–) 14.3–26.8 (–29.4) × (3–) 3.1–4.5 (–5) µm, smooth-walled, unbranched, septate, constricted septum, hyaline. Conidiogenous cell (3.1–) 3.2–5.8 (–7.5) × (2.6–) 3–4 (–4.5) µm (N=14), globose to sub-globose, smooth-walled, hyaline. Conidia (6.6–) 8.6–13.8 (–15) × (2.6–) 3.8–8.9 (–13.8) µm (N=22), L/W = 1.75, globose to ellipsoidal, both ends rounded, smooth-walled, hyaline.

Sexual morph on CMA. Ascomata (125.5–) 126.9–133.7 (–135.1) × (101.3–) 101.8–104.3 (–104.8) µm (N=10), sub-globose, closed, pale brown to brown. Peridium 3–11.5 µm thick, Asci (51.1–) 53.7–70.6 (–71.6) × (8.5–) 8.8–10.1 (–10.4) µm (N=8), cylindrical, slight curved, composed of pale to medium brown flattened angular cells, unitunicate, smooth-walled, 8–spored, hyaline. Ascospores (16.1–) 17.5–21.5 (–23.4) × (4.5–) 5.1–7.0 (–7.5) µm (N=20), L/W = 3.2, fusiform, blunt to somewhat acute or acute both ends, single guttule in the middle, septate, bi-seriately, smooth-walled, hyaline.

Cultures on CMA flat with entire margin. Fluffy, white, reverse same. Growth rate: 0.6cm/day, with 20-days for sporulation. Brown ring in the middle. Perithecia gregarious. Acervuli and ascomata in mass light brown to brown.

Material examined. Thailand, Chiang Rai, Wat Phra That Doi Tung (Temple of Doi Tung Pagodas), the host *Dendrobium* sp.2 was collected on 19 December 2013, Collector: Sureeporn Nontachaiyapoom, Natdanai Aewsakul, Xiaoya Ma.

Notes. *Colletotrichum doitungense* form an independent lineage from other strains with good support (66ML/1.00BI/73MP) in boninense species complex. The ITS sequence of MFLUCC 14-0128 100% matches with unpublished pathogenic *C. cymbidiicola* strain OORC18 (GenBank JX902424) isolated from orchid in India and *C. karstii*

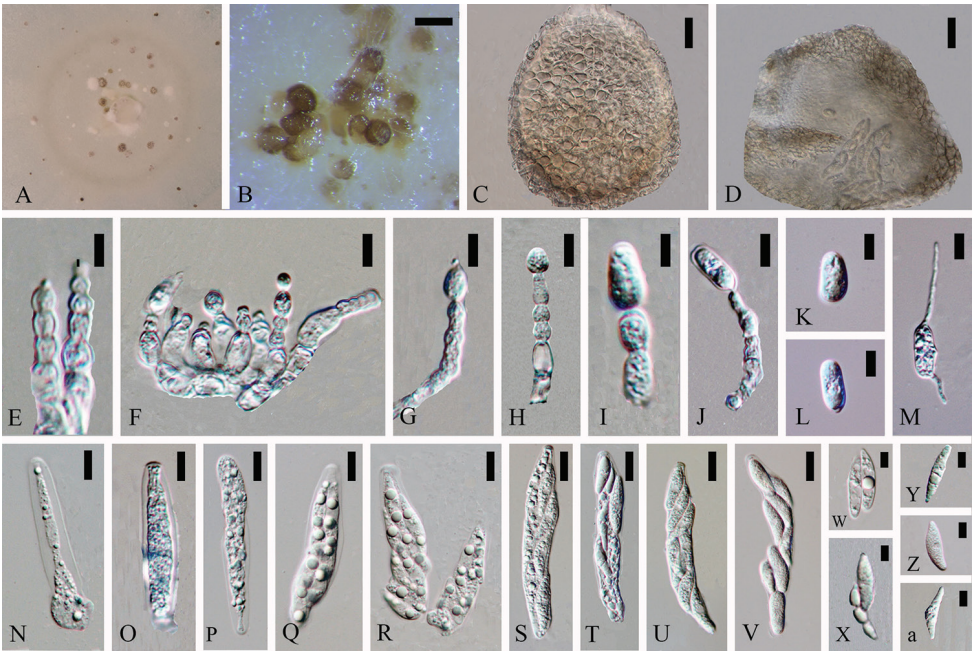

Figure 5. *Colletotrichum doitungense* (holotype). **A** Colony **B** Fruiting body **C–D** Ascomata **E–J** Conidiophores **K–L** Conidia **M** Spore germination **N–V** Asci **W–a** Ascospores. Scale bars: 100 μm (**B**), 20 μm (**C–D**), 5 μm (**E–M**), 10 μm (**N–V**), 5 μm (**W–a**).

strain R001 (GenBank JN715846) isolated from blackberry in Colombia (Unpublished). Blastn researches with sequences of MFLUCC 14-0128 results in 98% identity with GAPDH sequence of endophytic *C.boninense* strain CGMCC 3.15168 (GenBank KC843491) isolated from *Bletilla ochracea* in China (Tao et al. 2013), 99% identity with ACT sequence of *C. boninense* strain CBS 125502 (GenBank KJ954462) and 99% identity with TUB2 sequence of *C. citricola* strain SXC 151 (GenBank KC293656) as mentioned above. Its conidiogenus cell is globose to sub-globose, which differ from cylindrical to ellipsoidal conidiogenus cell in *C. boninense* (Damm et al. 2012). This strain has 2 and 0 in ITS, 6 and 1 in GAPDH, 3 and 2 in ACT, 17 and 16 base pair differences from its sister taxon *C. torulosum* and MFLUCC 14-0261 respectively. Here we introduce *Colletotrichum doitungense* isolated from root of *Dendrobium* sp.2 as a new species.

Colletotrichum parallelophorum **X.Y. Ma, K.D. Hyde & Jayawardena, sp. nov.**
Fungal Name Number: FN570515
Figure 6

Etymology. In reference to the parallel conidiophores.

Holotype. MFLU 17-1198 (ex-holotype culture: MFLUCC 14-0083).

Description. Asexual morph on CMA. Vegetative hyphae 2–4.3 μm diam (N=30), smooth-walled, septate, branched, hyaline to pale brown. Chlamydospores not ob-

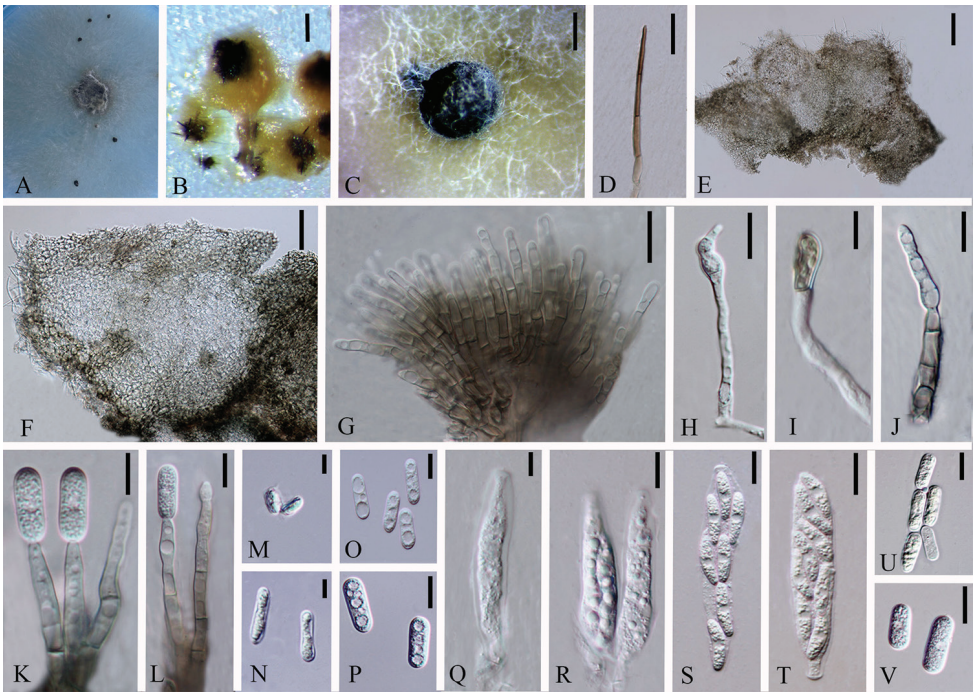

Figure 6. *Colletotrichum parallelophorum* (holotype). **A** Colony **B, C** Fruiting body **D** Setae **E–F** Ascomata **G, J–L** Conidiophores **I** Appressoria **M–P** Conidia **Q–T** Asci **U–V** Ascospore. Scale bars: 50 μm (**B**), 500 μm (**C**), 20 μm (**D**), 100 μm (**E**), 50 μm (**F**), 20 μm (**G**), 10 μm (**H–L**), 5 μm (**M, N**), 10 μm (**O–V**).

served. Conidiomata acervular, orange. Appressoria (56.7–) 60.2–79.2 (–81.2) × (2.8–) 2.9–3.7 (–3.9) μm (N=8), single, sub-globose, brown, rare. Conidiophores and setae formed on a cushion of pale brown cells (1.9–) 2.4–4 (–4.6) μm diam. Setae medium brown, smooth-walled, 2 or 3-septate; base cylindrical, constricted at the base, apex acute. Conidiophores (18.3–) 20.8–34 (–41.2) × (2.6–) 2.8–4.3 (–5.4) μm (N=20), smooth-walled, 2 to 3-septate, branched, hyaline to pale brown. Conidiophores and setae formed on a cushion of pale brown prismatic cells, sometimes with guttules. Conidia (12.1–) 13.8–16.8 (–18.9) × (3.3–) 4.4–7.5 (–7.9) μm (N=50), L/W = 2.6, hyaline, smooth-walled, with 1 to 4 guttules, cylindrical with both ends rounded.

Sexual morph on CMA. Ascomata (267–) 261.4–342.3 (–346.2) × (190.4–) 173.0–272.5 (–280) μm (N=3), globose, glabrous, Ascomata isolated, scattered, irregular and asymmetrical, black. Peridium 13.6–46.4 μm thick, consist of pale to medium brown flattened angular cells. Ascogenous hyphae hyaline, smooth-walled. Asci (43.3–) 44.1–63.3 (–66.5) × (7.6–) 8.0–9.8 (–10) μm (N=7), cylindrical, straight, unitunicate, 8–spored. Ascospores (13.9–) 14.1–18 (–20.9) × (3.1–) 3.9–5.4 (–5.8) μm (N=23), L/W = 3.5, uni-to bi-seriately, aseptate, smooth-walled, ellipsoidal, single guttules in the middle, both ends rounded, hyaline.

Cultures on CMA flat with entire margin. Growth rate: 0.4cm/d, with 20-days for sporulation. With fluffy, light green and white mycelia. Ascomata sometimes growing together with acervuli.

Material examined. Thailand, Chiang Rai, Wat Phra That Doi Tung (Temple of Doi Tung Pagodas), the host *Dendrobium* sp.1 was collected on 19 December 2013, Collector: Sureeporn Nontachaiyapoom, Natdanai Aewsakul, Xiaoya Ma.

Notes. Strains MFLUCC 14-0077, MFLUCC 14-0079 and MFLUCC 14-0083 had identical sequence data and they formed a single clade with MFLUCC 14-0082 and MFLUCC 14-0085. They are closely related to *Colletotrichum excelsum-altitudum* and *C. tropicicola*. MFLUCC 14-0077, MFLUCC 14-0079, MFLUCC 14-0082, MFLUCC 14-0083 and MFLUCC 14-0085 have similar morphological characteristics. Therefore, the five strains are regarded as the same species. There were totally 103bp and 101bp differences between MFLUCC 14-0083 and *C. excelsum-altitudum*/*C. tropicicola* respectively (mainly in GAPDH). Blastn researches with four-gene sequences of five strains presented 99% identity with ITS sequence of *C. cordylinicola* strain LC0886, 80% identity with GAPDH (GenBank JN050229), 90% identity with ACT (GenBank JN050218) and 93% identity with TUB2 (GenBank JN050246) sequences of *C. tropicola* strain LC0598 respectively as mentioned above. Conidia size and shape were very similar among MFLUCC 14-0083, *C. excelsum-altitudum* and *C. tropicicola*. Appressoria were rare and in strain MFLUCC–14–0083 appressoria were not variable like that in *C. excelsum-altitudum* and *C. tropicicola*. Here we introduced strains MFLUCC 14-0077, MFLUCC 14-0079, MFLUCC 14-0082 and MFLUCC 14-0083 and MFLUCC–14–0085 isolated from stems and roots of *Dendrobium* sp.1 as *Colletotrichum parallelophorum* sp.nov.

Colletotrichum citricola F. Huang, L. Cai, K.D. Hyde & H.Y. Li

Figure 7

Description. Asexual morph on CMA. Vegetative hyphae 3.1 ± 1.1 µm diam (N=20), smooth-walled, septate, branched, hyaline. Chlamydospores globose, hyaline. Conidiomata ovoid, orange. Setae (51.8–) 54.1–67.8 (–68.5) × (2.3–) 2.4–5.8 (–7.2) µm (N=6), smooth-walled, 1 or 3–septate, contracted to slightly inflated base, tapering to the apex, apex acute, pale brown to brown. Conidiophores (10.8–) 16.7–25.6 (–30.6) × (3.1–) 4–5.3 (–5.6) µm (N=27), smooth-walled, septate, hyaline. Conidia (12.5–) 13.4–15 (16.5–) × (5–) 5.9–6.9 (–7.2) µm (N=40), L/W = 2.2, ellipsoidal, smooth-walled, hyaline.

Sexual morph on CMA. Ascomata (34.5–) 46.4–84.9 (–87.1) × (31.7–) 33.8–46.5 (–50.9) µm (N=5), globose, ostiolate, clustered, pale brown to dark brown. Peridium 1.7–5.8 µm thick, composed of pale to medium brown, flattened, angular cells. Ascogenous hyphae hyaline, smooth-walled. Asci (41.3–) 49.4–65 (–71.6) × (8.3–) 9.5–12.9 (–14.3) µm (N=36), cylindrical, unitunicate, straight or curved, 8–spored. Ascospores (14.4–) 14.8–17.5 (–19.3) × (5.4–) 5.7–7.1 (–7.6) µm (N=25), L/W = 2.5, uni-or bi-seriately, smooth-walled, hyaline, fusiform or one end slightly rounded, with a single guttule in the middle.

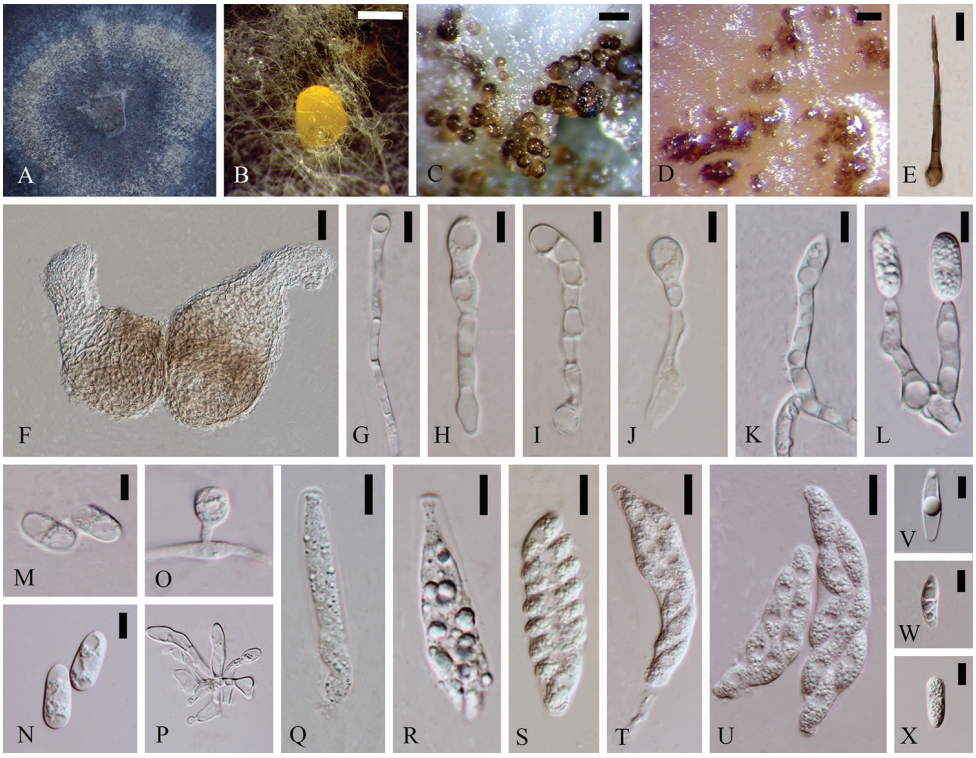

Figure 7. *Colletotrichum citricola*. **A** Colony **B** Conidiomata **C** Fruiting bodies **D** Fruiting body with setae **E** Setae **F** Ascomata **G–L** Conidiophores **M, N** Conidia **O** Chlamydospore **P–U** Young asci **V–X** Ascospores. Scale bars: 500 μm (**B**), 200 μm (**C**), 10 μm (**E–F**), 5 μm (**G**), 5 μm (**M–N**), 10 μm (**Q–U**), 5 μm (**V–X**).

Cultures on CMA flat with entire margin. Growth rate: 0.6cm/day, with18-days for sporulation. Fluffy, pale mycelia float on the dark scarlet pigment medium, reverse dark brown. Perithecia gregarious. Orange acervuli and ascomata in mass form thick globules.

Notes. Strains MFLUCC 14-0129 and MFLUCC 14-0131 had similar sequence data, cultures and conidia. There were 5bp and 7bp difference between the strains and *Colletotrichum camelliae-japonicae* and *C. citricola* respectively. ITS sequence is 99% identity with unpublished *C. boninense* strain LD3–8–1 isolated from strawberry in China (Unpublished). Blastn searches sequences results in GAPDH (GenBank KC293736) and TUB2 (GenBank KC293656) sequences of *C. citricola* strain SXC 151 as mention above. ACT sequence is closest to *C. karstii* strain 42a (GenBank KT122921) isolated from *Coffea arabica* in Mexico (Cristobal-Martinez et al. 2016). All morphological characteristics of the two strains were nearly the same as the protologue of *C. citricola.* Therefore, we name strains MFLUCC 14-0129 and MFLUCC 14-0131 as *C. citricola*. When compared with *C. camelliae-japonicae* (conidia: 11–14.5 ×5–6.5μm, mean ±SD = 12.5 ±0.8 ×5.5 ±0.3μm, L/W=1.5; ascospores: 13.5–18.5 ×4–5.5 μm, mean ± SD = 16.5 ±1.1×5±0.4μm, L/W = 3.3), strains MFLUCC 14-0129 and MFLUCC 14-0131 have shorter conidia and wider ascospores.

Colletotrichum fructicola **Prihastuti, L. Cai & K.D. Hyde**
Figure 8

Description. Asexual morph formed on CMA. Vegetative hyphae 2.6–5 µm diam (N=20), smooth-walled, septate, branched, hyaline. Appressoria and chlamydospores not observed. Conidiomata 500 × 400 µm (N=3), clustered, sub-globose, smooth-walled, orange. Conidiophores rare, septate, hyaline. Conidia (12.8–) 13.8–16.6 (–18.6) × (2.7–) 3.5–7.8 (–16) µm (N=21), L/W = 2.9, ellipsoidal, smooth-walled, septate, hyaline.

Sexual morph forming on CMA. Ascomata globose, pale brown to dark brown. Peridium (131.9–) 138.4–163.6 (–171.5) × (120.9–) 123.6–142.1 (–143.2) µm (N=4), composed of medium brown, flattened, angular cells. Setae (53–) 57.2–73.1 (–83.3) × (3.4–) 3.5–4(–4.1) µm (N=6), grow on the fruiting body, 2-septate, smooth-walled, contracted at the base, apex slightly rounded, brown to dark brown. Asci (57.6–) 61.2–82.6 (–94.3) × (8.7–) 9.3–13.3 (–15.8) µm (N=12), cylindrical, unitunicate, 8–spored. Ascospores (10–) 12–20 (–20.9) × (3.6–) 4.1–5.2 (–5.3) µm (N=10), L/W = 3.4, ellipsoidal to reniform, somewhat fusiform or acute both ends, 1 to 4 guttules, uni-to bi-seriate, smooth-walled, hyaline.

Cultures on CMA flat with slight serrated margin. Growth rate: 0.9cm/day, with 14-days for sporulation. Cottony, light brown to white from middle to the margin, reverse white to light brown with black spots. Ascomata gregarious and/or isolated. Acervuli and ascomata sometimes gregarious.

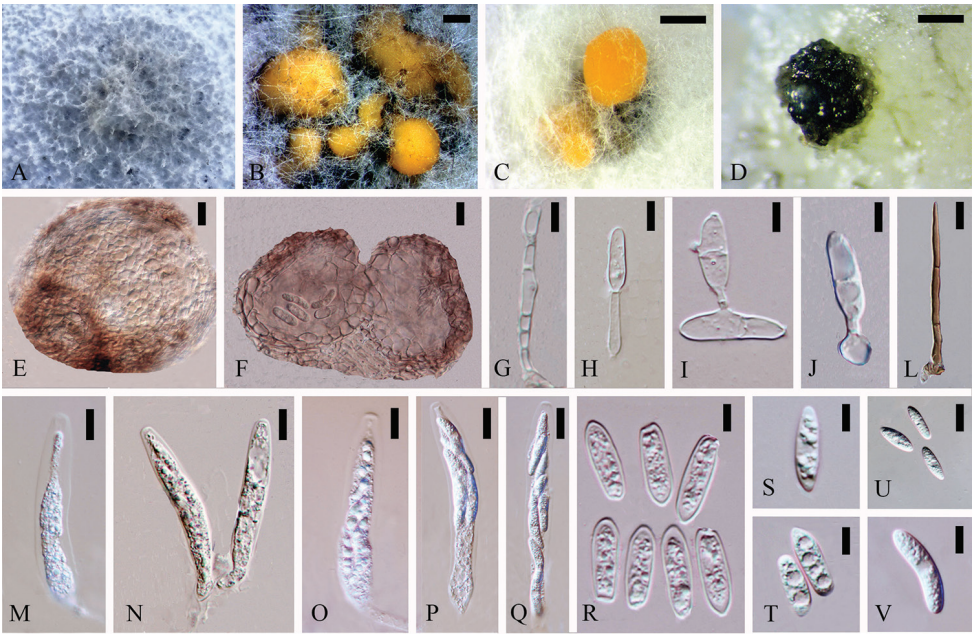

Figure 8. *Colletotrichum fructicola.* **A** Colony **B** Conidiomata and ascomata **C, D** Conidiomata **E, F** Ascomata **G–J** Conidiophores **L** Setae **M–Q** Asci **R–V** Ascospores Scale bars: 500 µm (**B–D**), 20 µm (**E, F**), 5 µm (**G–J**), 10 µm (**L**), 10 µm (**M–Q**), 5 µm (**R–V**).

Notes. Strains MFLUCC 14-0087, MFLUCC 14-0148 and MFLUCC 15-0262 had the identical sequences to *Colletotrichum fructicola*. The ITS and GAPDH sequences of them 100% match with many different unpublished species. Blastn researches with ACT sequence of them results in 99% identity with the ex-holotype culture of *C. fructicola* strain ICMP 18581 (GenBank JX009501) isolated from *Coffea arabica* in Thailand (Weir et al. 2012), which we involved it in phylogenetic analysis. TUB2 sequences of them are 99% identity with *C. boninense* strain CBS 125502 (GenBank KJ955336) as mentioned above. Their ascomata, conidia, asci and ascospores were also similar. Conidia were the same size as the ex-type strain of the pathogen *Colletotrichum fructicola* (9.7–14 × 3–4.3μm) found in coffee berries (Prihastuti et al. 2009). However, ascomata were much smaller and asci as well as ascospores were much larger than the ex-type from coffee berries. In the protologue, *C. fructicola* was introduced with ascomata as 345.67 ± 36.83 × 431.33 ± 69.89 μm, asci as 41.22 ± 7.02 × 7.61 ± 0.58 μm and ascospores as 11.91 ± 1.38 × 3.32 ± 0.35 μm. Here we name strains MFLUCC 14-0087, MFLUCC 14-0148 and MFLUCC 15-0262 isolated from leaves of *Dendrobium* sp.1 and *Dendrobium* sp.3, root of *Dendrobium* sp.2 as *Colletotrichum fructicola*.

Colletotrichum jiangxiense **F. Liu & L. Cai**
Figure 9

Description. *Sexual morph* not observed.

Sexual morph not observed. Asexual morph on PDA. Vegetative hyphae 1.3–2.1 μm diam (N=20), smooth-walled, septate, branched, hyaline. Setae and chlamydospores not observed. Conidiophores (12.7–) 13.5–21.4 (–23.4) × (1.9–) 2–3 (–3.2) μm (N=8), branched, hyaline. Conidia (8.6–) 9–12.4 (–13.2) × (3.5–) 3.6–4.4 (–4.5) μm (N=4), L/W = 2.6, ellipsoidal to cylindrical, smooth-walled, aseptate, one end more blunt than the other end, hyaline.

Cultures on PDA flat with entire margin. Growth rate: 0.4cm/day, with 18-days for sporulation. Aerial mycelia dense, cottony, pale to light brown, with brown outline ring close to the edge, mycelia in the middle dark brown, reverse white to light brown.

Notes. Strains MFLUCC 14-0091 and MFLUCC 14-0092 were the same species as they grouped with high support (98ML/1.0BI/87MP). They formed a very close clade with the pathogen *C. jiangxiense* isolated from *Camellia.* However, different media were used in these two studies. Blastn researches with ITS sequences results in 100% identity with *C. gloeosporioides* strain SS1-MS1 (GenBank KP900279) isolated from *Huperzia serrate* in China (Wang et al. 2016). GAPDH, ACT and TUB2 sequences of MFLUCC 14-0091 and MFLUCC 14-0092 are closest to *C. kahawae* subsp. *ciggaro* strain ICMP 18534 (GenBank JX009904) with 98% identity isolated from *Kunzea ericoides* in New Zealand, 99% identity with strain ICMP 12952 (GenBank JX009431) isolated from *Persea Americana* in New Zealand, and 99% identity with strain CO22-1 (GenBank KJ001124) isolated from *Rubus glaucus* in Colombia respectively (Weir et al. 2012;

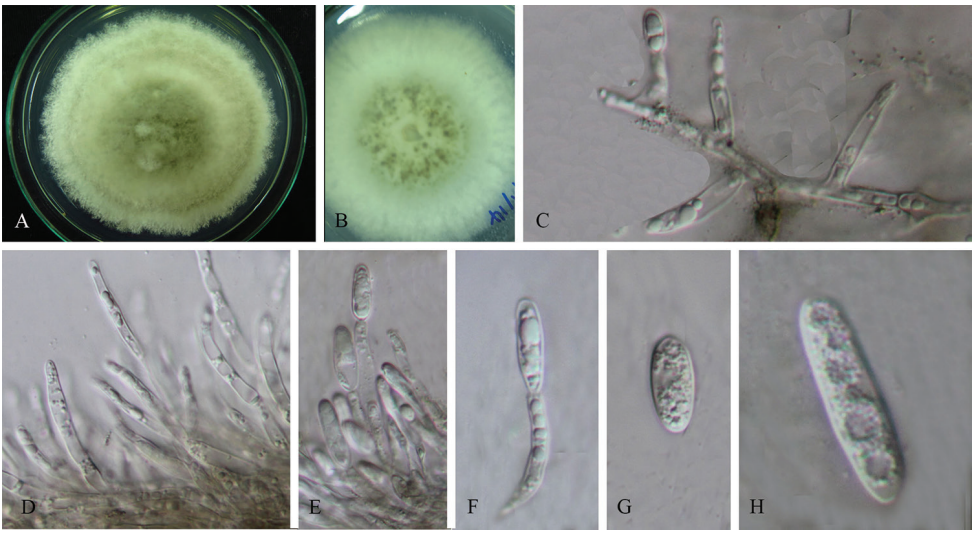

Figure 9. *Colletotrichum jiangxiense.* **A** Colony **B** Colony from below **C–F** Conidiophores **G–H** Conidia. Scale bars: 5 μm (**C–F**), 2.5 μm (**G–H**).

Afanador-Kafuri et al. 2014). Conidia size reported for *C. jiangxiense* was 15.2 ± 1 × 5.2 ± 0.4 μm, which was larger and faster growing than the strains isolated in this study. There were 5bp differences between strain MFLUCC 14-0091 and *C. jiangxiense*. Here we name both of isolates from leaves of *Dendrobium* sp.1 as *C. jiangxiense*.

Colletotrichum orchidophilum Damm, P.F. Cannon & Crous

Figure 10

Description. *Sexual morph* not observed.

Sexual morph not observed. Asexual morph on SDA. Vegetative hyphae 1.9–5.4 μm diam, smooth-walled, septate, branched, hyaline to pale brown. Chlamydospores not observed. Appressoria brown, smooth-walled. Conidiomata superficial or under mycelia, smooth-walled, 200 × 300 μm, black. Conidiophores smooth-walled, branched or unbranched, hyaline. Conidiophores and appressoria rare. Conidia (9.6–) 11.7–14.1 (–14.7) × (2.9–) 3.5–4.4 (–4.8) μm, L/W = 3.3, cylindrical, straight, with 1 to 4 guttules, one end somewhat acute, hyaline.

Cultures on SDA flat with entire margin. Growth rate: 0.44cm/day, with nearly 20-days for sporulation. White with dark green mycelia around the middle, white edge, reverse white. Cultures on PDA flat with entire margin. Growth rate: 0.45cm/day, with 30-days for sporulation. Fluffy, white, reverse light brown. Acervuli in mass black, irregular, asymmetrical, merging in media.

Notes. Strains MFLUCC–14–0161 and MFLUCC–14–0162 belong to a single species as they have similar conidia, cultures and the nearly identical sequence data. The

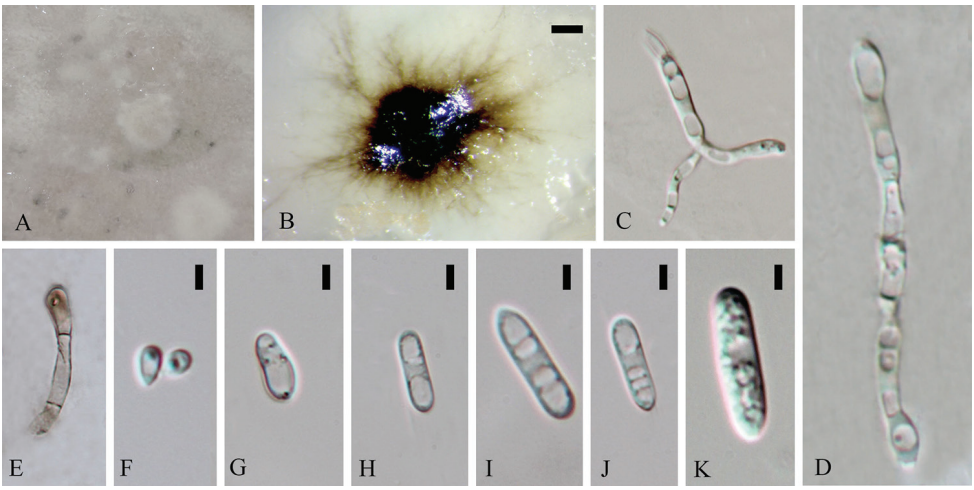

Figure 10. *Colletotrichum orchidophilum.* **A** Colony **B** Fruiting body **C–D** Conidiophores **E** Appressoria **F–K** Conidia. Scale bars: 200 μm (**B**), 5 μm (**F–K**).

support values of 100/1.00/100 totally grouped them with *C. orchidophilum* and their branch lengths are slightly different. Blastn researches sequences of MFLUCC 14-0161 and MFLUCC 14-0162 results in 99% identity with ITS (GenBank NR111729), GAPDH (GenBank JQ948481) and ACT (GenBank JQ949472) sequences of ex-holotype culture of *C. orchidophilum* strain CBS 632.80 isolated from *Dendrobium* sp. in USA (Damm et al. 2012). TUB2 sequence is 99% identity with pathogenic *C. fructicola* strain AV24 (GenBank KX786459) isolated from grapevine shoots in Brazil (Santos et al. 2018) and *C. gloeosporioides* strain TL-2 (GenBank KC913205) isolated from *Camellia sinensis* in China (Guo et al. 2014). Because no conidiophores were detected in culture, no measurement for the conidiophores could be given. In this study, strains MFLUCC 14-0161 and MFLUCC 14-0162 of *C. orchidophilum* were isolated from leaves of *D. harveyanum.*

Colletotrichum boninense **Moriwaki, Toy. Sato & Tsukib.**

For an illustrated description please refer Damm et al. (2012a).

Notes. Strains MFLUCC 14-0086, MFLUCC 14-0124 and MFLUCC 15-0261 grouped with *C. boninense* and MFLUCC 14-0128. All have very similar sequences as those as the ex-type of with *C. boninense* (only 2bp difference), while there was 11 base pair deviations between these strains and *Colletotrichum doitungense* sp. nov. Blastn researches with ITS sequences of them result in 100% identity with ITS sequence of endophytic *C. boninense* strain SL-ML18 (GenBank KP900269) isolated from *Huperzia serrate* in China (Wang et al. 2016) and strain CGMCC 3.15168 (GenBank KC244158) as mentioned above. GAPDH and ACT sequences of them are 97% identity with *C. boninense* CGMCC 3.15168 (GenBank KC843491) and 100% identity

with *C. fructicola* strain 1104-7 (GenBank KX885159) isoalted from *Malus domestica* in China (Liang et al. 2017). TUB2 blastn result are 99% identity with *C. fructicola* strain AV24 (GenBank KX786459) and *C. gloeosporioides* strain TL-2 (GenBank KC913205) as mentioned above. Here we identify these three strains isolated from leaves of *D. catenatum* and *Dendrobium sp.*1, stem of *D.* sp.2 respectively as *Colletotrichum boninense*.

Colletotrichum sp. indet

Notes. Strain MFLUCC 14-0120 failed to sporulate and lacks a complete morphological description. It formed a single branch close to *C. camelliae-japonicae,* MFLUCC 14-0129 / MFLUCC 14-0131 with 67ML/1.00BI/62MP support. There were 15bp and 11bp differences mainly in the ACT gene region among MFLUCC 14-0120 and *C. camelliae-japonicae,* MFLUCC 14-0129/MFLUCC 14-0131 respectively. ITS sequence blastn of MFLUCC 14-0120 showed many different kinds of species with 99% identity. Blastn searches with GAPDH (GenBank KC293736) and TUB2 (GenBank KC293656) sequences result in 99% identity with *C. citricola* strain SCX 151 as mentioned above. The ACT of MFLUCC–14–0120 is 98% identity with *C. boninense* strain CBS 125502 (GenBank KJ954462) as mentioned above. Here we listed it as an unidentified species.

Discussion

Colletotrichum species associated with orchid species

Many *Colletotrichum* species have been isolated from Orchidaceae plants sampled in China in previous studies (e.g. Yang et al. 2011; Chen et al. 2012; Tao et al. 2008, 2013). Eighteen *Colletotrichum* species have been reported from these studies. For example, *Colletotrichum beeveri* isolated from *Pleione bulbocodioides*; *C. bletillum* and *C. caudasporum* isolated from *Bletilla ochracea*; *C. oncidii* isolated from *Oncidium* sp. (Yang et al. 2011; Damm et al. 2012a; Tao et al. 2013). The present study is the first to report endophytic fungi from *Dendrobium* spp. in Thailand combining both multi-loci sequence data and morphological characteristics. *Colletotrichum* species in this study were diverse and present in every *Dendrobium* sample collected from all sites. Therefore, we conclude that *Orchidaceae* plants are rich source of endophytic *Colletotrichum* species.

Methods affecting the identification

Hyde and Zhang (2008) and Hyde et al. (2009b) suggested that nucleotide sequence data of holotypes or epitypes is essential for analysing phylogenetic relationships among *Colletotrichum* species. A polyphasic method combining morphological characteristics

and molecular phylogenetics has been applied to define and re-order species in this genus (Cai et al. 2009; Hyde et al. 2009; Damm et al. 2012a, b, c; Jayawardena et al. 2016a, b).

We found some differences in the *Colletotrichum gloeosporioides* species complex backbone tree as compared to that constructed with more genes in Weir et al (2012), Udayanga et al (2013) and Jayawardena et al. (2016a). *Colletotrichum jiangxiense* clusters with *C. rhexiae* rather than *C. kahawae*. *C. fructicola* is closer to *C. siamense* rather than *C. nupharicola.* The genes CHS-1 and HIS3 were not involved in this study and may be responsible for the differences. Actually CHS-1 and HIS3 could resolve species in sevaral other species complexes of *Colletotrichum* (Jayawardena et al. 2016a). However, the combination of ApMat and GS turned out to be the most effective genes in species resolution in the *Colletotrichum gloeosporioides* species complex (Liu et al. 2015). Our study is the first to use multiple gene sequences to analyse fungal endophytes from *Dendrobium* orchids.

Relationship between *Colletotrichum* and *Dendrobium*

Few species identified in this study showed host-specificity. Nevertheless, this study provides evidence that *C. orchidophilum* colonizes a wide range of hosts in *Orchidaceae* (Damm et al. 2012b). In addition, we found that leaves contained higher numbers of *Colletotrichum* species (11 strains from leaves) than other parts (4 strains from roots and 7 strains from stems). All *Dendrobium* leaves in this study were colonized by *Colletotrichum* strains. Our results are similar to those of Chen et al. (2011) who isolated more *Colletotrichum* species from stems and leaves of *Dendrobium* species than that from roots.

The majority of *Colletotrichum* species isolated from *Dendrobium* species in this study were fungal endophytes. This was also reported by Chen et al. (2011) and Yuan et al. (2009). The most common fungal endophytes in leaves of *Lepanthes rupestris* (*Orchidaceae*) sampled in a Puerto Rican forest were a *Colletotrichum* species which showed antagonism against other fungal taxa (Bayman et al. 2002). Most *Colletotrichum* species have been identified as plant pathogens living a hemibiotrophic life strategy, they adopt a biotrophic phase at an early stage and switch to a necrotrophic phase later (Damm et al. 2010; Cannon et al. 2012).

Here we speculate that most isolates in this study might be latent pathogens (Photita et al. 2004), since in the phylogenies, they were nested with pathogenic strains or have previously been reported to cause plant diseases (Tao et al. 2013, Hou et al 2016). *Colletotrichum jiangxiense* was isolated as a pathogen from leaf lesions of *Camellia* sp. (Liu et al. 2015). *Colletotrichum boninense* was reported as an anthracnose causing agent from *Dendrobium kingianum* in Japan (Moriwaki et al. 2003).

Acknowledgements

This work was funded by the grants of National Natural Science Foundation of China (Grants Nos. 31670027 & 31460011 & 30870009) and the Agricultural Science and

Technology Foundation of Guizhou Province, China (Grant No. NY[2013]3042). We sincerely acknowledge great help from Santi Watthana on identification of orchids collected in Thailand.

References

Altschul SF, Madden TL, Schäffer AA, Zhang J, Zhang Z, Miller W, Lipman DJ (1997) Gapped BLAST and PSI–BLAST: a new generation of protein database search programs. Nucleic Acids Research 25: 3389–3402. https://doi.org/10.1093/nar/25.17.3389

Bailey JA, O'Connell RJ, Pring RJ, Nash C (1992) Infection strategies of *Colletotrichum* species. In: Bailey JA, Jeger MJ (Eds) Biology, Pathology and Control. CAB, International Press, Wallingford, 88–120.

Bayman P, Gonzalez EJ, Fumero JJ, Tremblay RL (2002) Are fungi necessary? How fungicides affect growth and survival of the orchid *Lepanthes rupestris* in the field. Journal of Ecology 90(6): 1002–1008. https://doi.org/10.1046/j.1365-2745.2002.00733.x

Bulpitt CJ, Li Y, Bulpitt PF, Wang J (2007) The use of orchids in Chinese medicine. Journal of the Royal Society of Medicine 100(12): 558–563. https://doi.org/10.1177/0141076807100012014

Cannon PF, Damm U, Johnston PR, Weir BS (2012) *Colletotrichum*–current status and future directions. Studies in Mycology 73: 181–213. https://doi.org/10.3114/sim0014

China Plant Specialist Group (2004) *Dendrobium catenatum*. The IUCN red list of threatened species e.T46665A11074270. http://dx.doi.org/10.2305/IUCN.UK.RLTS.T46665A11074270.en

Chen J, Hu KX, Hou XQ, Guo SX (2011) Endophytic fungi assemblages from 10 *Dendrobium* medicinal plants (*Orchidaceae*). World Journal of Microbiology and Biotechnology 27(5): 1009–1016. https://doi.org/10.1007/s11274-010-0544-y

Crouch JA, Clarke BB, White JrJF, Hillman BI (2009) Systematic analysis of the falcate-spored graminicolous *Colletotrichum* and a description of six new species from warm season grasses. Mycologia 101: 717–732. https://doi.org/10.3852/08-230

Curry KJ, Abril M, Avant JB, Smith BJ (2002) Strawberry anthracnose: Histopathology of *Colletotrichum acutatum* and *C. fragariae*. Phytopathology 92(10): 1055–1063. https://doi.org/10.1094/PHYTO.2002.92.10.1055

Damm U, Baroncelli R, Cai L, Kubo Y, O'Connell R, Weir B, Yoshino K, Cannon PF (2010) *Colletotrichum*: species, ecology and interactions. IMA fungus 1(2): 161–165. https://doi.org/10.5598/imafungus.2010.01.02.08

Damm U, Cannon PF, Liu F (2013) The *Colletotrichum orbiculare* species complex: important pathogens of field and weeds. Fungal Diversity 61: 29–59. https://doi.org/10.1007/s13225-013-0255-4

Damm U, Cannon PF, Woudenberg JHC, Johnston PR, Weir BS, Tan YP, Shivas RG, Crous PW (2012a) The *Colletotrichum boninense* species complex. Studies in Mycology 73: 1–36. https://doi.org/10.3114/sim0002

Damm U, Cannon PF, Woudenberg JHC, Crous PW (2012b) The *Colletotrichum acutatum* species complex. Studies in Mycology 73: 37–113. https://doi.org/10.3114/sim0010

Damm U, O'Connell RJ, Groenewald JZ, Crous PW (2014) The *Colletotrichum destructivum* species complex – hemibiotrophic pathogens of forage and field crops. Studies in Mycology 79: 49–84. https://doi.org/10.1016/j.simyco.2014.09.003

Dean R, Van Kan JAL, Pretorius ZA, Hammond-Kosack KE, Di Pietro A, Spanu PD, Rudd JJ, Dickman M, Kahmann R, Ellis J, Foster GD (2012) The Top 10 fungal pathogens in molecular plant pathology. Molecular Plant Pathology 13: 414–430. https://doi.org/10.1111/j.1364-3703.2011.00783.x

Diao YZ, Zhang C, Liu F, Wang WZ, Liu L, Cai L, Liu XL (2017) *Colletotrichum* species causing anthracnose disease of chili in China. Persoonia 38: 20–37. https://doi.org/10.3767/003158517X692788

Ding G, Li X, Ding X, Qian L (2009) Genetic diversity across natural populations of *Dendrobium catenatum*, the endangered medicinal herb endemic to China, revealed by ISSR and RAPD markers. Russian Journal of Genetics 45(3): 327–334. https://doi.org/10.1134/S1022795409030119

Gan P, Nakata N, Suzuki T, Shirasu K (2017) Markers to differentiate species of anthracnose fungi identify *Colletotrichum fructicola* as the predominant virulent species in strawberry plants in Chiba Prefecture of Japan. Journal of General Plant Pathology 83(1): 14–22. https://doi.org/10.1007/s10327-016-0689-0

Gu S, Ding XY, Wang Y et al. (2007) Isolation and characterization of microsatellite markers in *Dendrobium officinale*, an endangered herb endemic to China. Molecular Ecology Resources 7(6): 1166–1168. https://doi.org/10.1111/j.1471-8286.2007.01817.x

Guo M, Pan YM, Dai YL, Gao ZM (2014) First report of brown blight disease caused by *Colletotrichum gloeosporioides* on *Camellia sinensis* in Anhui Province, China. Plant Disease 98(2): 284–284. https://doi.org/10.1094/PDIS-08-13-0896-PDN

Hall TA (1999) BioEdit: a user-friendly biological sequence alignment editor and analysis program for Windows 95/98/NT. Nucleic Acids Symposium Series 41: 95–98.

Hongsanan S, Maharachchikumbura SSN, Hyde KD, Samarakoon MC, Jeewon R, Zhao Q, Al-Sadi AM, Bahkali AH (2017) An updated phylogeny of Sordariomycetes based on phylogenetic and molecular clock evidence. Fungal Diversity 84(1): 25–41. https://doi.org/10.1007/s13225-017-0384-2

Hou LW, Liu F, Duan WJ, Cai L (2016) *Colletotrichum aracearum* and *C. camelliae-japonicae*, two holomorphic new species from China and Japan. Mycosphere 7: 1111–1123. https://doi.org/10.5943/mycosphere/si/2c/4

Hyde KD, Cai L, Cannon PF, Cannon PF, Crouch JA, Crous PW, Damm U, Goodwin PH, Chen H, Johnston PR, Jones EB, Liu ZY (2009a) *Colletotrichum* names in current use. Fungal Diversity 39(1): 147–182.

Hyde KD, Cai L, McKenzie EHC, Yang YL, Zhang JZ, Prihastuti H (2009b) *Colletotrichum*: a catalogue of confusion. Fungal Diversity 39: 1–17.

Hyde KD, Abd-Elsalam K, Cai L (2010) Morphology: still essential in a molecular world. Mycotaxon 114(1): 439–451. https://doi.org/10.5248/114.439

Hyde KD, Nilsson RH, Alias SA, Ariyawansa HA, Blair JE, Cai L, de Cock AW, Dissanayake AJ, Glockling SL, Goonasekara ID, Gorczak M (2014) One stop shop: backbones trees for important pytopathogenic genera: I. Fungal Diversity 67: 21–125. https://doi.org/10.1007/s13225-014-0298-1

Huang F, Chen GQ, Hou X, Fu YS, Cai L, Hyde KD, Li HY (2013) *Colletotrichum* species associated with cultivated citrus in China. Fungal Diversity 61(1): 61–74. https://doi.org/10.1007/s13225-013-0232-y

Jadrane I, Kornievsky M, Desjardin DE, He ZH, Cai L, Hyde K (2012) First report of flower anthracnose caused by *Colletotrichum karstii* in white *Phalaenopsis* orchids in the United States. European Journal of Plant Pathology 146(3): 465–481. https://doi.org/10.1094/PDIS-04-12-0360-PDN

Jayawardena RS, Hyde KD, Damm U, Cai L, Liu M, Li XH, Zhang W, Zhao WS, Yan JY (2016a) Notes on currently accepted species of *Colletotrichum*. Mycosphere 7: 1192–1260. https://doi.org/10.5943/mycosphere/si/2c/9

Jayawardena RS, Cai L, McKenzie EHC, Li XH, Liu M, Yan JY (2016b) Why is it important to correctly name *Colletotrichum* species? Mycosphere 7(8): 1076–1092. https://doi.org/10.5943/mycosphere/si/2c/1

Jeewon R, Hyde KD (2016) Establishing species boundaries and new taxa among fungi: recommendations to resolve taxonomic ambiguities. Mycosphere 7(11): 1669–1677. https://doi.org/10.5943/mycosphere/7/11/4

Jiang J, Zhai H, Li H, Wang Z, Chen Y, Hong N, Wang G, Chofong GN, Xu W (2014) Identification and characterization of *Colletotrichum fructicola* causing black spots on young fruits related to bitter rot of pear (*Pyrus bretschneideri* Rehd.) in China. Crop Protection 58: 41–48. https://doi.org/10.1016/j.cropro.2014.01.003

Katoh K, Toh H (2008) Recent developments in the MAFFT multiple sequence alignment program. Brief Bioinform 9: 276–285. https://doi.org/10.1093/bib/bbn013

Kalyaanamoorthy S, Minh BQ, Wong TKF, von Haeseler A, Jermiin LS (2017) ModelFinder: Fast Model Selection for Accurate Phylogenetic Estimates, Nature Methods 14: 587–589. https://doi.org/10.1038/nmeth.4285

Kleemann J, Rincon-RiveraLJ, Takahara H, Neumann U, van Themaat EV, van der Does HC, Hacquard S, Stüber K, Will I, Schmalenbach W, Schmelzer E (2012) Sequential delivery of host-induced virulence effectors by appressoria and intracellular hyphae of the phytopathogen *Colletotrichum higginsianum*. PLoS pathogens 8(4): pe1002643. https://doi.org/10.1371/journal.ppat.1002643

Li H, Zhou GY, Liu JA, Xu J (2016) Population genetic analyses of the fungal pathogen *Colletotrichum fructicola* on tea-oil trees in China. PloS one 11(6): e0156841. https://doi.org/10.1371/journal.pone.0156841

Li HN, Jiang JJ, Hong N, Wang GP, Xu WX (2016) First report of *Colletotrichum fructicola* causing bitter rot of pear (*Pyrus bretschneideri*) in China. Plant Disease 100(6): 1235.

Liang X, Tian X, Liu W, Wei T, Wang W, Dong Q, Wang B, Meng Y, Zhang R, Gleason ML (2017) Comparative analysis of the mitochondrial genomes of *Colletotrichum gloeosporioides* sensu lato: insights into the evolution of a fungal species complex interacting with diverse plants. BMC Genomics 18(1): 171. https://doi.org/10.1186/s12864-016-3480-x

Lichtemberg PSF, Moral J, Morgan DP, Felts DG, Sanders RD, Michailides TJ (2017) First report of anthracnose caused by *Colletotrichum fioriniae* and *C. karstii* in California Pistachio Orchards. Plant Disease 101(7): 1320. https://doi.org/10.1094/PDIS-01-17-0144-PDN

Lin Y, Li J, Li B, He T, Chun Z (2011) Effects of light quality on growth and development of protocorm – like bodies of *Dendrobium catenatum* in vitro. Plant Cell, Tissue and Organ Culture 105(3): 329–335. https://doi.org/10.1007/s11240-010-9871-9

Lin Y, Wang F, Yang L, Chun Z, Bao JK, Zhang GL (2013) Anti-inflammatory phenanthrene derivatives from stems of *Dendrobium denneanum*. Phytochemistry 95: 242–251. https://doi.org/10.1016/j.phytochem.2013.08.008

Liu F, Damm U, Cai L, Crous PW (2013) Species of the *Colletotrichum gloeosporioides*, complex associated with anthracnose diseases of Proteaceae. Fungal Diversity 61(1): 89–105. https://doi.org/10.1007/s13225-013-0249-2

Liu F, Cai L, Crous PW, Damm U (2014) The *Colletotrichum gigasporum* species complex. Persoonia – Molecular Phylogeny and Evolution of Fungi 33(1): 83–97. https://doi.org/10.3767/003158514X684447

Liu F, Weir BS, Damm U, Crous PW, Wang Y, Liu B, Wang M, Zhang M, Cai L (2015) Unravelling *Colletotrichum* species associated with *Camellia*: employing ApMat and GS loci to resolve species in the *C. gloeosporioides* complex. Persoonia–Molecular Phylogeny and Evolution of Fungi 35(1): 63–86. https://doi.org/10.3767/003158515X687597

Lu G, Cannon PF, Alex RE, Simmons CM (2004) Diversity and molecular relationships of endophytic *Colletotrichum* isolates from the Iwokrama Forest Reserve, Guyana. Mycological Research 108: 53–63. https://doi.org/10.1017/S0953756203008906

Ma XY, Kang JC, Nontachaiyapoom S, Wen T, Hyde KD (2015) Non-mycorrhizal endophytic fungi from orchids. Current Science 109(1): 72–87.

Maharachchikumbura SSN, Guo LD, Cai L, Chukeatirote E, Wu WP, Sun X, Crous PW, Bhat DJ, McKenzie EH, Bahkali AH, Hyde KD (2012) A multi – locus backbone tree for *Pestalotiopsis* with a polyphasic characterization of 14 new species. Fungal Diversity 56(1): 95–129. https://doi.org/10.1007/s13225-012-0198-1

Maharachchikumbura SSN, Hyde KD, Jones EBG, McKenzie EH, Bhat JD, Dayarathne MC, Huang SK, Norphanphoun C, Senanayake IC, Perera RH, Shang QJ (2016) Families of Sordariomycetes. Fungal Diversity 79(1): 1–317. https://doi.org/10.1007/s13225-016-0369-6

Maharachchikumbura SSN, Hyde KD, Jones EBG, McKenzie EH, Huang SK, Abdel-Wahab MA, Daranagama DA, Dayarathne M, D'souza MJ, Goonasekara ID, Hongsanan S (2015) Towards a natural classification and backbone tree for Sordariomycetes. Fungal Diversity 72(1): 199–301. https://doi.org/10.1007/s13225-015-0331-z

Mangunwardoyo W, Suciatmih IG (2011) Frequency of endophytic fungi isolated from *Dendrobium crumenatum* (Pigeon orchid) and antimicrobial activity. Biodiversitas 13(1): 34–39. https://doi.org/10.13057/biodiv/d130107

Moriwaki J, Sato T, Tsukiboshi T (2003) Morphological and molecular characterization of *Colletotrichum boninense* sp. nov. from Japan. Mycoscience 44(1): 47–53. https://doi.org/10.1007/S10267-002-0079-7

Mendgen K, Hahn M (2002) Plant infection and the establishment of fungal biotrophy. Trends in plant science 7(8): 352–356. https://doi.org/10.1016/S1360-1385(02)02297-5

NG TB, Liu J, Wong JH, Ye X, Sze SC, Tong Y, Zhang KY (2012) Review of research on *Dendrobium*, a prized folk medicine. Applied Microbiology and Biotechnology 93(5): 1795–1803. https://doi.org/10.1007/s00253-011-3829-7

Noireung P, Phoulivong S, Liu F, Cai L, Mckenzie EH, Chukeatirote E, Jones EB, Bahkali AH, Hyde KD (2012) Novel species of *Colletotrichum* revealed by morphology and molecular analysis. Cryptogamie, Mycologie 33(3): 347–362. https://doi.org/10.7872/crym.v33.iss3.2012.347

Nontachaiyapoom S, Sasirat S, Manoch L (2010) Isolation and identification of *Rhizoctonia*-like fungi from roots of three orchid genera, *Paphiopedilum*, *Dendrobium*, and *Cymbidium* collected in Chiang Rai and Chiang Mai provinces of Thailand. Mycorrhiza 20: 459–471. https://doi.org/10.1007/s00572-010-0297-3

Nylander JA (2004) MrModeltest v2. Program distributed by the author. Evolutionary Biology Centre, Uppsala University. Uppsala, Sweden.

Otero JT, Ackerman JD, Bayman P (2002) Diversity and host specificity of endophytic *Rhizoctonia* – like fungi from tropical orchids. American Journal of Botany 89: 1852–1858. https://doi.org/10.3732/ajb.89.11.1852

Ping L (2003) Advances in studies on pharmacology of plants from *Dendrobium* Sw. Chinese Traditional & Herbal Drugs 36(12): e215–e217.

Photita W, Lumyong S, Lumyong P, McKenzie EH, Hyde KD (2004) Are some endophytes of *Musa acuminata* latent pathogens. Fungal Diversity 16(1): 131–140.

Prihastuti H, Cai L, Chen H, McKenzie EH, Hyde KD (2009) Characterization of *Colletotrichum* species associated with coffee berries in northern Thailand. Fungal Diversity 39(1): 89–109.

Prusky D, Plumbley RA (1992) Quiescent infections of *Colletotrichum* in tropical and subtropical fruit in: *Colletotrichum*. In: Bailey JA, Jeger MJ (Eds) Biology, Pathology and Control, CABI Press, Wallingford, 289–307.

Radiastuti N, Mutea D, Sumarlin LO (2017) Endophytic *Colletrotrichum* spp. from *Cinchona calisaya* Wedd and it's potential quinine production as antibacterial and antimalaria. In: AIP Conference Proceedings 1813(1): 020022.

Redman RS, Dunigan DD, Rodriguez RJ (2001) Fungal symbiosis from mutualism to parasitism: who controls the outcome, host or invader? New Phytologist 151(3): 705–716. https://doi.org/10.1046/j.0028-646x.2001.00210.x

Rojas EI, Rehner SA, Samuels GJ, Van Bael SA, Herre EA, Cannon P, Chen R, Pang J, Wang R, Zhang Y, Peng YQ (2010) *Colletotrichum gloeosporioides* s.l. associated with *Theobroma cacao* and other plants in Panama: multilocus phylogenies distinguish pathogen and endophyte clades. Mycologia 102: 1318–1338. https://doi.org/10.3852/09-244

Santos RF, Ciampi-Guillardi M, Amorim L, Massola Júnior NS, Spósito MB (2017) Aetiology of anthracnose on grapevine shoots in Brazil. Plant Pathology Oct 24.

Sharma G, Shenoy BD (2014) *Colletotrichum fructicola* and *C. siamense* are involved in chilli anthracnose in India. Archives of Phytopathology and Plant protection 47(10): 1179–1194. https://doi.org/10.1080/03235408.2013.833749

Shi NN, Du YX, Chen FR, Ruan HC, Yang XJ (2017) First report of leaf spot caused by *Colletotrichum fructicola* on Japan Fatsia (*Fatsia japonica*) in Fujian Province in China. Plant Disease 101(8):1552. https://doi.org/10.1094/PDIS-12-16-1720-PDN

Silvestro D, Michalak I (2012) RaxmlGUI: a graphical front-end for RAxML. Organisms Diversity & Evolution 12(4): 335–337. https://doi.org/10.1007/s13127-011-0056-0

Swofford DL (2002) PAUP* 4.0: phylogenetic analysis using parsimony (* and other methods). Sinauer Associates, Sunderland.

Tao G, Liu ZY, Hyde KD, Liu XZ, Yu ZN (2009) Whole rDNA analysis reveals novel and endophytic fungi in *Bletilla ochracea* (Orchidaceae). Fungal Diversity 33: 101–122.

Tao G, Liu ZY, Liu F, Gao YH, Cai L (2013) Endophytic *Colletotrichum* species from *Bletilla ochracea* (*Orchidaceae*) with descriptions of seven new species. Fungal Diversity 61(1): 139–164. https://doi.org/10.1007/s13225-013-0254-5

The Plant List (2013) Version 1.1. Published on the Internet. http://www.theplantlist.org [accessed 1st January]

Udayanga D, Manamgoda DS, Liu X, Chukeatirote E, Hyde KD (2013) What are the common anthracnose pathogens of tropical fruits? Fungal Diversity 61(1): 165–179. https://doi.org/10.1007/s13225-013-0257-2

Wang H, Fang H, Wang Y, Duan L, Guo S (2011) In situ seed baiting techniques in *Dendrobium catenatum* Kimuraet Migo and *Dendrobium nobile* Lindl.: the endangered Chinese endemic *Dendrobium* (*Orchidaceae*). World Journal of Microbiology and Biotechnology 27(9): 2051–2059. https://doi.org/10.1007/s11274-011-0667-9

Wang Y, Lai Z, Li XX, Yan RM, Zhang ZB, Yang HL, Zhu D (2016) Isolation, diversity and acetylcholinesterase inhibitory activity of the culturable endophytic fungi harboured in *Huperzia serrata* from Jinggang Mountain, China. World Journal of Microbiology & Biotechnology 32(2): 20. https://doi.org/10.1007/s11274-015-1966-3

Weir BS, Johnston PR, Damm U (2012) The *Colletotrichum gloeosporioides* species complex. Studies in Mycology 73(1): 115. https://doi.org/10.3114/sim0011

Xia L, Liu X, Guo H, Zhang H, Zhu J, Ren F (2012) Partial characterization and immunomodulatory activity of polysaccharides from the stem of *Dendrobium officinale* (Tie pi shi hu) in vitro. Journal of functional foods 4(1): 294–301. https://doi.org/10.1016/j.jff.2011.12.006

Xia X, Xie Z, Salemi M, Chen L, Wang Y (2003) An index of substitution saturation and its application. Molecular Phylogenetics & Evolution 26(1): 1. https://doi.org/10.1016/S1055-7903(02)00326-3

Xing YM, Chen J, Cui JL, Chen XM, Guo SX (2011) Antimicrobial activity and biodiversity of endophytic fungi in *Dendrobium devonianum* and *Dendrobium thyrsiflorum* from Vietman. Current microbiology 62(4): 1218– 1224. https://doi.org/10.1007/s00284-010-9848-2

Xu FQ, Xu FC, Hou B, Fan WW, Zi CT, Li Y, Dong FW, Liu YQ, Sheng J, Zuo ZL, Hu JM (2014) Cytotoxic bibenzyl dimers from the stems of *Dendrobium fimbriatum* Hook. Bioorganic & Medicinal Chemistry Letters 24(22): 5268–5273. https://doi.org/10.1016/j.bmcl.2014.09.052

Xu JH, Li L, Chen LZ (1995) Studies on the effects of white *Dendrobium* (*Dendrobium candicum*) and American ginseng (*Panax quinquefolius*) on nourishing the Yin and promoting glandular secretion in mice and rabbits. Chinese Traditional Herb Drug 6: 79–80.

Yuan Z, Chen YC, Yang Y (2009) Diverse non-mycorrhizal fungal endophytes inhabiting an epiphytic, medicinal orchid (*Dendrobium nobile*): estimation and characterization. World Journal of Microbiology and Biotechnology 25(2): 295. https://doi.org/10.1007/s11274-008-9893-1

Yang Y, Cai L, Yu Z, Liu Z, Hyde KD (2011) *Colletotrichum* species on *Orchidaceae* in southwest China. Cryptogamie, Mycologie 32(3): 229–253. https://doi.org/10.7872/crym.v32.iss3.2011.229

Yang YL, Liu ZY, Cai L, Hyde KD, Yu ZN, McKenzie EHC (2009) *Colletotrichum* anthracnose of Amaryllidaceae. Fungal Diversity 39: 123–146.

Appendix A

Fungal isolates and sequences of region/genes used in *Colletotrichum* phylogenetic analysis.

Species	Isolate[a]	GenBank accession number			
		ITS	GAPDH	ACT	ß–tubulin
C. acutatum	CBS 128531*	JQ005776	JQ948677	JQ005839	JQ005860
C. aeschynomenes	CBS 128532*	JX010176	JX009930	JX009483	JX010392
C. alcornii	CBS 128534*	JX076858	–	–	–
C. alienum	ICMP 12071*	JX010251	JX010028	JX009572	JX010411
C. annellatum	CBS 128536*	JQ005222	JQ005309	JQ005570	JQ005656
C. anthrisci	CBS 125334*	GU227845	GU228237	GU227943	GU228139
C. aotearoa	CBS 128538*	JX010205	JX010005	JX009564	JX010420
C. arxii	CBS 132511*	NR132055	KF687843	KF687802	KF687881
C. australe	CBS 128540*	JQ948455	JQ948786	JQ949776	JQ950106
C. beeveri	CBS 128541*	JQ005171	JQ005258	JQ005519	JQ005605
C. bidentis	CBS 128542*	KF178481	KF178506	KF178578	KF178602
C. bletillum	CBS 128543*	JX625178	KC843506	KC843542	JX625207
C. boninense	CBS 123755*	JQ005153	JQ005240	JQ005501	JQ005588
C. brasiliense	CBS 128545*	JQ005235	JQ005322	JQ005583	JQ005669
C. brassicola	CBS 128546*	JQ005172	JQ005259	JQ005520	JQ005606
C. brevisporum	CBS 128547*	JQ247623	JQ247599	JQ247647	JQ247635
C. camelliae	ICMP 10643	JX010224	JX009908	JX009540	JX010436
C. camelliae–japonicae	CGMCC3.18117*	KX853165	KX893583	KX893575	KX893579
C. caudasporum	CGMCC 3.15106*	JX625162	KC843512	KC843526	JX625190
C. cereale	CBS 129663	JQ005774	–	JQ005837	JQ005858
C. chlorophyti	IMI 103806*	GU227894	GU228286	GU227992	GU228188
C. chrysanthemi	IMI 364540	JQ948273	JQ948603	JQ949594	JQ949924
C. citricola	SXC 151*	KC293576	KC293736	KC293616	KC293656
C. clidemiae	ICMP 18658*	JX010265	JX009989	JX009537	JX010438
C. cliviae	CBS 125375*	JX519223	GQ856756	JX519240	JX519249
C. coccodes	CBS 369.75	JQ005775	HM171673	JQ005838	JQ005859
C. colombiense	CBS 129818*	JQ005174	JQ005261	JQ005522	JQ005608
C. cordylinicola	ICMP 18579*	JX010226	JX009975	HM470234	JX010440
C. curcumae	IMI 288937*	GU227893	GU228285	GU227991	GU228187
C. cymbidiicola	IMI 347923*	JQ005166	JQ005253	JQ005514	JQ005600
C. dematium	CBS 125.25*	GU227819	GU228211	GU227917	GU228113
C. dracaenophilum	CBS 118199*	JX519222	–	JX519238	JX519247
C. echinochloae	MAFF 511473*	AB439811	–	–	–
C. eleusines	MAFF 511155*	JX519218	–	JX519234	JX519243
C. endophytum	CGMCC 3.15108*	JX625177	KC843521	KC843533	JX625206
C. eremochloae	CBS 129661*	CBS 129661	–	JX519236	JX519245
C. excelsum–altitudum	CGMCC 3.15130*	HM751815	KC843502	KC843548	JX625211
C. falcatum	CBS 147945*	JQ005772	–	JQ005835	JQ005856
C. fioriniae	CBS 128517*	JQ948292	JQ948622	JQ949613	JQ949943
C. fructi	CBS 346.37*	GU227844	GU228236	GU227942	GU228138
C. fructicola	ICMP 18581*	JX010165	JX010033	FJ907426	JX010405
C. fructivorum	Coll1414*	JX145145	–	–	JX145196
C. fusiforme	MFLU 130291*	NR138010	KT290255	KT290251	KT290256

Species	Isolate[a]	GenBank accession number			
		ITS	GAPDH	ACT	ß–tubulin
C. gigasporum	MUCL 44947*	AM982797	–	–	FN557442
C. godetiae	CBS 133.44*	JQ948402	JQ948733	JQ949723	JQ950053
C. graminicola	CBS 130836*	JQ005767		JQ005830	JQ005851
C. grevilleae	CBS 132879*	KC297078	KC297010	KC296941	KC297102
C. guizhouensis	CGMCC 3.15112*	JX625158	KC843507	KC843536	JX625185
C. hanaui	MAFF 305404*	JX519217	–	–	JX519242
C. henanense	LF238*	KJ955109	KJ954810	–	KJ955257
C. hippeastri	CBS 125376*	JQ005231	JQ005318	JQ005579	JQ005665
C. hemerocallidis	CDLG5*	JQ400005	JQ400012	JQ399991	JQ400019
C. horii	ICMP 10492	GQ329690	GQ329681	JX009438	JX010450
C. incanum	ATCC 64682*	KC110789	KC110807	KC110825	KC110816
C. jasminigenum	MFU 10–0273*	HM131513	HM131499	HM131508	HM153770
C. jiangxiense	LF 488*	KJ955149	KJ954850	KJ954427	–
C. kahawae	ICMP 17816*	JX010231	JX010012	JX009452	JX010444
C. kartsii	CORCG 6*	HM585409	HM585391	HM581995	HM585428
C. laticiphilum	CBS 112989*	JQ948289	JQ948619	JQ949610	JQ949940
C. lilii	CBS 109214	GU227810	GU228202	GU227908	GU228104
C. lindemuthianum	CBS 144.31*	JQ005779	JX546712	JQ005842	JQ005863
C. linicola	CBS 172.51	JQ005765	–	JQ949476	JQ949806
C. liriopes	CBS 119444*	GU227804	GU228196	GU227902	GU228098
*C. magnisporu*m	CBS 398.84	KF687718	KF687842	KF687803	KF687882
C. malvarum	CBS 527.97*	KF178480	KF178504	KF178577	KF178601
C. menispermi	MFLU 14–0625*	KU242357	KU242356	KU242353	KU242354
C. miscanthi	MAFF 510857*	JX519221	–	JX519237	JX519246
C. musae	ICMP 19119*	JX010146	JX010050	JX009433	HQ596280
C. navitas	CBS 125086*	JQ005769	–	JQ005832	JQ005853
C. nicholsonii	MAFF 511115*	JQ005770	–	JQ005833	JQ005854
C. novae–zelandiae	CBS 128505*	JQ005228	JQ005315	JQ005576	JQ005662
C. nupharicola	ICMP 18187*	JX010187	JX009972	JX009437	JX010398
C. ochraceae	CGMCC 3.15104*	JX625156	KC843513	KC843527	JX625183
C. oncidii	CBS 129828*	JQ005169	JQ005256	JQ005517	JQ005603
C. orchidophilum	CBS 632.80*	JQ948151	JQ948481	JQ949472	JQ949802
C. parsonsiae	CBS 128525*	JQ005233	JQ005320	JQ005581	JQ005667
C. paspali	MAFF 305403*	JX519219	–	JX519235	JX519244
C. petchii	CBS 378.94*	JQ005223	JQ005310	JQ005571	JQ005657
C. phaseolorum	CBS 157.36	GU227896	GU228288	GU227994	GU228190
C. phyllanthi	CBS 175.67*	JQ005221	JQ005308	JQ005569	JQ005655
C. pseudoacutatum	CBS 436.77*	JQ948480	JQ948811	JQ949801	JQ950131
C. pseudomajus	CBS 571.88*	NR132059	KF687826	KF687801	KF687883
C. psidii	ICMP 19120	JX010219	JX009967	JX009515	JX010443
C. radicis	CBS 529.93*	NR132057	KF687825	KF687785	KF687869
C. rhexiae	Coll 1026*	JX145128	–	–	JX145179
C. rhombiforme	CBS 129953*	JQ948457	JQ948788	JQ949778	JQ950108
C. riograndense	COAD 928*	KM655299	KM655298	KM655295	KM655300
C. rusci	CBS 119206*	GU227818	GU228210	GU227916	GU228112
C. salsolae	ICMP 19051*	JX010242	JX009916	JX009562	JX010403
C. siamense	ICMP 18578*	JX010171	JX009924	FJ907423	JX010404

Species	Isolate[a]	GenBank accession number			
		ITS	GAPDH	ACT	ß–tubulin
C. sichuanensis	LJTJ3	KP748193	KP823773	KP823738	KP823850
C. spinaciae	CBS 128.57	GU227847	GU228239	GU227945	GU228141
C. sublineola	CBS 131301*	JQ005771	–	JQ005835	JQ005855
C. syzygicola	DNCL 021*	KF242094	KF242156	KF157801	KF254880
C. tanaceti	CBS 132693*	–	JX218243	JX218238	JX218233
C. tebeestii	CBS 522.97*	KF178473	KF178505	KF178570	KF178594
C. temperatum	Coll 883*	JX145159	–	–	JX145211
C. theobromicola	ICMP 18649	JX010294	JX010006	JX009444	JX010447
C. ti	ICMP 4832*	JX010269	JX009952	JX009520	JX010442
C. torulosum	CBS 128544*	JQ005164	JQ005251	JQ005512	JQ005598
C. trichellum	CBS 217.64*	GU227812	GU228204	GU227910	GU228106
C. trifolii	CBS 158.83*	KF178478	KF178502	KF178575	KF178599
C. tropicicola	BCC 38877*	JN050240	JN050229	JN050218	JN050246
C. trucatum	CBS 151.35	GU227862	GU228254	GU227960	GU228156
C. verruculosm	IMI 45525*	GU227806	GU228198	GU227904	GU228100
C. vietnamense	CBS 125478*	KF687721	KF687832	KF687792	KF687877
C. viniferum	GZAAS 5.0860*1**	JN412804	JN412798	JN412795	JN412813
C.$1×anthorrhoeae	ICMP 17903*	JX010261	JX009927	JX009478	JX010448
C. yunnanense	CGMCC AS3.9167*	EF369490	–	JX519239	JX519248
Australiasca queenslandica	BRIP 24607	HM237327	–	–	–
Monilochaetes guadalcanalensis	CBS 346.76	GU180625	–	–	–
Monilochaetes infuscans	CBS 869.96	JQ005780	JX546612	JQ005843	JQ005864

[a]Isolates marked with "*" are extype or ex-epitype strains.

Appendix B

Fungal isolates and sequences of region/genes in this study.

Species	Isolate	GenBank accession number			
		ITS	GAPDH	ACT	ß–tubulin
C. boninense	MFLU 14-0124	MG792809	MK165700	–	MH351286
	MFLU 14-0086	MG792816	MH673668	MH376390	MH351281
	MFLU 14-0261	MG792815	MK165703	MH376400	MH351292
C. cariniferi	MFLU 14-0100	MF448521	–	–	MH351274
C. chiangraiense	MFLU 14-0119	MF448522	–	MH376383	MH351275
C. citricola	MFLU 14-0129	MG792821	MK165697	MH376395	MH351287
	MFLU 14-0131	MG792822	MK165696	MH376396	MH351288
C. doitungense	MFLU 14-0128	MF448524	MH049480	MH376385	MH351277
C. fructicola	MFLU 14-0087	MG792812	MK165691	MH376391	MH351282
	MFLU 14-0262	MG792814	MK165698	MH376401	MH351293
	MFLU 14-0148	MG792813	MK165701	MH376397	MH351289
C. jiangxiense	MFLU 14-0091	MG792806	MH673669	MH376392	MH351283
	MFLU 14-0092	MG792807	MH673670	MH376393	MH351284
C. orchidophilum	MFLU 14-0161	MG792818	MK165702	MH376398	MH351290
	MFLU 14-0162	MG792819	MK165704	MH376399	MH351291
C. parallelophorum	MFLU 14-0085	MF448525	MK165695	–	MH351280
	MFLU 14-0077	MG792808	MK165692	MH376387	MH351279
	MFLU 14-0079	MG792820	MK165693	MH376388	–
	MFLU 14-0082	MG792810	MK165694	MH376389	–
	MFLU 14-0083	MG792811	MH049478	MH376386	MH351278
C. sp. indet.	MFLU 14-0120	MG792817	MK165699	MH376394	MH351285
C. watphraense	MFLU 14-0123	MF448523	MH049479	MH376384	MH351276

MycoKeys 43: 59–74 (2018)
doi: 10.3897/mycokeys.43.30203
http://mycokeys.pensoft.net

RESEARCH ARTICLE

A peer-reviewed open-access journal
MycoKeys
Launched to accelerate biodiversity research

Lecanicillium cauligalbarum sp. nov. (Cordycipitaceae, Hypocreales), a novel fungus isolated from a stemborer in the Yao Ren National Forest Mountain Park, Guizhou

Ye-Ming Zhou[1,2], Jun-Rui Zhi[1], Mao Ye[1], Zhi-Yuan Zhang[2], Wen-Bo Yue[1], Xiao Zou[2]

1 *The Provincial Key Laboratory for Agricultural Pest Management of the Mountainous Region, Institute of Entomology, Guizhou University, Guiyang 550025, Guizhou, China* **2** *Institute of Fungus Resources, Guizhou University, Guiyang, Guizhou 550025, China*

Corresponding authors: *Jun-Rui Zhi* (jrzhi@gzu.edu.cn); *Xiao-Zou* (xzou@gzu.edu.cn)

Academic editor: *T. Lumbsch* | Received 30 September 2018 | Accepted 8 November 2018 | Published 4 December 2018

Citation: Zhou Y-M, Zhi J-R, Ye M, Zhang Z-Y, Yue W-B, Zou X (2018) *Lecanicillium cauligalbarum* sp. nov. (Cordycipitaceae, Hypocreales), a novel fungus isolated from a stemborer in the Yao Ren National Forest Mountain Park, Guizhou. MycoKeys 43: 59–74. https://doi.org/10.3897/mycokeys.43.30203

Abstract

A new species of entomopathogenic fungi, *Lecanicillium cauligalbarum*, was discovered from a survey of invertebrate-associated fungi in the Yao Ren National Forest Mountain Park in China. The synnemata of this species emerged from the corpse of a stemborer (Lepidoptera), which was hidden amongst pieces of wood on the forest floor. It differs from morphologically similar *Lecanicillium* species mainly in its short conidiogenous cells and ellipsoid to ovoid and aseptate conidia. Phylogenetic analysis of a combined data set comprising ITS, *SSU*, *LSU*, *TEF*, *RPB1* and *RPB2* sequence data supported the inclusion of *L. cauligalbarum* in the *Lecanicillium* genus and its recognition as a distinct species.

Keywords

Entomopathogenic fungi, *Lecanicillium*, multiple genes, phylogeny, new species

Introduction

The entomopathogenic fungal genus *Lecanicillium* W. Gams & Zare belongs to Ophiocordycipitaceae. It is typified by *Lecanicillium lecanii* with *Torrubiella confragosa* as the sexual morph (Zare and Gams 2001, Wijayawardene et al. 2017). *Lecanicillium lecanii*

was first named as *Cephalosporium lecanii* Zimm. by Zimmermann in 1898. Viegas incorporated the species in *Verticillium* Nees in 1939 (Gams and Zare 2001). The genus *Verticillium* has a wide host range, including arthropods, nematodes, plants and fungi (Goettel et al. 2008). Zare and Gams (2001) recircumscribed the genus following analyses of morphological data and sequence data for the internal transcribed spacer (ITS) rDNA region (which comprises the ITS1 spacer, 5.8S coding region and ITS2 spacer). All insect pathogens formerly included in *Verticillium* were reclassified in a newly established genus, *Lecanicillium*. In more recent studies, a multilocus nuclear DNA dataset combining sequence data for the nuclear small subunit rDNA (*SSU*), nuclear large subunit rDNA (*LSU*), translation elongation factor 1α (*TEF*), DNA-dependent RNA polymerase II largest subunit (*RPB1*) and DNA-dependent RNA polymerase II second largest subunit (*RPB2*) genes suggests that the genus *Lecanicillium* is paraphyletic (Sung et al. 2007). Phylogenetic analysis of ITS sequence data also supports this conclusion (Sukarno et al. 2009). Kepler et al. (2017) revisited the taxonomic affinities of the Cordycipitaceae (Hypocreales) and proposed that *Lecanicillium* should be rejected because *L. lecanii* is included within the *Akanthomyces* clade and the name *Akanthomyces* Lebert has nomenclatural priority over *Lecanicillium* (Kepler et al. 2017). However, Kepler et al. (2017) transferred to *Akanthomyces* only several species for which sufficient information was available. The phylogenetic affinities of the majority of species in the original circumscription of *Lecanicillium* remain uncertain. Given that there remain unresolved phylogenetic and taxonomic matters concerning *Lecanicillium*, Huang et al. (2018) and Crous et al. (2018) chose to describe new taxa in *Lecanicillium* to avoid creating further confusion in the taxonomy (Crous et al. 2018; Huang et al. 2018).

Presently, 29 *Lecanicillium* species have been formally described and are listed in the Index Fungorum (http://www.indexfungorum.org). Zare and Gams (2001) recognised 14 *Lecanicillium* species based primarily on morphology and ITS sequence data (Zare and Gams 2001). Subsequently, an additional five new *Lecanicillium* species, based on ITS sequence data, were described (Kope and Leal 2006, Sukarno et al. 2009, Kaifuchi et al. 2013). In order to add more sequence information with ITS, Zare and Gams (2008) reassessed the genus *Verticillium* and transferred four species to *Lecanicillium* based on ITS and *SSU* sequence data (Zare and Gams 2008). Except for the *SSU* and ITS gene, more and more researchers have labelled the *Lecanicillium* genus by *TEF* gene. Based on this, two new *Lecanicillium* species were confirmed based on combined with ITS and *TEF* sequence data (Crous et al. 2018). With combined multigene identification of species gradually becoming the convention, two new *Lecanicillium* species were identified based on multilocus (*TEF*, *RPB1*, *RPB2*, *LSU* and *SSU*) sequence data (Park et al. 2016, Chen et al. 2017). *Lecanicillium sabanense* was identified based on phylogenetic analysis of combined multilocus and ITS sequences (Chiriví-Salomón et al. 2015). *Lecanicillium subprimulinum* was identified based on combined analysis of *LSU*, *SSU*, *TEF* and ITS sequence data (Huang et al. 2018).

We carried out a survey of invertebrate-associated fungi in the Yao Ren National Forest Mountain Park near Sandu county in Guizhou province, China. A parasitic

fungus was found on a stemborer (Lepidoptera) hiding amongst pieces of wood. Attempting to identify the fungus, we determined it to be a member of *Lecanicillium* but its morphological traits and gene sequences did not correspond with those of any known *Lecanicillium* species. On the basis of its morphology and molecular phylogenetic analysis of multilocus nuclear genes (*TEF*, *RPB1*, *RPB2*, *LSU* and *SSU*) and ITS sequence data, this fungus was suggested to be an unnamed species of *Lecanicillium* and is here described and named *Lecanicillium cauligalbarum* sp. nov.

Materials and methods

Specimen collection and fungus isolation

The specimen was collected from Yao Ren National Forest Mountain Park, Sandu county, Guizhou, China (107°53', 107°58'E; 24°54', 25°59'N, approximately 560–1365 m above sea level), in September 2015 by Yeming Zhou and Xiao Zou. The synnemata of this species emerged from a dead stemborer (Lepidoptera) hidden amongst pieces of wood on the forest floor. The specimen GZUIFR–2015ZHJ and two isolated strains of the fungal asexual stage, GZUIFRZHJ01 and GZUIFRZHJ02, were deposited at the Institute of Fungal Resources of Guizhou University (GZUIFR). The fungal strains were isolated on potato dextrose agar (PDA) medium; one strain was isolated from part of the body and the second strain was isolated from the synnemata.

Strain culture and identification

The isolated strains were inoculated on PDA at 25 °C for 14 d under 12-h light/12-h dark conditions. The fresh hyphae were observed with an optical microscope (OM, BK5000, OPTEC, USA) following pretreatment with lactophenol cotton blue solution or normal saline.

DNA extraction, PCR amplification and sequencing

Genomic DNA was extracted using a previously described method (Chiriví-Salomón et al. 2015, Zou et al. 2016). The primers used for PCR amplification of the ITS region, *SSU*, *LSU*, *TEF*, *RPB1* and *RPB2* are listed in Table 1. The PCR reaction conditions employed for each genetic region followed those used in the references listed in Table 1.

To conduct phylogenetic analysis of the sequences obtained, sequences for selected taxa based on recent phylogenetic studies of *Lecanicillium* (Chen et al. 2017, Huang et al. 2018) and Cordycipitaceae (Sung et al. 2007, Kepler et al. 2017, Mongkolsamrit et al. 2018) were downloaded from the National Center for Biotechnology Infor-

Table 1. Primer information and provenance in this study.

Gene	Primer	Provenance
ITS	F: 5'-TCCGTAGGTGAACCTGCGG-3'	White et al. 1990
	R: 5'-TCCTCCGCTTATTGATATGC-3'	
SSU	F: GTAGTCATATGCTTGTCTC	White et al. 1990
	R: CTTCCGTCAATTCCTTTAAG	
LSU	F: GTTTCCGTAGGTGAACCTGC	Curran et al. 1994
	R: ATATGCTTAAGTTCAGCGGGT	
TEF	F: 5'-GCCCCCGGCCATCGTGACTTCAT-3'	van den Brink et al. 2011
	R: 5'-ATGACACCGACAGCGACGGTCTG-3'	
RPB1	F: 5'-CCWGGYTTYATCAAGAARGT-3'	Castlebury et al. 2004
	R: 5'-CAYCCWGGYTTYATCAAGAA-3'	
RPB2	F: 5'-GACGACCGTG ATCACTTTGG-3'	van den Brink et al. 2011
	R: 5'-CCCATGGCCTGTTTGCCCAT-3'	

mation GenBank database (https://www.ncbi.nlm.nih.gov/genbank/). A total of 79 accessions of Cordycipitaceae were selected for this study. The sequences used in the study are listed in Table 2.

Sequence alignment and phylogenetic analyses

The DNA sequences used in this study were edited using the LASERGENE software (version 6.0; DNASTAR, Madison, WI, USA). Multiple sequence alignments for *TEF*, *RPB1* and *RPB2* were performed in MAFFT (Katoh and Standley 2013) with the default settings. Multiple sequence alignments for ITS, *LSU* and *SSU* were conducted using MUSCLE algorithm (Edgar 2004) from MEGA 6 (Tamura et al. 2013). The sequences were edited manually. A multiple alignment of the combined partial ITS+*SSU*+*LSU*+*TEF*+*RPB1*+*RPB2* sequences were assembled with MEGA 6 (Tamura et al. 2013) and SEQUENCEMATRIX 1.7.8 (Vaidya et al. 2011). The command 'hompart' in PAUP* 4.0b10 was used for assessment of concordance amongst the genes and the ITS region (Swofford 2001). Bayesian inference (BI) was performed using MRBAYES 3.2 (Ronquist et al. 2012) and maximum likelihood (ML) analysis was performed using RAxML (Alexandros 2014) to analyse the combined data which were divided into twelve separate partitions (Kepler et al. 2017; Mongkolsamrit et al. 2018). Two maximum likelihood (ML) analysis and Bayesian inference (BI) analysis were performed. The first analysis was performed as reported by Huang et al. (2018), using the *Simplicillium lanosoniveum* as the outgroup. The second analysis was performed with *Akanthomyces*, *Samsoniella*, *Blackwellomyces*, *Hevansia*, *Simplicillium*, all the *lecanicillium* and use of *Beauveria* as outgroup (Mongkolsamrit et al. 2018). Nucleotide substitution models were determined by MrModeltest 2.3 (Nylander 2004). For BI, 10 000 000 generations were performed with one tree selected every 500th generation and the GTR+I+G evolutionary model was used. For ML, the model GTRGAMMA was used and a bootstrap analysis with 500 replicates was performed to assess statistical support for the tree topology. Phylogenetic trees were viewed with TREEGRAPH.

Table 2. Specimen information and GenBank accession numbers used in this study.

Species	Voucher Information	ITS	*SSU*	*LSU*	*TEF*	*RPB1*	*RPB2*
Akanthomyces waltergamsii	TBRC 7250	MF140749		MF140715	MF140835		
A. waltergamsii	TBRC 7251	MF140747		MF140713	MF140833	MF140781	MF140805
A. sulphureus	TBRC 7248	MF140758		MF140722	MF140843	MF140787	MF140812
	TBRC 7249	MF140757		MF140721	MF140842	MF140786	MF140734
A. thailandicus	TBRC 7246	MF140755		MF140719	MF140840		MF140810
	TBRC 7245	MF140754			MF140839		MF140809
A. kanyawimiae	TBRC 7242	MF140751		MF140718	MF140838	MF140784	MF140808
	TBRC 7244	MF140752		MF140716	MF140836		
A. aculeatus	HUA 186145		MF416572	MF416520	MF416465		
A. pistillariaeformis	HUA 186131		MF416573	MF416521	MF416466		
A. coccidioperitheciatus	NHJ 6709	JN049865	EU369110	EU369042	EU369025	EU369067	EU369086
A. aculeatus	TS 772	KC519371	KC519368	KC519370	KC519366		
A. tuberculatus	BCC16819		MF416600	MF416546	MF416490	MF416647	MF416490
Ascopolyporus villosus	ARSEF 6355			AY886544	DQ118750	DQ127241	
Asc. polychrous	P.C. 546			DQ118737	DQ118745	DQ127236	
Beauveria bassiana	ARSEF 1564	HQ880761			HQ880974	HQ880833	HQ880905
Bea. brongniartii	BCC 16585	JN049867	JF415951	JF415967	JF416009	JN049885	JF415991
Blackwellomyces cardinalis	OSC 93610	JN049843	AY184974	AY184963	EF469059	EF469088	EF469106
Bla. cardinalis	OSC 93609		AY184973	AY184962	DQ522325	DQ522370	DQ522422
Bla. pseudomilitaris	NBRC 101409	JN943305	JN941748	JN941393		JN992482	
	NBRC 101410	JN943307	JN941747	JN941394		JN992481	
Gibellula longispora	NHJ 12014		EU369098		EU369017	EU369055	EU369075
Gibellula sp.	NHJ 7859		EU369107			EU369064	EU369085
	NHJ 10788		EU369101	EU369036	EU369019	EU369058	EU369078
	NHJ 5401		EU369102			EU369059	EU369079
G. ratticaudata	ARSEF 1915	JN049837	DQ522562	DQ518777	DQ522360	DQ522408	DQ522467
Hevansia nelumboides	BCC 41864	JN201871	JN201863	JN201873	JN201867		
Hev. novoguineensis	NHJ 11923		EU369095	EU369032	EU369013	EU369052	EU369072
Hev. arachnophila	NHJ 10469		EU369090	EU369031	EU369008	EU369047	
Hev. cinerea	NHJ 3510		EU369091		EU369009	EU369048	EU369070
Lecanicillium acerosum	CBS418.81	EF641893	KM283762	KM283786	KM283810	KM283832	KM283852
L. antillanum	CBS350.85	AJ292392	AF339585	AF339536	DQ522350	DQ522396	DQ522450
L. aphanocladii	CBS797.84		KM283763	KM283787	KM283811	KM283833	KM283853
L. aranearum	CBS726.73a	AJ292464	AF339586	AF339537	EF468781	EF468887	EF468934
L. araneicola	BTCC-F35	AB378506					
L. araneogenum	GZU1031Lea		KX845705	KX845703	KX845697	KX845699	KX845701
L. attenuatum	CBS402.78	AJ292434	AF339614	AF339565	EF468782	EF468888	EF468935
	KACC42493		KM283756	KM283780	KM283804	KM283826	KM283846
L. cauligalbarum	**GZUIFRZHJ01**	**MH730663**	**MH730665**	**MH730667**	**MH801920**	**MH801922**	**MH801924**
	GZUIFRZHJ02	**MH730664**	**MH730666**	**MH730668**	**MH801921**	**MH801923**	**MH801925**
L. dimorphum	CBS345.37		KM283764	KM283788	KM283812	KM283834	KM283854
L. flavidum	CBS300.70D	EF641877	KM283765	KM283789	KM283813		KM283855
L. fungicola var. aleophilum	CBS357.80	NR_111064	KM283767	KM283791	KM283815	KM283835	KM283856
L. fungicola var. fungicola	CBS992.69	NR_119653	KM283768	KM283792	KM283816		KM283857
L. fusisporum	CBS164.70	AJ292428	KM283769	KM283793	KM283817	KM283836	KM283858
L. kalimantanense	BTCC-F23	AB360356					
L. lecanii	CBS101247	JN049836	KM283770	KM283794	DQ522359	KM283837	KM283859
	CBS102067		KM283771	KM283795	KM283818	KM283838	KM283860
L. longisporum	CBS102072		KM283772	KM283796	KM283819	KM283839	KM283861
	CBS126.27		KM283773	KM283797	KM283820	KM283840	KM283862
L. muscarium	CBS143.62		KM283774	KM283798	KM283821	KM283841	KM283863

Species	Voucher Information	ITS	*SSU*	*LSU*	*TEF*	*RPB1*	*RPB2*
L. nodulosum	IMI 338014R	EF513012	EF513075				
L. pissodis	CBS118231		KM283775	KM283799	KM283822	KM283842	KM283864
L. primulinum	JCM 18525	AB712266		AB712263			
	JCM 18526	AB712267		AB712264			
L. psalliotae	CBS532.81	JN049846	AF339609	AF339560	EF469067	EF469096	EF469112
	CBS101270		EF469128	EF469081	EF469066	EF469095	EF469113
	CBS363.86		AF339608	AF339559	EF468784	EF468890	
L. restrictum	CCF5252	LT548279			LT626943		
L. sabanense	JCHA5	KC633232	KC633251	KC875225	KC633266		KC633249
L. saksenae	IMI 179841	AJ292432					
L. subprimulinum	HKAS99548	MG585314	MG585316	MG585315	MG585317		
	HKAS99549	MG585318	MG585320	MG585319	MG585321		
L. testudineum	UBOCC-A112180	LT992874			LT992868		
	UBOCC-A116026	LT992871			LT992867		
L. tenuipes	CBS309.85	JN036556	KM283778	KM283802	DQ522341	KM283844	KM283866
L. uredinophilum	KACC44082		KM283758	KM283782	KM283806	KM283828	KM283848
	KACC47756		KM283759	KM283783	KM283807	KM283829	KM283849
L. wallacei	CBS101237	EF641891	AY184978	AY184967	EF469073	EF469102	EF469119
Samsoniella inthanonensis	TBRC 7915	MF140761		MF140725	MF140849	MF140790	MF140815
Sam. inthanonensis	TBRC 7916	MF140760		MF140724	MF140848	MF140789	MF140814
Sam. aurantia	TBRC 7271	MF140764		MF140728	MF140846	MF140791	MF140818
	TBRC 7272	MF140763		MF140727	MF140845		MF140817
Sam. alboaurantium	CBS 240.32	AY624178	JF415958	JF415979	JF416019	JN049895	JF415999
	CBS 262.58	MH857775		MH869308	JQ425685	MF416654	MF416448
Simplicillium lamellicola	CBS 116.25	AJ292393	AF339601	AF339552	DQ522356	DQ522404	DQ522462
Sim. lanosoniveum	CBS 704.86	AJ292396	AF339602	AF339553	DQ522358	DQ522406	DQ522464
	CBS 101267	AJ292395	AF339603	AF339554	DQ522357	DQ522405	DQ522463
Sim. obclavatum	CBS 311.74		AF339567	AF339517	EF468798		

Results

Sequencing and phylogenetic analysis

The first sequence dataset consisted of 3793 bases, including inserted gaps (ITS: 506 bp; *SSU*: 579 bp; *LSU*: 490 bp; *TEF*: 772 bp; *RPB1*: 561 bp; *RPB2*: 885 bp). The second sequence dataset consisted of 2944 bases, including inserted gaps (ITS: 526 bp; *SSU*: 456 bp; *LSU*: 409 bp; *TEF*: 386 bp; *RPB1*: 500 bp; *RPB2*: 667 bp). No significant differences in topology were observed between the BI and ML phylogenies. The first tree formed with almost all the *Lecanicillium* species (only *Lecanicillium evansii* could not be found in the NCBI) and one *Simplicillium* species (*Simplicillium lanosoniveum*). The phylogeny was resolved into 4 clades obviously. *Lecanicillium cauligalbarum* formed an independent branch in a polytomy together with a clade containing *L. flavidum* and *L. fungicola* and a major clade consisting of 27 accessions. The *L. cauligalbarum* lineage received maximum statistical support (BI posterior probabilities 1, ML boostrap 100%), which still remains unnamed (Figure 1). In the second tree, the four *Lecanicillium* clades were also be supported. *Lecanicillium cauligalbarum* formed an independent branch in a polytomy together with a clade containing *Blackwellomyces cardinalis* and *Blackwellomyces pseudomilitaris* (BI posterior probabilities 1, ML boostrap 85%) (Figure 2).

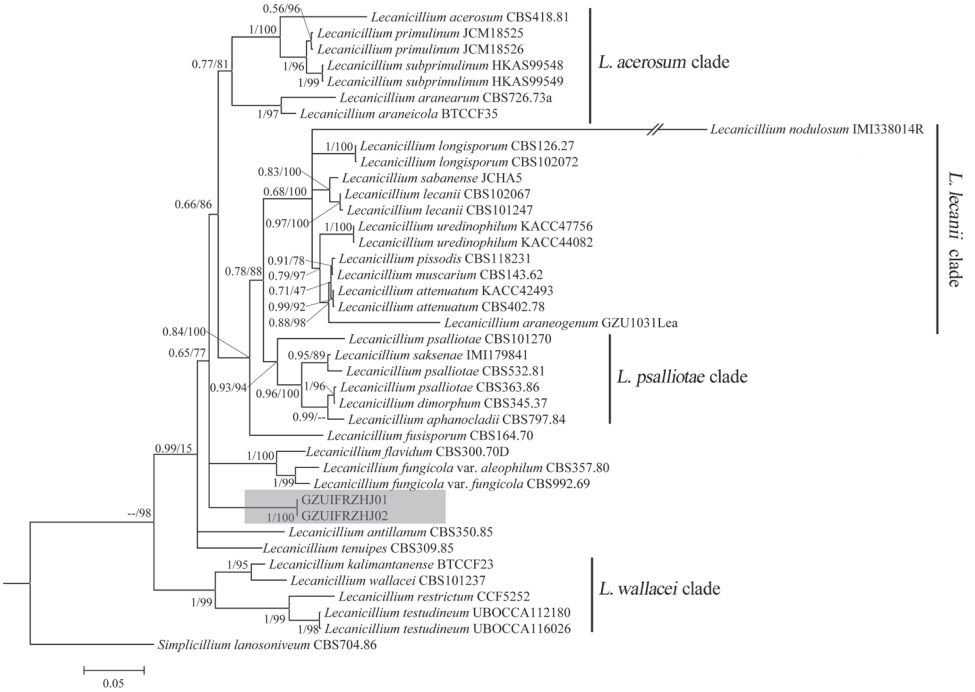

Figure 1. Phylogenetic analysis of the isolated strains GZUIFRZHJ01 and GZUIFRZHJ02 and related species derived from a combined dataset of partial ITS+*SSU*+*LSU*+*TEF*+*RPB1*+*RPB2* sequences. Statistical support values (≥ 0.5/50%) are shown at the nodes for BI posterior probabilities/ML boostrap support.

Taxonomy

Lecanicillium cauligalbarum **X. Zou, J.R. Zhi & Y.M. Zhou, sp. nov.**
MycoBank: MB827984
Figure 3

Diagnosis. Characterised by phialides gradually tapering towards the apex, solitary or 2–3 whorls, 9–14.4 × 1.4–1.8 µm. Conidia cylindric, aseptate, 3.6–6.3 × 0.9–1.8 µm.

Type. CHINA, Guizhou Province, Sandu county (107°53', 107°58'E; 24°54', 25°59'N, approximately 560–1365 m above sea level), September 2015, Yeming Zhou & Xiao Zou. Sequences from isolated strains (GZUIFRZHJ01 and GZUIFRZHJ02) have been deposited in GenBank (accession numbers to be provided).

Description. Colony on PDA 15 mm in diameter after 7 days, 33 mm in diameter after 14 days at 25 °C, colony circular, white, cottony, umbonate, with radiating surface texture from above, with clear radial crack and primrose-yellow from reverse. Mycelium 0.9–1.8 µm wide, hyaline, smooth, septated, branched. Conidiophores usually arising from aerial hyphae, sporulate abundant. Phialides gradually tapering towards the apex, solitary or 2–3 whorls, 9–14.4 × 1.4–1.8 µm. Conidia cylindric, aseptate, 3.6–6.3 × 0.9–1.8 µm. In culture, both phialides and conidia are of similar general shape and size to those found on the host stemborer.

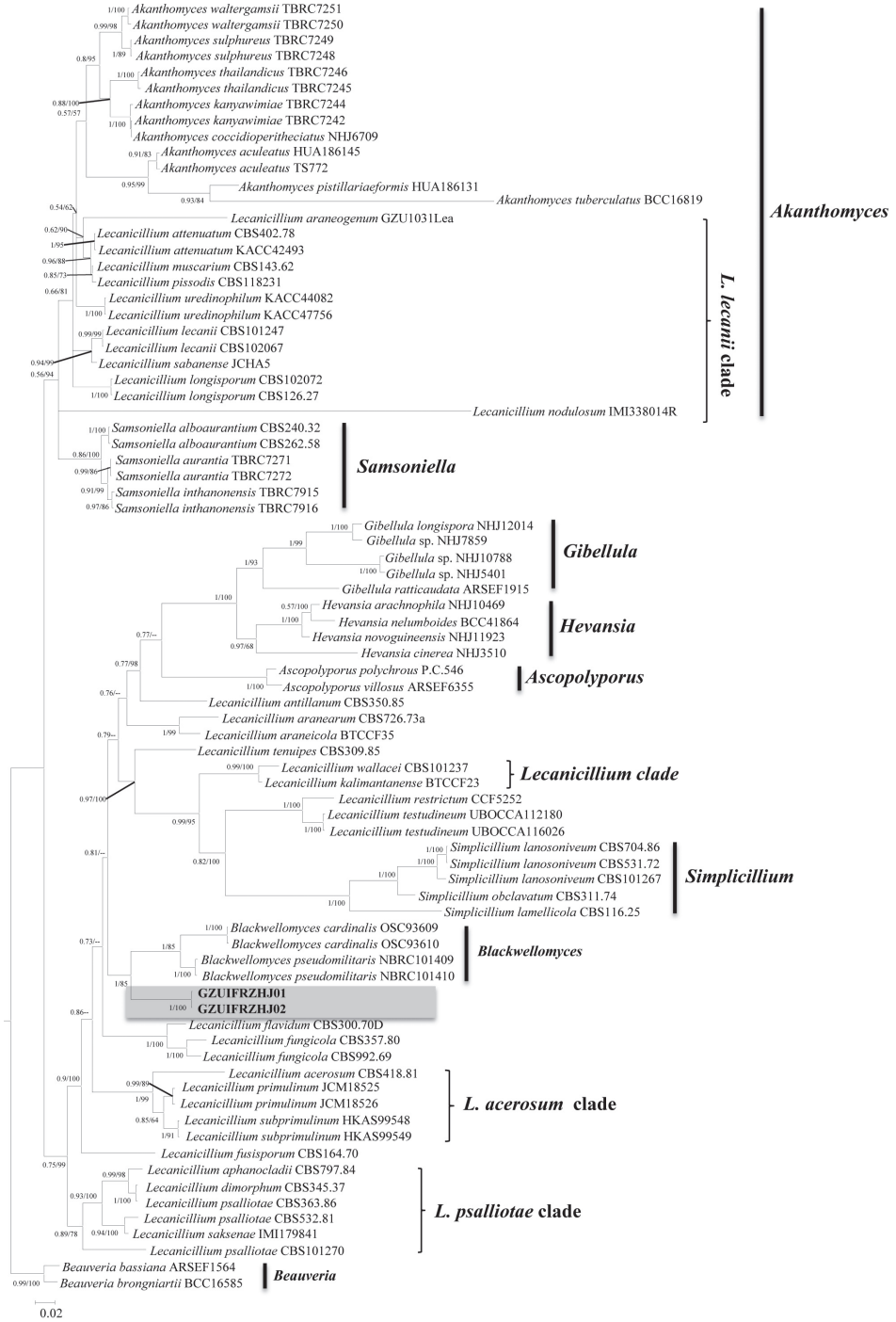

Figure 2. Phylogenetic relationships of the form genus *Lecanicillium*, *Akanthomyces*, *Samsoniella*, *Blackwellomyces*, *Hevansia* and related genera in the Cordycipitaceae. Statistical support values (≥ 0.5/50%) are shown at the nodes for BI posterior probabilities/ML boostrap support.

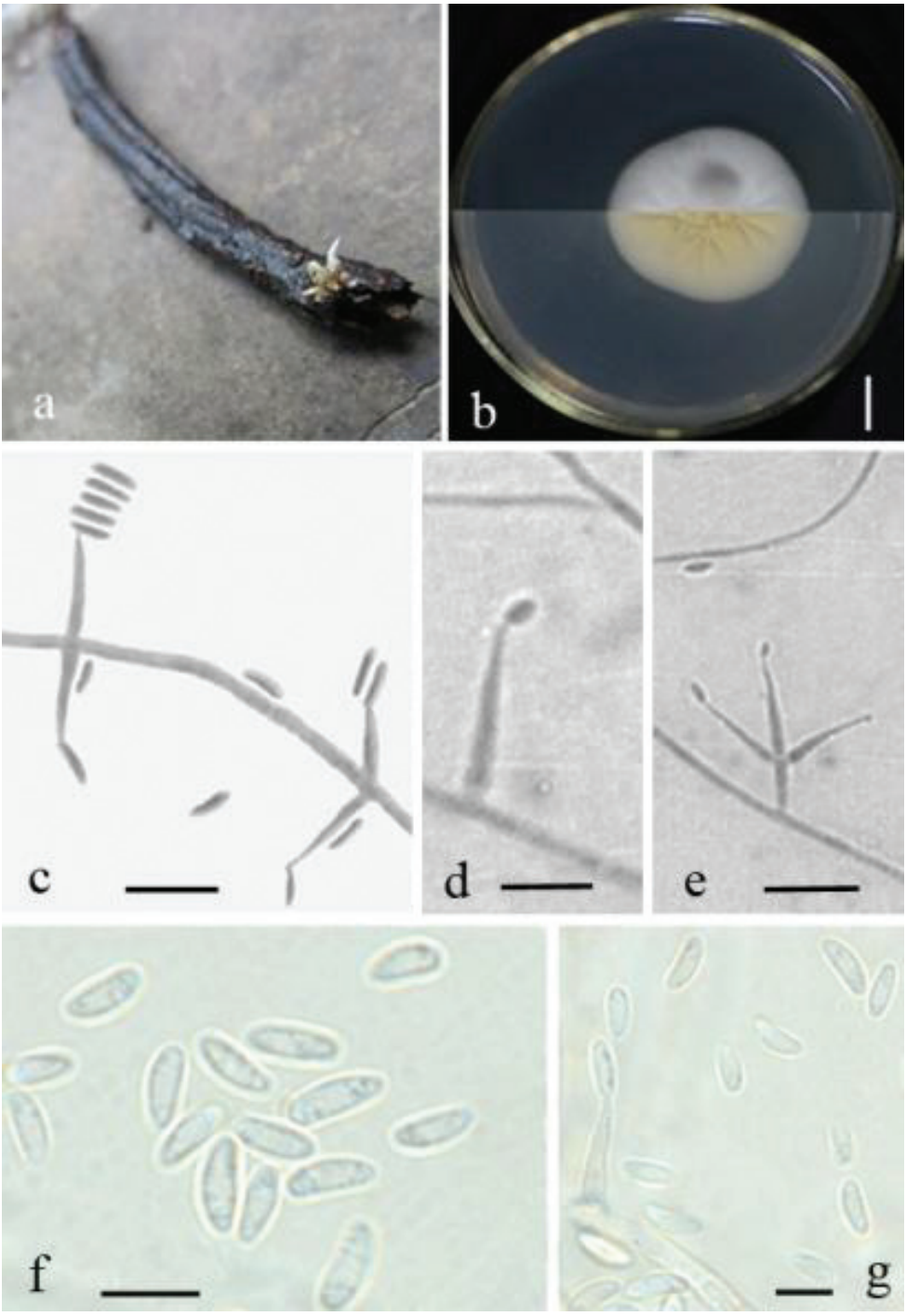

Figure 3. *Lecanicillium cauligalbarum*. **a** Synnemata emerged from the corpse of a stemborer (Lepidoptera) **b** Culture plate, showing the front (upper) and the back (lower) of the colony, cultured on PDA medium **c–e** Phialides solitary or in 2–3 whorls **f–g** Conidia. Scale bars: 10 mm (**b, c, e**), 5 μm (**d, f, g**).

Host. Stemborer (Lepidoptera) hidden amongst wooden sticks.

Habitat and distribution. Hidden amongst pieces of wood in humid forests of southwest China.

Etymology. The epithet '*cauligalbarum*' refers to the host (stemborer).

Teleomorph. Not known.

Remarks. With regard to phylogenetic relationships, *L. cauligalbarum* is closely related to the *L. fungicola* clade and *L. fusisporum*. The two strains (GZUIFRZHJ01 and GZUIFRZHJ02) formed a distinct lineage. All *Lecanicillium* species were included in the phylogenetic analysis except for *L. evansii* for which sequence data could not be located in public databases, although Zare and Gams (2001) published ITS sequences. The morphological features of *L. evansii* include brownish-cream to brown reverse, phialides solitary or up to 3–4 per node and two types of the conidia, slightly falcate with a pointed end macroconidia 4.5–7.5 × 0.8–1.2 μm and slightly curved microconidia 2.0–3.0 × 0.8–1.2 μm (Zare and Gams 2001). *L. evansii* is distinct from *L. cauligalbarum*, which has conidia of 3.6–6.3 × 0.9–1.8 μm and 9–14.4 × 1.4–1.8 μm phialides.

In morphology *L. cauligalbarum*is is similar to *L. aphanocladii*, *L. attenuatum* and *L. nodulosum* with regard to the short conidiogenous cell (Table 3). However, *L. cauligalbarum* is distinguished by the pattern of spore production and the frequency of the wheel structure.

Table 3. Morphological comparison among *Lecanicillium cauligalbarum* and the other related species.

Species	Colonies	Conidiogenous cell	Conidia	Refrence
Lecanicillium acerosum	White, yellow reverse	Solitary or up to 4–5, 30–32×1.8–2.2 μm	Macroconidia fusiform, straight to slightly falcate, 15–20×1.6–2.2 μm, microconidia fusiform, 4.5–7.5×1.0–1.5 μm	Zare and Gams 2001
L. antillanum	White, cream-coloured reverse	Solitary or up to 6, subulate, 18–31×1 μm (at the top)	Macroconidia fusiform, 11–18×0.8–1.5 μm, microconidia ellipsoidal, 3–4×0.8–1.2 μm	Zare and Gams 2001
L. aphanocladii	White, red, reddish-white to cream-coloured reverse	Solitary, in pairs, verticillate, flask-shaped in the beginning, tapering into a thread-like neck, 4.5–11×1.0–1.8 μm	Solitary, oval to sub-globose, 2.7–4×1.5–2.2 μm	Zare and Gams 2001
L. aranearum	White, yellowish-cream reverse	Tapering towards the apex, 20–30×1.2–1.5 μm	Straight or curved, usually asymmetrically narrowed or subacute at the ends, 5–8×0.7–1.5 μm	Zare and Gams 2001
L. araneicola	White, creamy-white reverse	Solitary or in whorls of 2–4, slender, tapering toward the tip, (14-)19–31.5×1–2 μm	Macroconidia slightly curved to nearly straight, (7.5-)8.5–12(-14)×1.5–2 μm, microconidia allantoid to ellipsoidal with round ends, 3–5×1–2 μm	Sukarno et al. 2009
L. araneogenum	White to light grey, light yellow reverse	Produced in whorls of (1-)2–6(-8), 30–64×1.1–3.2 μm	Forming mostly globose heads, cylindric, 3.2–8.6×1.3–1.6 μm	Chen et al. 2017
L. attenuatum	White, yellowish-white reverse	Up to 3–5 per node, 9–15.5×1–2 μm	Cylindrical with attenuate base, 4.5–6.5×1.5–2.0 μm	Zare and Gams 2001
L. cauligalbarum	White, primrose-yellow reverse	Solitary or 2–3 whorls, 9–14.4×1.4–1.8 μm	Cylindrical, 3.6–6.3×0.9–1.8 μm	**This work**
L. dimorphum	White, cream to brownish-cream, red reverse	Two kinds: solitary or 4–5 whorls, 14–30×1.0–1.5μm; short, 5–12×0.7–1.5 μm	Macroconidia falcate with sharply pointed ends, usually evenly curved, 6–11×1.5–2.5μm, microconidia oval to ellipsoidal, 2.5–4.5×1.0–1.5 μm	Zare and Gams 2001
L. evansii	White, creamy, brownish-cream to brown reverse,	Solitary or up to 3–4 per node, 20–45×1–1.2 μm	Macroconidia slightly falcate, 4.5–7.5×0.8–1.2μm, microconidia ellipsoidal or curved, 2.0–3.0×0.8–1.2 μm	Zare and Gams 2001

Species	Colonies	Conidiogenous cell	Conidia	Refrence
L. flavidum	Greyish-white to citron-yellow, citron-yellow reverse	In whorls, 12–35×1.5–2.5 µm, 0.5–1 µm at the tips	Mostly fusiform, long-ellipsoidal to almost cylindrical, slightly sickle-shaped, 4–8×1.5–2 µm	Zare and Gams 2008
L. fungicola var. *aleophilum*	White, reverse uncoloured	Whorls of 3–10, 15–30×1.5–2.5 µm, 0.5–1.5 µm at the tips	Oblong, fusiform, long ellipsoidal to almost cylindrical, irregular size, 4.5–8×1–2.5 µm	Zare and Gams 2008
L. fungicola var. *fungicola*	Dirty white, reverse uncoloured	Whorls of 3–7, 14–20(-45)×1.5–3µm, 0.5–1 µm at the tip	Fusiform, long-ellipsoidal to almost cylindrical, sickle-shaped, very unequal size, 4–9(-12)×1.5–2.5(-3.5) µm	Zare and Gams 2008
L. fusisporum	White, with red reverse and pigment diffusing	Solitary or up to 5, 16–26×1.0–1.5 µm	Fusiform, straight and rather broad, 3–5×1.5–2.0 µm	Zare and Gams 2001
L. kalimantanense	White, creamy-white reverse	Solitary or more often in whorls of 2–5, slender, tapering toward the apex, 12.5–36×1–2 µm	Acerose to fusoid with pointed ends, slightly curved, of varying size, (3.5-)4.5–12×1–2 µm	Sukarno et al. 2009
L. lecanii	Yellowish-white, deep yellow reverse	Aculeate and strongly tapering, singly or up to 6, 11–20(-30)×1.3–1.8 µm	Typically short-ellipsoidal, 2.5–3.5(-4.2)×1–1.5 µm, homogeneous in size and shape	Zare and Gams 2001
L. longisporum	White to sulphur-yellow, cream-coloured to pale yellow reverse	Tapering towards the apex(sub-aculeate), singly or up to 5–6 or on secondary phialides, 20–40×1.2–2.7 µm	Produced in globose heads, ellipsoidal to oblong-oval, 5.0–10.5×1.5–2.5 µm	Zare and Gams 2001
L. muscarium	White, cream-coloured or uncoloured reverse	Solitary or up to 6 (less frequent than in *L. lecanii*), (15-)20–35×1–1.5 µm	Produced in globose heads, ellipsoidal to subcylindrical, more irregular in size and shape, (2-)2.5–5.5(-6)×1–1.5(-1.8) µm	Zare and Gams 2001
L. nodulosum	White, cream-coloured reverse	Subulate, up to 6, 10–20×1.5 µm	Produced in heads of about 10µm diam., oval, 2.5–4.5×1.2–1.5 µm	Zare and Gams 2001
L. pissodis	White, ceram to yellow reverse	Solitary, up to 3, 16-(18–28)-38×1–2 µm	Up to more than 50 formed in globose droplets, cylindrical to oval, very variable in size and shape, 4–9.2×1.6–2.4 µm	Kope and Leal 2006
L. primulinum	Pale yellow, yellowish-brown reverse, brownish-yellow pigment	Solitary or in whorls of 2–5, tapering toward the tip, 20–50(-85)×0.8–1.8 µm	Macroconidia ellipsoidal to cylindrical, 5.0–9.5×1.2–2.5 µm, microconidia oval to ellipsoidal, 3.0–4.8×1.0–2.5 µm	Kaifuchi et al. 2013
L. psalliotae	White and red, reddish-cream to cream-coloured reverse, red to purple pigment	Aculeate, solitary or more often 3–4(-6) in whorls on each node, 25–35×1.0–1.5 µm	Macroconidia curved, falcated, 5–10×1.2–1.7 µm, microconidia oval or ellipsoidal, 2.7–3.7×1–1.5 µm	Zare and Gams 2001
L. restrictum	Yellowish-white, reverse yellowish-white to pale yellow	Solitary or in whorls of 2–5, tapering toward the tip, (12-)17–30(-36)×0.5–1.5 µm, 0.3–0.5 µm wide on the tip	Macroconidia fusiform or slightly falcate, (5-)6–10(-12)×1–1.5 µm, microconidia ovate, ellipsoidal, obovate or fusoid, frequently slightly curved, 2.5–3×1–1.5 µm	Crous et al. 2018
L. sabanense	Pale yellow to duller yellow, orange reverse	Solitary or in whorls of 2–4, 13–19×1.0–2.0 µm, gradually tapering to 0.5–1.0 µm	Forming mostly globose heads, 9–20 µm diam, ellipsoidal to ovoid, 3.5–4.5×1.5–2.0 µm	Chiriví-Salomón et al. 2015
L. saksenae	White, creamy white reverse	Solitary or often in whorls of 2–4, slender, tapering towards the apex, 14.5–36×1.0–2.0 µm	Macroconidia slightly curved, 6–13×1.5–2 µm, microconidia ellipsoidal to fusoid with round ends, nearly straight to slightly curved, 2.5–5×1.5–2 µm	Sukarno et al. 2009
L. subprimulinum	Creamy, primrose-yellow reverse	Tapering towards apex, discrete, solitary or up to 2–3 per node, 19–32×1.5–3.5 µm	Ovoid to ellipsoidal, elongated, straight or slightly curved, 4–15×2–6 µm	Huang et al. 2018
L. testudineum	White, centrally raised, wrinkled, reverse pale yellow to greyish-yellow	Solitary or in whorls of 2–4, tapering toward the tip, (13-)16–45(-53)×0.5–1 µm (exceptionally 80 µm long), 0.5–1 µm wide on the tip	Macroconidia fusiform or slightly falcate, 3.5–6(-6.5)×1–1.5 µm, microconidia ovate, ellipsoidal or fusoid, curved to reniform, 2–3.5×1–1.5 µm	Crous et al. 2018
L. tenuipes	White, reverse uncoloured	Arising singly or in scanty whorls, 20–35(-40)×1.2–1.5 µm	Microconidia ellipsoidal, straight, 3.0–5.5(-6.5)×1.0–1.5 µm, microconidia fusiform to falcate, 8–17×1.5–1.8 µm	Gams et al. 1984; Zare and Gams 2001
L. uredinophilum	White to cream coloured, reverse cream coloured	Produced singly or in whorls of up to 3–5, 20–60×1–2.5(-3) µm	Cylindric, oblong or ellipsoid, 3–9×1.8–3 µm	Park et al. 2016
L. wallacei	White, cream-coloured to creamish-brown reverse	Sollitary or up to 3–4, aculeate, (14-)17–25(29)×0.7–1.2 µm	Macroconidia, fusiform to falcate, (7.0-)8.5–10.5(-12.5)×1.0–1.5 µm, microconidia ellipsoidal to slightly falcate, (3.0-)4.0–5.5(-6.5)×0.7–1.2 µm	Zare and Gams 2001, 2008

Discussion

The genera *Lecanicillium* and *Simplicillium* belong to the Cordycipitaceae (Sung et al. 2007). The two genera are indistinguishable in morphological traits (Sung et al. 2001; Zare and Gams 2001). However, *Lecanicillium* and *Simplicillium* are clearly separated in molecular phylogenetic analyses (Kouvelis et al. 2008; Maharachchikumbura et al. 2015; Nonaka et al. 2013). As an insect pathogen, *Lecanicillium* spp. has potential for development as effective biological control agents against a number of plant diseases, insect pests and plant-parasitic nematodes (Goettel et al. 2008). Fifteen commercial preparations based on *Lecanicillium* spp. have been developed or are in the process of being developed (Faria and Wraight 2007). Kepler et al. (2017) concluded that *Lecanicillium* should be incorporated into *Akanthomyces* and formally transferred a number of *Lecanicillium* species. However, the compatibility of *Lecanicillium* was not so good in this study. Species that have been transferred to *Akanthomyces* were all assembled in the *L. lecanii* clade in the present study. The remaining species included in the present analyses were divided into multiple clades similar to those retrieved by Kepler et al. (2017). Relationships amongst *Lecanicillium* species thus appear to be more complicated than expected. Thus, we also prefer to describe the new taxon as a *Lecanicillium* species, consistent with Huang et al. (2018), owing to the uncertainty in generic boundaries.

In a comparison of all *Lecanicillium* species included in the present study, we were unable to identify morphological synapomorphies that characterise the phylogenetic groups. However, the species that show a close phylogenetic relationship are more similar in morphology than those that are phylogenetically distant. For example, the *L. lecanii* clade, which has globose heads with a higher number of conidia, are distinguishable from those clades that usually have one conidium visible at the top of the phialide in the phylogenetic tree presented here. In our phylogeny study, the node connecting *L. antillanum* and *L. tenuipes* is the basal node for the major clade. So the relationships of all of the lineages involved may change with more data or a different dataset. Therefore, more species are needed to enrich the phylogenetic study of *Lecanicillium* spp.

We know that *Lecanicillium* has a different origin into the Cordycipitaceae. We consider that the ones '*L. lecanii* clade' in pig.1 form a strong clade inside of *Akanthomyces*. Maybe all these should be moved to the *Akanthomyces* including *Lecanicillium longisporum*. In addition, the elimination of the genus may create more chaos considering the unsolved other clades.

Blackwellomyces Spatafora & Luangsa-ard is diagnosed by the unique characters of the ascospore, which have irregularly spaced septa and do not disarticulate into partspores at maturity as advised by Kepler et al. (2017). It includes *Blackwellomyces cardinalis* and *Blackwellomyces pseudomilitaris*. Asexual morphs have been described as similar to species in *Clonostachys*, *Hirsutella*, *Isaria* and *Mariannaea* (Hywel-Jones 1994; Sung and Spatafora 2004). Although the new species are close to the *Blackwellomyces* in the phylogenetic tree, we think they are clearly distinguished from *Blackwellomyces* by

the morphology. We also treat the new species as *Lecanicillium* considering the small sample and the unknown teleomorph. Thus, based on the present molecular phylogeny, derived from nuclear and ribosomal DNA sequence data, together with morphological evidence, a distinct new *Lecanicillium* species, *L. cauligalbarum*, is proposed.

Acknowledgements

This study was supported by the National Science Foundation of China (Project number: 31860507; 31860037), Guizhou international science and technology cooperation base (Project number: G[2016]5802), Major special projects of Guizhou tobacco company (201603; 201712). We thank Robert McKenzie, PhD, from Liwen Bianji, Edanz Group China (www.liwenbianji.cn/ac), for editing the English text of a draft of this manuscript. We also thank Konstanze Bensch, from mycobank web site (www.mycobank.org/), for the suggested epithet of "cauligalbarum" to replace "bristletailum".

References

Alexandros S (2014) RAxML version 8: a tool for phylogenetic analysis and post-analysis of large phylogenies. Bioinformatics 30: 1312–1313. https://doi.org/10.1093/bioinformatics/btu033

Castlebury LA, Rossman AY, Sung G-H, Hyten AS, Spatafora JW (2004) Multigene phylogeny reveals new lineage for Stachybotrys chartarum, the indoor air fungus. Mycological Research 108: 864–872. https://doi.org/10.1017/S0953756204000607

Chen WH, Han YF, Liang ZQ, Jin DC (2017) *Lecanicillium araneogenum* sp. nov., a new araneogenous fungus. Phytotaxa 305: 29–34. https://doi.org/10.11646/phytotaxa.305.1.4

Chiriví-Salomón JS, Danies G, Restrepo S, Sanjuan T (2015) *Lecanicillium sabanense* sp. nov. (Cordycipitaceae) a new fungal entomopathogen of coccids. Phytotaxa 234: 63–74. https://doi.org/10.11646/phytotaxa.234.1.4

Crous PW, Wingfield MJ, Burgess TI, Hardy GESJ, Gené J, Guarro J, Baseia IG, García D, Gusmão LFP, Souza-Motta CM, Thangavel R, Adamčík S, Barili A, Barnes CW, Bezerra JDP, Bordallo JJ, Cano-Lira JF, de Oliveira RJV, Ercole E, Hubka V, Iturrieta-González I, Kubátová A, Martín MP, Moreau PA, Morte A, Ordoñez ME, Rodríguez A, Stchigel AM, Vizzini A, Abdollahzadeh J, Abreu VP, Adamčíková K, Albuquerque GMR, Alexandrova AV, Álvarez Duarte E, Armstrong-Cho C, Banniza S, Barbosa RN, Bellanger JM, Bezerra JL, Cabral TS, Caboň M, Caicedo E, Cantillo T, Carnegie AJ, Carmo LT, Castañeda-Ruiz RF, Clement CR, Čmoková A, Conceição LB, Cruz RHSF, Damm U, da Silva BDB, da Silva GA, da Silva RMF, Santiago ALCMdA, de Oliveira LF, de Souza CAF, Déniel F, Dima B, Dong G, Edwards J, Félix CR, Fournier J, Gibertoni TB, Hosaka K, Iturriaga T, Jadan M, Jany JL, Jurjević Ž, Kolařík M, Kušan I, Landell MF, Leite Cordeiro TR, Lima DX, Loizides M, Luo S, Machado AR, Madrid H, Magalhães OMC, Marinho P, Matočec N, Mešić A, Miller AN, Morozova OV, Neves RP, Nonaka K, Nováková A, Oberlies NH, Oliveira-Filho JRC, Oliveira TGL, Papp V, Pereira OL, Perrone G, Peterson SW, Pham THG,

Raja HA (2018) Fungal Planet description sheets: 716–784. Persoonia-Molecular Phylogeny and Evolution of Fungi 40: 240–393. https://doi.org/10.3767/persoonia.2018.40.10

Curran J, Driver F, Ballard JWO, Milner RJ (1994) Phylogeny of Metarhizium : analysis of ribosomal DNA sequence data. Mycological Research 98: 547–552. https://doi.org/10.1016/S0953-7562(09)80478-4

Edgar R (2004) MUSCLE: multiple sequence alignment with high accuracy and high throughput. Nucleic Acids Research 32: 1792–1797. https://doi.org/10.1093/nar/gkh340

Faria MR, Wraight SP (2007) Mycoinsecticides and Mycoacaricides: A comprehensive list with worldwide coverage and international classification of formulation types. Biological Control 43: 237–256. https://doi.org/10.1016/j.biocontrol.2007.08.001

Gams W, Hoog D, Samson RA (1984) The hyphomycete genus Engyodontium a link between *Verticillium* and *Aphanocladium*. Persoonia 12: 135–147.

Gams W, Zare R (2001) A revision of *Verticillium* sect. Prostrata. III. Generic classification°). Nova Hedwigia 72: 47–55.

Goettel MS, Koike M, Kim JJ, Aiuchi D, Shinya R, Brodeur J (2008) Potential of *Lecanicillium* spp. for management of insects, nematodes and plant diseases. Journal of Invertebrate Pathology 98: 256–261. https://doi.org/10.1016/j.jip.2008.01.009

Huang SK, Maharachchikumbura SSN, Jeewon R, Bhat DJ, Phookamsak R, Hyde KD, Al-Sadi AM, Kang JC (2018) *Lecanicillium subprimulinum* (Cordycipitaceae, Hypocreales), a novel species from Baoshan, Yunnan. Phytotaxa 348: 99–108.

Hywel-Jones NL (1994) *Cordyceps khaoyaiensis*, and *C. pseudomilitaris*, two new pathogens of lepidopteran larvae from Thailand. Mycological Research 98: 939–942. https://doi.org/10.1016/S0953-7562(09)80267-0

Kaifuchi S, Nonaka K, Mori M, Shiomi K, Ōmura S, Masuma R (2013) *Lecanicillium primulinum*, a new hyphomycete (Cordycipitaceae) from soils in the Okinawa's main island and the Bonin Islands, Japan. Mycoscience 54: 291–296. https://doi.org/10.1016/j.myc.2012.10.006

Katoh K, Asimenos G, Toh H (2009) Multiple alignment of DNA sequences with MAFFT. Methods in Molecular Biology 537. https://doi.org/10.1007/978-1-59745-251-9_3

Kepler RM, Luangsa-ard JJ, Hywel-Jones NL, Quandt CA, Sung GH, Rehner SA, Aime MC, Henkel TW, Sanjuan T, Zare R, Chen MJ, Li ZZ, Rossman AY, Spatafora JW, Shrestha B (2017) A phylogenetically-based nomenclature for Cordycipitaceae (Hypocreales). IMA Fungus 8: 335–353. https://doi.org/10.5598/imafungus.2017.08.02.08

Kope HH, Leal I (2006) A new species of *Lecanicillium* isolated from the white pine weevil. Mycotaxon 94: 331–340.

Kouvelis VN, Sialakouma A, Typas MA (2008) Mitochondrial gene sequences alone or combined with ITS region sequences provide firm molecular criteria for the classification of *Lecanicillium* species. Mycological Research 112: 829–844. https://doi.org/10.1016/j.mycres.2008.01.016

Maharachchikumbura SSN, Hyde KD, Jones EBG, McKenzie EHC, Huang S-K, Abdel-Wahab MA, Daranagama DA, Dayarathne M, D'souza MJ, Goonasekara ID, Hongsanan S, Jayawardena RS, Kirk PM, Konta S, Liu J-K, Liu Z-Y, Norphanphoun C, Pang K-L, Perera RH, Senanayake IC, Shang Q, Shenoy BD, Xiao Y, Bahkali AH, Kang J, Som-

rothipol S, Suetrong S, Wen T, Xu J (2015) Towards a natural classification and backbone tree for Sordariomycetes. Fungal Diversity 72: 199–301. https://doi.org/10.1007/s13225-015-0331-z

Mongkolsamrit S, Noisripoom W, Thanakitpipattana D, Wutikhun T, Spatafora JW, Luangsaard J (2018) Disentangling cryptic species with isaria-like morphs in cordycipitaceae. Mycologia 110: 230–257.

Nonaka K, Kaifuchi S, Ōmura S, Masuma R (2013) Five new *Simplicillium* species (Cordycipitaceae) from soils in Tokyo, Japan. Mycoscience 54: 42–53. https://doi.org/10.1016/j.myc.2012.07.002

Park MJ, Hong SB, Shin HD (2016) *Lecanicillium uredinophilum* sp. nov. associated with rust fungi from Korea. Mycotaxon 130: 997–1005. https://doi.org/10.5248/130.997

Ronquist F, Teslenko M, van der Mark P, Ayres DL, Darling A, Höhna S, Larget B, Liu L, Suchard MA, Huelsenbeck JP (2012) MrBayes 3.2: Efficient Bayesian Phylogenetic Inference and Model Choice Across a Large Model Space. Systematic Biology 61: 539–542. https://doi.org/10.1093/sysbio/sys029

Sukarno N, Kurihara Y, Park J-Y, Inaba S, Ando K, Harayama S, Ilyas M, Mangunwardoyo W, Sjamsuridzal W, Yuniarti E, Saraswati R, Widyastuti Y (2009) *Lecanicillium* and *Verticillium* species from Indonesia and Japan including three new species. Mycoscience 50: 369–379. https://doi.org/10.1007/S10267-009-0493-1

Sung GH, Spatafora JW (2004) *Cordyceps cardinalis* sp. nov. a new species of *Cordyceps* with an east Asian-eastern North American distribution. Mycologia 96: 658–666. https://doi.org/10.1080/15572536.2005.11832962

Sung GH, Hywel-Jones NL, Sung JM, Luangsa-ard JJ, Shrestha B, Spatafora JW (2007) Phylogenetic classification of Cordyceps and the clavicipitaceous fungi. Studies in Mycology 57: 5–59. https://doi.org/10.3114/sim.2007.57.01

Sung GH, Spatafora JW, Zare R, Hodge KT, Gams W (2001) A revision of *Verticillium* sect. Prostrata. II. Phylogenetic analyses of SSU and LSU nuclear rDNA sequences from anamorphs and teleomorphs of the ClavicipitaceaeO). Nova Hedwigia 72: 311–328.

Swofford DL (2001) Paup*: Phylogenetic analysis using parsimony (and other methods) 4.0. b10. Sunderland, Massachusetts.

Tamura K, Stecher G, Peterson D, Filipski A, Kumar S (2013) MEGA6: Molecular Evolutionary Genetics Analysis Version 6.0. Molecular Biology and Evolution 30: 2725–2729. https://doi.org/10.1093/molbev/mst197

Vaidya G, Lohman DJ, Rudolf M (2011) SequenceMatrix: concatenation software for the fast assembly of multi-gene datasets with character set and codon information. Cladistics 27: 171–180. https://doi.org/10.1111/j.1096-0031.2010.00329.x

van den Brink J, Samson RA, Hagen F, Boekhout T, de Vries RP (2011) Phylogeny of the industrial relevant, thermophilic genera Myceliophthora and Corynascus. Fungal Diversity 52: 197–207. https://doi.org/10.1007/s13225-011-0107-z

White TJ, Bruns T, Lee S, Taylor J (1990) Amplification and direct sequencing of fungal ribosomal RNA genes for phylogenetics. In: Innis MA, Gelfand DH, Sninsky JJ, White TJ (Eds) PCR Protocols. Academic Press, San Diego, 315–322. https://doi.org/10.1016/B978-0-12-372180-8.50042-1

Wijayawardene NN, Hyde KD, Rajeshkumar KC, Hawksworth DL, Madrid H, Kirk PM, Braun U, Singh RV, Crous PW, Kukwa M, Lücking R, Kurtzman CP, Yurkov A, Haelewaters D, Aptroot A, Lumbsch HT, Timdal E, Ertz D, Etayo J, Phillips AJL, Groenewald JZ, Papizadeh M, Selbmann L, Dayarathne MC, Weerakoon G, Jones EBG, Suetrong S, Tian Q, Castañeda-Ruiz RF, Bahkali AH, Pang KL, Tanaka K, Dai DQ, Sakayaroj J, Hujslová M, Lombard L, Shenoy BD, Suija A, Maharachchikumbura SSN, Thambugala KM, Wanasinghe DN, Sharma BO, Gaikwad S, Pandit G, Zucconi L, Onofri S, Egidi E, Raja HA, Kodsueb R, Cáceres MES, Pérez-Ortega S, Fiuza PO, Monteiro JS, Vasilyeva LN, Shivas RG, Prieto M, Wedin M, Olariaga I, Lateef AA, Agrawal Y, Fazeli SAS, Amoozegar MA, Zhao GZ, Pfliegler WP, Sharma G, Oset M, Abdel-Wahab MA, Takamatsu S, Bensch K, de Silva NI, De Kesel A, Karunarathna A, Boonmee S, Pfister DH, Lu YZ, Luo ZL, Boonyuen N, Daranagama DA, Senanayake IC, Jayasiri SC, Samarakoon MC, Zeng X-Y, Doilom M, Quijada L, Rampadarath S, Heredia G, Dissanayake AJ, Jayawardana RS, Perera RH, Tang LZ, Phukhamsakda C, Hernández-Restrepo M, Ma X, Tibpromma S, Gusmao LFP, Weerahewa D, Karunarathna SC (2017) Notes for genera: Ascomycota. Fungal Diversity 86: 1–594. https://doi.org/10.1007/s13225-017-0386-0

Zare R, Gams W (2001) The genera *Lecanicillium* and *Simplicillium* gen. nov. Nova Hedwigia 73: 1–50.

Zare R, Gams W (2008) A revision of the *Verticillium* fungicola species complex and its affinity with the genus *Lecanicillium*. Mycological Research 112: 811–824. https://doi.org/10.1016/j.mycres.2008.01.019

Zou X, Zhou YM, Liang ZQ, Xu FL (2016) A new species of the genus *Hirsutella* with helical twist neck of phialides parasitized on Tortricidae. Mycosystema 35: 807–813.

MycoKeys 43: 75–90 (2018)
doi: 10.3897/mycokeys.43.29365
http://mycokeys.pensoft.net

RESEARCH ARTICLE

A peer-reviewed open-access journal
MycoKeys
Launched to accelerate biodiversity research

Coryneum heveanum sp. nov. (Coryneaceae, Diaporthales) on twigs of Para rubber in Thailand

Chanokned Senwanna[1,2], Kevin D. Hyde[2,3,4], Rungtiwa Phookamsak[2,3,4,5], E. B. Gareth Jones[1], Ratchadawan Cheewangkoon[1]

1 *Department of Entomology and Plant Pathology, Faculty of Agriculture, Chiang Mai University, Chiang Mai 50200, Thailand* **2** *Center of Excellence in Fungal Research, Mae Fah Luang University, Chiang Rai 57100, Thailand* **3** *Key Laboratory for Plant Diversity and Biogeography of East Asia, Kunming Institute of Botany, Chinese Academy of Sciences, Kunming 650201, Yunnan, People's Republic of China* **4** *World Agroforestry Centre, East and Central Asia, Heilongtan, Kunming 650201, Yunnan, People's Republic of China* **5** *Department of Biology, Faculty of Science, Chiang Mai University, Chiang Mai 50200, Thailand*

Corresponding author: *Ratchadawan Cheewangkoon* (ratchadawan.c@cmu.ac.th)

Academic editor: *Andrew Miller* | Received 28 August 2018 | Accepted 14 November 2018 | Published 6 December 2018

Citation: Senwanna C, Hyde KD, Phookamsak R, Jones EBG, Cheewangkoon R (2018) *Coryneum heveanum* sp. nov. (Coryneaceae, Diaporthales) on twigs of Para rubber in Thailand. MycoKeys 43: 75–90. https://doi.org/10.3897/mycokeys.43.29365

Abstract

During studies of microfungi on para rubber in Thailand, we collected a new *Coryneum* species on twigs which we introduce herein as *C. heveanum* with support from phylogenetic analyses of LSU, ITS and TEF1 sequence data and morphological characters. *Coryneum heveanum* is distinct from other known taxa by its conidial measurements, number of pseudosepta and lack of a hyaline tip to the apical cell.

Keywords

1 new species, Ascomycota, *Hevea brasiliensis*, Phylogeny, Taxonomy

Introduction

The para rubber tree (*Hevea brasiliensis*) is a tropical plant belonging to family Euphorbiaceae (Priyadarshan et al. 2009). Para rubber tree is the major commercial source of natural rubber, which is used in all kinds of manufactured products, including tyres, medical appliances and agricultural equipment, in addition, rubber-wood is used in the furniture industry (Priyadarshan et al. 2009, Rippel and Galembeck 2009, Häu-

ser et al. 2015, Herrmann et al. 2016). The total para rubber tree plantation area in South East Asia exceeds more than 5 million hectares (Vongkhamheng et al. 2016). In Thailand, para rubber tree plantation area covers more than 3 million hectares and this number has increased every year (Kromkratoke and Suwanmaneepong 2017, Romyen et al. 2018). This important perennial crop is currently often affected by plant pathogenic fungi which can substantially decrease the quality and quantity of rubber yield (Liu et al. 2018). Many taxa have proven to be serious pathogens worldwide, causing severe leaf spot formation, defoliation, shoot die-back and stem cankers (Jayasinghe 2000, Nyaka Ngobisa et al. 2015, Trakunyingcharoen et al. 2015, Liyanage et al. 2016, Liu et al. 2018). Nonetheless, information about the diversity of phytopathogenic taxa on para rubber from Thailand is generally lacking and currently there are only thirteen reports (Farr and Rossman 2018). Thus, the main objective of our project is to survey and study the diversity of microfungi associated with para rubber trees in Thailand. During the survey, we found a *Coryneum* species associated with canker disease on twigs of para rubber. This work is based on a combination of morphology and molecular data for identification this taxon.

Many *Coryneum* species have been reported as phytopathogens causing tree canker (Strouts 1972, Gadgil and Dick 2007, Horst 2013, Senanayake et al. 2017). This genus was introduced by Nees von Esenbeck (1817) to accommodate *C. umbonatum* as the type species. Historically, *Coryneum* species have relied on morphological studies and only a few species are supported by sequence data in GenBank. Many species causing tree canker, previously known as *Coryneum* were transferred to other genera e.g. *Seiridium*, *Seimatosporium* and *Wilsonomyces* (Sutton 1980, Raddi and Panconesi 1981, Marin-Felix et al. 2017). Recently, research has clarified the taxonomic position of the family Coryneaceae based on morphological and molecular data (Rossman et al., 2015; Senanayake et al., 2017; Wijayawardene et al., 2018). Currently 123 *Coryneum* species are listed in Index Fungorum (2018). Molecular analyses, using sequence data of LSU, ITS and TEF1 regions, has supplemented traditional taxonomic methods, enabling a more precise and rapid identification of species in the genus *Coryneum* (Senanayake et al. 2017, 2018, Fan et al. 2018). The correct identification of pathogenic fungi is necessary to implement appropriate quarantine decisions, suitable control strategies and to promote an understanding of the evolution of new pathogens and the movement of fungi between continents.

Material and methods

Collections, morphological studies and isolation

Fresh materials were collected from Chiang Rai, Thailand in 2016. Specimens were taken to the laboratory in zip lock bags and observed with a Motic SMZ 168 series stereomicroscope and photographed with an Axio camera on a Zeiss Discover V8 stereomicroscope. Sections of the conidiomata were mounted in double-distilled water (ddH_2O) for morphological structures and photography. Images were taken us-

ing a Canon 600D camera on a Nikon ECLIPSE 80i microscope. All measurements were calculated using Tarosoft® Image Framework programme v.0.9.0.7. Photoplates were made using Adobe Photoshop CS6 version 13.0 (Adobe Systems U.S.A.). The specimens were deposited in the Mae Fah Luang University Herbarium, Chiang Rai, Thailand (MFLU). Living cultures were deposited in Mae Fah Luang University Culture Collection (MFLUCC) in Thailand and duplicated at the Kunming Culture Collection (KUMCC). Faces of Fungi and Index Fungorum numbers are registered as described in Jayasiri et al. (2015) and Index Fungorum (2018).

DNA extraction, PCR and DNA sequencing

Genomic DNA was extracted from mycelium using Biospin Fungus Genomic DNA Extraction Kit (BioFlux®, Hangzhou, P.R. China) following the manufacturer's protocol. The DNA product was kept at 4 °C for the DNA amplification and maintained at -20 °C for long term storage. The DNA amplification was carried out by polymerase chain reaction (PCR) using three genes, the 28S large subunit (LSU), internal transcribed spacer (ITS) and translation elongation factor 1 alpha gene (TEF1). The LSU gene was amplified by using the primers LROR and LR5 (Vilgalys and Hester 1990), the ITS gene was amplified by using the primers ITS5 and ITS4 (White et al. 1990) and the TEF1 gene was amplified using the primers EF1-728F (Carbone and Kohn 1999) and EF2 (O'Donnell 1998). The amplification reactions were performed in 25 µl final volumes contained of 8.5 µl of sterilized ddH_2O, 12.5 µl of 2 × Easy Taq PCR Super Mix (mixture of Easy Taq TM DNA Polymerase, dNTPs and optimised buffer (Beijing Trans Gen Biotech Co., Chaoyang District, Beijing, PR China), 1 µl of each forward and reverse primers (10 pM) and 2 µl of DNA template. The PCR thermal cycle programme for LSU and ITS gene amplification was provided as initially 94 °C for 3 mins, followed by 35 cycles of denaturation at 94 °C for 1 min, annealing at 55 °C for 50 secs, elongation at 72 °C for 1 min and final extension at 72 °C for 10 mins. The PCR thermal cycle programme for TEF1 gene amplification was provided as initially 94 °C for 5 mins, followed by 40 cycles of denaturation at 94 °C for 45 secs, annealing at 52 °C for 30 secs, elongation at 72 °C for 1.30 mins and final extension at 72 °C for 6 mins. PCR products were sequenced by Sangon Biotech Co., Shanghai, China. Nucleotide sequences were deposited in GenBank (Table 1).

Phylogenetic analysis

Phylogenetic analyses were conducted based on a combined gene of LSU, ITS and TEF1 sequence data. Sequence data of Coryneaceae from previous studies and representative strains of major classes in Diaporthales were downloaded from GenBank to supplement the dataset (Table 1). The combined dataset consisted of 45 sequences including our newly generated sequences. *Phaeoacremonium aleophilum* (CBS 63194) and *P. vibratile* (CBS 117115) were selected as the outgroup taxa. The combined LSU, ITS

Table 1. Isolates utilized in the phylogenetic tree and their GenBank and culture accession numbers.

Taxa	Culture AC no.	GenBank Accession number		
		ITS	LSU	TEF1
Asterosporium asterospermum	KT2125	_	AB553743	_
Asterosporium asterospermum	KT2138	_	AB553744	_
Chaetoconis polygoni	CBS 405.95	_	EU754141	_
Coryneum castaneicola	43-1	_	MH683551	_
Coryneum castaneicola	43-2	MH683560	MH683552	_
Coryneum depressum	AR 3897	_	EU683074	_
Coryneum heveanum	**MFLUCC 17-0369**	**MH778707**	**MH778703**	**MH780881**
Coryneum heveanum	**MFLUCC 17-0376**	**MH778708**	**MH778704**	_
Coryneum modonia	AR 3558	_	EU683073	_
Coryneum perniciosum	CBS 130.25	MH854812	MH866313	_
Coryneum umbonata	CBS 199.68	MH859114	MH870828	_
Coryneum umbonatum	AR 3541*	_	EU683072	_
Coryneum umbonatum	MFLUCC 13-0658*	MF190120	MF190066	MF377574
Coryneum umbonatum	MFLUCC 15-1110*	MF190121	MF190067	MF377575
Crinitospora pulchra	CBS 138014	KJ710466	KJ710443	_
Cytospora centravillosa	MFLUCC 17-1660	MF190122	MF190068	_
Cytospora centravillosa	MFLU 17-0887	MF190123	MF190069	_
Cytospora melanodiscus	Jimslanding2	JX438621	_	JX438605
Cytospora translucens	CZ320	FJ755269	FJ755269	_
Diaporthe azadirachtae	TN 01	KC631323	_	_
Diaporthe eres	AR 5193*	KJ210529	_	KJ210550
Diaporthe eres	MFLUCC 17-1668	MF190138	MF190081	MF377595
Diaporthe maytenicola	CBS 136441	KF777157	KF777210	_
Hyaliappendispora galii	MFLUCC 16-1208	MF190150	MF190095	MF377587
Lamproconium desmazieri	MFLUCC 15-0870*	KX430134	KX430135	MF377591
Lamproconium desmazieri	MFLUCC 15-0872	KX430138	KX430139	MF377593
Macrohilum eucalypti	CPC 10945*	DQ195781	DQ195793	_
Macrohilum eucalypti	CPC 19421*	KR873244	KR873275	_
Pachytrype princeps	Rogers s.n.*	_	FJ532382	_
Pachytrype rimosa	FF1066	_	FJ532381	_
Phaeoacremonium aleophilum	CBS 631.94	AF266647	AB278175	KF764643
Phaeoacremonium vibratile	CBS 117115	KF764573	DQ649065	KF764645
Phaeoappendispora thailandensis	MFLUCC 13-0161*	MF190157	MF190102	_
Phaeoappendispora thailandensis	MFLU 12-2131	MF190158	MF190103	_
Phaeodiaporthe appendiculata	CBS 123821*	KF570156	KF570156	_
Prosopidicola mexicana	CBS 113529*	AY720709	KX228354	_
Prosopidicola mexicana	CBS 113530*	AY720710	_	_
Rossmania ukurunduensis	AR 3484*	_	EU683075	_
Stegonsporium acerophilum	CBS 117025	EU039982	EU039993	EU040027
Stegonsporium pyriforme	CBS 117023	EU039971	EU039987	EU040001
Stilbospora ellipsosporum	WJ 1840	_	AY616229	_
Stilbospora macrosperma	CBS 121883*	JX517290	JX517299	_
Sydowiella depressula	CBS 813.79	_	EU683077	_
Sydowiella fenestrans	CBS 125530*	JF681956	EU683078	_
Valsella salicis	AR 3514	_	EU255210	EU222018

Note: AR: AR, Amy Rossman; ATCC: American Type Culture Collection, Virginia, USA; BCRC, Bioresource Collection and Research Center, Taiwan; CBS: Westerdijk Fungal Biodiversity Institute, Utrecht, Netherlands; CFCC: China Forestry Culture Collection Center, Beijing, China; CPC: Culture Collection of Pedro Crous, Netherlands; FF: F.A. Fernández; KT: K. Tanaka; MFLU: MAFF: MAFF Genebank, Ministry of Agriculture Forestry and Fisheries, USA; Mae Fah Luang University Herbarium, Chiang Rai, Thailand; MFLUCC: Mae Fah Luang University Culture Collection, Chiang Rai, Thailand; WJ: W. Jaklitsch. The newly generated sequences are indicated in bold. The strains from generic type species are marked by an asterisk (*).

and TEF1 gene dataset were initially aligned by using MAFFT version 7 (Katoh et al. 2017; http://mafft.cbrc.jp/alignment/server/) and improved manually, where necessary, in BioEdit v.7.0.9.1 (Hall 1999) and MEGA7 (Kumar et al. 2015). The final alignment of the combined LSU, ITS and TEF1 sequence datasets was analysed and inferred the phylogenetic tree based on maximum likelihood (ML), maximum parsimony (MP) and Bayesian inference analyses (BI).

The estimated evolutionary model of Bayesian inference and maximum likelihood were performed independently for each locus using MrModeltest v. 2.3 (Nylander 2004) implemented in PAUP v. 4.0b10 (Swofford 2002). The best-fit model resulted as GTR+I+G model for each locus under the Akaike Information Criterion (AIC).

Maximum likelihood analysis was performed by Randomized Accelerated Maximum Likelihood (RAxML) (Stamatakis 2008) version 7.4.2 (released by Alexandros Stamatakis on November 2012) implemented in raxmlGUI v.1.0 (Stamatakis et al. 2008, Silvestro and Michalak 2011). The search strategy was set to rapid bootstrapping at 1,000 replicates.

Maximum parsimony analysis was performed using PAUP v 4.0b10 (Swofford 2002). Trees were inferred using the heuristic search function with 1,000 random stepwise addition replicates and tree bisection-reconnection (TBR) as the branch-swapping algorithm. All informative characters were unordered and of equal weight. The consistency index (CI), retention index (RI), rescaled consistency index (RC) and homoplasy index (HI) were calculated. Statistical supports for branches of the most parsimonious tree were estimated using maximum parsimony bootstrap (BS) analysis with 1,000 bootstrap replicates.

Bayesian inference was performed in MrBayes v. 3.2.2 (Ronquist and Huelsenbeck 2003) with the best-fit model of sequences evolution under the Akaike Information Criterion (AIC). Bayesian posterior probabilities (BY) (Rannala and Yang 1996, Zhaxybayeva and Gogarten 2002) were determined by Markov Chain Monte Carlo Sampling (BMCMC). Six simultaneous Markov chains were run from random trees for one million generations and trees were sampled every 100th generation. The first 20% of generated trees representing the burn-in phase of the analysis were discarded and the remaining trees were used for calculating posterior probabilities (BY) in the majority rule consensus tree.

The phylogenetic tree was shown in FigTree V.1.4.3 (Rambaut 2016) and drawn and converted to tiff file in Microsoft PowerPoint 2013 and Adobe Photoshop CS6 version 13.0 (Adobe Systems U.S.A.). The final alignment and tree were deposited in TreeBASE (http://www.treebase.org/) under the submission ID 23550.

Results

Phylogenetic analysis

The dataset consisted of 45 taxa including the new taxa (Figure 1). The combined LSU, ITS and TEF1 sequence data including 2040 total characters, were analysed based on Bayesian inference, maximum likelihood and maximum parsimony analysis. RAxML analysis of the combined dataset had 996 distinct alignment patterns and 39.23% of

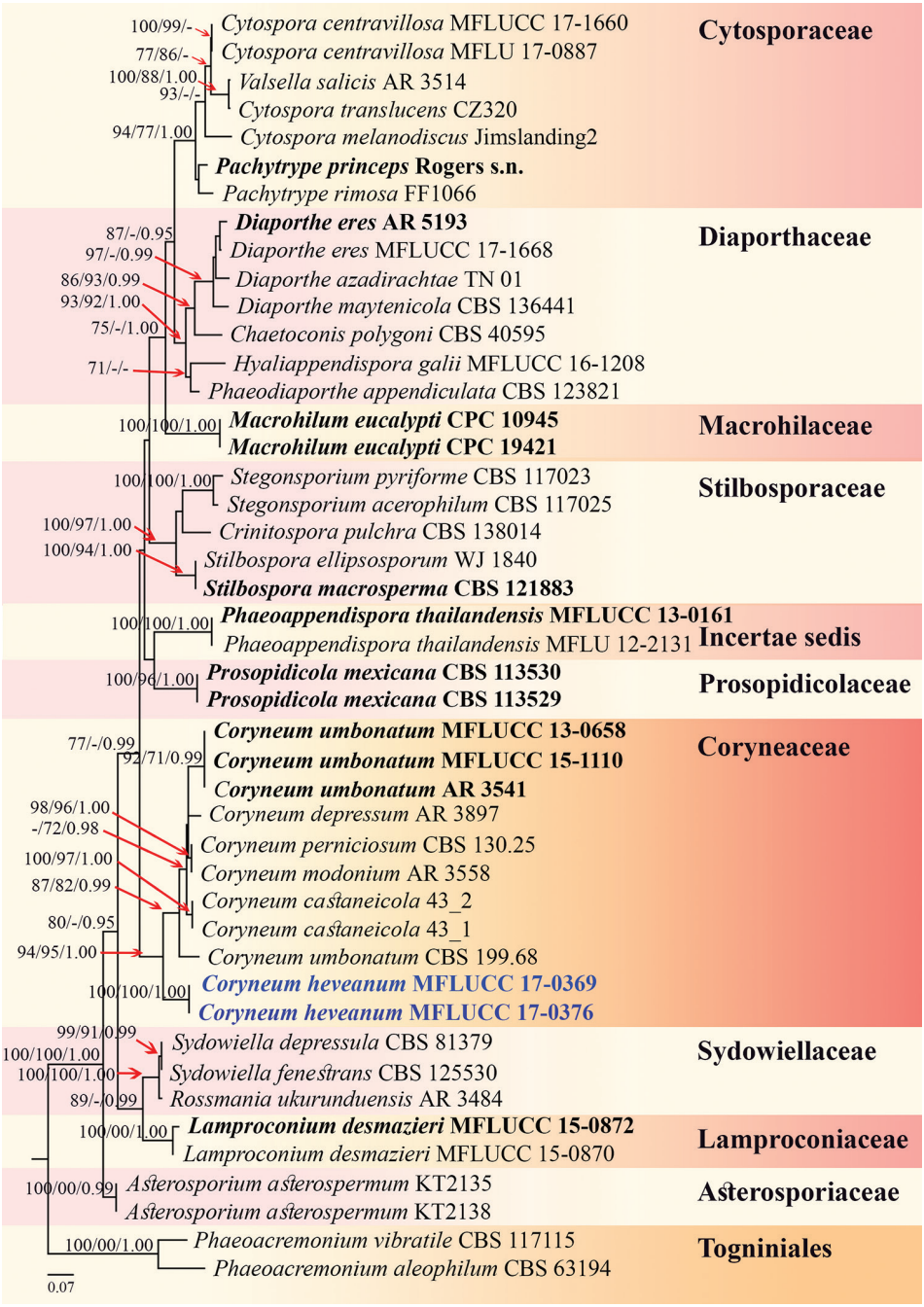

Figure 1. Maximum likelihood (RAxML) based on analysis of a combined dataset of LSU, ITS and TEF1 sequence data representing Diaporthales. Bootstrap support values for maximum likelihood (ML, left), maximum parsimony (MP, middle) greater than 70% and Bayesian posterior probabilities (BY, right) equal to or greater than 0.95 are indicated at the nodes. The tree is rooted to *Phaeoacremonium aleophilum* (CBS 63194) and *P. vibratile* (CBS 117115). The newly generated sequences are in blue. The strains from generic type species are in black bold.

undetermined characters or gaps. Maximum parsimony had 1191 constant characters, 151 variable parsimony-uninformative characters and 690 parsimony-informative characters. The most parsimonious tree is shown where TL = 2336, CI = 0.607, RI = 0.716, RC = 0.435, HI = 0.393. Bayesian posterior probabilities (BY) from MCMC were evaluated with the final average standard deviation of split frequencies = 0.005452. Phylogenetic analysis from ML, MP and BI gave trees with similar overall topologies of the generic placement and in agreement with previous studies (Senanayake et al. 2017, Fan et al. 2018, Yang et al. 2018). The final RAxML tree of the combined dataset is shown in Figure 1, with a final ML optimisation likelihood value of -13004.6966291. The phylogeny shows that *Coryneum heveanum* forms a distinct lineage in *Coryneum* with strong support (94% ML, 95%MP and 1.00 BY) and in a sister clade to *C. umbonatum*, *C. depressum*, *C. modonium*, *C. perniciosum* and *C. castaneicola*.

Taxonomy

Coryneum heveanum **Senwanna, Cheewangkoon & K.D. Hyde sp. nov.**
Index Fungorum number: IF555338
Facesoffungi number: FoF 04873
Figure 2

Etymology. Named after the host on which it occurs, *Hevea brasiliensis.*

Type. THAILAND, Chiang Rai Province, Wiang Chiang Rung District, on twigs (attached on tree) of *Hevea brasiliensis*, 1 November 2016, C. Senwanna, RBCR003 (MFLU 18-0936, holotype), ex-type living culture MFLUCC 17-0369, KUMCC 18-0106; Dry culture from ex-type MFLU 18-0936); *ibid.*, RBCR016 (MFLU 17-1982, living culture MFLUCC 17-0376, dry culture MFLU 18-0937, MFLU 18-0938)

Description. *Associated with canker* on twigs of *Hevea brasiliensis*. Asexual morph: *Conidiomata* acervular, solitary, erumpent through the outer periderm layers of host, scattered, surface tissues above slightly dome-shaped, black, velvety, formed of brown cell, thick-walled *textura angularis*, 145–540 µm diam. *Conidiophores* short, cylindrical, apically pale brown, paler at the base, smooth, septate, branched at the base, arising from basal stroma, 22–37 × 4–8 µm ($\bar{x}$ = 28.5 × 5.6 µm, n = 15). *Conidiogenous cell* annellidic, integrated, terminal, cylindrical, medium brown, truncate apex, with 1-3 slightly percurrent proliferations, 6–17 µm long ($\bar{x}$ = 10.7 µm, n = 20). *Conidia* curved, clavate to fusiform, dark brown, smooth-walled, 4–6-pseudo-septa, sometimes with apical and basal cells darker than other cells, rounded or sometime truncate at apex, truncate and black at the base, (40–)43–53(–68) × (14–)15–20 µm ($\bar{x}$ = 48.7 × 17.3 µm, n = 85). *Appressoria* hyaline, globose to sub globose, thick-walled, 4–11 µm wide ($\bar{x}$ = 7.1 µm, n = 20).

Cultural characteristics. Conidia germinated on MEA within 24 h with germ tubes produced from one or both end cells, mostly from basal cell of conidia. Colonies on MEA reaching 20–25 mm diam. after 4 weeks at 25–30 °C, colonies circular, medium dense, cottony, margin wavy, superficial, slightly effuse, radially striated; colony

Figure 2. *Coryneum heveanum* (MFLU 18-0936). **a–d** Conidiomata on host surface **e–f** Acervuli **g** Conidiogenesis (annellidic; red arrow, proliferation; blue arrow) **h–j** Conidiophores, conidiogeneous cells with conidia **k** Conidia **l** Germinated spores **m–p** Appressoria **q–r** Mass of conidia on PDA after 6 months **s** Mycelium on PDA after 6 months. Scale bars: 5 mm (**a**), 1000 µm (**b**), 200 µm (**c, d, r**), 100 µm (**e, f, q**), 20 µm (**g–k**), 50 µm (**l, s**), 5 µm (**m–p**).

from above, white, edges with more aerial mycelium than centre in the beginning and later become white grey, smooth with edge entire; from below: white to cream at the margin, yellowish-green in the centre in the beginning and later become dark green; not producing pigmentation in agar. Colonies on PDA reaching 10–15 mm diam. after 4 weeks at 25–30 °C, colonies circular, medium dense, cottony, slightly effuse, dark green with brown aerial mycelium on surface; not producing pigmentation in agar. Conidial masses were observed in PDA culture after 6 months at 25–30 °C. Mass of conidia dark brown to black, extruding on colony or tip of mycelium (Figure 2 q, r). Mycelium superficial and immersed, dark brown, hyphae branched, septate, constricted at septa, thick, smooth-walled (Figure 2 s).

Additional GenBank number. SSU (primer NS1 and NS4; White et al. 1990) MH778705; MFLUCC 17-0369, MH778706; MFLUCC 17-0376, TEF1 (primer EF1-983F and EF1-2218R; Rehner 2001) MH780882; MFLUCC 17-0376.

Notes. Phylogenetically, *Coryneum heveanum* clustered in the same clade with *C. umbonatum*, *C. depressum*, *C. modonium*, *C. perniciosum* and *C. castaneicola* with high statistical support. Based on morphological characters, the conidia of *C. castaneicola*, *C. depressum*, *C. elevatum*, *C. modonium* and *C. umbonatum* have slightly curved conidia with an apical cell with a hyaline tip, while *C. heveanum*, *C. castaneicola* and *C. perniciosum* lack a hyaline tip (Table 2) (Briosi and Farneti 1908, Sutton 1980, Gadgil and Dick 2007, Senanayake et al. 2017, 2018). *Coryneum heveanum* is similar to *C. betulinum*, *C. perniciosum*, *C. psidi* and *C. pyricola* in having broadly fusiform or clavate conidia but differs in size of conidia and number of pseudosepta (Table 2).

Discussion

Fungi on para rubber (*Hevea brasiliensis*) can be pathogens, saprobes or endophytes (Rocha et al. 2011, Seephueak et al. 2011, Ghazali 2013, Nyaka Ngobisa et al. 2015, Hyde et al. 2018, Senwanna 2017, 2018). Fungal endophytes on para rubber have been comparatively well-studied (Gasiz and Chaverri 2010, Rocha et al. 2011, Déon et al. 2012, Martin et al. 2015), while few studies have investigated saprobic fungi or fungi associated with para rubber (Cai et al. 2013, Trakunyingcharoen et al. 2015). However, previous studies reporting saprobic taxa based on morphology, are available (Seephueak et al. 2011, Seephueak 2012). In this study, we introduced a new species, *Coryneum heveanum*, found on twigs of para rubber, based on morphological characters and phylogenetic analyses.

Coryneum species are phytopathogenic fungi associated with twig blight, canker and dieback disease with some species reported as saprobes (Carter 1914, Strouts 1972, Gadgil and Dick 2007, Senanayake et al. 2018). Host-specificity of *Coryneum* has not yet been clarified and species have been recorded from various plant families worldwide (i.e. Betulaceae, Clusiaceae, Cupressaceae, Fagaceae, Hippocastanoideae, Malvaceae, Myrtaceae, Rosaceae, Ulmaceae) (Wehmeyer 1926, Strouts 1972, Sutton 1980, Senanayake et

Table 2. Synopsis of recorded *Coryneum* species (asexual morph) (Related to this research).

Taxa	Size (µm)			Host records
	Conidiomata	Conidiophores	Conidia; Number of pseudo-septate	
Coryneum betulinum (Sutton 1980)	–	–	31–36 × 14–17; 4–5	*Betula rubrum* (Betulaceae)
C. castaneicola (Sutton 1980)	–	–	57–80 × 10–13; apical cell with a hyaline tip; 6–7	*Castanea dentata* (Fagaceae)
C. depressum (Sutton 1980)	–	–	44–53 × 19–23; apical cell with a hyaline tip; 4–5(–6)	*Quercus* spp. (Fagaceae)
C. elevatum (Sutton 1980)			56–70 × 24–32; apical cell with a hyaline tip; 6–7	*Quercus* spp. (Fagaceae)
C. heveanum This study	145–540	22–37 × 4–8	(40–)43–53(–68) × (14–)15–20; 4–6	*Hevea brasiliensis* (Euphorbiaceae)
C. modonium (Sutton 1980)	–	–	50–71 × 14–19; apical cell with a hyaline tip; 5–8	*Castanea* spp. (Fagaceae)
C. perniciosum (Briosi and Farneti 1908)	–	–	40–50 × 13–15; 5–7	*Castanea* sp. (Fagaceae)
C. psidi (Sutton 1980)	–	–	25–40 × 14–17; 5–6	*Psidium guajava* (Myrtaceae)
C. pyricola (Sutton 1980)	–	–	61–70 × 24–32; 5–7	*Pyrus* sp. (Rosaceae)
C. umbonatum (*Pseudovalsa longipes*) (Wehmeyer 1926)	–	–	47–104 × 10–14; 3–8	*Quercus coccinea* (Fagaceae)
C. umbonatum (Gadgil and Dick 2007, Sutton 1980)	1500–2200	(10–) 27.5–47	57–72 × 14–16; apical cell with a hyaline tip; 5–7	*Quercus* spp. (Fagaceae), *Castanea sativa* (Fagaceae)
C. umbonatum (Senanayake et al. 2017)	1000–1300 × 500–550	20–35 × 4–7	42–56 × 13–16; apical cell with a hyaline tip; 4–6	*Quercus* sp. (Fagaceae)
C. umbonatum (Senanayake et al. 2018)	450 × 700	20–30 × 3–6	35–45 × 8–10; apical cell with a hyaline tip; 4–6	*Quercus petraea* (Fagaceae)

al. 2017, 2018, Farr and Rossman 2018). Until recently, these taxa have primarily been identified by their morphology i.e. Sutton (1980) and only a few species are supported by molecular data with nine sequences from six species available in GenBank. However, we do not include *Coryneum foliicola* (CBS 153.32) sequence data in our analyses as its phylogenetic affinities are distant from Coryneaceae (data not shown). Therefore, we use reliable sequences from GenBank to determine the taxonomic placement of our new species.

Based on morphological characters, there are some similarities between *Coryneum heveanum* and related *Coryneum* species, such as acervular conidiomata, fusiform or clavate conidia with pseudosepta (Sutton 1980, Maharachchimbura et al. 2016, Senanayake et al. 2017, 2018). However, *C. heveanum* is distinct from other known taxa including *Coryneum umbonatum* (type species) by conidial measurements, number of pseudosepta and lack of a hyaline tip to the apical cell (Table 2) (Briosi and Farneti 1908, Sutton 1980, Gadgil and Dick 2007, Senanayake et al. 2017, 2018).

Current phylogenetic analyses of combined LSU, ITS and TEF1 alignment are used to clarify the species relationships in *Coryneum* (Figure 1), following Senanayake et al. (2017) and Fan et al. (2018). The phylogenetic tree shows that our species clearly groups with *Coryneum*. In addition, pairwise dissimilarities of DNA sequences of ITS regions between *C. heveanum* and other *Coryneum* species also provide further evidence to justify *C. heveanum* as a new species (Jeewon & Hyde, 2016). Comparison of 599 nucleotides of the ITS nucleotides between *C. heveanum* and *C. umbonatum* (MFLUCC 13-0658 and

MFLUCC 15-1110) reveals 90 base pair differences. Comparison of 536 nucleotides of the ITS nucleotides between *C. heveanum* and *C. castaneicola* (43_2) reveals 90 base pair differences. Comparison of 620 nucleotides of the ITS nucleotides between *C. heveanum* and *C. umbonatum* (CBS 199.68) reveals 91 base pair differences. Comparison of 598 nucleotides of the ITS nucleotides between *C. heveanum* and *C. perniciosum* (CBS 130.25) reveals 77 base pair differences. *Coryneum umbonatum* strains (AR3541, MFLUCC 13-0658 and MFLUCC 15-1110) form a distinct lineage, which is in agreement with the results of Fan et al. (2018). However, *Coryneum umbonatum* (CBS 199.68) forms a separate clade with *C. umbonatum* strain AR 3541, MFLUCC 13-0658 and MFLUCC 15-1110 and we cannot verify this taxon based on morphological characters. Previous studies have described the morphological features of *Coryneum umbonatum* but conidial dimensions and number of pseudosepta reported varies significantly from each other (Sutton 1980, Gadgil and Dick 2007, Senanayake et al. 2017, 2018) (Table 2). In addition, some of the *Coryneum* sequences deposited in GenBank (i.e. *C. castaneicola*, *C. depressum*, *C. foliicola*, *C. monodia* and *C. perniciosum*, *C. umbonatum*) lack morphological characteristics and their identities cannot be confirmed. Therefore, these taxa need to be recollected, described and sequenced to determine their taxonomic placement in this family.

Acknowledgements

We would like to thank the Thailand Research Fund (TRF) grant no. MRG5580163, DGB6080013 and Chiang Mai University for financial support. C. Senwanna would like to thank the Key Research Program of Frontier Sciences, CAS (grant no. QYZDY-SSW-SMC014 and 973 key project of the National Natural Science Foundation of China (grant no. 2014CB954101) for supporting DNA molecular experiments of this study. R. Phookamsak expresses appreciation to the Research Fund from China Postdoctoral Science Foundation (grant no. Y71B283261), the Yunnan Provincial Department of Human Resources and Social Security (grant no. Y836181261), the National Nature Science Foundation of China (NSFC; grant no. 31850410489) and Chiang Mai University for financial support. We thank Milan C. Samarakoon and Sirinapa Konta for their valuable suggestions and helping in phylogenetic analyses. Dr. *Shaun Pennycook* is thanked for his essential nomenclatural review.

References

Barr ME (1978) The Diaporthales in North America: with emphasis on *Gnomonia* and its segregates. Mycologia Memoirs 7: 1–232.

Briosi G, Farneti R (1908) Sulla moria dei castagni (mal dell'inchiostro), prima nota. Atti dell'Istituto Botanico della Università e Laboratorio Crittogamico di Pavia 13: 291–307.

Cai Z, Li G, Lin C, Shi T, Zhai L, Chen Y, Huang G (2013) Identifying pathogenicity genes in the rubber tree anthracnose fungus *Colletotrichum gloeosporioides* through random in-

sertional mutagenesis. Microbiological Research 168: 340–350. http://doi.org /10.1016/j.micres.2013.01.005

Carbone I, Kohn LM (1999) A method for designing primer sets for speciation studies in filamentous ascomycetes. Mycologia 91: 553–556. https://doi.org/10.2307/3761358

Castlebury LA, Rossman AY, Jaklitsch WJ, Vasilyeva LN (2002) A phylogeny overview of the Diaporthales based on large subunit nuclear ribosomal DNA sequences. Mycologia 94: 1017–1031. https://doi.org/10.1080/15572536.2003.11833157

Corda ACI (1839) *Coniomycetes* Nees ab Esenb. Icones Fungorum hucusque Cognitorum 3: 1–55.

Déon M, Scomparin A, Tixier A, Mattos CRR, Leroy T, Seguin M, Roeckel-Drevet P, Pujade-Renaud V (2012) First characterization of endophytic *Corynespora cassiicola* isolates with variant cassiicolin genes recovered from rubber trees in Brazil. Fungal Diversity 54: 87–99. https://doi.org/10.1007/s13225-012-0169-6

de Silva H, Castlebury LA, Green S, Stone JK (2009) Characterisation and phylogenetic relationships of *Anisogramma virgultorum* and *A. anomala* in the Diaporthales (Ascomycota). Mycological Research 113: 73–81. http://doi.org/10.1016/j.mycres.2008.08.008

Fan XL, Bezerra JDP, Tian CM, Crous PW (2018) Families and genera of diaporthalean fungi associated with canker and dieback of tree hosts. Persoonia 40: 119–134. https://doi.org/10.3767/persoonia.2018.40.05

Farr DF, Rossman AY (2018) Fungal Databases, U.S. National Fungus Collections, ARS, USDA. https://nt.ars-grin.gov/fungaldatabases/

Gadgil PD, Dick M (2007) Fungi Silvicolae Novazelandiae: 7. New Zealand Journal of Forestry Science 37: 329–335. http://10.1186/s40490-014-0030-7

Gazis R, Chaverri P (2010) Diversity of fungal endophytes in leaves and stems of wild rubber trees (*Hevea brasiliensis*) in Peru. Fungal Ecology 3: 240–254. https://doi.org/10.1016/j.funeco.2009.12.001

Ghazali NIB (2013) Isolation and identification of fungi associated with leaf diseases of *Hevea Brasiliensis*. http://ir.unimas.my/8746/

Hall TA (1999) BioEdit: a user-friendly biological sequence alignment editor and analysis program for Windows 95/98/NT. Nucleic Acids Symposium Series 41: 95–98.

Häuser I, Martin K, Germer J, He P, Blagodatskiy S, Liu H, Krauß M, Rajaona A, Shi M, Pelz S, Langenberger G, Zhu C, Cotter M, Stürz S, Waibel H, Steinmetz H, Wieprecht S, Frör O, Ahlheim M, Aenis T, Cadisch G (2015) Environmental and socio-economic impacts of rubber cultivation in the Mekong region: challenges for sustainable land use. CAB Reviews 10: 1–11. https://doi.org/10.1079/PAVSNNR201510027

Herrmann L, Lesueur D, Bräu L, Davison J, Jairus T, Robain H, Robin A, Vasar M, Wiriyakitnateekul W, Öpik M (2016) Diversity of root-associated arbuscular mycorrhizal fungal communities in a rubber tree plantation chronosequence in Northeast Thailand. Mycorrhiza 26: 863–877. http://doi.org/10.1007/s00572-016-0720-5

Horst RK (2013) Field Manual of Diseases on Trees and Shrubs. 2013th Edition. Springer, Netherlands, 207 pp. http://doi.org/10.1007/978-94-007-5980-0_4

Hyde KD, Chaiwan N, Norphanphoun C, Boonmee S, Camporesi E, Chethana KWT, Dayarathne MC, de Silva NI, Dissanayake AJ, Ekanayaka AH, Hongsanan S, Huang SK, Jayasiri SC, Jayawardena R, Jiang HB, Karunarathna A, Lin CG, Liu JK, Liu NG, Lu YZ, Luo

ZL, Maharachchimbura SSN, Manawasinghe IS, Pem D, Perera RH, Phukhamsakda C, Samarakoon MC, Senwanna C, Shang QJ, Tennakoon DS, Thambugala KM, Tibpromma S, Wanasinghe DN, Xiao YP, Yang J, Zeng XY, Zhang JF, Zhang SN, Bulgakov TS, Bhat DJ, Cheewangkoon R, Goh TK, Jones EBG, Kang JC, Jeewon R, Liu ZY, Lumyong S, Kuo CH, McKenzie EHC, Wen TC, Yan JY, Zhao Q (2018) Mycosphere notes 169–224. Mycosphere 9: 271–430. http://doi.org /10.5943/mycosphere/9/2/8

Index Fungorum (2018) http://www.indexfungorum.org/ Names/Names.asp

Jayasinghe CK (2000) Checklist of Rubber Pathogens in Srilanka. National Science Foundation Colombo.

Jayasiri SC, Hyde KD, Ariyawansa HA, Bhat J, Buyck B, Cai L, Dai YC, Abd-Elsalam KA, Ertz D, Hidayat I, Jeewon R, Jones EBG, Bahkali AH, Karunarathna SC, Liu JK, Luangsaard JJ, Lumbsch HT, Maharachchikumbura SSN, McKenzie EHC, Moncalvo JM, GhobadNejhad M, Nilsson H, Pang KA, Pereira OL, Phillips AJL, Raspé O, Rollins AW, Romero AI, Etayo J, Selçuk F, Stephenson SL, Suetrong S, Taylor JE, Tsui CKM, Vizzini A, AbdelWahab MA, Wen TC, Boonmee S, Dai DQ, Daranagama DA, Dissanayake AJ, Ekanayaka AH, Fryar SC, Hongsanan S, Jayawardena RS, Li WJ, Perera RH, Phookamsak R, de Silva NI, Tambugala KM, Tian Q, Wijayawardene NN, Zhao RL, Zhao Q, Kang JC, Promputtha I (2015) The Faces of Fungi database: fungal names linked with morphology, phylogeny and human impacts. Fungal Diversity 74: 3–18. https://doi.org/10.1007/s13225-015-0351-8

Jeewon R, Hyde KD (2016) Establishing species boundaries and new taxa among fungi: recommendations to resolve taxonomic ambiguities. Mycosphere 7: 1669–1677. https://doi.org/10.5943/mycosphere/7/11/4

Katoh K, Rozewicki J, Yamada KD (2017) MAFF online service: multiple sequence alignment, interactive sequence choice and visualization. Briefings in Bioinformatics 1–7. https://doi.org/10.1093/bib/bbx108

Kowalski T, Kehr RD (1922) Endophytic fungal colonization of branch bases in several forest tree species. Sydowia 44: 137–168.

Kromkratoke K, Suwanmaneepong S (2017) Socio-economic Characteristics of Rubber Farmer in the Drought Area in SaKaeo Province, Thailand. International Journal of Agricultural Technology 13: 1947–1957.

Kumar S, Stecher G, Tamura K (2015) MEGA7: Molecular Evolutionary Genetics Analysis version 7.0 for bigger datasets. Molecular Biology and Evolution 33: 1870–1874. http://doi.org10.1093/molbev/msw054

Liu X, Li B, Cai L, Zheng X, Feng Y, Huang G (2018) Colletotrichum Species Causing Anthracnose of Rubber Trees in China. Science reports 8:10435. http://doi.org /10.1038/s41598-018-28166-7

Liyanage KK, Khan S, Mortimer PE, Hyde KD, Xu J, Brooks S, Ming Z (2016) Powdery mildew disease of rubber tree. Forest Pathology 46: 90–103. http://doi.org/10.1111/efp.12271

Maharachchikumbura SSN, Hyde KD, Jones EBG, McKenzie EHC, Bhat JD, Dayarathne MC, Huang SK, Norphanphoun C, Senanayake IC, Perera RH, Shang QJ, Xiao YP, D'souza MJ, Hongsanan S, Jayawardena RS, Daranagama DA, Konta S, Goonasekara ID, Zhuang WY, Jeewon R, Phillips AJL, AbdelWahab MA, Al-Sadi AM, Bahkali AH, Boon-

mee S, Boonyuen N, Cheewangkoon R, Dissanayake AJ, Kang JC, Li QR, Liu JK, Liu XZ, Liu ZY, Luangsa-ard JJ, Pang KL, Phookamsak R, Promputtha I, Suetrong S, Stadler M, Wen TC, Wijayawardene NN (2016) Families of Sordariomycetes. Fungal Diversity 79: 1–317. https://doi.org/10.1007/s13225-016-0369-6

Marin-Felix Y, Groenewald L, Cai L, Chen Q, Marincowitz S, Barnes I, Bensch K, Braun U, Camporesi E, Damn U, de Beer ZW, Dissanayake A, Edward J, Giraldo A, Hernández-Restrepo M, Hyde KD, Jayawardena RS, Lombard L, Luangsa-ard J, McTaggart AR, Rossman AY, Sandoval-Denis M, Shen M, Shivas RG, Tan YP, van der Linde EJ, Wingfield MJ, Wood AR, Zhang JQ, Zhang Y, Crous PW (2017) Genera of phytopathogenic fungi: GOPHY 1. Studies in Mycology 86: 99–216. https://doi.org/10.1016/j.simyco.2017.04.002

Martin R, Gazis R, Skaltsas D, Chaverri P, Hibbett D (2015) Unexpected diversity of basidiomycetous endophytes in sapwood and leaves of *Hevea*. Mycologia 107: 284–297. http://doi.org/10.3852/14-206

Nyaka Ngobisa AIC, Zainal Abidin MA, Wong MY, Abbas N, Ntsomboh NG, Owona NP (2015) Susceptibility of rubber (*Hevea brasiliensis*) clones to *Neofusicoccum ribis*. World Journal of Agricultural Research 3: 198–202. http://doi.org/10.12691/wjar-3-6-3

Nylander JAA (2004) MrModeltest 2.3. Program distributed by the author. Evolutionary Biology Centre, Uppsala University.

O'Donnell K, Kistler HC, Cigelnik E, Ploetz RC (1998) Multiple evolutionary origins of the fungus causing Panama disease of banana: Concordant evidence from nuclear and mitochondrial gene genealogies. Proceedings of the National Academy of Sciences, USA 95: 2044–2049. https://doi.org/10.1073/pnas.95.5.2044

Priyadarshan PM, Gonçalves PDS, Omokhafe KO (2009) Breeding Hevea rubber. In: Jain SM, Priyadarshan PM (Eds) Breeding Plantation Tree Crops: Tropical Species. Springer, New York, 469–522. https://doi.org/10.1007/978-0-387-71201-7_13

Raddi P, Panconesi A (1981) Cypress canker disease in Italy: biology control possibilities and genetic improvement for resistance. European Journal of Forest Pathology 11: 340–347. http://doi.org/10.1111/j.1439-0329.1981.tb00104.x

Rambaut A (2016) FigTree, version 1.4.3. University of Edinburgh, Edinburgh.

Rannala B, Yang Z (1996) Probability distribution of molecular evolutionary trees: a new method of phylogenetic inference. Journal of Molecular Evolution 43: 304–311. https://doi.org/10.1007/BF02338839

Rehner SA (2001) Primers for elongation factor 1-alpha (EF1-alpha). http://ocid.nacse.org/research/deephyphae/EF1primer.pdf

Rippel MM, Galembeck F (2009) Nanostructures and Adhesion in Natural Rubber: New Era for a Classic. Journal of the Brazilian Chemical Society 20: 1024–1030.

Rocha ACS, Garcia D, Uetanabaro APT, Carneiro RTO, Araújo IS, Mattos CRR, Góes-Neto A (2011) Foliar endophytic fungi from *Hevea brasiliensis* and their antagonism on *Microcyclus ulei*. Fungal Diversity 47: 75–84. http://doi.org/10.1007/s13225-010-0044-2

Romyen A, Sausue P, Charenjiratragul S (2018) Investigation of rubber-based intercropping system in Southern Thailand. Kasetsart Journal of Social Sciences 39: 135–142. https://doi.org/10.1016/j.kjss.2017.12.002

Ronquist F, Huelsenbeck JP (2003) MrBayes 3: Bayesian phylogenetic inference under mixed models. Bioinformatics 19: 1572–1574. https://doi.org/10.1093/bioinformatics/btg180

Rossman AY, Adams GC, Cannon PF, Castlebury LA, Crous PW, Gryzenhout M, Jaklitsch WM, Mejia LC, Stoykov D, Udayanga D, Voglmayr H, Walker DM (2015) Recommendations of generic names in Diaporthales competing for protection or use. IMA Fungus 6: 145–154. http://doi.org/10.5598/imafungus.2015.06.01.09

Rossman AY, Farr DF, Castlebury LA (2007) A review of the phylogeny and biology of the Diaporthales. Mycoscience 48: 135–144. https://doi.org/10.1007/S10267-007-0347-7

Seephueak P (2012) Fungal associated with degradation of rubber wood logs and leaf little. PhD Thesis, Prince of Songkla University, Hat Yai Campus, Songkhla, Thailand.

Seephueak P, Phongpaichit S, Hyde KD, Petcharat V (2011) Diversity of saprobic fungi on decaying branch litter of the rubber tree (*Hevea brasiliensis*). Mycosphere 2(4): 307–330.

Senanayake IC, Crous PW, Groenewald JZ, Maharachchikumbura SSN, Jeewon R, Phillips AJL, Bhat JD, Perera RH, Li QR, Li WJ, Tangthirasunun N, Norphanphoun C, Karunarathna SC, Camporesi E, Manawasighe IS, Al-Sadi AM, Hyde KD (2017). Families of Diaporthales based on morphological and phylogenetic evidence. Studies in Mycology 86: 217–296. http://doi.org/10.1016/j.simyco.2017.07.003

Senanayake IC, Jeewon R, Chomnunti P, Wanasinghe DN, Norphanphoun C, Karunarathna A, Pem D, Perera RH, Campores E, McKenzie EHC, Hyde KD, Karunarathna SC (2018) Taxonomic circumscription of Diaporthales based on multigene phylogeny and morphology. Fungal Diversity. 1–203. https://doi.org/10.1007/s13225-018-0410-z

Senwanna C, Phookamsak R, Doilom M, Hyde KD, Cheewangkoon R (2017) Novel taxa of Diatrypaceae from Para rubber (*Hevea brasiliensis*) in northern Thailand; introducing a novel genus *Allocryptovalsa*. Mycosphere 8: 1835–1855. http://doi.org/10.5943/mycosphere/8/10/9

Senwanna C, Phookamsak R, Bahkali AH, Elgorban AM, Cheewangkoon R, Hyde KD (2018) *Neolinocarpon phayaoense* sp. nov. (Linocarpaceae) from Thailand. Phytotaxa 362: 077–086. https://doi.org/10.11646/phytotaxa.362.1.6

Silvestro D, Michalak I (2011) raxmlGUI: a graphical front-end for RAxML. Organisms Diversity, Evolution 12: 335–337. https://doi.org/10.1007/s13127-011-0056-0

Stamatakis A, Hoover P, Rougemont J (2008) A rapid bootstrap algorithm for the raxml web servers. Systematic Biology 57: 758–771. https://doi.org/10.1080/10635150802429642

Strouts RG (1972) Canker of cypresses caused by *Coryneum cardinale* Wag. in Britain. European Journal of Forest Pathology 3: 13–24. https://doi.org/10.1111/j.1439-0329.1973.tb00372.x

Sutton BC (1975) Coelomycetes V. *Coryneum*. Myc. Papers. 138:1–224.

Sutton BC (1980) The Coelomycetes Fungi imperfect with pycnidia, acervuli and stromata. Commonwealth Mycological Institute, Kew, UK.

Swofford DL (2002) PAUP*: phylogenetic analysis using parsimony (*and other methods). Version 4. Sinauer Associates, Sunderland.

Trakunyingcharoen T, Cheewangkoon R, To-anun C (2015) Phylogenetic study of the Botryosphaeriaceae species associated with avocado and para rubber in Thailand. Chiang Mai University Journal of Natural Sciences 42: 104–116.

Vilgalys R, Hester M (1990) Rapid genetic identification and mapping of enzymatically amplified ribosomal DNA from several *Cryptococcus* species. Journal of Bacteriology 172(8): 4238–4246. https://doi.org/10.1128/jb.172.8.4238-4246.1990

Vongkhamheng C, Zhou J, Beckline M, Phimmachanh S (2016) Socioeconomic and ecological impact analysis of rubber cultivation in Southeast Asia. Open Access Library Journal, 3: e2339. https://doi.org/10.4236/oalib.1102339

White T, Bruns T, Lee S, Taylor JW (1990) Amplification and direct sequencing of fungal ribosomal RNA genes for phylogenetics. In: Innis M, Gelfand D, Shinsky J, White T (Eds) PCR protocols: a guide to methods and applications. 18(1): 315–322. https://doi.org/10.1016/B978-0-12-372180-8.50042-1

Wijayawardene NN, Hyde KD, Rajeshkumar KC, Hawksworth DL, Madrid H, Kirk PM, Braun U, Singh RV, Crous PW, Kukwa M, Lücking R, Kurtzman CP, Yurkov A, Haelewaters D, Aptroot A, Lumbsch HT, Timdal E, Ertz D, Etayo J, Phillips AJL, Groenewald JZ, Papizadeh M, Selbmann L, Dayarathne MC, Weerakoon G, Gareth Jones EB, Suetrong S, Tian Q, Castañeda-Ruiz RF, Bahkali AH, Pang K, Tanaka K, Dai DQ, Sakayaroj J, Hujslová M, Lombard L, Shenoy BD, Suija A, Maharachchikumbura SSN, Thambugala KM, Wanasinghe DN, Sharma DO, Gaikwad S, Pandit G, Zucconi L, Onofri S, Egidi E, Raja HA, Kodsueb R, Cáceres MES, Pérez-Ortega S, Fiuza PO, Monteiro JS, Vasilyeva LN, Shivas RG, Prieto M, Wedin M, Olariaga I, Lateef AA, Agrawal Y, Fazeli SAS, Amoozegar MA, Zhao GZ, Pfliegler WP, Sharma G, Oset M, Abdel-Wahab MA, Takamatsu S, Bensch K, de Silva NI, De Kesel A, Karunarathna A, Boonmee S, Pfister DH, Lu Y, Luo Z, Boonyuen N, Daranagama DA, Senanayake IC, Jayasiri SC, Samarakoon MC, Zeng X, Doilom M, Quijada L, Rampadarath S, Heredia G, Dissanayake AJ, Jayawardana RS, Perera RH, Tang LZ, Phukhamsakda C, Hernández-Restrepo M, Ma X, Tibpromma S, Gusmao LFP, Weerahewa D, Karunarathna SC (2017) Notes for genera: Ascomycota. Fungal Diversity 86: 1–594. http://doi.org/10.1007/s13225-017-0386-0

Wijayawardene NN, Hyde KD, Lumbsch HT, Liu JK, Maharachchikumbura SSN, Ekanayaka AH, Tian Q, Phookamsak R (2018) Outline of Ascomycota: 2017. Fungal Diversity 88(1): 167–263. http://doi.org/10.1007/s13225-018-0394-8

Yang Q, Fan XL, Du Z, Tian CM (2018) Diaporthosporellaceae, a novel family of Diaporthales (Sordariomycetes, Ascomycota). Mycoscience 59: 229–235. https://doi.org/10.1016/j.myc.2017.11.005

Zhaxybayeva O, Gogarten JP (2002) Bootstrap, Bayesian probability and maximum likelihood mapping: exploring new tools for comparative genome analyses. Genomics 3(4): 1–15. https://doi.org/10.1186/1471-2164-3-4

MycoKeys 43: 91–113 (2018)
doi: 10.3897/mycokeys.43.29093
http://mycokeys.pensoft.net

RESEARCH ARTICLE

A peer-reviewed open-access journal
MycoKeys
Launched to accelerate biodiversity research

Population genomic analyses of RAD sequences resolves the phylogenetic relationship of the lichen-forming fungal species *Usnea antarctica* and *Usnea aurantiacoatra*

Felix Grewe[1], Elisa Lagostina[2], Huini Wu[1,3], Christian Printzen[2], H. Thorsten Lumbsch[1]

1 *Integrative Research Center, Science and Education, Field Museum of Natural History, 1400 S Lake Shore Drive, Chicago, IL 60605, USA* **2** *Department of Botany and Molecular Evolution, Senckenberg Research Institute and Natural History Museum Frankfurt, Senckenberganlage 25, 60325 Frankfurt/Main, Germany* **3** *Department of Cell and Molecular Physiology, Stritch School of Medicine, Loyola University Chicago, 2160 S First Avenue, Maywood, IL 60153, USA*

Corresponding author: *Felix Grewe* (fgrewe@fieldmuseum.org)

Academic editor: *E. Kraichak* | Received 15 August 2018 | Accepted 23 November 2018 | Published 12 December 2018

Citation: Grewe F, Lagostina E, Wu H, Printzen C, Lumbsch HT (2018) Population genomic analyses of RAD sequences resolves the phylogenetic relationship of the lichen-forming fungal species *Usnea antarctica* and *Usnea aurantiacoatra*. MycoKeys 43: 91–113. https://doi.org/10.3897/mycokeys.43.29093

Abstract

Neuropogonoid species in the lichen-forming fungal genus *Usnea* exhibit great morphological variation that can be misleading for delimitation of species. We specifically focused on the species delimitation of two closely-related, predominantly Antarctic species differing in the reproductive mode and representing a so-called species pair: the asexual *U. antarctica* and the sexual *U. aurantiacoatra*. Previous studies have revealed contradicting results. While multi-locus studies based on DNA sequence data provided evidence that these two taxa might be conspecific, microsatellite data suggested they represent distinct lineages. By using RADseq, we generated thousands of homologous markers to build a robust phylogeny of the two species. Furthermore, we successfully implemented these data in fine-scale population genomic analyses such as DAPC and fineRADstructure. Both *Usnea* species are readily delimited in phylogenetic inferences and, therefore, the hypothesis that both species are conspecific was rejected. Population genomic analyses also strongly confirmed separated genomes and, additionally, showed different levels of co-ancestry and substructure within each species. Lower co-ancestry in the asexual *U. antarctica* than in the sexual *U. aurantiacoatra* may be derived from a wider distributional range of the former species. Our results demonstrate the utility of this RADseq method in tracing population dynamics of lichens in future analyses.

Keywords
Antarctica, Ascomycota, lichens, Parmeliaceae, phylogeny, RADseq

Introduction

Over the last decades, the use of DNA sequence data to delimit species and reconstruct phylogenetic relationships has become standard (Barraclough and Nee 2001; de Queiroz 2007; Holder and Lewis 2003; Huelsenbeck et al. 2001; Taylor et al. 2000; Wiens and Penkrot 2002). In groups with high morphological plasticity and homoplasy in phenotypical data sets, such as fungi, molecular data have dramatically changed our understanding of evolution and coinciding taxonomic interpretations (Hibbett et al. 2007; James et al. 2006; Lutzoni et al. 2004; McLaughlin et al. 2009; Robbertse et al. 2006; Schoch et al. 2009; Spatafora et al. 2017; Spatafora and Robbertse 2010; Stajich et al. 2009).

The general lineage species concept (de Queiroz 2007) allows researchers to use different empirical data to test the hypothesis of lineage separation, including phenotypical characters and molecular data. The latter dataset often provides strong evidence if analysed within a rigorous statistical framework (Rannala 2015). With regards to species delimitation, numerous studies of lichen-forming fungi detected distinct lineages lacking obvious distinguishing phenotypical characters, the so-called cryptic species (Bickford et al. 2007; Crespo and Lumbsch 2010; Crespo and Pérez-Ortega 2009; Lumbsch and Leavitt 2011). However, some studies also demonstrated that morphologically distinct populations could not be separated using single- or multi-locus genetic data. These results have been interpreted either as an indication of recent diversification and incomplete lineage sorting (Leavitt et al. 2016a; Zhao et al. 2017) or that the phenotypes represented populations of the same species (Articus et al. 2002; Buschbom and Mueller 2006; Kotelko and Piercey-Normore 2010; Lohtander et al. 1998; Myllys et al. 2001; Velmala et al. 2009). The latter result was often found in so-called species pairs. These are lichens that differ in forming either ascomata and reproducing sexually or forming asexual diaspores (soredia), which propagate the fungal and photosynthetic partner simultaneously (Mattsson and Lumbsch 1989; Poelt 1970; Tehler 1982). Otherwise, these species are morphologically identical, but were traditionally regarded as distinct species due to their different reproductive modes (Poelt 1972). The *Parmotrema perforatum* group was used as a model system of species delimitation based on the reproductive mode and secondary metabolites (Culberson and Culberson 1973). However, a recent study suggests that the phylogenetic relationships between sexual and asexual populations might be more complex (Widhelm et al. 2016).

We here focus on a complex of two morphologically similar species that differ in their reproductive mode and are considered a species pair in the genus *Usnea*: *U. aurantiacoatra* and *U. antarctica*, the latter reproducing by asexual soredia (Walker 1985). Within the genus, there is group of species predominantly occurring in Antarctica and adjacent cool-temperate to polar regions with a thallus that consists of yellow (containing usnic acid) and blackish areas (caused by melanins). Species in this group, which is also called neuropogonoid (Lumbsch and Wirtz 2011; Wirtz et al. 2008), can be difficult to

distinguish by their general appearance and hence, molecular data, such as DNA marker sequencing, can be helpful in delimiting lineages (Articus 2004; Lumbsch and Wirtz 2011; Seymour et al. 2007; Wirtz et al. 2008; Wirtz et al. 2012). Earlier studies based on morphological and chemical data considered the neuropogonoid species as a subgenus *Neuropogon* in *Usnea* (Lamb 1964; Walker 1985) or as a distinct genus *Neuropogon* (Krog 1976; 1982; Lamb 1939). Molecular studies confirmed *Usnea* (including *Neuropogon*) as a monophyletic genus within Parmeliaceae (Crespo et al. 2007); however, the relationship of *Neuropogon* and *Usnea* remained ambiguous. A two-marker DNA analysis of *Usnea* elevated *Neuropogon* to a generic rank (Articus 2004), but subsequent studies provided evidence that *Neuropogon* is polyphyletic with a core group nested within *Usnea* (Seymour et al. 2007; Wirtz et al. 2008; Wirtz et al. 2012; Wirtz et al. 2006). Multilocus DNA sequence data could not delimit individuals of the species *U. antarctica* and *U. aurantiacoatra* (Seymour et al. 2007; Wirtz et al. 2012) suggesting that they might be conspecific. In contrast, a recent microsatellite study provided evidence that the two species represent isolated lineages (Lagostina et al. 2018). Given the contradicting results of multi-locus and microsatellite data, we decided to employ a reduced genomic dataset to revisit the species delimitation of *U. antarctica* and *U. aurantiacoatra*.

The advent of next-generation sequencing (NGS), also referred to as high-throughput sequencing, drastically changed the scale of molecular datasets for systematic analyses and revolutionised our ability to assess evolutionary histories of organisms (Kraus and Wink 2015; Wachi et al. 2018; Zimmer and Wen 2015). Many molecular studies, such as the former species delimitation efforts for neuropogonoid *Usnea* spp., were limited to, at most, a dozen markers because their production would require tedious lab work and costly Sanger-sequencing (Hoffman and Lendemer 2018; Wilkinson et al. 2017). Population genomics of closely related organisms often relied on the descriptive power of microsatellite markers (Hodel et al. 2016). Compared to these traditional lab methods, NGS techniques allow a relatively straight-forward production of genome-scale datasets. Direct sequencing NGS methods, such as de-novo genome sequencing (Ellegren 2014), re-sequencing (Stratton 2008) or RNAseq of expressed genes (Ozsolak and Milos 2011; Wickett et al. 2014), can provide whole genome-scale data but may still be limited by high sequencing costs. Therefore, these methods are rarely applied to population studies which require the sequencing of many individuals. However, often a subset of the genome entails sufficient polymorphisms to answer questions of phylogenetic or population genomic studies. Hence, many NGS methods for systematic analyses are designed to be economical and generate reduced genome representation datasets (Allendorf 2017; Davey et al. 2011). One of these reduced representation methods is genotype-by-sequencing and its altered approach, which is known as restriction associated DNA sequencing (RADseq) (Baird et al. 2008). We recently designed a RADseq approach for metagenomic data derived from symbiotic lichen genomes, which allows reduced representation genomic analyses of numerous individuals for population-scale studies (Grewe et al. 2017).

By using genome-wide single nucleotide polymorphisms (SNPs) produced by restriction site-associated DNA sequencing (RADseq) of predominantly Antarctic li-

chen-forming fungi, our main aim in this study was to clarify the taxonomy of asexual *Usnea antarctica* and sexual *Usnea aurantiacoatra* and test their hypothesised species pair relationship. To further support our findings, we applied population genomic methods to measure the degree of genomic divergence and infer the levels of co-ancestry for each species.

Methods

Sample collection and site description

Samples were collected in Antarctica between December 2015 and January 2017. From these collected specimens, we chose to compare 105 representative specimens of the species *U. antarctica* and *U. aurantiacoatra* for this study (see details of specimens in Suppl. material 1). All selected specimens were either collected on King George Island (65) and Elephant Island (19) of the South Shetland Islands or in the Northern part of the Antarctic Peninsula (21) near the research bases Esperanza and Primavera. Fifty-eight of the 105 selected specimens were identified as *U. antarctica* and 47 specimens were identified as *U. aurantiacoatra* based on their phenotypical characters (Walker 1985). As a reference sequence to filter for lichen-fungal loci of *U. antarctica* and *U. aurantiacoatra* during the RADseq processing, we sequenced a specimen of *U. strigosa* that was collected in Arkansas, U.S.A. (Suppl. material 1).

DNA extraction

Total metagenomic DNA was extracted either by following a cetyltrimethylammonium bromide (CTAB) protocol as modified by Cubero et al. (1999) or by using the ZR Fungal/Bacterial DNA MiniPrep Kit (Zymo Research, Irvine, CA, USA) as recommended by the manufacturer. We used the whole lichen thalli for DNA extraction from *U. antarctica* and *U. aurantiacoatra*, but only the central axis in *U. strigosa* to preferentially extract DNA from the lichen fungus (to avoid the photobiont). DNA concentrations of all samples were quantified with a Qubit fluorometer (Thermo Fisher Scientific, Waltham, MA, USA).

Reference Sequencing and Assembly

We first deep-sequenced and assembled a reference sequence of an *Usnea strigosa* specimen to aid in mapping lichen-fungal loci during the processing of metagenomic RADseq data. A paired-end Illumina sequencing library of 150 bp read length was constructed from total DNA with the Nextera XT DNA Library Prep Kit (Illumina, San Diego, CA, USA) and sequenced on a NextSeq platform at the University of Il-

linois Chicago's Sequencing Core Facility (Chicago, IL, USA). The resulting reads were quality trimmed using the programme Trimmomatic v0.36 (Bolger et al. 2014). Bases were trimmed when the average quality of 4-base sliding windows was below 15 and bases at the start and end of reads had a quality below 10. Subsequently, all trimmed reads, shorter than 25 bp, were filtered out (LEADING:10 TRAILING:10 SLIDINGWINDOW:4:15 MINLEN:25). The trimmed reads were used for a genome assembly with the programme SPAdes v3.5 (Bankevich et al. 2012) with default parameter settings. The assembled metagenomic scaffolds were loaded into the programme MetaWatt v3.5.3 (Strous et al. 2012) for a binning based on tetranucleotide frequencies. Scaffolds of fungal origin that clustered together were separated from the remaining scaffolds. All selected scaffolds that were larger than 10 kb were then included into the final reference sequence of *U. strigosa*. We used the Core Eukaryotic Gene Mapping Approach (CEGMA) to estimate the genomic completeness of the assembly (Parra et al. 2009). Finally, we created a Bowtie2 (Langmead and Salzberg 2012) database from the selected scaffolds for the mapping approach to filter for fungal RAD loci.

RADseq Library Preparation and Sequencing

RADseq libraries for *Usnea antarctica* and *U. aurantiacoatra* were prepared as described previously (Grewe et al. 2017). In short, for the RADseq library production, DNA isolations were pooled with sequence adapters (Rubin and Moreau 2016), subsequently digested with the restriction enzyme ApeKI (New England Biolabs, Ipswich, MA, USA) and ligated using T4 ligase (New England Biolabs). Up to 48 samples with compatible barcodes were pooled and selected for fragments of sizes between 300 and 500 bp using the BluePippin DNA size selection system (Sage Science, Beverly, MA, USA). The pooled libraries were amplified using the REDTaq ReadyMix (Sigma-Aldrich, St. Louis, MO, USA) prior to sequencing on an Illumina MiSeq using the MiSeq Reagent Kit v3 for 150 cycles (Illumina, San Diego, CA, USA) to produce single-end sequences with a length of 150 bp.

Assembly of RADseq datasets

The raw reads of *U. antarctica* and *U. aurantiacoatra* from the MiSeq sequencing were processed and assembled as described earlier for metagenomic datasets of lichens (Grewe et al. 2017). This process used a combination of the ipyRAD (https://github.com/dereneaton/ipyrad/blob/master/docs/index.rst) and pyRAD (Eaton and Ree 2013) pipelines with an additional mapping step that filtered for lichen-fungal loci with a reference sequence. Subsequently, we refer to the raw Illumina RAD sequences as 'read' and name the clustered reads per individual sample 'loci'; the final matrices are alignments of homologous loci from multiple samples with nucleotide substitutions referred to as 'SNP'. In pyRAD, we set the datatype to genotype-by-sequencing

(gbs), ploidy to haploid (1), a similarity threshold for the clustering of reads within and between individuals to 90% (.90) and a minimum coverage of four individuals per locus (4). For the reference-based filtering of RAD loci, we used Bowtie2 with adjusted parameters to allow one permitted mismatch (–N 1), a seed length of 20 (–L 20), up to 20 seed extension attempts (–D 20) and a maximum "re-seeding" of 3 (–R 3). Following an initial round with all sequenced samples, we re-ran step 7 of pyRAD and excluded samples with less than 1000 recovered loci. We used the filtered pyRAD output files, such as unlinked_snps, alleles and vcf, for further analyses.

Phylogenetic reconstructions

Phylogenetic trees were calculated from all unlinked SNPs of the filtered RADseq dataset, i.e. a matrix that was limited to one SNP per RAD locus. This matrix was used for a RAxML v7.2.8 (Stamatakis 2006) maximum likelihood analysis using the GTR + G model. For each analysis, 100 bootstrap replicates were calculated using the fast bootstrapping option implemented in RAxML (Stamatakis et al. 2008). The resulting phylogenetic tree was midpoint rooted and drawn to scale with FigTree v1.4.3 (http://tree.bio.ed.ac.uk/software/figtree/).

Analysis of population structure

To calculate differences in the population structure between *U. antarctica* and *U. aurantiacoatra*, we created a reduced dataset that included all sites with a minor allele frequency (MAF) greater than or equal to 0.05 and greater than 50% coverage using vcftools v0.1.15 (Danecek et al. 2011). This reduced vcf file was converted into a genind object from the R package adegenet v2.0.2 (Jombart and Ahmed 2011; Jombart et al. 2010). The genind object was appended with additional information settings for haploid genomes and the population memberships for samples according to their initial identification based on morphological characters. With all information enclosed, the genind object became subject to population genetics analyses encoded in R.

To determine the degree to which both populations are subdivided, we estimated Gst (Nei 1973) and Hedrick's standardised genetic differentiation measures G'st (Hedrick 2005) and Jost's D (Jost 2008) by using the R package mmod v1.3.3 (Winter 2012). Gst is a good measure when the mutation rate is small relative to migration rate; contrarily, G'st and D fit to data with high mutation rates and two populations (Whitlock 2011). We used these multiple statistics to get a comprehensive measure of genomic differentiation. In a population pairwise comparison, we calculated these indices per site and plotted the values by frequency in separate histograms for Gst, G'st and D.

The genetic structure of samples of *U. antarctica* and *U. aurantiacoatra* was evaluated with the Discriminant Analysis of Principal Components (DAPC) implemented in the R package adegenet v2.02. This non-parametric method first transforms the data

using a principle components analysis (PCA) and subsequently distinguishes between two or more groups using a discriminant analysis (DA). The DAPC was conducted by using the first 60 principal components and all (two) DA-eigenvalues. In addition to the display of the genetic variation in genomic space, the DAPC allows a prediction of the group membership probability for each sample which is visualised in a STRUCTURE-like plot.

In addition to the nonparametric approach with DAPC, we used a model-based method to detect population subdivision using the programme fineRADstructure (Malinsky et al. 2018). This software is specifically designed to measure population structure amongst haplotypes inferred from RADseq datasets. We used the script finerad_input.py included in fineRADstructure-tools (https://github.com/edgardomortiz/fineRADstructure-tools) to convert the pyRAD alleles output into the input format for fineRADstructure. During the conversion, we also reduced the dataset to only unlinked loci (default parameter) with a minimum sample number of 4 (--minsample 4). As recommended by the authors, we then re-ordered the unsorted RAD loci with the script sampleLD.R which is part of the fineRADstructure package. Next, we used the scripts, RADpainter and fineSTRUCTURE, which are both implemented in fineRADstructure, to measure the population structure. First, we calculated the co-ancestry matrix with RADpainter for haploid datasets (-p 1). We then used fineSTRUCTURE for the Markov chain Monte Carlo (MCMC) clustering algorithm with the following arguments: -x 100,000, -z 100,000 and -y 1,000. We also started fineSTRUCTURE with the arguments -m T and -x 10,000 to run a simple tree-building algorithm on the data of the co-ancestry matrix. Finally, the co-ancestry matrix, MCMC output and the coalescence tree were loaded into the programme 'Finestructure GUI' for visualisation.

Reproducibility

The *U. strigosa* reference sequence and all scripts that were used in this study are available online (https://github.com/felixgrewe/Usnea). All RAD sequences were deposited in the NCBI Sequence Read Archive (SRA) with accession number PRJNA505526.

Results

Reference assembly and RADseq results

We assembled a draft reference genome of *U. strigosa* to filter for fungal RAD loci from *U. antarctica* and *U. aurantiacoatra*. The Illumina NextSeq sequencing of the whole *U. strigosa* lichen resulted in 8,552,530 metagenomic paired-end reads. First, we trimmed these raw data which reduced the paired-end reads to 8,366,962 (97.78% of raw data). The trimmed read pairs were then assembled into 16,932 scaffolds (N50 = 12,750 bp) with a total size of 40.9 Mbp (including 1,187 scaffolds of sizes larger than 10 kb).

Metagenomic binning identified 28.92 Mbp of the assembly as fungal derived from which we selected 1,100 scaffolds (N50 = 23,562 bp) with sizes larger than 10 kb; all but two of these scaffolds were continuous assemblies (contigs). The sorted draft genome of *U. strigosa* had a total size of 24.1 Mbp and an estimated completeness of 72.18%.

We included 105 specimens of *U. antarctica* and *U. aurantiacoatra* that were collected in Antarctica in four RADseq libraries (Suppl. material 2). The sequence read number of each sample varied widely from 13,659 for sample EL0059 to 1,942,819 for sample EL0074 with an average sequence read number of 488,468 (sd = 313,604). The number of loci (within sample clusters) that pyRAD generated from these sequences directly correlated with the initial number of sequences (R2 = 0.8017, Suppl. material 3). An average of 21.8% (sd = 2.9%) of all loci mapped to the lichen fungus reference genome and, of these, an average of 85.4% (sd = 5.5%) were included into the final pyRAD dataset. The numbers of loci before and after the mapping were directly correlated (R2 = 0.7598, Suppl. material 3); however, the number of mapped loci reached saturation at an average of 6,496 (sd = 801) for samples with more than 40,000 initial loci. In addition, the number of mapped loci were strongly correlated to the number of loci included in the final dataset (R2 = 0.9869, Suppl. material 3). Two samples of *U. antarctica* (EL0059, EL0281) and two samples of *U. aurantiacoatra* (EL0415, EL0437) had less than 1,000 loci in the final dataset and were removed from the analysis. All remaining 101 samples in the final dataset had on average of 4,143 (sd = 1,316) loci (Suppl. material 2).

Phylogenetic analysis of RADseq data

The phylogenetic analysis of the RADseq data showed two distinct and highly supported clades corresponding to the phenotypically circumscribed species *U. antarctica* and *U. aurantiacoatra* (Figure 1). The phylogenetic tree was calculated from a matrix with 7,087 positions and 53.24% gaps. Most internal relationships within each clade remained unresolved; however, the *U. antarctica* clade showed higher internal support values than the *U. aurantiacoatra* clade. Within the *U. antarctica* clade, three sister relationships of *U. antarctica* (EL0001 and EL0409, EL0382 and EL0390, EL0713 and EL0743) had a 100% bootstrap support and short branches, indicating low genomic divergence.

Population genomic analyses of RADseq data

We determined the degree to which both species complexes are subdivided by Gst, G'st and D measurements. For these analyses, we included only SNPs with a MAF greater than 0.05 and more than 50% coverage. This reduced the RAD dataset to a total of 4,132 SNPs. We plotted the frequency of Gst, G'st and D measures for each SNP (Figure 2). A strong tendency towards 1 for most SNPs in all three measures strongly indicated that genomes of both species were completely isolated. This was also supported by the average measures of Gst, G'st and D of 0.70, 0.93 and 0.60, respectively.

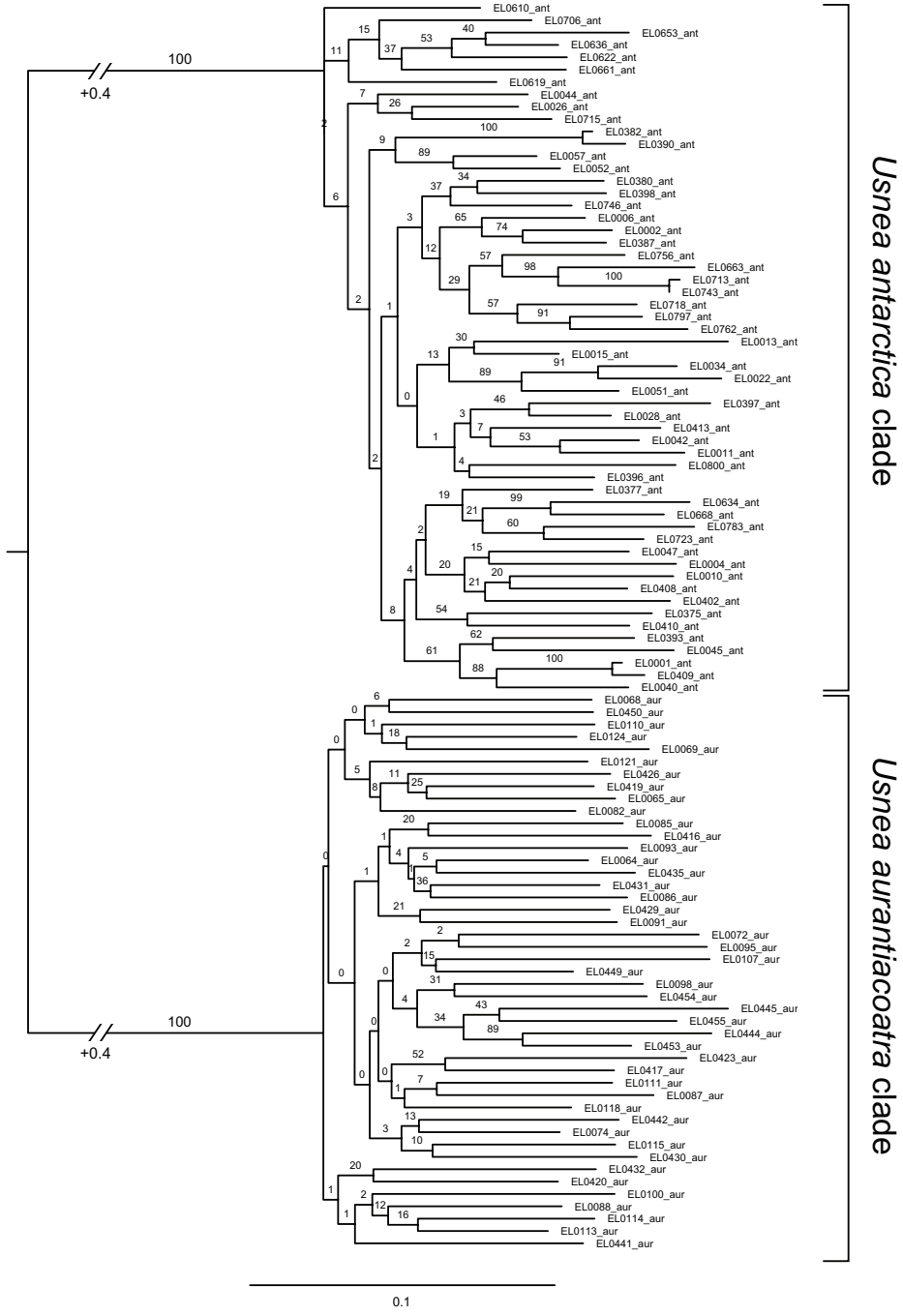

Figure 1. Phylogenetic tree inferred from the *U. antarctica* and *U. aurantiacoatra* RADseq data. The clades of each species are highlighted by brackets. Bootstrap values are indicated at the branches. The unit of branch length is substitutions per site. Note that branches leading to both major clades were abbreviated by 0.4 substitutions per site.

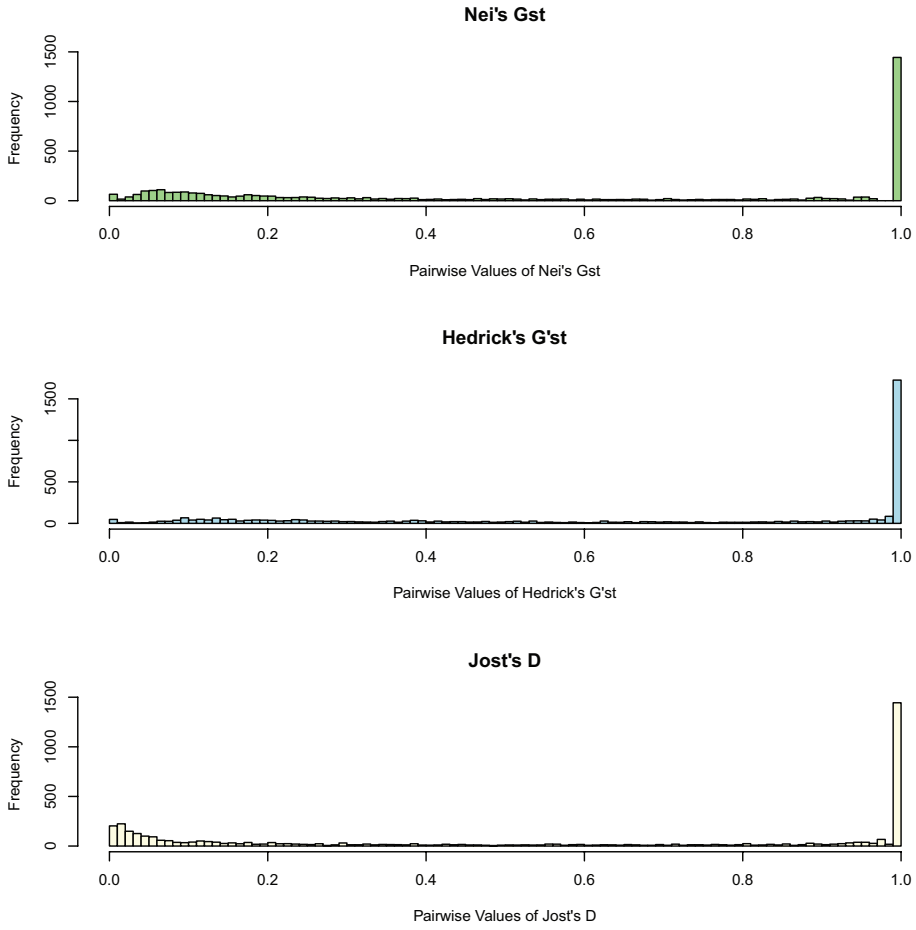

Figure 2. Pairwise Gst, G'st and D distribution. Pairwise values of Nei's Gst (green), Hedrick's G'st (blue) and Jost's D (yellow) are plotted by their frequency.

The same reduced dataset of 4,132 SNPs was used to differentiate the genomes by their variation in a non-parametric approach with a DAPC (Figure 3A). The DAPC combines a PCA with a DA for a separation of genomes based on their variance between groups rather than the total variance of the sample. The resulting clusters of both species were clearly separated in genomic space and showed no evidence for admixture. In addition, the group membership probabilities indicated absolute discrimination of the two species by the DAPC assigning each individual with 100% probability to their respective species (Figure 3B).

The separation of *U. antarctica* and *U. aurantiacoatra* was further supported by the results of a Bayesian model-based approach with the programme fineRADstructure. By converting the pyRAD allele output for fineRADstructure, we reduced the dataset to 3,803 unlinked SNPs with a minimum coverage of 4 samples. The resulting clustered

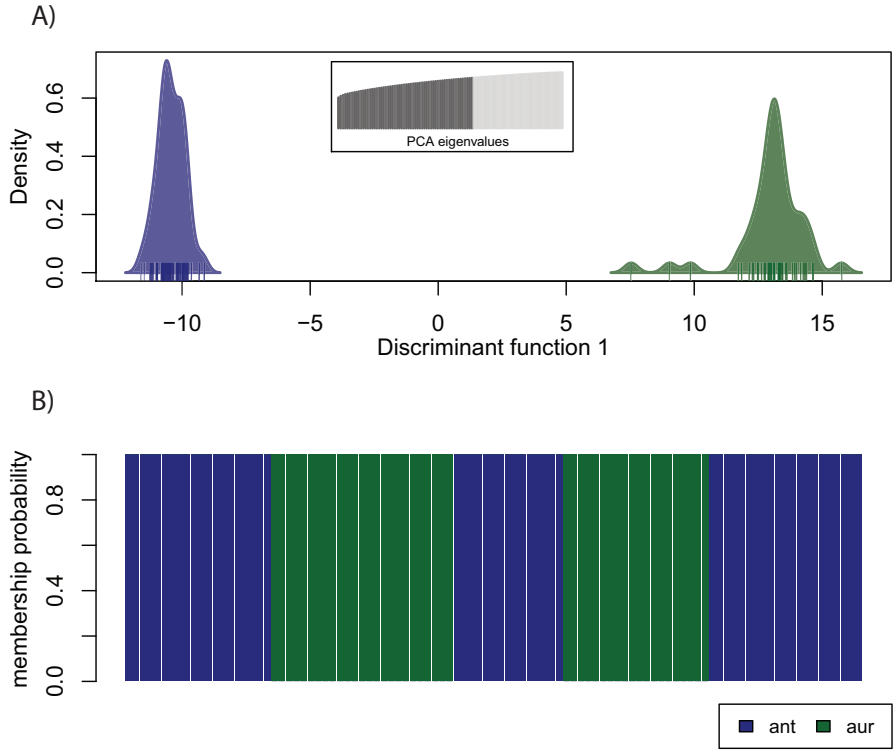

Figure 3. Genomic variation by non-parametric DAPC. **A** DAPC plot of the densities of *U. antarctica* (blue) and *U. aurantiacoatra* (green) on the first retained discriminant function **B** Bar plot of group membership probabilities.

co-ancestry matrix showed that both species shared more co-ancestry within each other than between species (Figure 4). By comparing both species clusters, *U. aurantiacoatra* showed a higher estimated co-ancestry than *U. antarctica* (Figure 4A). To avoid a sampling bias, we reduced the dataset for the fineRADstructure analysis to include only samples collected on King George Island and Elephant Island. This reduced the dataset to 80 samples and 3,652 unlinked SNPs with a minimum coverage of 4 samples. The resulting plot of the reduced dataset also showed higher shared co-ancestry within each species compared to that between species, but estimated higher co-ancestry of *U. antarctica* than *U. aurantiacoatra* (Figure 4B), opposite to the entire dataset. In addition, both matrices visualised different degrees of intraspecific co-ancestry and suggested substructure for a group of three specimens of *U. antarctica* from Potter Peninsula, King George Island (EL0022, EL0034 and EL0051) and for six specimens of *U. aurantiacoatra* from Fildes Peninsula, King George Island (EL0444, EL0435, EL0445, EL450, EL0455 and EL0453). Moreover, two *U. antarctica* specimen pairs collected on King George Island (EL0001 and EL0409, EL0382 and EL390) and one pair col-

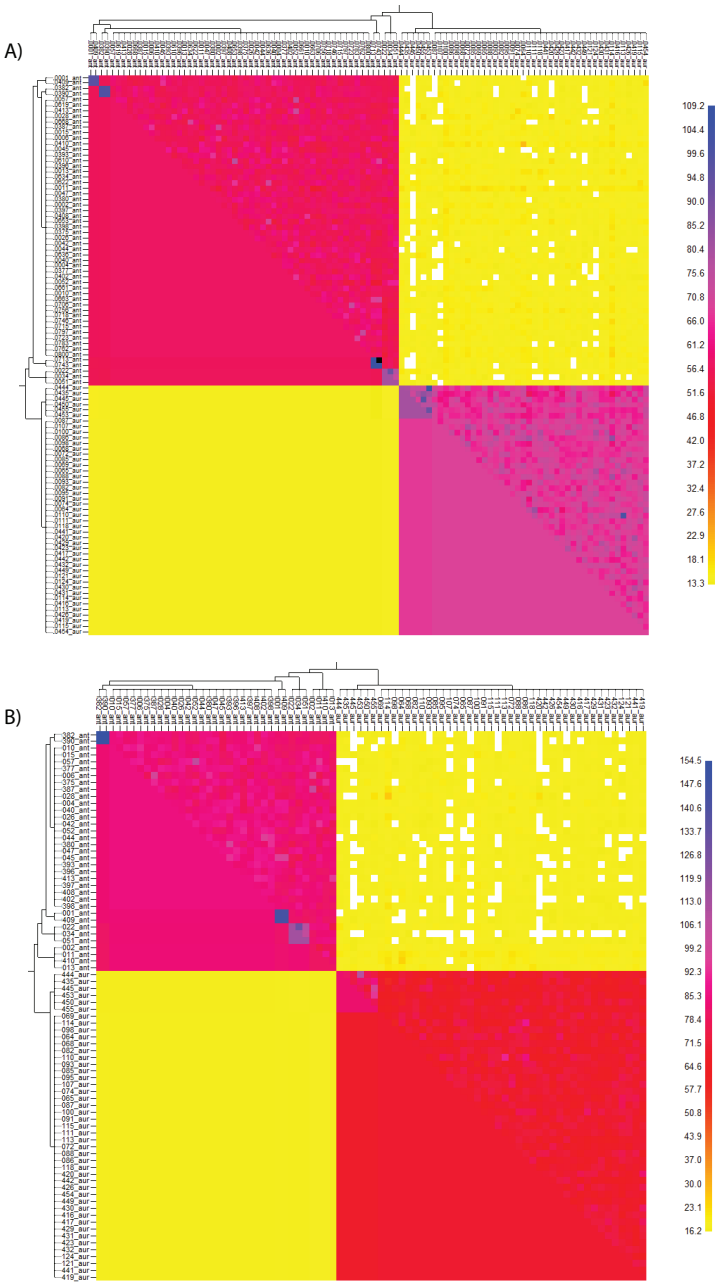

Figure 4. Clustered fineRADstructure co-ancestry matrix. **A** Full dataset including *U. antarctica* collected on the Antarctic Peninsula in addition to *U. antarctica* and *U. aurantiacoatra* collected on King George Island and Elephant Island **B** Reduced dataset with all *U. antarctica* and *U. aurantiacoatra* collected on King George Island and Elephant Island. Two major clades are corresponding to the two species *U. antarctica* (top-left) and *U. aurantiacoatra* (bottom-right). The top and left trees were calculated from the co-ancestry matrix to sort the individuals by their population structure. The matrix is diagonally split into the top-right half showing raw data and the bottom-left half displaying aggregated data.

lected on the Antarctic Peninsula (EL0713 and EL0743) showed the highest degrees of co-ancestry demonstrating very close relatedness, such as sister or clonal relationships. These results agreed with the phylogenetic inference (see above) in which the same *U. antarctica* specimens were close sister taxa.

Discussion

In this study, we used RAD sequencing for evaluating the delimitation of two predominantly Antarctic *Usnea* species. Phylogenetic evidence and population genomic analyses of the RADseq data strongly supported that the two species represent independent lineages. Although both species showed no overlapping genomic structure in a DAPC, we could compare levels of co-ancestry and detect genomic substructure within each species in a fineRADstructure plot.

In previous studies using multi-locus approaches, including the ITS barcoding marker (Schoch et al. 2012), the relationship of *U. antarctica* and *U. aurantiacoatra* remained unresolved and, since specimens of both species did not separate as different clades, conspecificity of the species was not ruled out (Seymour et al. 2007; Wirtz et al. 2012). Our study using RADseq supports the results obtained using microsatellite data that suggested the two species are distinct lineages (Lagostina et al. 2018). In *U. antarctica* and *U. aurantiacoatra*, the taxonomic interpretation of species pairs as separate species (Poelt 1972) is supported.

We developed a RADseq method for lineages involved in intimate symbiotic associations (Grewe et al. 2017), which we here successfully implemented for the use of delimiting two species. Different to the previously described RADseq method that used a reference genome from a lichen-fungal culture, we successfully generated a reference genome from a metagenomic *de-novo* assembly of *U. strigosa*. The filtering of the metagenomic assembly for fungal derived content reduced the size and completeness of the fungal reference (28.92 Mbp, CEGMA: 72.18%) compared to the reference genome assembly from a lichen-fungal culture which was used in earlier studies (31.6 Mbp, CEGMA: 96.77%) (Grewe et al. 2017; Leavitt et al. 2016b). However, the saturation of successfully mapped loci to the reference (Suppl. material 3) suggested that the maximum number of possible mapped loci was reached for samples with many initial loci. Therefore, although using a smaller reference and less fungal derived loci than in our initial study (Grewe et al. 2017), this RADseq approach still was successful in mapping a large number of fungal loci sufficient for phylogenetic and population genomic methods. This widens the potential application of RADseq for intimate symbiotic organisms and includes studies where cultures of one symbiotic partner are not readily available.

RADseq data are extremely powerful, since the method generates a matrix of thousands of homologous loci derived from randomly distributed regions across the genome. Many studies have successfully used large RADseq datasets for phylogenetic analysis which were difficult to resolve due to insufficient signals in available markers

(Eaton and Ree 2013; Escudero et al. 2014; Hipp et al. 2014; Vargas et al. 2017; Wagner et al. 2018). Our phylogenetic and population genomic results from the RADseq dataset clearly delimited *U. antarctica* and *U. aurantiacoatra* into two lineages (Figures 1–4) supporting the acceptance of two species. This confirms that closely related species are difficult to separate using sequence-based multi-locus approaches and great care should be taken when interpreting results from molecular studies when it comes to testing for conspecificity. On the other hand, the microsatellite-based multi-locus approach by Lagostina et al. (2018) rendered almost identical results, including nearly 100 % correct assignment of samples to their species.

The fineRADstructure matrix estimated lower co-ancestry (and hence higher genotypic variation) for the sexually-reproducing *U. aurantiacoatra*, compared to the asexually-reproducing *U. antarctica* when comparing samples that were collected in the same geographic range (Figure 4B). This result agrees with earlier observations that asexual populations have lower genotypic variation than sexual populations in modelling approaches (Balloux et al. 2003) and empirical measures (Delmotte et al. 2002). Moreover, Lagostina et al. (2018) inferred lower genetic variability for *U. antarctica* than *U. aurantiacoatra* using 23 microsatellite loci. These authors also used samples collected in mixed stands of both species from King George and Elephant Island. When we increased our sampling of *U. antarctica* to include a much wider geographical range (Antarctic Peninsula in addition to King George and Elephant Island) compared to the sampling of *U. aurantiacoatra* (King George and Elephant Island only), the matrix indicated increased levels of co-ancestry and a lower genotypic variation (Figure 4A). Although this comparative analysis is lacking collections of *U. aurantiacoatra* from the Antarctic Peninsula for a direct comparison, it should be noted that *U. antarctica* covers a wider geographical range than *U. aurantiacoatra* (Walker 1985) and this wider species distribution might increase genetic variability. The difference in distribution may result from the main form of reproductive units of both *Usnea*. The exclusively sexual *U. aurantiacoatra* reproduces via the dispersal of fungal spores which are required to meet with an appropriate photobiont after germination. The asexual *U. antarctica* on the other hand is in majority vegetatively reproducing via soredia, which already include the photobiont. Therefore, even if both reproductive units are dispersed over similar distances, the success rate of colonisation may be higher for soredia and explain the overall wider distribution and therefore genetic variability of *U. antarctica*. Finally, it was predicted that a small number of sexual individuals per generation — and *U. antarctica* rarely can be found with apothecia — is sufficient to make an apparently asexual population highly variable (Bengtsson 2003).

Despite the lower co-ancestry of *U. antarctica* compared to *U. aurantiacoatra*, we detected three pairs of very close relatives with high co-ancestry of *U. antarctica* (Figure 4). The three pairs were collected on Elephant Island, King George Island and on the Antarctic Peninsula, respectively and may indicate almost immediately related clones. On Elephant Island and the Antarctic Peninsula, the pairs were collected in the same locations with a greater chance to pick up clones. However, the clonal pair from King George Island must have dispersed between Fildes and Potter Peninsula over ice or water bounda-

ries prior to our collection. Contrarily, none of the individuals of *U. aurantiacoatra* expressed similarly close relationships. However, we could detect substructure for a group of six individuals of *U. aurantiacoatra* collected at the same location and three specimens of *U. antarctica* collected at different locations on King George Island, which indicates the potential of this analysis to identify (sub)population structure. Using this detailed method to measure co-ancestry on a deeper sampling of individuals of *Usnea* may, in future, provide a comprehensive picture of population structure and diversification.

Conclusion

We successfully used RADseq for phylogenetic and population genomic studies on two species of the lichen-fungal genus *Usnea*. Phylogenetic inference using RAD data clearly delimited the species *U. antarctica* and *U. aurantiacoatra* into two lineages, which were irresolvable using multi-locus DNA sequence markers. Furthermore, the RADseq approach offered sufficient genotyping data for conclusive population genomic analyses. We used RADseq to measure lower co-ancestry in the asexual *U. antarctica* than in the sexual *U. aurantiacoatra*, potentially derived from a wider geographical distribution of *U. antarctica* in our sample. These results show that RADseq has much potential for future phylogenetic and population genomic studies on lichens, particularly for groups of organisms which remained unresolved by multi-locus markers.

Acknowledgements

The authors thank the Robert A. Pritzker Center for Meteoritics and Polar Studies and Tawani Foundation for financial support. We want to acknowledge the Lauer family for the generous gift of a MiSeq sequencer to the Pritzker Lab for Molecular Systematics at the Field Museum. Fieldwork by Elisa Lagostina was funded by the German Science Foundation through grant Pr 567/18-1. Mikhael Andreev, Aline Lorenz and Mayara Scur are gratefully acknowledged for contributing samples from Elephant and King George Island and the Antarctic Peninsula. We also thank Marta Ribeiro and Kevin Feldheim (Chicago) for their invaluable help in the laboratory and Sarah Cowles (Miami), Steve D. Leavitt (Provo) and Pradeep K. Divakar (Madrid) for comments on the manuscript.

References

Allendorf FW (2017) Genetics and the conservation of natural populations: allozymes to genomes. Molecular Ecology 26: 420–430. https://doi.org/10.1111/mec.13948

Articus K (2004) *Neuropogon* and the phylogeny of *Usnea* s.l. (Parmeliaceae, lichenized Ascomycetes). Taxon 53: 925–934. https://doi.org/10.2307/4135560

Articus K, Mattsson JE, Tibell L, Grube M, Wedin M (2002) Ribosomal DNA and beta-tubulin data do not support the separation of the lichens *Usnea florida* and *U. subfloridana* as distinct species. Mycological Research 106: 412–418. https://doi.org/10.1017/S0953756202005786

Baird NA, Etter PD, Atwood TS, Currey MC, Shiver AL, Lewis ZA, Selker EU, Cresko WA, Johnson EA (2008) Rapid SNP discovery and genetic mapping using sequenced RAD markers. Plos One 3(10): e3376. https://doi.org/10.1371/journal.pone.0003376

Balloux F, Lehmann L, de Meeûs T (2003) The Population Genetics of Clonal and Partially Clonal Diploids. Genetics 164: 1635–1644.

Bankevich A, Nurk S, Antipov D, Gurevich AA, Dvorkin M, Kulikov AS, Lesin VM, Nikolenko SI, Son P, Prjibelski AD, Pyshkin AV, Sirotkin AV, Vyahhi N, Tesler G, Alekseyev MA, Pevzner PA (2012) SPAdes: A new genome assembly algorithm and its applications to single-cell sequencing. Journal of Computational Biology 19: 455–477. https://doi.org/10.1089/cmb.2012.0021

Barraclough TG, Nee S (2001) Phylogenetics and speciation. Trends in Ecology & Evolution 16: 391–399. https://doi.org/10.1016/S0169-5347(01)02161-9

Bengtsson BO (2003) Genetic variation in organisms with sexual and asexual reproduction. Journal of Evolutionary Biology 16: 189–199. https://doi.org/10.1046/j.1420-9101.2003.00523.x

Bickford D, Lohman DJ, Sodhi NS, Ng PKL, Meier R, Winker K, Ingram KK, Das I (2007) Cryptic species as a window on diversity and conservation. Trends in Ecology & Evolution 22: 148–155. https://doi.org/10.1016/j.tree.2006.11.004

Bolger AM, Lohse M, Usadel B (2014) Trimmomatic: a flexible trimmer for Illumina sequence data. Bioinformatics 30: 2114–2120. https://doi.org/10.1093/bioinformatics/btu170

Buschbom J, Mueller GM (2006) Testing "species pair" hypotheses: Evolutionary processes in the lichen-forming species complex *Porpidia flavocoerulescens* and *Porpidia melinodes*. Molecular Biology and Evolution 23: 574–586. https://doi.org/10.1093/molbev/msj063

Crespo A, Lumbsch HT (2010) Cryptic species in lichen-forming fungi. IMA Fungus 1: 167–170. https://doi.org/10.5598/imafungus.2010.01.02.09

Crespo A, Lumbsch HT, Mattsson JE, Blanco O, Divakar PK, Articus K, Wiklund E, Bawingan PA, Wedin M (2007) Testing morphology-based hypotheses of phylogenetic relationships in Parmeliaceae (Ascomycota) using three ribosomal markers and the nuclear RPB1 gene. Molecular Phylogenetics and Evolution 44: 812–824. https://doi.org/10.1016/j.ympev.2006.11.029

Crespo A, Pérez-Ortega S (2009) Cryptic species and species pairs in lichens: A discussion on the relationship between molecular phylogenies and morphological characters. Anales Del Jardin Botanico De Madrid 66: 71–81. https://doi.org/10.3989/ajbm.2225

Cubero OF, Crespo A, Fatehi J, Bridge PD (1999) DNA extraction and PCR amplification method suitable for fresh, herbarium-stored, lichenized, and other fungi. Plant Systematics and Evolution 216: 243–249. https://doi.org/10.1007/BF01084401

Culberson WL, Culberson CF (1973) Parallel evolution in the lichen-forming fungi. Science 180: 196–198. https://doi.org/10.1126/science.180.4082.196

Danecek P, Auton A, Abecasis G, Albers CA, Banks E, DePristo MA, Handsaker RE, Lunter G, Marth GT, Sherry ST, McVean G, Durbin R, 1000 Genomes Project Analysis Group (2011) The variant call format and VCFtools. Bioinformatics 27: 2156–2158. https://doi.org/10.1093/bioinformatics/btr330

Davey JW, Hohenlohe PA, Etter PD, Boone JQ, Catchen JM, Blaxter ML (2011) Genome-wide genetic marker discovery and genotyping using next-generation sequencing. Nature Reviews Genetics 12: 499–510. https://doi.org/10.1038/nrg3012

de Queiroz K (2007) Species concepts and species delimitation. Systematic Biology 56: 879–886. https://doi.org/10.1080/10635150701701083

Delmotte F, Leterme N, Gauthier JP, Rispe C, Simon JC (2002) Genetic architecture of sexual and asexual populations of the aphid *Rhopalosiphum padi* based on allozyme and microsatellite markers. Molecular Ecology 11: 711–723. https://doi.org/10.1046/j.1365-294X.2002.01478.x

Eaton DAR, Ree RH (2013) Inferring phylogeny and introgression using RADseq data: An example from flowering plants (*Pedicularis*: Orobanchaceae). Systematic Biology 62: 689–706. https://doi.org/10.1093/sysbio/syt032

Ellegren H (2014) Genome sequencing and population genomics in non-model organisms. Trends in Ecology & Evolution 29: 51–63. https://doi.org/10.1016/j.tree.2013.09.008

Escudero M, Eaton DAR, Hahn M, Hipp AL (2014) Genotyping-by-sequencing as a tool to infer phylogeny and ancestral hybridization: A case study in *Carex* (Cyperaceae). Molecular Phylogenetics and Evolution 79: 359–367. https://doi.org/10.1016/j.ympev.2014.06.026

Grewe F, Huang JP, Leavitt SD, Lumbsch HT (2017) Reference-based RADseq resolves robust relationships among closely related species of lichen-forming fungi using metagenomic DNA. Scientific Reports 7: 9884. https://doi.org/10.1038/s41598-017-09906-7

Hedrick PW (2005) A standardized genetic differentiation measure. Evolution 59: 1633–1638. https://doi.org/10.1111/j.0014-3820.2005.tb01814.x

Hibbett DS, Binder M, Bischoff JF, Blackwell M, Cannon PF, Eriksson OE, Huhndorf S, James T, Kirk PM, Lücking R, Lumbsch HT, Lutzoni F, Matheny PB, McLaughlin DJ, Powell MJ, Redhead S, Schoch CL, Spatafora JW, Stalpers JA, Vilgalys R, Aime MC, Aptroot A, Bauer R, Begerow D, Benny GL, Castlebury LA, Crous PW, Dai YC, Gams W, Geiser DM, Griffith GW, Gueidan C, Hawksworth DL, Hestmark G, Hosaka K, Humber RA, Hyde KD, Ironside JE, Koljalg U, Kurtzman CP, Larsson KH, Lichtwardt R, Longcore J, Miadlikowska J, Miller A, Moncalvo JM, Mozley-Standridge S, Oberwinkler F, Parmasto E, Reeb V, Rogers JD, Roux C, Ryvarden L, Sampaio JP, Schussler A, Sugiyama J, Thorn RG, Tibell L, Untereiner WA, Walker C, Wang Z, Weir A, Weiss M, White MM, Winka K, Yao YJ, Zhang N (2007) A higher-level phylogenetic classification of the Fungi. Mycological Research 111: 509–547. https://doi.org/10.1016/j.mycres.2007.03.004

Hipp AL, Eaton DAR, Cavender-Bares J, Fitzek E, Nipper R, Manos PS (2014) A framework phylogeny of the American Oak clade based on sequenced RAD data. Plos One 9(4): e102272. https://doi.org/10.1371/journal.pone.0093975

Hodel RDGJ, Segovia-Salcedo MC, Landis JB, Crowl AA, Sun M, Liu X, Gitzendanner MA, Douglas NNA, Germain-Aubrey CC, Chen S, Soltis DE, Soltis PS (2016) The report of my death was an exaggeration: a review for researchers using microsatellites in the 21st century. Applications in Plant Sciences 4. https://doi.org/10.3732/apps.1600025

Hoffman JR, Lendemer JC (2018) A meta-analysis of trends in the application of Sanger and next-generation sequencing data in lichenology. Bryologist 121: 133–147. https://doi.org/10.1639/0007-2745-121.2.133

Holder M, Lewis PO (2003) Phylogeny estimation: Traditional and Bayesian approaches. Nature Reviews Genetics 4: 275–284. https://doi.org/10.1038/nrg1044

Huelsenbeck JP, Ronquist F, Nielsen R, Bollback JP (2001) Evolution – Bayesian inference of phylogeny and its impact on evolutionary biology. Science 294: 2310–2314. https://doi.org/10.1126/science.1065889

James TY, Kauff F, Schoch CL, Matheny PB, Hofstetter V, Cox CJ, Celio G, Gueidan C, Fraker E, Miadlikowska J, Lumbsch HT, Rauhut A, Reeb V, Arnold AE, Amtoft A, Stajich JE, Hosaka K, Sung GH, Johnson D, O'Rourke B, Crockett M, Binder M, Curtis JM, Slot JC, Wang Z, Wilson AW, Schussler A, Longcore JE, O'Donnell K, Mozley-Standridge S, Porter D, Letcher PM, Powell MJ, Taylor JW, White MM, Griffith GW, Davies DR, Humber RA, Morton JB, Sugiyama J, Rossman AY, Rogers JD, Pfister DH, Hewitt D, Hansen K, Hambleton S, Shoemaker RA, Kohlmeyer J, Volkmann-Kohlmeyer B, Spotts RA, Serdani M, Crous PW, Hughes KW, Matsuura K, Langer E, Langer G, Untereiner WA, Lücking R, Büdel B, Geiser DM, Aptroot A, Diederich P, Schmitt I, Schultz M, Yahr R, Hibbett DS, Lutzoni F, McLaughlin DJ, Spatafora JW, Vilgalys R (2006) Reconstructing the early evolution of Fungi using a six-gene phylogeny. Nature 443: 818–822. https://doi.org/10.1038/nature05110

Jombart T, Ahmed I (2011) adegenet 1.3–1: new tools for the analysis of genome-wide SNP data. Bioinformatics 27: 3070–3071. https://doi.org/10.1093/bioinformatics/btr521

Jombart T, Balloux F, Dray S (2010) adephylo: new tools for investigating the phylogenetic signal in biological traits. Bioinformatics 26: 1907–1909. https://doi.org/10.1093/bioinformatics/btq292

Jost L (2008) GST and its relatives do not measure differentiation. Molecular Ecology 17: 4015–4026. https://doi.org/10.1111/j.1365-294X.2008.03887.x

Kotelko R, Piercey-Normore MD (2010) *Cladonia pyxidata* and *C. pocillum*; genetic evidence to regard them as conspecific. Mycologia 102: 534–545. https://doi.org/10.3852/09-030

Kraus RHS, Wink M (2015) Avian genomics: fledging into the wild! Journal of Ornithology 156: 851–865. https://doi.org/10.1007/s10336-015-1253-y

Krog H (1976) *Lethariella* and *Protousnea*, two new lichen genera in the Parmeliaceae. Norwegian Journal of Botany 23: 83–106.

Krog H (1982) Evolutionay trends in foliose and fruticose lichens of the Parmeliaceae. Journal of the Hattori Botanical Laboratory 52: 303–311.

Lagostina E, Dal Grande F, Andreev M, Printzen C (2018) The use of microsatellite markers for species delimitation in Antarctic *Usnea* subgenus *Neuropogon*. Mycologia. https://doi.org/10.1080/00275514.2018.1512304

Lamb IM (1939) A review of the genus *Neuropogon* (Nees.) Nyl., with special reference to the Antarctic species. Journal of the Linnean Society, Botany 52: 199–237. https://doi.org/10.1111/j.1095-8339.1939.tb01602.x

Lamb IM (1964) Antarctic lichens. I. The genera *Usnea*, *Ramalina*, *Himantormia*, *Alectoria*, *Cornicularia*. 38: 1–34.

Langmead B, Salzberg SL (2012) Fast gapped-read alignment with Bowtie 2. Nature Methods 9: 357–354. https://doi.org/10.1038/nmeth.1923

Leavitt SD, Divakar PK, Crespo A, Lumbsch HT (2016a) A matter of time – understanding the limits of the power of molecular data for delimiting species boundaries. Herzogia 29: 479–492. https://doi.org/10.13158/heia.29.2.2016.479

Leavitt SD, Grewe F, Widhelm T, Muggia L, Wray B, Lumbsch HT (2016b) Resolving evolutionary relationships in lichen-forming fungi using diverse phylogenomic datasets and analytical apporaches. Scientific Reports 6: 22262. https://doi.org/10.1038/srep22262

Lohtander K, Källersjö M, Tehler A (1998) Dispersal strategies in *Roccellina capensis* (Arthoniales). Lichenologist 30: 341–350. https://doi.org/10.1006/lich.1998.0154

Lumbsch HT, Leavitt SD (2011) Goodbye morphology? A paradigm shift in the delimitation of species in lichenized fungi. Fungal Diversity 50: 59–72. https://doi.org/10.1007/s13225-011-0123-z

Lumbsch HT, Wirtz N (2011) Phylogenetic relationships of the neuropogonoid core group in the genus *Usnea* (Ascomycota: Parmeliaceae). Lichenologist 43: 553–559. https://doi.org/10.1017/S0024282911000417

Lutzoni F, Kauff F, Cox C, McLaughlin D, Celio G, Dentinger B, Padamsee M, Hibbett D, James TY, Baloch E, Grube M, Reeb V, Hofstetter V, Schoch C, Arnold AE, Miadlikowska J, Spatafora J, Johnson D, Hambleton S, Crockett M, Shoemaker R, Sung G-H, Lücking R, Lumbsch HT, O'Donnell K, Binder M, Diederich P, Ertz D, Gueidan C, Hansen K, Harris RC, Hosaka K, Lim Y-W, Matheny B, Nishida H, Pfister D, Rogers J, Rossman A, Schmitt I, Sipman H, Stone J, Sugiyama J, Yahr R, Vilgalys R (2004) Assembling the fungal tree of life: progress, classification, and evolution of subcellular traits. American Journal of Botany 91: 1446–1480. https://doi.org/10.3732/ajb.91.10.1446

Malinsky M, Trucchi E, Lawson DJ, Falush D (2018) RADpainter and fineRADstructure Population Inference from RADseq Data. Molecular Biology and Evolution 35: 1284–1290. https://doi.org/10.1093/molbev/msy023

Mattsson J-E, Lumbsch HT (1989) The use of the species pair concept in lichen taxonomy. Taxon 38: 238–241. https://doi.org/10.2307/1220840

McLaughlin DJ, Hibbett DS, Lutzoni F, Spatafora JW, Vilgalys R (2009) The search for the fungal tree of life. Trends in Microbiology 17: 488–497. https://doi.org/10.1016/j.tim.2009.08.001

Myllys L, Lohtander K, Tehler A (2001) beta-tubulin, ITS and group I intron sequences challenge the species pair concept in *Physcia aipolia* and *P. caesia*. Mycologia 93: 335–343. https://doi.org/10.2307/3761655

Nei M (1973) Analysis of gene diversity in subdivided populations. Proceedings of the National Academy of Sciences 70: 3321–3323. https://doi.org/10.1073/pnas.70.12.3321

Ozsolak F, Milos PM (2011) RNA sequencing: advances, challenges and opportunities. Nature Reviews Genetics 12: 87–98. https://doi.org/10.1038/nrg2934

Parra G, Bradnam K, Ning Z, Keane T, Korf I (2009) Assessing the gene space in draft genomes. Nucleic Acids Research 37: 289–297. https://doi.org/10.1093/nar/gkn916

Poelt J (1970) Das Konzept der Artenpaare bei den Flechten. Vorträge aus dem Gesamtgebiet der Botanik. Neue Folge 4: 187–198.

Poelt J (1972) Die taxonomische Behandlung von Artenpaaren bei den Flechten. Botaniska Notiser 125: 77–81.

Rannala B (2015) The art and science of species delimitation. Current Zoology 61: 846–853. https://doi.org/10.1093/czoolo/61.5.846

Robbertse B, Reeves JB, Schoch CL, Spatafora JW (2006) A phylogenomic analysis of the Ascomycota. Fungal Genetics and Biology 43: 715–725. https://doi.org/10.1016/j.fgb.2006.05.001

Rubin BER, Moreau CS (2016) Comparative genomics reveals convergent rates of evolution in ant-plant mutualisms. Nature Communications 7: 12679. https://doi.org/10.1038/ncomms12679

Schoch CL, Seifert KA, Huhndorf S, Robert V, Spouge JL, Levesque CA, Chen W, Bolchacova E, Voigt K, Crous PW, Miller AN, Wingfield MJ, Aime MC, An KD, Bai FY, Barreto RW, Begerow D, Bergeron MJ, Blackwell M, Boekhout T, Bogale M, Boonyuen N, Burgaz AR, Buyck B, Cai L, Cai Q, Cardinali G, Chaverri P, Coppins BJ, Crespo A, Cubas P, Cummings C, Damm U, de Beer ZW, de Hoog GS, Del-Prado R, Dentinger B, Dieguez-Uribeondo J, Divakar PK, Douglas B, Duenas M, Duong TA, Eberhardt U, Edwards JE, Elshahed MS, Fliegerova K, Furtado M, Garcia MA, Ge ZW, Griffith GW, Griffiths K, Groenewald JZ, Groenewald M, Grube M, Gryzenhout M, Guo LD, Hagen F, Hambleton S, Hamelin RC, Hansen K, Harrold P, Heller G, Herrera G, Hirayama K, Hirooka Y, Ho HM, Hoffmann K, Hofstetter V, Högnabba F, Hollingsworth PM, Hong SB, Hosaka K, Houbraken J, Hughes K, Huhtinen S, Hyde KD, James T, Johnson EM, Johnson JE, Johnston PR, Jones EB, Kelly LJ, Kirk PM, Knapp DG, Koljalg U, Kovacs GM, Kurtzman CP, Landvik S, Leavitt SD, Liggenstoffer AS, Liimatainen K, Lombard L, Luangsa-Ard JJ, Lumbsch HT, Maganti H, Maharachchikumbura SS, Martin MP, May TW, McTaggart AR, Methven AS, Meyer W, Moncalvo JM, Mongkolsamrit S, Nagy LG, Nilsson RH, Niskanen T, Nyilasi I, Okada G, Okane I, Olariaga I, Otte J, Papp T, Park D, Petkovits T, Pino-Bodas R, Quaedvlieg W, Raja HA, Redecker D, Rintoul T, Ruibal C, Sarmiento-Ramirez JM, Schmitt I, Schussler A, Shearer C, Sotome K, Stefani FO, Stenroos S, Stielow B, Stockinger H, Suetrong S, Suh SO, Sung GH, Suzuki M, Tanaka K, Tedersoo L, Telleria MT, Tretter E, Untereiner WA, Urbina H, Vagvolgyi C, Vialle A, Vu TD, Walther G, Wang QM, Wang Y, Weir BS, Weiss M, White MM, Xu J, Yahr R, Yang ZL, Yurkov A, Zamora JC, Zhang N, Zhuang WY, Schindel D, Fungal Barcoding C (2012) Nuclear ribosomal internal transcribed spacer (ITS) region as a universal DNA barcode marker for Fungi. Proceedings of the National Academy of Sciences of the United States of America 109: 6241–6246. https://doi.org/10.1073/pnas.1117018109

Schoch CL, Sung GH, Lopez-Giraldez F, Townsend JP, Miadlikowska J, Hofstetter V, Robbertse B, Matheny PB, Kauff F, Wang Z, Gueidan C, Andrie RM, Trippe K, Ciufetti LM, Wynns A, Fraker E, Hodkinson BP, Bonito G, Groenewald JZ, Arzanlou M, de Hoog GS, Crous PW, Hewitt D, Pfister DH, Peterson K, Gryzenhout M, Wingfield MJ, Aptroot A, Suh SO, Blackwell M, Hillis DM, Griffith GW, Castlebury LA, Rossman AY, Lumbsch HT, Lücking R, Büdel B, Rauhut A, Diederich P, Ertz D, Geiser DM, Hosaka K, Inderbitzin P, Kohlmeyer J, Volkmann-Kohlmeyer B, Mostert L, O'Donnell K, Sipman H, Rogers JD, Shoemaker RA, Sugiyama J, Summerbell RC, Untereiner W, Johnston PR, Stenroos S, Zuccaro A, Dyer PS, Crittenden PD, Cole MS, Hansen K, Trappe JM, Yahr R, Lutzoni F, Spatafora JW (2009) The Ascomycota tree of life: A phylum-wide phylogeny clarifies the origin and evolution of fundamental reproductive and ecological traits. Systematic Biology 58: 224–239. https://doi.org/10.1093/sysbio/syp020

Seymour FA, Crittenden PD, Wirtz N, Øvstedal DO, Dyer PS, Lumbsch HT (2007) Phylogenetic and morphological analysis of Antarctic lichen-forming *Usnea* species in the group *Neuropogon*. Antarctic Science 19: 71–82. https://doi.org/10.1017/S0954102007000107

Spatafora JW, Aime MC, Grigoriev IV, Martin F, Stajich JE, Blackwell M (2017) The fungal tree of life: from molecular systematics to genome-scale phylogenies. Microbiology Spectrum 5(5): FUNK-0053-2016.

Spatafora JW, Robbertse B (2010) Chapter 4 : phylogenetics and phylogenomics of the Fungal Tree of Life. In: Borkovich KA, Ebbole DJ (Eds) Cellular and Molecular Biology of Filamentous Fungi. ASM Press, 36–49. http://dx.doi.org/10.1128/9781555816636.ch4

Stajich JE, Berbee ML, Blackwell M, Hibbett DS, James TY, Spatafora JW, Taylor JW (2009) The Fungi. Current Biology 19: 840–845. https://doi.org/10.1016/j.cub.2009.07.004

Stamatakis A (2006) RAxML-VI-HPC: maximum likelihood-based phylogenetic analyses with thousands of taxa and mixed models. Bioinformatics 22: 2688–2690. https://doi.org/10.1093/bioinformatics/btl446

Stamatakis A, Hoover P, Rougemont J (2008) A rapid bootstrap algorithm for the RAxML web servers. Systematic Biology 57: 758–771. https://doi.org/10.1080/10635150802429642

Stratton M (2008) Genome resequencing and genetic variation. Nature Biotechnology 26: 65–66. https://doi.org/10.1038/nbt0108-65

Strous M, Kraft B, Bisdorf R, Tegetmeyer HE (2012) The binning of metagenomic contigs for microbial physiology of mixed cultures. Frontiers in Microbiology 3: 410. https://doi.org/10.3389/fmicb.2012.00410

Taylor JW, Jacobson DJ, Kroken S, Kasuga T, Geiser DM, Hibbett DS, Fisher MC (2000) Phylogenetic species recognition and species concepts in fungi. Fungal Genetics and Biology 31: 21–32. https://doi.org/10.1006/fgbi.2000.1228

Tehler A (1982) The species pair concept in lichenology. Taxon 31: 708–714. https://doi.org/10.2307/1219689

Vargas OM, Ortiz EM, Simpson BB (2017) Conflicting phylogenomic signals reveal a pattern of reticulate evolution in a recent high-Andean diversification (Asteraceae: Astereae: *Diplostephium*). New Phytologist 214: 1736–1750. https://doi.org/10.1111/nph.14530

Velmala S, Myllys L, Halonen P, Goward T, Ahti T (2009) Molecular data show that *Bryoria fremontii* and *B. tortuosa* (Parmeliaceae) are conspecific. Lichenologist 41: 231–242. https://doi.org/10.1017/S0024282909008573

Wachi N, Matsubayashi KW, Maeto K (2018) Application of next-generation sequencing to the study of non-model insects. Entomological Science 21: 3–11. https://doi.org/10.1111/ens.12281

Wagner ND, Gramlich S, Hörandl E (2018) RAD sequencing resolved phylogenetic relationships in European shrub willows (*Salix* L. subg. *Chamaetia* and subg. *Vetrix*) and revealed multiple evolution of dwarf shrubs. Ecology and Evolution 2018(00): 1–13. https://doi.org/10.1002/ece3.4360

Walker FJ (1985) The lichen genus *Usnea* subgenus *Neuropogon*. Bulletin of the British Museum (Natural History), Botany Series 13: 1–130.

Whitlock MC (2011) G ‘(ST) and D do not replace F-ST. Molecular Ecology 20: 1083–1091. https://doi.org/10.1111/j.1365-294X.2010.04996.x

Wickett NJ, Mirarab S, Nam N, Warnow T, Carpenter E, Matasci N, Ayyampalayam S, Barker MS, Burleigh JG, Gitzendanner MA, Ruhfel BR, Wafula E, Der JP, Graham SW, Mathews S, Melkonian M, Soltis DE, Soltis PS, Miles NW, Rothfels CJ, Pokorny L, Shaw AJ, DeGironimo L, Stevenson DW, Surek B, Villarreal JC, Roure B, Philippe H, dePamphilis CW, Chen T, Deyholos MK, Baucom RS, Kutchan TM, Augustin MM, Wang J, Zhang Y, Tian Z, Yan Z, Wu X, Sun X, Wong GK-S, Leebens-Mack J (2014) Phylotranscriptomic analysis of the origin

and early diversification of land plants. Proceedings of the National Academy of Sciences of the United States of America 111: 4859–4868. https://doi.org/10.1073/pnas.1323926111

Widhelm TJ, Egan RS, Bertoletti FR, Asztalos MJ, Kraichak E, Leavitt SD, Lumbsch HT (2016) Picking holes in traditional species delimitations: an integrative taxonomic reassessment of the *Parmotrema perforatum* group (Parmeliaceae, Ascomycota). Botanical Journal of the Linnean Society 182: 868–884. https://doi.org/10.1111/boj.12483

Wiens JJ, Penkrot TA (2002) Delimiting species using DNA and morphological variation and discordant species limits in spiny lizards (*Sceloporus*). Systematic Biology 51: 69–91. https://doi.org/10.1080/106351502753475880

Wilkinson MJ, Szabo C, Ford CS, Yarom Y, Croxford AE, Camp A, Gooding P (2017) Replacing Sanger with Next Generation Sequencing to improve coverage and quality of reference DNA barcodes for plants. Scientific Reports 7. https://doi.org/10.1038/srep46040

Winter DJ (2012) MMOD: an R library for the calculation of population differentiation statistics. Molecular Ecology Resources 12: 1158–1160. https://doi.org/10.1111/j.1755-0998.2012.03174.x

Wirtz N, Printzen C, Lumbsch HT (2008) The delimitation of Antarctic and bipolar species of neuropogonoid *Usnea* (Ascomycota, Lecanorales): a cohesion approach of species recognition for the *Usnea perpusilla* complex. Mycological Research 112: 472–484. https://doi.org/10.1016/j.mycres.2007.05.006

Wirtz N, Printzen C, Lumbsch HT (2012) Using haplotype networks, estimation of gene flow and phenotypic characters to understand species delimitation in fungi of a predominantly Antarctic *Usnea* group (Ascomycota, Parmeliaceae). Organisms Diversity & Evolution 12: 17–37. https://doi.org/10.1007/s13127-011-0066-y

Wirtz N, Printzen C, Sancho LG, Lumbsch HT (2006) The phylogeny and classification of *Neuropogon* and *Usnea* (Parmeliaceae, Ascomycota) revisited. Taxon 55: 367–376. https://doi.org/10.2307/25065584

Zhao X, Fernández-Brime S, Wedin M, Locke M, Leavitt SD, Lumbsch HT (2017) Using multi-locus sequence data for addressing species boundaries in commonly accepted lichen-forming fungal species. Organisms Diversity & Evolution 17: 351–363. https://doi.org/10.1007/s13127-016-0320-4

Zimmer EA, Wen J (2015) Using nuclear gene data for plant phylogenetics: Progress and prospects II. Next-gen approaches. Journal of Systematics and Evolution 53: 371–379. https://doi.org/10.1111/jse.12174

Supplementary material 1

Origin of samples used for this study

Authors: Felix Grewe, Elisa Lagostina, Huini Wu, Christian Printzen, H. Thorsten Lumbsch

Data type: species data

Link: https://doi.org/10.3897/mycokeys.43.29093.suppl1

Supplementary material 2

Overview of RADseq results after individual steps of RAD analyses

Authors: Felix Grewe, Elisa Lagostina, Huini Wu, Christian Printzen, H. Thorsten Lumbsch

Data type: molecular data

Link: https://doi.org/10.3897/mycokeys.43.29093.suppl2

Supplementary material 3

Correlation of RADseq results after individual steps of RAD analyses

Authors: Felix Grewe, Elisa Lagostina, Huini Wu, Christian Printzen, H. Thorsten Lumbsch

Data type: molecular data

Link: https://doi.org/10.3897/mycokeys.43.29093.suppl3

MycoKeys 43: 115–130 (2018)
doi: 10.3897/mycokeys.43.30776
http://mycokeys.pensoft.net

RESEARCH ARTICLE

A peer-reviewed open-access journal
MycoKeys
Launched to accelerate biodiversity research

Two new African siblings of *Pulveroboletus ravenelii* (Boletaceae)

Sylvestre A. Badou[1], André De Kesel[2], Olivier Raspé[2,3], Martin K. Ryberg[4], Atsu K. Guelly[5], Nourou S. Yorou[1]

1 *Research Unit Tropical Mycology and Soil-Plant-Fungi Interaction, Laboratory of Ecology, Botany and Plant Biology, Faculty of Agronomy, University of Parakou, 03 BOX: 125, Parakou, Benin* **2** *Meise Botanic Garden, Nieuwelaan 38, 1860 Meise, Belgium* **3** *Fédération Wallonie-Bruxelles, Rue A. Lavallée 1, 1080 Bruxelles, Belgium* **4** *Systematic Biology program, Department of Organismal Biology, Uppsala University, Norbyvägen 17D, 752 36 Uppsala, Sweden* **5** *Département de Botanique et Écologie Végétale, Faculté des Sciences, Université de Lomé, BP1515 Lomé, Togo*

Corresponding author: *André De Kesel* (andre.dekesel@botanicgardenmeise.be)

Academic editor: *M.P. Martín* | Received 23 October 2018 | Accepted 25 November 2018 | Published 12 December 2018

Citation: Badou AS, De Kesel A, Raspé O, Ryberg MK, Guelly AK, Yorou NS (2018) Two new African siblings of *Pulveroboletus ravenelii* (Boletaceae). MycoKeys 43: 115–130. https://doi.org/10.3897/mycokeys.43.30776

Abstract

This paper sorts out the taxonomy of species affiliated with *Pulveroboletus ravenelii* in the Guineo-soudanian and Zambezian woodlands of Africa. Morphological and genetic characters of African *Pulveroboletus* collections were studied and compared to those of North American and Asian species. A phylogenetic analysis showed that the African specimens form a subclade, sister to the Asian and American taxa. Although clamp connections have previously never been reported from *Pulveroboletus*, all specimens of the African subclade show very small clamp connections. Two new African species, *Pulveroboletus africanus* **sp. nov.** and *P. sokponianus* **sp. nov.**, are described and illustrated. Comments concerning morphology and identification, as well as distribution and ecology, are given for both species.

Keywords

Boletales, Africa, *Pulveroboletus*, morphology, phylogeny, taxonomy

Introduction

Boletes belonging to *Pulveroboletus* Murrill are morphologically characterised by boletoid basidiomata with a pulverulent arachnoid veil. As originally indicated by Murrill (1909), this veil or cleistoblema *sensu* Clémençon (2012), is most often yellowish to vivid yellow and already present at a very early stage of development. Alterations broadening the circumscription of *Pulveroboletus* (Singer 1945, 1947, 1986), are not followed here as they have rendered the genus morphologically heterogeneous (Watling 2008) and polyphyletic (Binder and Hibbett 2006, Wu et al. 2014, Zeng et al. 2017). In its strict sense, *Pulveroboletus* holds few species, all of which are similar to the type, *Pulveroboletus ravenelii* (Berk. & M.A. Curtis) Murrill. Based on molecular data, Raspé et al. (2016) stated that what is called *Pulveroboletus ravenelii* outside North America belongs to a complex of different taxa. The name *P. ravenelii* has been used erroneously for lookalikes in Asia, Australia (Watling 2001, Horak 2011) and also Africa (Thoen and Ducousso 1989, Watling and Turnbull 1992, De Kesel et al. 2002, Yorou and De Kesel 2011, Vanié-Léabo et al. 2017, Kamou et al. 2017). So far, Raspé et al. (2016) and Zeng et al. (2017) have resolved part of the Asian complex around *P. ravenelii*, which now counts ten species. In a similar way, this paper aims to resolve and clarify the identity of some of the African, non-viscid, *Pulveroboletus* that have been kept under "*Pulveroboletus* aff. *ravenelii*".

Materials and methods

Sampling, microscopy and morphology

Specimens were obtained from our own fieldwork or from herbarium specimens at our disposal. Protocols for field collecting, macroscopic description, drying and preservation follow Eyi Ndong et al. (2011). Codes and names of colours are according to the Methuen Handbook of Colour (Kornerup and Wanscher 1978). Microscopic structures were revived and examined in 5% potassium hydroxide (KOH) or in 10% ammonia with Congo Red. Measurements and drawings of microscopic structures were undertaken using an Olympus (BX51) compound microscope equipped with digital camera and drawing tube. Dimensions of microscopic structures are presented in the following format: (a–)b–c–d(–e), in which c represents the average, b = c – 1.96 * SD and d = c + 1.96 * SD and a and e are extreme values. *Q* is the length/width ratio based on at least 50 spores and is presented in the same format as spore dimensions (Eyi Ndong et al. 2011). Unless otherwise stated, herbarium specimens are deposited in BR. Duplicates from material from Togo are deposited in TOGO (Université de Lomé, Togo). Herbarium specimens from S. Badou (Benin) are deposited in UNIPAR (University of Parakou, Benin Republic). Abbreviations of herbaria follow Thiers (continuously updated). MycoBank (CBS-KNAW Fungal Biodiversity Centre, continuously updated) numbers are provided for the new species.

DNA extraction, amplification and sequencing

Genomic DNA was isolated from CTAB-preserved tissues or dry specimens using a CTAB isolation procedure adapted from Doyle and Doyle (1990). The genes *atp*6, *tef*1 and *rpb*2 were amplified by PCR using the following primers: ATP6-1M40F and ATP6-2M (Raspé et al. 2016), EF1-983F and EF1-2218R (Rehner and Buckley 2005) and bRPB2-6F and bRPB2-7.1R (Matheny 2005). PCR products were purified by adding 1 U of Exonuclease I and 0.5 U FastAP Alkaline Phosphatase (Thermo Scientific, St. Leon-Rot, Germany) and incubated at 37 °C for 1 h, followed by inactivation at 80 °C for 15 min. Sequencing was performed by Macrogen Europe (The Netherlands) with PCR primers, except for *atp*6, for which universal primers M13F-pUC(-40) and M13F(-20) were used. For *tef*1, additional sequencing was performed with two internal primers, EF1-1577F and EF1-1567R (Rehner and Buckley 2005).

Alignment and phylogeny inference

Sequences of *Pulveroboletus* species, including the type species *P. ravenelii*, along with sequences of various genera of the *Pulveroboletus* group (Wu et al. 2014) and three Leccinoideae species as outgroup were generated or retrieved from GenBank (Table 1). The sequences were assembled in GENEIOUS Pro v. 6.0.6 (Biomatters). All sequences were aligned using MAFFT (Katoh and Standley 2013) on the server accessed at http://mafft.cbrc.jp/alignment/server/ and introns in *rpb*2 and *tef*1 were identified based on the amino acid sequence of previously published DNA sequences. Maximum Likelihood (ML) phylogenetic tree inference was performed using RAxML (Stamatakis 2006) on the CIPRES web server (RAxML-HPC2 on XSEDE; Miller et al. 2009). The phylogenetic tree was inferred by a single analysis with four partitions (one for the exons of each gene and a fourth for the introns of *rpb*2 and *tef*1), using the GTRCAT model with 25 categories. Statistical support of nodes was obtained with 1,000 rapid bootstrap replicates.

Results

DNA analyses

The alignment contained sequences from 50 specimens and was 2,649 characters long (TreeBase number 23416). In the phylogram obtained (Fig. 1), *Pulveroboletus* formed a highly supported clade (BS = 100%). Interestingly, the African species formed a highly supported sub-clade sister to the Asian and American species, which together formed another highly supported sub-clade.

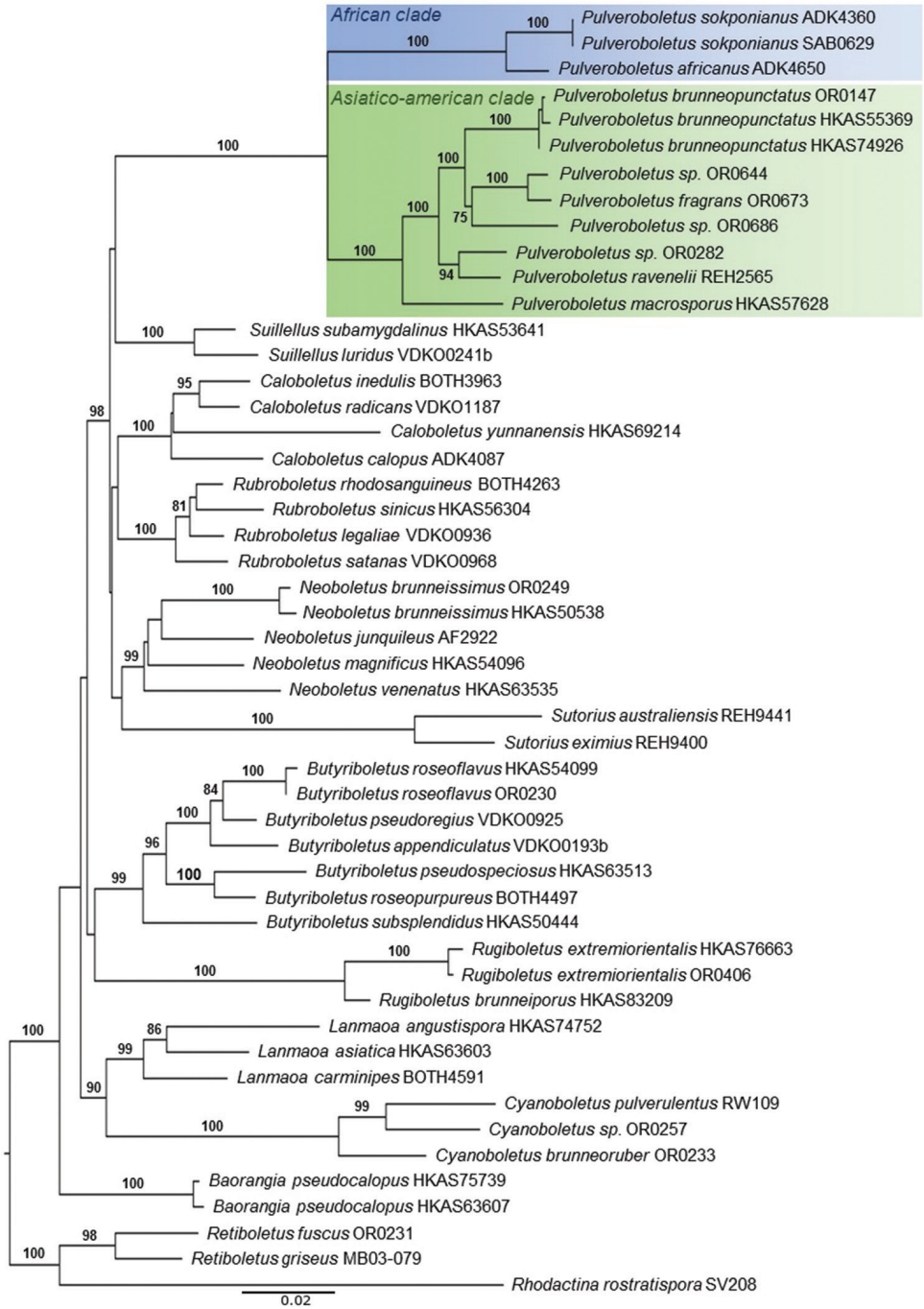

Figure 1. Maximum likelihood phylogenetic tree inferred from the three-gene dataset (*atp*6, *rpb*2, *tef*1), including *Pulveroboletus africanus* sp. nov. and *Pulveroboletus sokponianus* sp. nov and selected Boletaceae. The three Leccinoideae species (*Retiboletus fuscus* (Hongo) N.K. Zeng & Zhu L. Yang, *R. griseus* (Frost) Manfr. Binder & Bresinsky and *Rhodactina rostratispora* S. Vadthanarat, O. Raspé & S. Lumyong) were used as outgroup taxa. Bootstrap frequencies > 70% are shown above supported branches.

Table 1. List of collections used for DNA analyses, with origin, GenBank accession numbers and references.

Species	Voucher	Origin	*atp6*	*tef1*	*rpb2*	Reference
Baorangia pseudocalopus	HKAS63607	China	–	KF112167	KF112677	Wu et al. 2014
Baorangia pseudocalopus	HKAS75739	China	–	KJ184570	KM605179	Wu et al. 2015
Butyriboletus appendiculatus	VDKO0193b	Belgium	MG212537	MG212582	MG212624	Vadthanarat et al. 2018
Butyriboletus pseudoregius	VDKO0925	Belgium	MG212538	MG212583	MG212625	Vadthanarat et al. 2018
Butyriboletus pseudospeciosus	HKAS63513	China	–	KT990743	KT990380	Wu et al. 2016
Butyriboletus roseoflavus	HKAS54099	China	–	KF739779	KF739703	Wu et al. 2014
Butyriboletus roseopurpureus	BOTH4497	USA	MG897418	MG897428	MG897438	Phookamsak et al. 2018
Butyriboletus subsplendidus	HKAS50444	China	–	KT990742	KT990379	Wu et al. 2016
Butyriboletus cf. *roseoflavus*	OR230	China	KT823974	KT824040	KT824007	Raspé et al. 2016
Caloboletus calopus	ADK4087	Belgium	MG212539	KJ184566	KP055030	Vadthanaratet al. 2018, Zhao et al. 2014a, 2014b
Caloboletus inedulis	BOTH3963	USA	MG897414	MG897424	MG897434	Phookamsak et al. 2018
Caloboletus radicans	VDKO1187	Belgium	MG212540	MG212584	MG212626	Vadthanarat et al. 2018
Caloboletus yunnanensis	HKAS69214	China	–	KJ184568	KT990396	Zhao et al. 2014a, Wu et al. 2016
Cyanoboletus brunneoruber	OR0233	China	MG212542	MG212586	MG212628	Vadthanarat et al. 2018
Cyanoboletus pulverulentus	RW109	Belgium	KT823980	KT824046	KT824013	Raspé et al. 2016
Cyanoboletus sp.	OR0257	China	MG212543	MG212587	MG212629	Vadthanarat et al. 2018
Lanmaoa angustispora	HKAS74752	China	–	KM605154	KM605177	Wu et al. 2015
Lanmaoa asiatica	HKAS63603	China	–	KM605153	KM605176	Wu et al. 2015
Lanmaoa carminipes	BOTH4591	USA	MG897419	MG897429	MG897439	Phookamsak et al. 2018
Neoboletus brunneissimus	HKAS50538	China	–	KM605150	KM605173	Wu et al. 2015
Neoboletus brunneissimus	OR0249	China	MG212551	MG212595	MG212637	Vadthanarat et al. 2018
Neoboletus junquilleus	AF2922	France	MG212552	MG212596	MG212638	Vadthanarat et al. 2018
Neoboletus magnificus	HKAS54096	China	–	KF112149	KF112654	Wu et al. 2014
Neoboletus venenatus	HKAS63535	China	–	KT990807	KT990448	Wu et al. 2016
Pulveroboletus africanus (type)	ADK4650	Togo	KT823959	KT824025	KT823992	Raspé et al. 2016
Pulveroboletus brunneopunctatus	OR0147	China	MG897420	MG897430	MG897440	Phookamsak et al. 2018
Pulveroboletus brunneopunctatus	HKAS55369	China	–	KT990814	KT990455	Wu et al. 2016
Pulveroboletus brunneopunctatus	HKAS74926	China	–	KT990815	KT990456	Wu et al. 2016
Pulveroboletus fragrans	OR0673	Thailand	KT823977	KT824043	KT824010	Raspé et al. 2016
Pulveroboletus macrosporus	HKAS57628	China	–	KT990812	KT990453	Wu et al. 2016
Pulveroboletus sokponianus (type)	ADK4360	Togo	KT823957	KT824023	KT823990	Raspé et al. 2016
Pulveroboletus sokponianus	SAB0629	Benin	MH983001	MH983002	MH983003	This study
Pulveroboletus ravenelii	REH2565	U.S.A.	KU665635	KU665636	KU665637	Raspé et al. 2016
Pulveroboletus sp.	OR0282	China	MK058515	MK058518	MK058521	This study

Species	Voucher	Origin	*atp6*	*tef1*	*rpb2*	Reference
Pulveroboletus sp.	OR0644	Thailand	MK058516	MK058519	MK058522	This study
Pulveroboletus sp.	OR0686	Thailand	MK058517	MK058520	MK058523	This study
Retiboletus fuscus	OR0231	China	MG212556	MG212600	MG212642	Vadthanarat et al. 2018
Retiboletus griseus	MB03-079	U.S.A.	KT823964	KT824030	KT823997	Raspé et al. 2016
Rhodactina rostratispora	SDBR-CMU-SV208	Thailand	MG212561	MG212606	MG212646	Vadthanarat et al. 2018
Rubroboletus legaliae	VDKO0936	Belgium	KT823985	KT824051	KT824018	Raspé et al. 2016
Rubroboletus rhodosanguineus	BOTH4263	USA	MG897416	MG897426	MG897436	Phookamsak et al. 2018
Rubroboletus satanas	VDKO0968	Belgium	KT823986	KT824052	KT824019	Raspé et al. 2016
Rubroboletus sinicus	HKAS56304	China	–	KJ619483	KP055031	Zhao et al. 2014a; Zhao et al. 2014b
Rugiboletus brunneiporus	HKAS83209	China	–	KM605144	KM605168	Wu et al. 2015
Rugiboletus extremiorientalis	HKAS76663	China	–	KM605147	KM605170	Wu et al. 2015
Rugiboletus extremiorientalis	OR0406	Thailand	MG212562	MG212607	MG212647	Vadthanarat et al. 2018
Suillellus luridus	VDKO0241b	Belgium	KT823981	KT824047	KT824014	Raspé et al. 2016
Suillellus subamygdalinus	HKAS53641	China	–	KT990841	KT990478	Wu et al. 2016
Sutorius australiensis	REH9441	Australia	MG212567	JQ327032*	MG212652	Halling et al. 2012*, Vadthanaratet al. 2018
Sutorius eximius	REH9400	U.S.A.	MG212568	JQ327029*	MG212653	Halling et al. 2012*, Vadthanaratet al. 2018

Taxonomy

***Pulveroboletus africanus* De Kesel & Raspé, sp. nov.**
Mycobank MB 827970
Fig. 2a–f

Illustr. Sharp (2011, page 41, ut *Pulveroboletus* aff. *ravenelii*).

Holotype. Togo, Central Province, Fazao National Park, 08°44'31.9"N, 0°48'17.4"E, 6 June 2008, elev. 500 m, on the ground in a gallery forest with *Berlinia grandiflora* (Vahl) Hutch. & Dalziel, *Uapaca guineensis* Müll.-Arg. and *Pandanus* sp., leg. A. De Kesel, De Kesel 4650 (BR!, BR 5020165390056, duplicate in TOGO).

Etymology. Epithet refers to its very wide distribution throughout tropical Africa.

Description. Basidiomata medium-sized, covered by a general veil when young. Pileus 60–70 mm diam., at first broadly convex then pulvinate to plano-convex, upper layer dark brown (6E6–6F6), dry, mat, tomentose to felty, very soon cracking, becoming tomentose-scaly, bright yellow (2A4–5) in the deeper layers, predominantly yellow with age; scales appressed, slightly fibrillose, leather brown to greyish-brown (6E4–5), thicker and darker in the centre, thinner, paler and more diffused towards the margin; margin at first incurved, appendiculate with age, vivid yellow, beset with sulphur-yellow pulverulent material. Hymenophore tubulate, separable, straight to

slightly sinuate, almost free around the stipe or depressed and then only slightly decurrent with a tooth; tubes up to 10 mm long, yellow to greyish-yellow (1B3), cyanescent when cut; pores regular, mostly round or slightly angular, slightly elongated around the stipe, small (14–16/mm), yellow (1A2–2A2), with age greyish-brown (5E4–6), cyanescent. Stipe cylindrical, 60–80 × 8–12 mm, central, solid, uppermost part vivid yellow (2A4–5), often with some reddish fibrils and smooth, lower part sheathed from the base up with a mat, dry, fibrillose-cottony, greyish to brownish-grey (5–6EF3–4) layer, the latter cracking transversally, forming brownish-grey to olive brown patches (4DE4–6), first exposing a greyish-white layer, then the bright yellow deeper layers; ring at first prominent, loose membranous-cottony, vivid yellow (2AB3–5), covering the pores, later tearing, leaving fibrillose to membranous material on both pileus margin and upper third of the stipe, pulverulent, becoming greenish from spores.

Context yellowish-white in the pileus, marmorated yellow (1–2A2) – yellowish-white in the stipe, yellow towards the base of the stipe, cyanescent in all parts. Basal mycelium and rhizomorphs relatively thick, yellowish-white (2A2) to yellow. Odour strong fungoid. Taste not recorded. Spore print greenish-olive (fresh 3D4 in Rammeloo 5720).

Macrochemical reactions: tubes brown to reddish-brown with KOH and NH_4OH (in collections Rammeloo 5922 and De Kesel 2163).

Spores (8.4)8.6–9.5–10.3(–10.6) × (4.5)4.5–4.9–5.3(5.4) µm, Q = (1.77)1.79–1.93–2.07(2.09), broadly ellipsoid, smooth, pale yellowish-brown in 5% KOH and Melzer's reagent, thin-walled, inamyloid. Basidia 4-spored, 22–35 × 8–12 µm, clavate, hyaline, sterigmata up to 3–4 µm long, without clamp connection. Cheilocystidia abundant, cylindrical to narrowly fusiform, (31.9–)32.1–42.6–53(–48.8) × (6.1–)5.6–7.2–8.7(–8.6) µm, thin-walled, hyaline. Pleurocystidia similar to cheilocystidia, not abundant. Hymenophoral trama subregular, with poorly defined mediostratum. Pileipellis a tomentum composed of irregularly arranged hyphae, the latter cylindrical, of similar shape, 3.8–5.1(6.5) µm wide, slightly thick-walled (0.5 µm), with brownish intracellular pigment (persistent in 5% KOH), smooth, with pulverulence in places. Stipitipellis a tomentocutis composed of elements similar to the pileipellis. Partial veil composed of cylindrical hyphae, 3–6 µm wide, thin-walled and smooth. Clamp connections present in pileipellis tissue, small, frequent.

Additional collections. BENIN, Atacora Province, Kota, 10°12.680'N, 1°26.723'E, 30 Aug. 1997, 490 m a.s.l., gallery forest with *Berlinia grandiflora* and *Uapaca guineensis*, De Kesel 2023 (BR 5020074869827); ibidem, 10°12.699'N, 1°26.786'E, 17 Jun. 2000, 490 m a.s.l., De Kesel 2824 (BR 5020126377836); ibidem, 10°12.665'N, 1°26.750'E, 30 Jun. 2002, 510 m a.s.l., De Kesel 3500 (BR 5020152209163); Borgou Province, Wari Maro, 9°09.884'N, 2°09.595'E, 20 Jun. 1998, 300 m a.s.l., savannah woodland with *Isoberlinia doka* Craib & Stapf and *Uapaca togoensis* Pax, De Kesel 2163 (BR 5020112674574); BURUNDI, Bururi Province, Mugara, 04°02'S, 29°31'E, 16 Nov. 1978, 1050 m a.s.l., *Brachystegia* woodland, Rammeloo 5720 (BR 5020019368651);); ibid., 18 Nov. 1978, Rammeloo 5788 (BR 5020019374713); ibid., 20 Nov. 1978, Rammeloo 5811 (BR 5020032463654); ibid., 29 Nov. 1978, 950–1050 m a.s.l., *Brachystegia* woodland, Rammeloo 5922

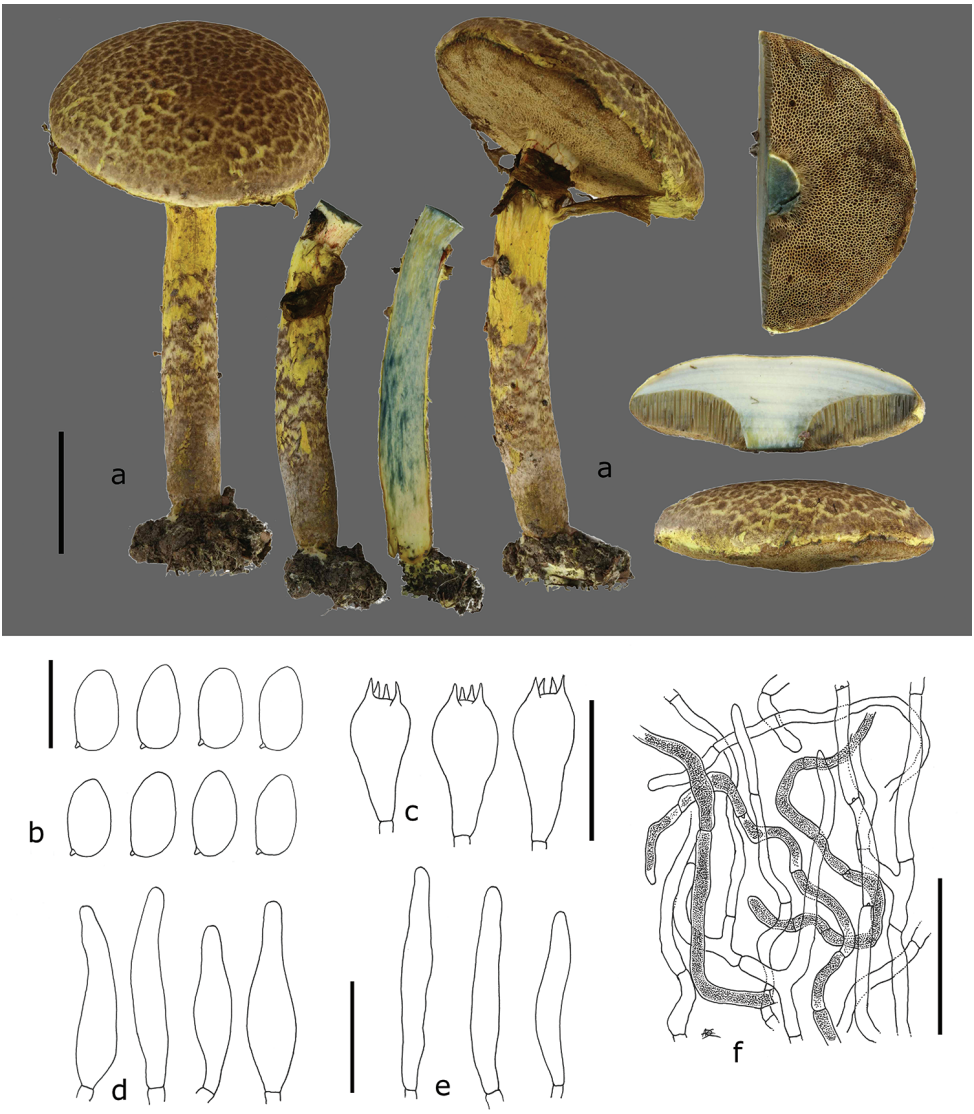

Figure 2. *Pulveroboletus africanus* (De Kesel 4650, holotype): **a** basidiomes **b** basidiospores **c** basidia **d** cheilocystidia **e** pleurocystidia **f** pileipellis hyphae with intracellular pigments and tiny clamps. Scale bars: 25mm (**a**), 10µm (**b**), 25µm (**c**), 25µm (**d, e**), 50µm (**f**).

(BR 5020019378759); ibid., Rumonge-Mutambara, 4°0.756'S, 29°29.599'E, 11 Jan. 2011, 950 m a.s.l., miombo woodland with *Brachystegia utilis* Burtt Davy & Hutch. and *B. bussei* Harms, Degreef 673 (BR); GUINEA, Labé Prefecture, Fouta Djalon, N of Tountourou, 13 Jul. 1988, 1000 m a.s.l., mountain woodland with *Uapaca chevalieri* Beille, Thoen 7977 (BR 5020003130264); DR CONGO, Upper Katanga Province, near Kisangwe, Mikembo sanctuary, 11°28.790'S, 27°40.367'E, 2 Feb. 2012,

1170 m a.s.l., miombo woodland with *Julbernardia globiflora* (Benth.) Troupin and *Brachystegia* spp, De Kesel 5026 (BR 5020212174363V); MALAWI, Nkhata bay district, Chisosira, 16 miles south of Chinteche, 3 Jan. 1978, woodland with *Brachystegia spiciformis* Benth., 450 m a.s.l., E. Tybaert 141 (BR 5020019389861, dupl. GENT); MOZAMBIQUE, Nambula Province, Natala, Reserva de Mecuburi, 27 Jan. 2011, leg. M. Härkönen, Marja Härkönen 201131 (H 7016064); TOGO, Central Province, Kparatao (towards Bassar), 09°11.630'N, 0°59.134'E, 14 Jul. 2007, 580 m a.s.l., miombo woodland with *Uapaca togoensis* and *Monotes kerstingii* Gilg., De Kesel 4359 (BR 5020163710719, duplicate in TOGO); ZIMBABWE, Midlands Province, Mtao Forest, 19°22.081'S, 30°40.383'E, 11 Feb. 1999, 1500 m a.s.l., extensively grazed miombo woodland, under *Brachystegia spiciformis*, De Kesel 2453 (BR 5020112623060).

Ethnomycological data. except for Mozambique and Zimbabwe, no local names or uses were collected. The local name in Mozambique (in Makua) is *Ettuli ya Khapa* (coll. Marja Härkönen 201131), which means tortoise shell. The local name in Zimbabwe (in chiShona) is *dindindi java* (Sharp 2011). The species is not used for consumption.

***Pulveroboletus sokponianus* Badou, De Kesel, Raspé & Yorou, sp. nov.**
Mycobank MB 827974
Fig. 3a–g

Illustr. Yorou and De Kesel (2011, fig 5.10, ut *Pulveroboletus ravenelii*).

Holotype. Togo, Central Province, Kparatao (towards Bassar), 09°11.630'N, 0°59.134'E, 14 July 2007, alt. 580 m, woodland on a slope with *Isoberlinia doka*, *Uapaca togoensis* and *Monotes kerstingii*, leg. A. De Kesel, De Kesel 4360 (BR!, BR 5020163695566, duplicate in TOGO).

Etymology. in honour of the late Prof. Dr. Ir. Nestor Sokpon, esteemed colleague of the University of Parakou (Benin), for his various contributions to the understanding of woodland ecology and regeneration.

Description. Basidiomata medium-sized, wrapped in a greenish-yellow (1A2–3) general veil when young. Pileus 40–55(60) mm diam., at first hemispherical to convex, then pulvinate or plano convex, upper layer pale yellow (1A2–4) to greenish-grey (1BC3–4), not cyanescent, dry, mat, tomentose to felty, becoming subtly to inconspicuously cracked, greenish-yellow (1A2–3) in the deeper layers; scales subtle, flat, slightly felty, greenish-grey (1BC3–4), darker in the centre, diffused towards the margin; margin at first incurved, appendiculate with age, greenish-yellow. Hymenophore tubulate, separable, straight to slightly sinuate, depressed around the stipe; tubes up to 7 mm long, yellow to greyish-yellow (1B3), cyanescent when cut; pores regular, mostly round or slightly angular, slightly elongated around the stipe, small (13–16/mm), pale yellow (1A2–2A2), cyanescent. Stipe cylindrical, 42–60 × 6–7(9) mm, central, solid, uppermost part yellowish-white (1A2–3), smooth, lower part sheathed with a mat, dry, fibrillose-cottony, thick, yellowish-white to pale yellow (1A2–4) or pale greenish-grey (1BC3–4) layer, the latter rather tearing than cracking in subtle fibrils;

Figure 3. *Pulveroboletus sokponianus* (**a, c–g** De Kesel 4360, holotype, **b** De Kesel 3593): **a** basidiomes **b** very young basidiomes **c** basidiospores **d** basidia **e** cheilocystidia **f** pleurocystidia **g** pileipellis with tiny clamps. Scale bars: 25mm (**a, b**), 10µm (**c**), 25µm (**d**), 25µm (**e, f**), 50µm (**g**).

ring at first woolly, cottony, pale greenish-yellow (1A2–4), then collapsing, leaving diffuse remains on pileus margin and stipe, sometimes pulverulent. Context whitish to whitish-yellow in the pileus, gradually yellowish-white (1A2) towards the base of the stipe. Slightly and slowly cyanescent, except in the base of the stipe. Basal mycelium and rhizomorphs usually white. Odour fungoid, when fresh like *Lepista nuda* (in collection De Kesel 1979). Spore print and macrochemical reactions not obtained.

Spores (8.5–)8.5–9.3–10.2(–10.5) × (4.4–)4.3–4.9–5.4(–5.6) µm, Q = (1.76)1.74–1.92–2.1(–2.14), broadly ellipsoid, smooth, pale yellowish-brown in 5% KOH and Melzer's reagent, thin-walled, inamyloid. Basidia 4-spored, 21–32 × 8–12 µm, clavate, hyaline, sterigmata 3–4 µm long, without clamp connection. Cheilocystidia abundant, fusiform to clavate, (36.8–)34.1–42.7–51.4(–52.8) × (6.6–)7.7–9.7–11.7(–11) µm, thin-walled, with yellow intracellular pigment (persistent in NH_4OH). Pleurocystidia similar to cheilocystidia, not abundant. Hymenophoral trama divergent, with regular mediostratum. Pileipellis a tomentum, composed of irregularly intertwined hyphae of similar shape, cylindrical, 3.3–5.1(6.2) µm wide, entirely hyaline, smooth, with small clamps. Stipitipellis a tomentum composed of elements similar to the pileipellis. Partial veil with cylindrical hyphae, 3–6 µm wide, thin-walled, smooth. Clamp connections small, frequent in the pileipellis.

Additional collections. BENIN, Atacora Province, Natitingou, Kota falls, 10°12.680'N, 1°26.723'E, 23 Aug. 1997, 520 m a.s.l., savannah woodland with *Isoberlinia*, A. De Kesel 1979 (BR 5020074831442); ibidem, 10°12.555'N, 001°26.793'E, 26 Jun. 2004, 480 m a.s.l., forest gallery with *Berlinia grandiflora* and *Uapaca* sp., A. De Kesel 3769 (BR 5020152060610); ibidem, Kouandé, 10°17.159'N, 1°40.890'E, 25/09/2000, 470 m a.s.l., savannah woodland with *Isoberlinia tomentosa* (Harms) Craib & Stapf, A. De Kesel 2942 (BR 5020129153468); ibidem, Borgou Province, Doguè, 9°07.249'N, 1°54.839'E, 10/10/2001, 350 m a.s.l., savannah woodland with *Afzelia africana* S.M. and *Isoberlinia doka*, A. De Kesel 3213 (BR 5020149693227); ibidem, Borgou Province, Okpara, 9°14.669'N, 2°43.377'E, 9 Aug. 2017, 360 m a.s.l., savannah woodland with *Isoberlinia doka*, S. Badou 0629 (UNIPAR); ibidem, Tamarou (forêt classée de N'dali), 9°44.680'N, 2°41.544'E, 31 Jul. 2017, 390 m a.s.l., savannah woodland with *Isoberlinia doka*, S. Badou 0624 (UNIPAR); ibidem, 4 Aug. 2017, 390m a.s.l., S. Badou 0625 (UNIPAR); ibidem, Wako, 9°09.457'N, 2°05.599'E, 11/09/2001, 300 m a.s.l., savannah woodland with *Isoberlinia doka*, *Uapaca togoensis* and *Burkea africana* Hook., A. De Kesel 3132 (BR 5020149809413); ibidem, Wari Maro, 9°10.038'N, 2°09.931'E, 20 Aug. 1997, 310 m a.s.l., savannah woodland with *Isoberlinia doka*, A. De Kesel 1943 (BR 5020074934501); ibidem, 9°09.884'N, 2°09.595'E, 22 Jun. 1998, 310 m a.s.l., savannah woodland with *Isoberlinia doka*, A. De Kesel 2183 (BR 5020112693766); ibidem, 9°08.110'N, 2°10.215'E, 09/10/2001, 290 m a.s.l., savannah woodland with *Isoberlinia doka* and *Uapaca togoensis*, A. De Kesel 3188 (BR 5020149726550); ibidem, 9°09.900'N, 2°09.511'E, 23/09/2001, 310 m a.s.l., savannah woodland with *Isoberlinia doka* and *Uapaca togoensis*, A. De Kesel 3237 (BR 5020149751804); ibidem, 9°10.027'N, 2°10.848'E, 16 Jun. 2002, 340 m a.s.l., savannah woodland with *Isoberlinia doka* and *Uapaca togoensis*, A. De Kesel 3411 (BR 5020152133376); ibidem, Collines Province, Toui-Kilibo, 8°32.746'N, 2°40.424'E, 19 Jul. 2017, 320 m a.s.l., savannah woodland with *Isoberlinia doka* and *I. tomentosa*, S. Badou 0519 (UNIPAR); ibidem, 5 Jul. 2017, S. Badou 0617 (UNIPAR); ibidem, 13 Jul. 2017, S. Badou 0621 (UNIPAR); ibidem, Donga Province, Bassila, 8°57.319'N, 1°38.391'E, 14 Jun. 2002, 380 m a.s.l., savannah woodland with *Berlinia grandiflora*, A. De Kesel 3403 (BR 5020152245529); ibidem, 8°59.516'N, 1°38.261'E, 26 Jun. 2002,

370 m a.s.l., gallery forest with *Berlinia grandiflora*, *Elaeis guineensis* Jacq. and *Raphia* sp., A. De Kesel 3467 (BR 5020152045464); ibidem, 9°0.073'N, 001°39.318'E, 17 Jun. 2004, 380 m a.s.l., gallery forest with *Berlinia grandiflora*, A. De Kesel 3668 (BR 5020157041959); ibidem, Penessoulou (south), 9°9.688'N, 1°34.793'E, 4 Jul. 2017, 380 m a.s.l., small gallery forest with *Isoberlinia doka*, S. Badou 0613 (UNIPAR); ibidem, 11 Aug. 2017, S. Badou 0630 (UNIPAR); ibidem, 22 Aug. 2017, S. Badou 0631 (UNIPAR); ibidem, Zou Province, Ouèssè, Gbadji forest (West side of the slope), 7°57.152'N, 001°58.095'E, 13 Jun. 2004, 310 m a.s.l., savannah woodland with *Isoberlinia doka*, *Burkea africana*, A. De Kesel 3593 (BR 5020157206662). TOGO, Central Province, Fazao (Parc National), 08°42.150'N, 0°46.383'E, 16 Jun. 2011, 520 m a.s.l., savannah woodland with *Afzelia africana*, A. De Kesel 4910 (BR 5020212173335V); ibidem, 08°43.963'N, 0°47.674'E, 16 Jul. 2007, 510 m a.s.l., savannah woodland with *Isoberlinia doka* and *Uapaca togoensis*, A. De Kesel 4382 (BR 5020163713741); ibidem, 08°38.737'N, 0°46.010'E, 17 Jul. 2007, 550 m a.s.l., gallery forest with *Berlinia grandiflora*, A. De Kesel 4393 (BR 5020163839069); ibidem, 08°43.145'N, 0°46.332'E, 20 Jul. 2007, 560 m a.s.l., savannah woodland on gravelly soil, with *Uapaca togoensis*, A. De Kesel 4469 (BR 5020163803671); ibidem, 08°40.872'N, 0°45.487'E, 04 Jun. 2008, 680 m a.s.l., savannah woodland with *Isoberlinia doka* and *Uapaca togoensis*, A. De Kesel 4625 (BR 5020165412277).

Ethnomycological data. Except for Benin, no local names or uses were collected. The local name in Nagot language is *osousou eti* (coll. De Kesel 2183) and this species is not eaten.

Discussion

Species delimitation

The African collections represent two separate species, *Pulveroboletus africanus* sp. nov. and *P. sokponianus* sp. nov., both macroscopically similar to *Pulveroboletus ravenelii*. In the latter, however, the disc becomes reddish-orange to reddish-brown at maturity and it grows in temperate conifer woods (Bessette et al. 2016), montane Quercus forests in Costa Rica (Halling and Mueller 2005) and Colombia (Franco-Molano et al. 2000) and Pine-oak forests in the Dominican Republic/Belize (Ortiz-Santana et al. 2007). The phylogenetic analysis showed that the African specimens form a well-supported subclade within *Pulveroboletus*, sister to the Asian and American taxa. Although clamp connections have previously been reported to be absent in *Pulveroboletus* (Watling 2008, Zeng et al. 2017), all specimens of the African subclade show very small clamp connections.

Macroscopically, both African taxa can be distinguished based on the colour of the scales on the pileus and the stipe, being brown in *P. africanus* and greenish-grey or yellow in *P. sokponianus*. In *P. africanus*, the basal mycelium and context in the base of the stipe is generally yellow whereas it is whitish to whitish-yellow in *P. sokponianus*. While bluing of the context depends on the freshness and the maturity of the basidiomes, it

seems more pronounced in *P. africanus*. Although cystidia have been reported to be rather constant and of little use to separate Asian taxa (Zeng et al. 2017), this seems to be true for the spores of the African taxa, but not for cystidia. In *P. africanus*, the cheilocystidia are hyaline and narrowly fusiform, whereas they are broadly fusiform and yellow pigmented in *P. sokponianus*. Further striking characters of distinction is the brownish intracellular pigmentation in the hyphae of the pileal and stipital scales, present in *P. africanus* but absent in *P. sokponianus*.

Young basidiomes of *Pulveroboletus sokponianus* are strongly reminiscent of the Asian *P. brunneopunctatus* G. Wu & Zhu L. Yang, but the latter has a viscid veil and smaller cheilocystidia. Using the key of the Chinese species (Zeng et al. 2017), *Pulveroboletus africanus* approaches closest to *P. brunneoscabrosus* Har. Takah. The latter has a viscid veil, reddish-brown scales and white to yellowish-white basal mycelium.

Distribution and ecology

Both new species are endemic to tropical Africa. *Pulveroboletus africanus* was found in Benin, Burundi, Guinea, DR Congo, Malawi, Mozambique, Togo, Zimbabwe and possibly also Zambia. It prefers regions with a pronounced wet/dry season alternance and occurs in a wide variety of woodlands, savannah woodlands and gallery forests across tropical Africa. It seems absent in the dense rainforests (Congolian region). The species is terricolous and most probably ectomycorrhizal (EcM), occurring in EcM dominated forests up to 1500 m elevation. It is difficult to ascertain if the species associates with Caesalpiniaceae (*Berlinia*, *Brachystegia*, *Isoberlinia*, *Julbernardia*) and/or with *Uapaca* (Phyllantaceae). Only *Uapaca* is well represented throughout its distribution range. In Eastern Africa (Zambezian region), it is also found under *Brachystegia* spp. and *Julbernardia* spp.; in West Africa (Soudano-Guinean region) under *Berlinia grandiflora* and *Isoberlinia* spp., Thoen and Ducousso (1989) mention it under *Uapaca chevalieri* Beille. The species may also occur in Zambia (ut *Pulveroboletus* aff. *ravenelii*, fig. 1H in Watling and Turnbull 1992).

Pulveroboletus sokponianus has so far only been found in a variety of savannah woodlands and gallery forests in the Soudano-Guinean transition zones of Benin and Togo, probably also in Ivory Coast (see fig. 3a in Léabo et al. 2017). The species is terricolous, most probably ectomycorrhizal (EcM) and most often found under *Isoberlinia doka* (Caesalpiniaceae). Since habitat destruction and felling of host trees is common practice in Benin, Yorou and De Kesel (2011) placed this species (mentioned as *P. ravenelii*) under the IUCN threat category 'vulnerable'.

Acknowledgements

Badou S. and Guelly A.K. acknowledge the Belgian focal point for the Global Taxonomy Initiative (CEBioS programme) for research grants at Meise Botanic Garden

(Belgium) and support for fieldwork in Togo, respectively. Badou S., Yorou N.S. and M. Ryberg are grateful to FORMAS (Sweden) for financially supporting part of the fieldwork in Benin (grant 226-2014-1109). Badou S. and Yorou N.S. thank the Volkswagen Foundation (grant 90-127), Meise Botanic Garden and the Global Taxonomy Initiative (CEBioS programme) for financing or supplying laboratory equipment to the University of Parakou (Benin).

De Kesel A. acknowledges grants and logistic support from MIKEMBO and BAK (Biodiversité au Katanga) for supporting the fieldwork in DR Congo (2012–2018). He acknowledges the King Léopold III Fund for Nature Exploration and Conservation, as well as the Foundation to Promote Scientific Research in Africa for financially supporting fieldwork in Benin (2002, 2004) and in Togo (2007, 2008, 2011).

We express our gratitude to Daniel Thoen (Belgium), Jan Rammeloo (Belgium), Marja Härkönen (Finland), Maba Dao (Togo), Bill Kasongo, Michel Hasson, Michel Anastassiou (DR Congo), Anxious Masuka (Zimbabwe), André De Groote (Benin) and Jean Claude Codjia (CECODI, Benin) for kindly providing specimens or help and logistic support during our fieldwork. Wim Baert and Myriam de Haan are acknowledged for assistance in the molecular lab of Meise Botanic Garden. We thank Roy Halling for indicating additional references.

References

Bessette A, Roody WC, Bessette AR (2016) Boletes of eastern North America. Syracuse, New York, 469 pp.

Binder M, Hibbett DS (2006) Molecular systematics and biological diversification of Boletales. Mycologia 98: 971–981. https://doi.org/10.1080/15572536.2006.11832626

Clémençon H (2012) Cytology and plectology of the Hymenomycetes (2nd revised edn). J. Cramer-Schweitzerbart, Stuttgart, 520 pp.

De Kesel A, Codjia JTC, Yorou SN (2002) Guide des champignons comestibles du Bénin. Jardin Botanique national Belgique, Bruxelles, 274 pp.

Doyle JJ, Doyle JL (1990) Isolation of plant DNA from fresh tissue. Focus 12: 13–15.

Eyi Ndong H, Degreef J, De Kesel A (2011) Champignons comestibles des forêts denses d'Afrique centrale. Taxonomie et identification. Abc Taxa volume 10, 254 pp.

Franco-Molano AE, Aldana-Gómez R, Halling RE (2000) Setas de Colombia (Agaricales, Boletales y otros hongos). Universidad de Antioquia, Colcencias, 156 pp.

Halling RE, Mueller GM (2005) Common Mushrooms of the Talamanca Mountains, Costa Rica. Mem. NY Bot Gard 90: 1–195.

Halling RE, Nuhn M, Fechner NA, Osmundson TW, Soytong K, Arora D, Hibbett DS, Binder M (2012) *Sutorius*: a new genus for *Boletus eximius*. Mycologia 104: 951–961. https://doi.org/10.3852/11–376

Horak E (2011) Revision of Malaysian species of Boletales s.l. (Basidiomycota) described by E.J.H. Corner (1972, 1974). Malayan Forest Record 51: 1–283.

Kamou H, Gbogbo KA, Yorou NS, Nadjombe P, Abalo-Loko AG, Verbeken A, De Kesel A, Batawila K, Akpagana K, Guelly A (2017) Inventaire préliminaire des macromycètes du Parc National Fazao-Malfakassa du Togo, Afrique de l'Ouest. Tropicultura 35(4): 275–287. http://www.tropicultura.org/text/v35n4/275.pdf

Katoh K, Standley DM (2013) MAFFT Multiple sequence alignment software version 7: Improvements in performance and usability. Molecular Biology and Evolution 30: 772–780. https://doi.org/10.1093/molbev/mst010

Kornerup A, Wanscher JH (1978) Methuen Handbook of Colour (3rd edn). Eyre Methuen Ltd, London, 252 pp.

Matheny PB (2005) Improving phylogenetic inference of mushrooms with RPB1 and RPB2 nucleotide sequences (Inocybe; Agaricales). Molecular Phylogenetics and Evolution 35: 1–20. https://doi.org/10.1016/j.ympev.2004.11.014

Miller MA, Holder MT, Vos R, Midford PE, Liebowitz T, Chan L, Hoover P, Warnow T (2009) The CIPRES portals. CIPRES. http://www.phylo.org/portal2/home

Murrill WA (1909) The Boletaceae of North America: I. Mycologia 1: 4–18.

Ortiz-Santana B, Lodge DJ, Baroni TJ, Both EE (2007) Boletes from Belize and the Dominican Republic. Fungal Diversity 27: 247–416.

Phookamsak R, Hyde KD, Wanasinghe DN, Jeewon R, Bhat DJ, Maharachchikumbura SSN, et al. (2018) Fungal diversity notes 933–1040: taxonomic and phylogenetic contributions on genera and species of fungal taxa. Fungal Diversity. [in press]

Raspé O, Vadthanarat S, De Kesel A, Degreef J, Hyde KD, Lumyong S (2016) *Pulveroboletus fragrans*, a new Boletaceae species from Northern Thailand, with a remarkable aromatic odor. Mycological Progress 15: 38. https://doi.org/10.1007/s11557-016-1179-7

Rehner SA, Buckley E (2005) A *Beauveria* phylogeny inferred from nuclear ITS and EF1-α sequences: evidence for cryptic diversification and links to *Cordyceps* teleomorphs. Mycologia 97: 84–98.

Sharp C (2011) A pocket guide to mushrooms in Zimbabwe. Vol. 1: some common species. Directory publishers, Bulawayo, 104 pp.

Singer R (1945) The Boletinae of Florida with notes on extralimital species, II. Farlowia 2: 223–302.

Singer R (1947) The Boletinae of Florida with notes on extralimital species, III. American Midland Naturalist 37: 1–135.

Singer R (1986) The Agaricales in Modern Taxonomy (4th edn). Koeltz Scientific Books, Koenigstein, 981 pp.

Stamatakis A (2006) Raxml-vi-hpc: maximum likelihood-based phylogenetic analyses with thousands of taxa and mixed models. Bioinformatics 22: 2688–2690. https://doi.org/10.1093/bioinformatics/btl446

Thoen D, Ducousso M (1989) Champignons et ectomycorrhizes du Fouta Djalon. Bois et forêts des tropiques 221: 45–63.

Thiers B (continuously updated) Index Herbariorum: A global directory of public herbaria and associated staff. New York Botanical Garden's Virtual Herbarium. http://sweetgum.nybg.org/science/ih

Vadthanarat S, Raspé O, Lumyong S (2018) Phylogenetic affinities of *Rhodactina* (Boletaceae), with a new species *R. rostratispora*. MycoKeys 29: 63–80. https://doi.org/10.3897/mycokeys.29.22572

Vanié-Léabo LPL, Yorou NS, Koné NA, Kouamé NF, De Kesel A, Koné D (2017) Diversity of ectomycorrhizal fungal fruiting bodies in Comoé National Park, a Biosphere and World Heritage in Côte d'Ivoire (West Africa). International Journal of Biodiversity and Conservation 9(2): 27–44. https://doi.org/10.5897/IJBC2016.0999

Watling R, Turnbull E (1992) Boletes from South and East Africa – I. Edinb. Journal of Botany 48(3): 343–361. https://doi.org/10.1017/S0960428600000585

Watling R (2001) The relationships and possible distribution patterns of boletes in south-east Asia. Mycological Research 105: 1440–1448. https://doi.org/10.1017/S0953756201004877

Watling R (2008) A manual and source book on the boletes and their allies. Synopsis Fungorum, vol 24. Fungiflora, Oslo.

Wu G, Feng B, Xu J, Zhu XT, Li YC, Zeng NK, Hosen MI, Yang ZL (2014) Molecular phylogenetic analyses redefine seven major clades and reveal 22 new generic clades in the fungal family Boletaceae. Fungal Diversity 69: 93–115. https://doi.org/10.1007/s13225-014-0283-8

Wu G, Li YC, Zhu XT, Zhao K, Han LH, Cui YY, Li F, Xu JP, Yang ZL (2016) One hundred noteworthy boletes from China. Fungal Diversity 81: 25–188. https://doi.org/10.1007/s13225-016-0375-8

Wu G, Zhao K, Li YC, Zeng NK, Feng B, Halling RE, Yang ZL (2015) Four new genera of the fungal family Boletaceae. Fungal Diversity 81: 1–24. https://doi.org/10.1007/s13225-015-0322-0

Yorou NS, De Kesel A (2011) Champignons supérieurs – Larger fungi. In : Neuenschwander P, Sinsin B, Goergen G (Eds) Protection de la Nature en Afrique de l'Ouest: Une Liste Rouge pour le Bénin. Nature Conservation in West Africa: Red List for Benin. International Institute of Tropical Agriculture, Ibadan, Chapter 5, 47–60.

Zeng NK, Liang ZQ, Tang LP, Li YC, Yang ZL (2017) The genus *Pulveroboletus* (Boletaceae, Boletales) in China. Mycologia 109: 422–442. https://doi.org/10.1080/00275514.2017.1331689

Zhao K, Wu G, Feng B, Yang ZL (2014a) Molecular phylogeny of *Caloboletus* (Boletaceae) and a new species in East Asia. Mycological Progress 13: 1127–1136. https://doi.org/10.1007/s11557-014-1001-3

Zhao K, Wu G, Yang ZL (2014b) A new genus, *Rubroboletus*, to accommodate *Boletus sinicus* and its allies. Phytotaxa 188: 61–77. https://doi.org/10.11646/phytotaxa.188.2.1